TECHNISCHE UNIVERSITÄT KAISERSLAUTERN

Multi-omics and functional analysis reveal novel consequences of monosomy

Vom Fachbereich Biologie
der Universität Kaiserslautern
zur Verleihung des akademischen Grades
„Doktor der Naturwissenschaften“ (Dr.rer.nat.)
genehmigte Dissertation

vorgelegt von **Narendra Kumar Chunduri**

Datum der wissenschaftlichen Aussprache:
14. July 2021

Prüfungskommission
1. Gutachter: Prof. Dr. Zuzana Storchová
2. Gutachter: Prof. Dr. Stefan Kins
Vorsitzender: Prof. Dr. Johannes M. Herrmann

Kaiserslautern, 2021

DECLARATION

I hereby declare that this thesis is a record of bonafide work carried out by me, under the supervision of Prof. Dr. Zuzana Storchová, for the award of a Doctorate degree at the Technische Universität Kaiserslautern. No other sources or aids for assistance, other than those specified, were used in the writing of this thesis.

I further declare that the work reported in this thesis has not been submitted and will not be submitted, either in part or full, for the award of any other degree or diploma in this institute or any other institute or University.

Narendra Kumar Chunduri

Kaiserslautern, 15. June 2021

…… dedicated to all the beautiful souls who lost fight against COVID-19

Table of Contents

List of publications

Research Articles:

1. Narendra Kumar Chunduri, Paul Menges, Vincent Leon Gotsmann, Xiaoxiao Zhang, Balca R. Mardin, Christopher Buccitelli, Jan O. Korbel, Felix Willmund, Maik Kschischo, Markus Raeschle, Zuzana Storchova. Haploinsufficiency of ribosomal genes limits the viability of monosomic human cells by activation of the p53 pathway. *(Accepted in Nature communications)*

2. Maria Krivega, Clara Marie Stiefel, Sahar Karbassi, Narendra Kumar Chunduri, Neysan Donnelly, Andreas Pichlmair, Zuzana Storchova. Genotoxic stress in constitutive trisomies induces autophagy and the innate immune response via the cGAS-STING pathway. *(Accepted in Communication Biology)*

3. Anand Vasudevan, Prasamit S Baruah, Joan C Smith, Zihua Wang, Nicole M Sayles, Peter Andrews, Jude Kendall, Justin Leu, Narendra Kumar Chunduri, Dan Levy, Michael Wigler, Zuzana Storchová, Jason M Sheltzer. Single-Chromosomal Gains Can Function as Metastasis Suppressors and Promoters in Colon Cancer. *Developmental Cell* 52 (4), 413-428. e6

4. Devon A. Lukow, Erin L. Sausville, Pavit Suri, Narendra Kumar Chunduri, Justin Leu, Jude Kendall, Zihua Wang, Zuzana Storchova, Jason M. Sheltzer. Chromosomal instability accelerates the evolution of resistance to anti-cancer drugs. *Developmental cell (In revisions)*

Reviews:

5. Narendra Kumar Chunduri, Zuzana Storchova. The diverse consequences of aneuploidy. *Nature Cell Biology*. 21 (1), 54-62

6. Narendra Kumar Chunduri, Zuzana Storchova. BCL9L and caspase-2—new guardians against aneuploidy. *Translational Cancer Research* 6, S139-S142

Summary

Every organism contains a characteristic number of chromosomes that have to be segregated equally into two daughter cells during mitosis. Any error during chromosome segregation results in daughter cells that lost or gained a chromosome, a condition known as aneuploidy. Several studies from our laboratory and across the world have previously shown that aneuploidy per se strongly affects cellular physiology. However, these studies were limited mainly to the chromosomal gains due to the availability of several model systems. Strikingly, no systemic study to evaluate the impact of chromosome loss in the human cells has been performed so far. This is mainly due to the lack of model systems, as chromosome loss is incompatible with survival and drastically reduces cellular fitness. During my PhD thesis, for the first time, I used diverse omics and biochemical approaches to investigate the consequences of chromosome losses in human somatic cells.

Using isogenic monosomic cells derived from the human cell line RPE1 lacking functional p53, we showed that, similar to the cells with chromosome gains, monosomic cells proliferate slower than the parental cells and exhibit genomic instability. Transcriptome and proteome analysis revealed that the expression of genes encoded on the monosomic chromosomes was reduced, as expected, but the abundance was partially compensated towards diploid levels by both transcriptional and post transcriptional mechanisms. Furthermore, we showed that monosomy induces global gene expression changes that are distinct to changes in response to chromosome gains. The most consistently deregulated pathways among the monosomies were ribosomes and translation, which we validated using polysome profiling and analysis of translation with puromycin incorporation experiments. We showed that these defects could be attributed to the haploinsufficiency of ribosomal protein genes (RPGs) encoded on monosomic chromosomes. Reintroduction of p53 into the monosomic cells uncovered that monosomy is incompatible with p53 expression and that the monosomic cells expressing p53 are either eliminated or outgrown by the p53 negative population. Given the RPG haploinsufficiency and ribosome biogenesis defects caused by monosomy, we show an evidence that the p53 activation in monosomies could be caused by the defects in ribosomes. These findings were further supported by computational analysis of cancer genomes revealing those cancers with monosomic karyotype accumulated frequently p53 pathway mutations and show reduced ribosomal functions.

Together, our findings provide a rationale as to why monosomy is embryonically lethal, but frequently occurs in p53 deficient cancers.

Zussamenfassung

Jeder Organismus enthält eine charakteristische Anzahl von Chromosomen, die während der Mitose gleichmäßig in zwei Tochterzellen segregiert werden müssen. Jeder Chromosomensegregation-Fehler führt zu Tochterzellen, die ein Chromosom verlieren oder gewinnen, bekannt als Aneuploidie. Mehrere Studien aus unserem Labor und weltweit haben bereits gezeigt, dass Aneuploidie per se die Zellphysiologie stark beeinflusst. Allerdings waren diese Studien aufgrund der Verfügbarkeit verschiedener Modellsysteme hauptsächlich auf die Chromosomengewinne beschränkt. Jedoch wurde bisher keine systemische Studie über die Auswirkungen von Chromosomenverlusten in menschlichen Zellen durchgeführt. Dies ist vor allem auf den Mangel an Modellsystemen zurückzuführen, da Chromosomenverlust mit dem Überleben unvereinbar ist und die zelluläre Fitness drastisch reduziert. Während meiner Doktorarbeit habe ich zum ersten Mal verschiedene Omics- und biochemische Ansätze verwendet, um die Folgen von Chromosomenverlusten in menschlichen somatischen Zellen zu untersuchen.

Mit isogenen monosomischen Zellen der Zelllinie RPE1, der funktionelles p53 fehlt, konnten wir zeigen, dass monosomische Zellen, ähnlich wie die Zellen mit Chromosomengewinnen, langsamer proliferieren als die elterlichen Zellen und eine genomische Instabilität aufweisen. Transkriptom- und Proteomanalysen zeigten eine reduzierte Expression von Genen, die auf den monosomischen Chromosomen kodiert werden, aber die Abundanz teilweise durch transkriptionelle und posttranskriptionelle Mechanismen in Richtung diploides Niveau kompensiert wurde. Darüber hinaus konnten wir zeigen, dass die Monosomie andere globale Veränderungen der Genexpression induziert, als bei Chromosomengewinne. Die am konsequentesten deregulierten Signalwege unter den Monosomien waren Ribosomen und Translation, was wir durch Polysomen rofiling und Analyse der Translation mit Puromycin inkorporations experimenten validierten. Wir zeigten, dass diese Defekte auf die Haploinsuffizienz von auf monosomischen Chromosomen kodierenden ribosomalen Protein-Genen (RPGs) zurückzuführen sind. Die Reintroduktion von p53 deckte auf, dass die Monosomie mit der p53-Expression inkompatibel ist und dass die monosomischen Zellen, die p53 exprimieren, entweder eliminiert oder von der p53-negativen Population überwuchert werden. Angesichts der durch Monosomie verursachten RPG-Haploinsuffizienz und defekte Ribosomenbiogenese zeigen wir einen Hinweis darauf, dass die p53-Aktivierung in Monosomien durch Ribosomendefekte verursacht werden könnte. Diese Befunde wurden weiter durch eine rechnerische Analyse von Krebsgenomen unterstützt, die zeigte, dass Krebserkrankungen mit monosomischem Karyotyp häufig p53-Signalweg-Mutationen akkumulieren und reduzierte ribosomale Funktionen aufweisen.

Zusammengenommen liefern unsere Ergebnisse eine Erklärung dafür, warum Monosomie embryonal letal ist, aber häufig in p53-defizienten Krebsarten auftritt.

1. Introduction

Faithful propagation of genetic information from parental to the daughter cells is essential for the perpetuation of life. In every organism, from unicellular to multicellular, the genetic information encoded on DNA is organized in cells as chromosomes, with characteristic number and sequence defining the organism. The faithful propagation of genetic information requires accurate duplication and segregation of chromosomes equally into the daughter cells. The chromosome duplication and segregation are highly dynamic processes orchestrated by several mechanisms ensuing that these processes occur in an error-free manner. Any errors in these processes result in unequal distribution of chromosomes, a condition commonly known as “aneuploidy”.

1.1 Aneuploidy – Types and occurrence

Aneuploidy can be broadly defined as an imbalance in the complement of chromosomes. Recent advances in the sequencing technologies have led to better classification of aneuploidy based on the karyotypes. Aneuploidy can be categorized into 3 types: 1) Whole chromosomal aneuploidy, characterized by a loss or gain of a whole chromosome; 2) Segmental or structural aneuploidy, characterized by arm level copy number changes; and 3) Somatic copy number variation (SCNV) involving chromosome alterations in range of kilobases to megabases. While the whole chromosomal aneuploidy is mainly caused due to the errors in chromosome segregation, segmental aneuploidy and SCNV occur mainly due to errors in DNA replication and repair (reviewed in (B. Orr, Godek, & Compton, 2015)).

At the organismal level, aneuploidy can be further classified into constitutional aneuploidy and somatic aneuploidy based on its origin and distribution. Constitutional aneuploidy is caused by chromosome segregation errors during meiosis, such as non-disjunction, precocious sister chromatid separation (Ottolini et al., 2015) as well as mitotic mechanisms including mitotic non-disjunction, anaphase lagging and endo-reduplication (Vazquez-Diez & FitzHarris, 2018). Errors in meiosis affect all embryonic cells uniformly after fertilization, resulting in whole organisms being aneuploid. In contrast, mitotic errors lead to chromosomal mosaicism. Severe chromosomal mosaicism is lethal to embryos (McCoy et al., 2015; Ottolini et al., 2017), whereas mild levels of mosaicism is compatible with growth and survival (Greco, Minasi, & Fiorentino, 2015). Constitutional aneuploidy is embryonically lethal in most cases. In rare instances, for example trisomy of chromosome 13, 18 and 21 (Patau, Edwards and Down syndrome respectively) can survive, albeit at a low frequency and with severe pathological consequences. Monosomy, or chromosome loss, has even more severe effects. Early cytogenetic studies showed that mice embryos with monosomic karyotype are eliminated much earlier than the trisomic embryos (Magnuson et al., 1985). Similar findings were observed in humans, where no monosomies survive till

birth. Somatic aneuploidy is mainly caused by errors in mitosis leading to random chromosome missegregation and karyotype heterogeneity among the tissues. Classical example for somatic aneuploidy is a disease called mosaic variegated aneuploidy (MVA). It is caused by mutations in *BUB1B* and *CEP57* that lead to frequent errors in chromosome segregation (Snape et al., 2011) (Hanks et al., 2004). Patients with MVA often suffer from growth retardation, developmental defects and structural central nervous system defects, and are prone to develop cancer (Garcia-Castillo, Vasquez-Velasquez, Rivera, & Barros-Nunez, 2008). Indeed, aneuploidy is frequently observed in cancers. About 90% of solid tumors and 35-60 % of hematopoietic cancers are aneuploid (Storchova & Kuffer, 2008; Taylor et al., 2018). Although the exact role of aneuploidy in tumor development is unclear, it is believed that aneuploidy promotes tumor growth by selecting for gain of oncogenes or loss of tumor suppressors.

Interestingly, aneuploidy was reported in liver and brain of healthy individuals. The occurrence of aneuploidy in liver is attributed to the polyploid hepatocytes that arise during the post-natal development (Guidotti et al., 2003). Investigation of hepatocyte ploidy using FISH suggested that about 50% of hepatocytes are aneuploid (Duncan et al., 2012). Similarly, FISH analysis revealed that about 20% of mouse and human brain cells are found to be aneuploid (Rehen et al., 2005) (Faggioli, Wang, Vijg, & Montagna, 2012). Spectral karyotyping of mouse embryonic neural progenitor cells implied that 33% of cells either lost or gained different chromosomes (Rehen et al., 2001). High aneuploidy in hepatocytes and brain cells was believed to be beneficial for the organs by providing genetic and phenotypic heterogeneity. However, single cell DNA sequencing (scSEQ) of the cells obtained from these tissues revealed that the aneuploidy levels are much lower in mammalian liver and brain tissues than it has been proposed by FISH. scSEQ identified that only about 1-4% of mammalian brain and liver cells are aneuploid (K. A. Knouse, Wu, Whittaker, & Amon, 2014). Interestingly, aneuploidy is commonly observed in unicellular organisms such as budding yeast (Peter et al., 2018) (Duan et al., 2018), in pathogenic yeast *Candida albicans* (Selmecki, Forche, & Berman, 2006) or other parasitic species, and in several multicellular species (Piló, Carvalho, Pereira, Gaspar, & Leitão, 2017) (Leitao, Boudry, & Thiriot-Quievreux, 2001). How aneuploidy on one hand causes embryonal lethality, but on the other hand can be often observed in pathological conditions such as cancer fuels the curiosity for understanding its consequences.

1.2 Causes of Aneuploidy

Aneuploidy is mainly caused by errors in chromosome segregation during mitosis or meiosis. These errors can be broadly classified into 4 types: spindle assembly checkpoint (SAC) defect, microtubule attachment defects, centrosomal defects and chromosome cohesion defects (Figure 1).

Spindle assembly checkpoint (SAC) defects: Spindle assembly checkpoint is a failsafe mechanism ensuring correct attachments of spindle microtubules to kinetochores (Figure 1A). Failure to form a correct attachment activates the proteins of SAC and delays anaphase onset until the attachments are corrected. Several *in vitro* and *in vivo* studies showed that reduced levels of SAC proteins, such as BUB1, BUB3, MAD1, MAD2, CENPE and MPS1 (Michel et al., 2001) (Babu et al., 2003; Foijer et al., 2014; Iwanaga et al., 2007; Jeganathan, Malureanu, Baker, Abraham, & van Deursen, 2007; Kalitsis et al., 2005; Ohashi et al., 2015; Schliekelman et al., 2009; B. A. Weaver, Silk, Montagna, Verdier-Pinard, & Cleveland, 2007) resulted in varying degree of aneuploidy. Further, these models showed in comparison to diploid organisms an increased tendency to develop tumors, either spontaneous or upon additional drug treatment, or in cancer predisposed mice models. However, it is unclear whether the tumors were caused by aneuploidy or by the gene depletion itself, because many of the SAC proteins have functions outside mitosis (B. A. A. Weaver & Cleveland, 2006). Interestingly, mutations in SAC proteins are rarely observed in cancers (Figure 2) (Giorgia Simonetti, Samantha Bruno, Antonella Padella, Elena Tenti, & Giovanni Martinelli, 2019). In fact, some of these proteins are often overexpressed in tumors. For example, MAD2 overexpression was commonly observed in cells with aberrant RB pathway. MAD2 is a transcriptional target of the E2F pathway and aberrant RB pathway leads to increased E2F activity (Hernando et al., 2004). Interestingly, increased MAD2 expression also causes aneuploidy due to hyper stabilization of microtubule-kinetochore attachments (Kabeche & Compton, 2012). Hence, impaired expression of SAC proteins influences chromosome segregation by multiple mechanisms and leads to aneuploidy.

Microtubule attachment defects: In mitosis, the microtubules connect with the chromosomes via kinetochore, large proteinaceous complex located at the centromeric region (Nicklas, 1997). Correct microtubule- kinetochore attachment is recognized by SAC and signals the progression from metaphase to anaphase. The complex of Aurora kinase B along with KIF2B and KIF2C (MCAK) plays an essential role to ensure proper (amphitelic) attachment (Manning et al., 2007) (Samuel F. Bakhoum, Thompson, Manning, & Compton, 2009) (Figure 1A). This complex destabilizes erroneous correction such as monotelic attachements (only single kinetochore is attached), syntelic attachments (both sister kinetochores attach to the same pole) and merotelic attachments (one of the kinetochores is attached to both poles). The progression of mitosis is arrested by monotelic and syntelic attachments due to SAC activation, but not by merotelic attachments, since this configuration satisfies the SAC (Gregan, Polakova, Zhang, Tolic-Norrelykke, & Cimini, 2011) (Figure 1B, C, D & E). Failure to correct merotelic attachment results in lagging chromosomes, which can be eventually missegregated.

Chromosome cohesion defects: Following chromosome duplication, the sister chromatids are held together by a protein complex called cohesin. When the cells enter mitosis, majority of the cohesin is removed in a phosphorylation dependent manner mediated by WAPL. The cohesin around the sister chromatid at the centromere remains intact and holds the sister chromatids together until all the spindles are attached to the kinetochores. SGO1 recruits a phosphatase to the centromere and inhibit the phosphorylation of cohesin by WAPL, thereby preventing premature sister chromatid separation (Shintomi & Hirano, 2009). Premature sister chromatid separation does not elicit robust SAC activation, which leads to erroneous mitosis and aneuploidy (Mirkovic, Hutter, Novak, & Oliveira, 2015) (Figure 1F).

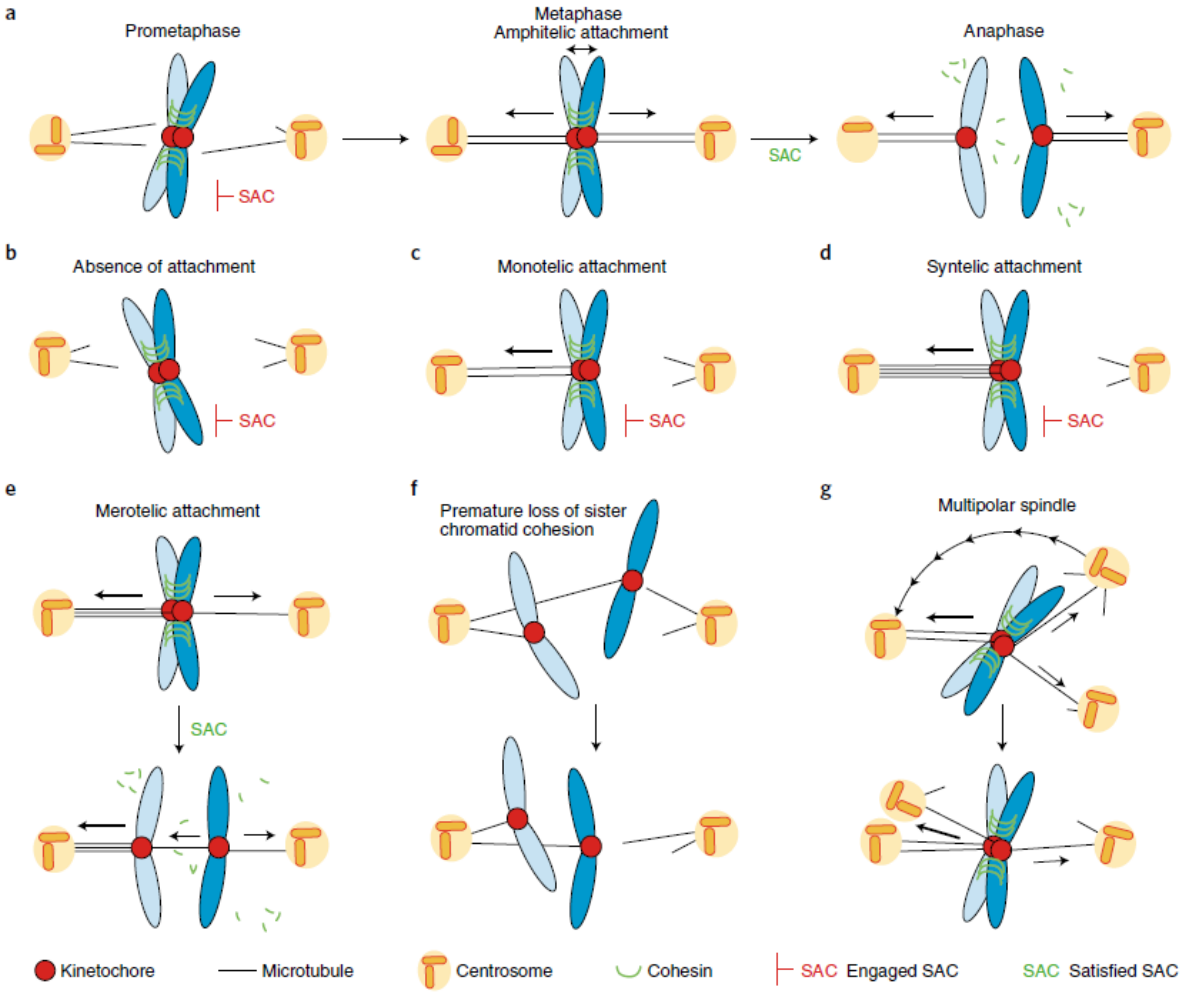

Figure 1. Different paths to chromosome missegregation. A. Schematics of normal chromosome segregation process. During prometaphase, the newly replicated sister chromatids are connected to the microtubules at their respective kinetochores. In metaphase, correct bipolar attachment generates tension between the sister chromatid cohesion and pulling forces of microtubules. Once the bipolar attachment is successfully established, spindle check point is silenced. In anaphase, cohesin is dissolved and the sister chromatids are pulled apart to the opposite poles. **B.** Absence of microtubule-kinetochore attachment activates SAC. **C, D and E.** Different types of spindle attachment

errors. Monotelic attachment - two microtubules from the same pole attach to the kinetochore of one of the sister chromatids and no attachment on the other one. This also elicits SAC. Syntelic attachment- both sister chromatids are connected to the microtubules emanating from the same pole. Both monotelic and syntelic attachments results in chromosome missegregation if left uncorrected. Merotelic attachment - one sister chromatid is connected to microtubules from both poles. This generates enough tension and inhibits SAC. Merotelically attached chromatids often lag during anaphase and become missegregated. **F.** Premature loss of cohesin results in premature chromatid segregation even before the microtubules are attached to kinetochores. **G.** Multi-polar mitosis caused by additional centrosomes. Clustering of additional centrosome leads to bipolar mitosis. Impaired clustering results in multipolar mitosis. (Adapted from (Chunduri & Storchova, 2019)).

Centrosome defects: Centrosomes are cellular organelles that serve as microtubule organizing center (MTOC). Each centrosome contains two centrioles aligned in right angle. Every cell contains one centrosome, which is duplicated during the S phase. Maintaining the number of centrosomes is essential for the faithful chromosome segregation (Wong & Stearns, 2003). Centrosome amplification is commonly found in cancers and is known to contribute to tumorigenesis. Centrosome amplification can occur directly through centrosome over-duplication, cell fusion, or due to cytokinesis failure. Cells with supernumerary centrosomes undergo normal chromosome segregation when the centrosomes cluster together to form two spindle poles (Sabat-Pospiech, Fabian-Kolpanowicz, Prior, Coulson, & Fielding, 2019) (Figure 1G). Failure to do so would eventually lead to attachment of microtubules to multiple centrosomes, causing multipolar mitosis. Often, cells with multipolar mitosis are eliminated due to excessive chromosome missegregation. However, cancers with centrosome amplification often suppress multipolar mitosis. HSET, a gene nonessential for cell division in normal cells, was shown to be essential for the suppressing multipolar mitosis in centrosome amplified cancer cells (Kwon et al., 2008). Therefore, drugs targeting HSET could be an ideal therapeutic candidate for targeting cancer with centrosome amplification.

Several *in vitro* and *in vivo* studies showed that mutations or impaired expression of genes involved in SAC, cohesin and centrosome maintenance lead to chromosome missegregation and aneuploidy. However, the mutations affecting these genes are rarely observed in cancers implying that other genes besides the ones involved in mitotic processes could be responsible for generating aneuploidy in cancers. Mutation frequency of SAC genes that exceeds 5% (threshold for frequently mutated genes) was observed only in uterine corpus endometrial carcinoma (UCEC, blue) and colon adeno carcinoma (COAD, red) (Figure. 2).

Further, mutations in different oncogenes and tumor suppressors are known to cause chromosomal instability (reviewed in (Bernardo Orr & Compton, 2013)). Recently, two genome wide screens identified several genes previously not known to be involved in chromosome segregation, to cause aneuploidy

(Conery & Harlow, 2010) (Meena et al., 2015). This, together with observations from cancer studies suggest that diverse pathways could indirectly influence chromosome segregation and cause aneuploidy.

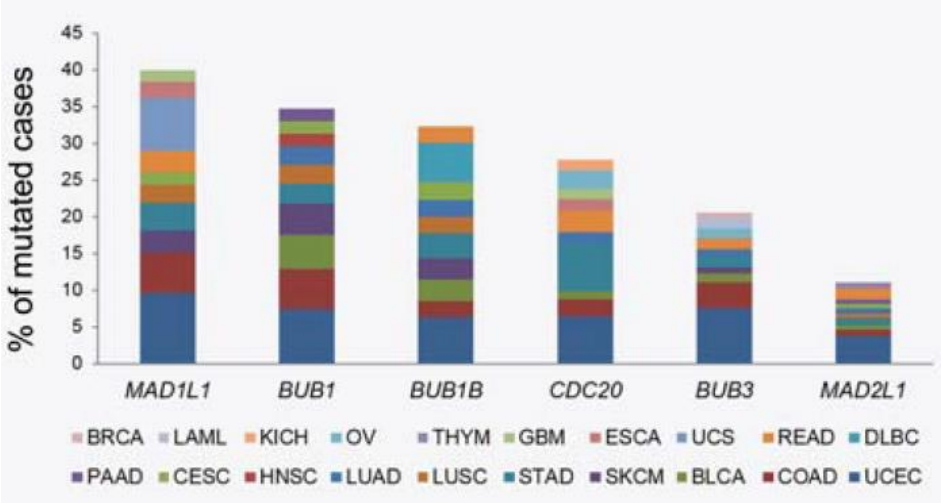

Figure 2. SAC gene mutation frequency distributions across pan-cancer TCGA cohorts. Adapted from (G. Simonetti, S. Bruno, A. Padella, E. Tenti, & G. Martinelli, 2019).

Following chromosome missegregation, the daughter cells with aneuploid karyotypes are often eliminated due to cell cycle arrest or apoptosis. Therefore, mutations in pathways that eliminate aneuploid cells could also increase aneuploidy levels. For example, tumor suppressor gene *TP53* limits the propagation of cells following chromosome missegregation. Consistently, tumors with *TP53* mutations are highly aneuploid (Lopez-Garcia et al., 2017). Frequent loss of heterozygosity and mutations in *BCL9L* was frequently observed in aneuploid tumors. Consistently, loss of *BCL9L* promoted tolerance to chromosome missegregation events (Lopez-Garcia et al., 2017). Therefore, identification of genes responsible for causing aneuploidy and facilitating survival would help to understand the how cancers survive despite being highly aneuploid.

1.3 Model systems to study aneuploidy and its consequences

Over the last decade, several labs were indulged in understanding the cellular consequences of aneuploidy due to its ubiquitous occurrence in diverse cancers. Several models had been employed by various laboratories to understand aneuploidy. Currently, there are two main approaches used. As a first approach, aneuploidy can be induced by mutating genes involved in chromosome segregation or using drugs affecting chromosome segregation in cell culture, specific tissues or whole organism (Santaguida et al., 2017) (Soto et al., 2017) (Ohashi et al., 2015) (Babu et al., 2003; Iwanaga et al., 2007; Jeganathan et al., 2007; Kalitsis et al., 2005; Schliekelman et al., 2009) (Figure 3A). Further, sporulation of odd ploidy

yeast strains produces strains with variable aneuploid progeny (Y. Chen et al., 2019; Tsai et al., 2019) (Figure 3H). While these approaches generate aneuploidy very robustly, the cell populations derived from these approaches are very heterogeneous, both genetically and phenotypically. These models allow to study the immediate consequences of chromosome missegregation. However, it is difficult to comprehend whether the observed phenotypes are because of aneuploidy itself or due to secondary changes caused by the treatment. Furthermore, the identity and number of chromosomes lost or gained cannot be known.

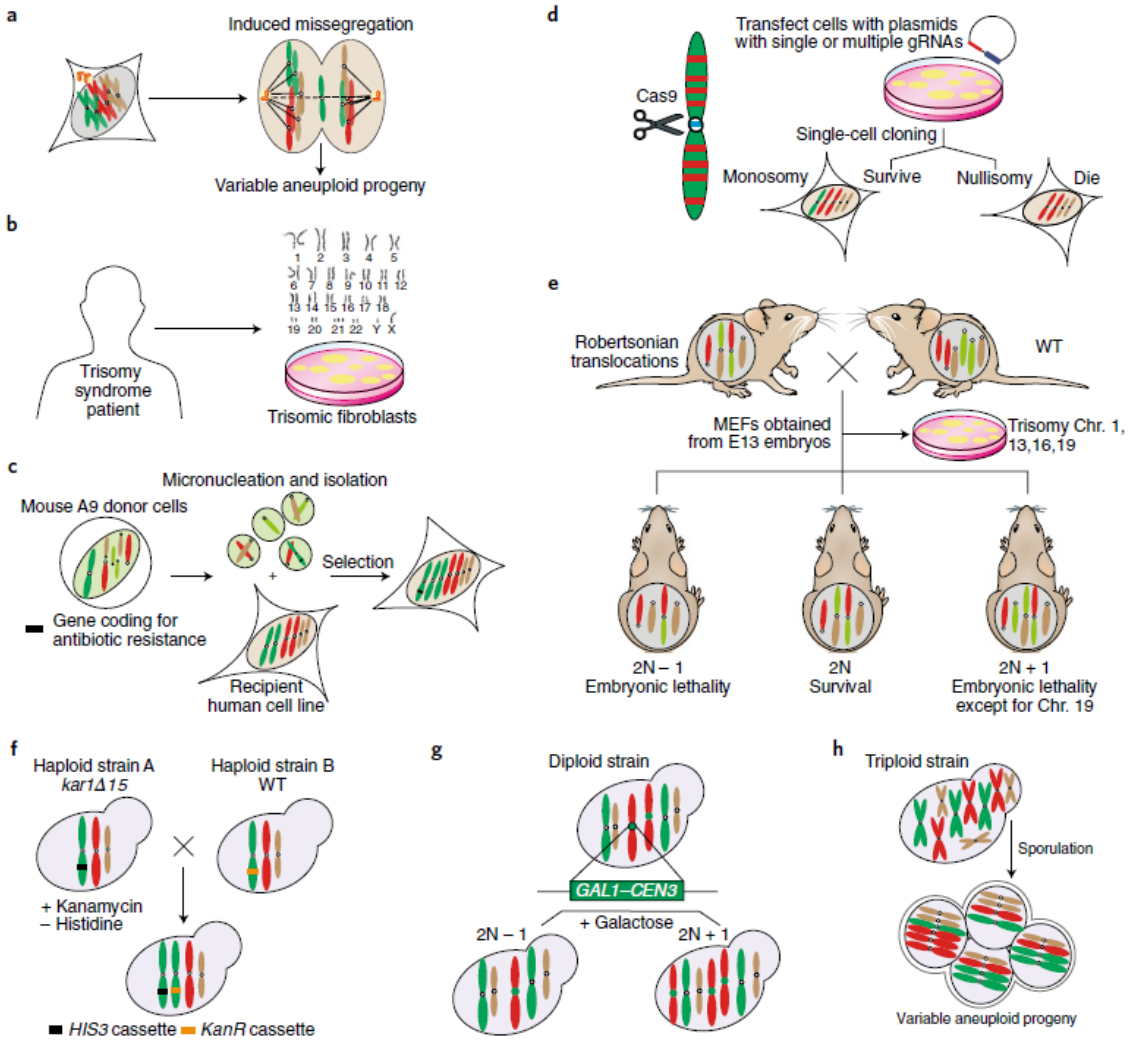

Figure 3. Model systems to understand consequences of aneuploidy. A. Chromosome missegregation can be induced by genetic manipulation of genes involved in chromosome segregation or drugs inhibiting the processes involved in chromosome segregation **B.** Primary cells obtained from different trisomy patients can be cultured *in vitro*. **C.** Micronuclei mediated chromosome transfer. Mouse donor cells harboring human chromosome are treated to induce micronuclei. Micronuclei are isolated and fused to the recipient cells. The recipient cells are treated with respective antibiotics to select for clones that received the chromosome. **D.** CRISPR-Cas9 can be used to delete an

entire chromosome or its part. Guide RNAs (gRNAs) are designed to target multiple parts of the chromosome or at the centromere. Viable single cell clones are verified either by FISH, PCR or by whole genome DNA sequencing. **E.** Wild type mice mates with mice harboring Robertsonian translocations. The resulting littermates are either monosomic, diploid or nullisomic. Embryos from E13 can be used to obtain mouse embryonic fibroblasts. **F.** Disomic yeast strains can be obtained by mating a haploid strain carrying a *kar1* mutation with a wild type strain. The mutation of Kar1 interferes with nuclear fusion and some chromosomes are randomly missegregated. The disomic strains can be selected using various selection markers. **G.** Conditional disruption of transcriptional activity at the centromere induces chromosome missegregation. Knocking in the *GAL1-CEN3* cassette into the desired chromosome allows for missegregation of selected chromosome. **H.** Sporulation of odd ploidy yeast strains, such as triploid and pentaploid, produces progeny with variable aneuploidy. (Adapted from (Chunduri & Storchova, 2019)).

The aim of the second approach is to generate aneuploidy models with a defined karyotype, such as a gain or loss of a defined chromosome. This approach allows comparison with an isogenic control that differs only by the defined chromosome(s). This approach is used particularly to study the changes caused by the chromosome copy number deviations.

So far, various techniques were used to obtain defined aneuploidy models. For example, in humans, chromosomal gain cell lines were generated using micronuclei mediated chromosome transfer (Fournier & Ruddle, 1977; Stingele et al., 2012) (Figure 3C), and chromosome loss cell lines using CRISPR mediated chromosomal deletions (He et al., 2015; Zuo et al., 2017) (Figure 3D). Further, cell lines can be obtained from the patients of different trisomy syndromes (Figure 3B). Mating mice carrying Robertsonian translocation with wild type mice generates viable aneuploid mice, although majority of the chromosomal gains and losses are embryonically lethal, except for chromosome 19 (Gropp, Kolbus, & Giers, 1975; Williams et al., 2008). However, it has been possible to obtain mouse embryonic fibroblasts from aneuploid embryos. In yeast, various genetic methods were used to generate aneuploid strains (Figure 3E). First, haploid yeasts carrying mutation in *KAR1* were mated with a WT strain. *KAR1* mutation interferes with nuclear fission during mating resulting in random transfer of chromosomes. Further, presence of a selection marker allows for the selection of strains with defined karyotype. In this way, several yeast disomic yeast strains were generated (Pavelka et al., 2010; Torres et al., 2007) (Figure 3F). Alternative approaches involve interfering with the transcription of centromere that disturb the microtubule-kinetochore attachments, thereby generating population of cells that gained or lost one defined chromosome (Beach et al., 2017) (Figure 3G). These model systems have significantly helped to improve our understanding of the consequences of aneuploidy. They also provided insights into the role of aneuploidy in cancers. Below, I will summarize the diverse consequences of aneuploidy.

1.4 Multiple consequences of aneuploidy

The advent of various model systems of aneuploidy elaborated the understanding of the consequences of aneuploidy. In particular, these systems helped to differentiate what the immediate consequences of chromosome missegregation (acute aneuploidy) are in comparison to the chronic or long-term effects of aneuploidy (chronic aneuploidy). While most of the consequences of aneuploidy are exhibited by both acute and chronic models as discussed below, the cells immediately after chromosome segregation activate different stress pathways.

1.4.1 Immediate consequences of chromosome missegregation

The immediate consequences of chromosome segregation errors are often severe and it is difficult to differentiate if they arise due to DNA damage during chromosome missegregation or due to the arising aneuploidy. Several independent studies addressing the immediate consequences of chromosome segregation errors showed that the guardian of genome, tumor suppressor protein TP53 was activated in response to chromosome segregation errors (Janssen, van der Burg, Szuhai, Kops, & Medema, 2011; M. Li et al., 2010; Ohashi et al., 2015; Santaguida et al., 2017; Soto et al., 2017; Thompson & Compton, 2010) (Figure 4). However, the triggers of the p53 activation remains unclear.

One study suggested that the missegregated chromosomes were frequently damaged during cytokinesis and subsequently activates p53 through ATM/CHK2 axis (Janssen et al., 2011). However, in another study, chromosome missegregation induced by monastrol or by depletion of the mitotic centromere-associated kinesin (MCAK) was shown to activate p53 by the p38 stress pathway and not by DNA damage, since no accumulation of γH2AX foci that marks the DNA damage was observed (Thompson & Compton, 2010). Similarly, MEFs derived from the spindle assembly checkpoint deficient mice models showed increased p53 levels, but no increase in DNA damage was observed. However, they observed an increased reactive oxygen species (ROS) following chromosome missegregation (M. Li et al., 2010). Increased ROS levels results in oxidative DNA damage and activates both ATM and p53. Nonetheless, an important limitation from all these studies was that the chromosome missegregation was induced by compounds that interfere with microtubule dynamics or microtubule-kinetochore attachment, which eventually activate SAC, prolong the mitosis. Interestingly, cells arrested in mitosis exceeding 100 min induced p53 irrespective of the cells missegregating a chromosome or not (Orth, Loewer, Lahav, & Mitchison, 2012; Uetake & Sluder, 2010, 2018). Therefore, it is difficult to distinguish whether p53 was activated by prolonged mitosis, or chromosome missegregation and its outcomes, such as DNA damage or aneuploidy.

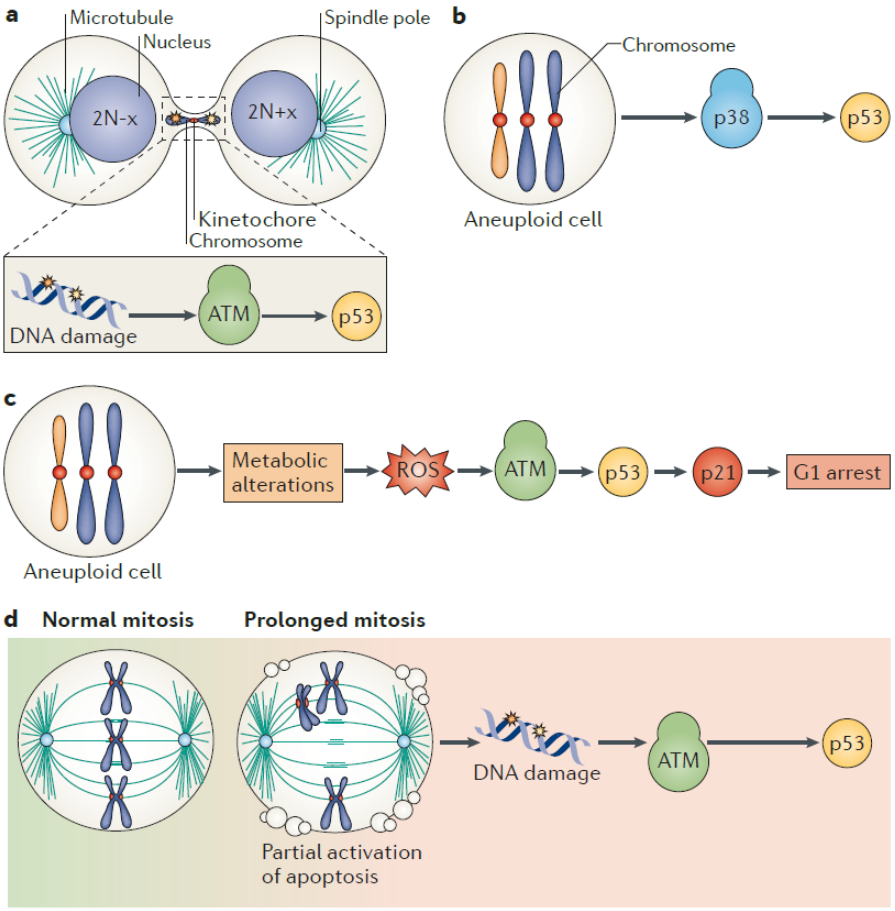

Figure 4. Immediate consequences of chromosome missegregation. A. Lagging chromosome trapped in the cytokinesis furrow is prone to severe DNA damage and activates p53 via ATM and arrest the cells. **B.** Monastrol induced chromosome segregation and aneuploidy was shown to activate p53 through p38 activation. The mechanism for increased p38 activity is unclear. **C.** Metabolic alterations caused by aneuploidy results in increased reactive oxygen species (ROS). ROS is known inducer of oxidative DNA damage which activates p53 through ATM and arrests cells in G1 phase. **D.** The chromosome mis-segregating cells spent longer time in mitosis. Prolonged mitosis partially activates apoptotic pathway and induces DNA damage leading to p53 activation. Adapted from (Santaguida & Amon, 2015).

Keeping these limitations in mind, two recent studies addressed how and what factors determine the activation of p53 following chromosome segregation errors. In both these studies, authors directly altered SAC (for example by using reversine, a SAC kinase MPS1 inhibitor), which accelerates the progression through mitosis despite incorrect spindle attachment. In this way, prolonged mitosis could be excluded as the cause of p53 activation. In one of these studies, using live cell imaging combined with single cell sequencing, the authors identified that about 40% of cells proliferate after chromosome missegregation in spite 80% of these cells being aneuploid. Further, they showed that p53 is not activated in all of the cells following missegregation event. This suggests that the aneuploidy per se does not activate p53 and

arrest all aneuploid cells after missegregation event (Soto et al., 2017). In other study, authors established a technique where they separated the G1 arrested aneuploid cells from the cycling aneuploid cells following chromosome missegregation. Intriguingly, they showed that p53 is activated in G1 arrested cells, but not in the cycling cells. While the arrested and cycling populations are both aneuploid, the percentage of genome changes in arrested cells is much higher than in the cycling cells. These findings confirm that the aneuploidy *per se* does not trigger p53. Another important difference between arrested and cycling cells was that the structural chromosome abnormalities were enriched in arrested cells. Structural chromosome abnormalities arise as a result of DNA damage that occurred during cytokinesis or accelerated anaphase entry or in the micronuclei. Consistently, authors showed that the inactivation of DNA damage checkpoint reduced the G1 arrest, thus suggesting that DNA damage caused during chromosome missegregation is probably the main trigger of the G1 arrest and p53 activation (Santaguida et al., 2017).

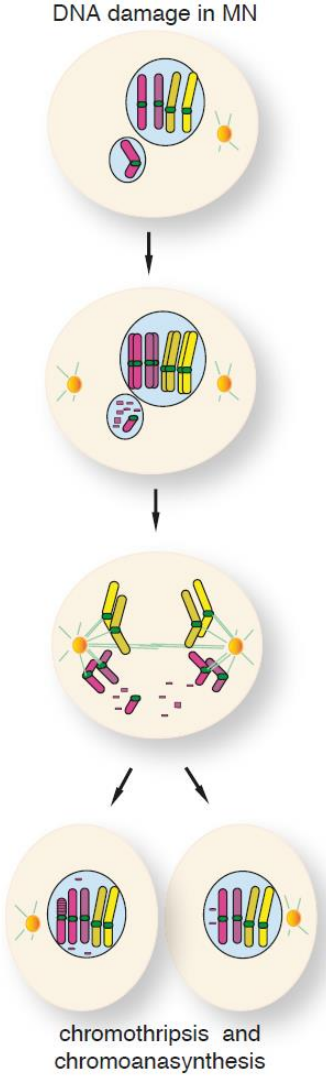

When the cells missegregate chromosomes, the lagging chromosome either eventually joins the rest of the chromosomes or they stay behind and become damaged during cytokinesis or entrapped by the nuclear membrane in a separate body commonly known as “micronucleus”. The chromosomes entrapped in the micronuclei are prone to DNA damage and leads to chromosome shattering, an event known as “chromothripsis” (C. Z. Zhang et al., 2015) (Kneissig, Keuper, et al., 2019) (Figure 5). Why is the DNA in micronuclei prone to DNA damage more than the DNA in regular nuclei? Several studies have shown that the cellular functions such as DNA transcription, replication and repair are impaired in micronuclei (Kneissig, Bernhard, & Storchova, 2019). Part of this defect was attributed to the defective nuclear membrane assembly in micronuclei.

Figure 5. Mechanism of chromothripsis during chromosome missegregation. Missegregated chromosome often lag between the two masses of chromosomes. The lagging chromosome will be enclosed by a nuclear envelope, thus forming a micronucleus. The chromosomes in micronuclei are prone to DNA damage owing to the defects in micronuclei membrane structure, transport and stability. The DNA damage shatters the chromosomes into multiple fragments in a single event causing chromothripsis. Adapted from (Kneissig, Bernhard, et al., 2019).

Immunostaining experiments showed that micronuclei failed to recruit nuclear pore complex proteins and non-core proteins such as lamins. Nuclear lamins are categorized into A-type (A or C) and B-type (B1 and

B2) lamins. A-type lamins form rigid and thick filament bundles and provides mechanical rigidity to the nucleus. B type lamins are rather thin but form highly organized meshwork essential for the integrity of nuclear envelope. Several studies showed that majority of the micronuclei lack lamin B and are prone to spontaneous nuclear membrane collapse. Defective nuclear pore complexes combined with lack of lamin B impairs the transport of proteins essential to maintain cellular functions such as DNA replication and repair, eventually leading to DNA damage (Hatch, Fischer, Deerinck, & Hetzer, 2013; S. Liu et al., 2018; Maass et al., 2018). Recent studies have shown that leaky micronuclear envelope exposes the DNA to cytoplasmic nucleases, which could also damage DNA (Mackenzie et al., 2017).

Taken together, while the DNA damage and p53 activation limit the viability of daughter cells derived from chromosome missegregation event, some cells survive with aneuploidy. In the next chapter, I will discuss the long-term implications of aneuploidy.

1.4.2 Long term impact of chromosome copy number changes

1.4.2.1 Impact of aneuploidy on cell proliferation

From unicellular to multicellular organisms analyzed so far, gain of even a single chromosome affects the cellular proliferation. However, whether the impact is positive or negative depends on the cell type, growth conditions and the karyotype involved. For instance, aneuploid budding yeast, aneuploid mouse embryonic fibroblasts (MEFs) derived from trisomic mice, human aneuploid cells derived from micronuclei mediated chromosome transfer and patient derived cell lines proliferate slower than their respective diploid controls (Beach et al., 2017; Segal & McCoy, 1974; Stingele et al., 2012; Torres et al., 2007; Williams et al., 2008). The slower proliferation was attributed to a delay in the G1-S transition of cell cycle. Aneuploidy induced in drosophila neural stem cells by genetic manipulation of spindle assembly checkpoint proteins *Mad2, Bub3* and centriole kinase *Sak* caused a delay in G1 phase of the cell cycle leading to pre-mature differentiation (Gogendeau et al., 2015). However, what determines the proliferation defect caused by aneuploidy is unclear. Interestingly, studies in yeast showed that the proliferation defect correlate with the amount of extra DNA content. Consistently, human tetrasomic cells for chromosome 5 proliferate much slower than trisomy of the chromosome 5. Is the extra DNA amount responsible for the proliferation defects? Yeast transcriptional machinery cannot support transcription of human and mouse genes. Budding yeast engineered to harbor artificial chromosome containing human and mouse DNA, which cannot be transcribed, did not suffer from the proliferation defects (Torres et al., 2007). These findings suggest that increased expression of genes from the extra chromosome is responsible for the proliferation defects caused by aneuploidy and not the extra DNA *per se*. In line with this, human aneuploidy syndromes of chromosome X, trisomy of X (Triple X syndrome) or monosomy of

X (Turner syndrome) affecting females, and XXY (Klinefelter syndrome) affecting males have lesser pathological consequences compared to other aneuploidy syndromes. Although they carry extra DNA content, the transcriptional activity from the extra X chromosome is silenced by non-coding RNA XIST. This is because in females, the gene expression of chromosome X is active only on one copy of the X chromosome. The expression of the second chromosome is silenced by long non-coding RNA XIST. In cells with extra chromosome X, all the extra copies are silenced by similar mechanism; therefore, the subsequent cellular phenotype is rather mild. Similarly, both transcriptional silencing and removal of extra chromosome 21 from the Down syndrome derived induced pluripotent stem cells (iPSCs) rescued the proliferation defects (Jiang et al., 2013; L. B. Li et al., 2012). Together, these findings suggest that the increased expression of genes from supernumerary chromosome is responsible for the observed defects caused by aneuploidy.

If the proliferation defects are indeed caused by increased gene expression, then what genes are responsible for it? Is it caused by the increased expression of a few detrimental genes or is it a combined effect of copy number changes of several genes that are not harmful when expressed individually? A genome wide study aimed to identify genes that limits the cell proliferation when present in excess copies identified 55 genes (dosage sensitive genes, DSG) that are not tolerated when expressed more than five copies (Bonney, Moriya, & Amon, 2015). However, expression of individual DSG in wild type haploid strain to the levels comparable to yeast aneuploid strains did not recapitulate the proliferation defects observed in aneuploid yeast strains. Further, depletion of individual DSGs in the aneuploid strains to the levels in wild type could not rescue the proliferation defect. Together, these finding suggest that the proliferation defect in aneuploidy is not caused by altered expression of a few DSGs, but a compound effect of several genes (Bonney et al., 2015).

Although it is evident from several studies that altered gene expression from supernumerary chromosome is responsible for proliferation defects, mechanistically, it is unclear what determines the proliferation defect. Several stresses associated with aneuploidy, such as proteotoxic stress and genotoxic stress (discussed below) are known to interfere with the G1-S transition of cell cycle. It is plausible to think that these stresses could be responsible for the proliferation defects. However, the specific responsible mechanism remains to be identified. Interestingly, loss of chromosome (monosomy) also impairs the proliferation negatively. Arm level depletion of chromosome 3 in human cells and whole chromosome loss in diploid yeast strains slowed the proliferation (Beach et al., 2017; Taylor et al., 2018). This impairment is probably due to the gene haploinsufficiency, where one copy of gene is not sufficient for cell viability, and a compound effect of loss of several genes.

In contrast, aneuploidy was shown to be beneficial under stressful conditions. For instance, *Candida albicans*, most prevalent human fungal pathogen, acquires resistance to anti-fungal drug fluconazole by becoming aneuploid (Selmecki et al., 2006). Aneuploidy provided growth advantage to cells that were grown in non-standard growth conditions such as hypoxia and cytotoxic drugs such as cisplatin, 5-fluorouracil etc., (Kuznetsova et al., 2015; Replogle et al., 2020; Rutledge et al., 2016). Cancer cells that can survive in diverse growth conditions are highly aneuploid. Aneuploidy is often observed in naturally occurring yeast strains (Hose et al., 2020; Hose et al., 2015) (Duan et al., 2018). Additionally, the impact on proliferation depends also on the identity of the chromosome. A majority of disomic budding yeast strains progress through G1-S with a delay of 10-20 min, except for the strains with aneuploidies of chromosome 1, 2, 5 and 9 (Torres et al., 2007). These strains do not show any proliferation defect. Trisomy of 12 in human pluripotent stem cells increases proliferation (Ben-David et al., 2014). Thus, although the impact of aneuploidy on the proliferation is largely negative, it depends on the cell type, growth conditions and the specific karyotype.

1.4.2.2 Impact of altered karyotype on the transcriptome and proteome

The detrimental consequences of aneuploidy have been attributed to the altered gene expression from the aneuploid chromosome. Using diverse multi-omics approaches, several studies investigated the gene expression changes caused by aneuploidy. Such studies determined that aneuploidy not only impairs the expression of the genes encoded on the supernumerary chromosome (cis effects), but across the whole genome (trans-effects). In this chapter, I will summarize how aneuploidy impacts the gene expression landscape of a cell.

1.4.2.2.1 Impact of aneuploidy on the gene dosage (cis-effects)

When the cells become aneuploid, does the mRNA and protein levels scale according to the DNA copy number changes? By quantifying global transcriptome and proteome of various aneuploid model systems, several laboratories addressed this important aspect of aneuploidy.

On the transcriptome level, mRNA expression from the supernumerary chromosome correlated closely with the DNA copy number in yeast, genetically engineered human and murine aneuploid cell lines, patient derived cell lines and tissues, *Arabidposis thaliana* and in maize. Further, gene expression analysis of prostate tumors, colon cancer and acute myeloid leukemia with different aneuploidies showed that the mRNA expression largely scales with the DNA levels (Phillips et al., 2001; Pollack et al., 2002; Virtaneva et al., 2001). These findings suggest a lack of general dosage compensation that would buffer the mRNA expression. However, there are few exceptions that mainly effects the sex chromosomes. In humans, the X chromosome is dosage compensated by a long non-coding RNA XIST which transcriptionally silences the

second copy of X chromosome in females. In *Drosophila melanogaster*, the dosage compensation occurs in males, where the transcription of X chromosome is doubled to match the female expression levels. In *Caenorhabditis elegans* that possess XX sex determination system, the gene expression is compensated by reducing to half, resulting in XX being hermaphrodite and XO as males (Ercan, 2015). Interestingly, aneuploidy of autosomes in *Drosophil*a *melanogaster* are compensated transcriptionally. Aneuploidy of chromosome 4 in *Drosophil*a *melanogaster*, which is evolutionarily derived from chromosome X, possess chromosome specific dosage compensation mediated by Painting of Forth (POF) (Y. Zhang et al., 2010) (Stenberg et al., 2009). What determines the dosage compensation of other autosomes remains unclear. Recent investigations revealed that MSL2, a member of male specific lethal complex (MSLc) involved in X chromosome dosage compensation in *Drosophila melanogaster*, regulates also the expression of several dosage sensitive genes encoded on the autosomes (Valsecchi et al., 2018). This suggests that the mechanisms known to be involved in the sex chromosome dosage compensation could regulate the gene expression of the autosomes as well. However, the existence of similar mechanisms in other mammalians remains to be investigated. The autosomal gene expression from aneuploid wild yeast strains was shown to be compensated towards diploid levels, but this observation was disputed owing to the normalization strategies authors employed (Hose et al., 2015; Torres, Springer, & Amon, 2016). *Candida albicans* strains with monosomy 5 and trisomy 4/7b compensated 25-30% of transcripts towards diploid levels (Tucker et al., 2018). Despite these few exceptions, mRNA expression of genes encoded on the aneuploid chromosome scales according to the DNA copy number.

In the recent past, advances in the measurement and quantification of global proteome increased the sensitivity and the accuracy of protein dosage determination. Analysis of aneuploid yeast and human protein abundances by mass spectrometry revealed that, similar to the mRNA levels, majority of proteins scale according to the DNA copy number (Dephoure et al., 2014; Y. Liu et al., 2017; Pavelka et al., 2010; Stingele et al., 2012; Torres et al., 2010; Vigano et al., 2018) (Figure 6). Interestingly, about 20-25% of the proteins encoded on the supernumerary chromosome are compensated towards diploid levels. Further investigation revealed that these proteins are enriched for multi-molecular protein complexes, such as ribosomes, spliceosome etc. (Stingele et al., 2012). The stability of the proteins in multi-molecular subunits is determined by their stoichiometry. When a protein subunit is produced in excess and if it does not integrate into the complex, the unassembled protein is rapidly degraded (Jacob, Brain, Dacie, Carrell, & Lehmann, 1968; Lippincott-Schwartz, Bonifacino, Yuan, & Klausner, 1988; Sung, Reitsma, Sweredoski, Hess, & Deshaies, 2016). This principle underlies the protein attenuation in anueploids (McShane et al., 2016). The attenuation is mediated by ubiquitin-proteasome degradation pathway, as the levels of

attenuated proteins are rescued when the proteasomal degradation is inhibited (Dephoure et al., 2014; McShane et al., 2016). Recently, investigation of complex aneuploid strains derived from pentaploid meiosis proposed an "over dosage hypothesis". This hypothesis suggests that when a subunit protein is present in 3 copies, then other proteins belonging to the complex are increased, leading to an increased expression of the entire complex (balanced). The authors propose that the proportion of balanced complexes and the imbalanced complexes determine the fitness of the organism (Y. Chen et al., 2019). Taken together, the expression of genes encoded on the supernumerary chromosomes scales according to the DNA copy number and the expression of some class of proteins are determined by the balance of individual subunit in multi-protein complexes. Together, these findings suggest the lack of general dosage compensation mechanisms in response to aneuploidy. While a majority of work had been performed using model systems with chromosome gains, whether the gene dosage regulation of cells with chromosome losses remained to be investigated.

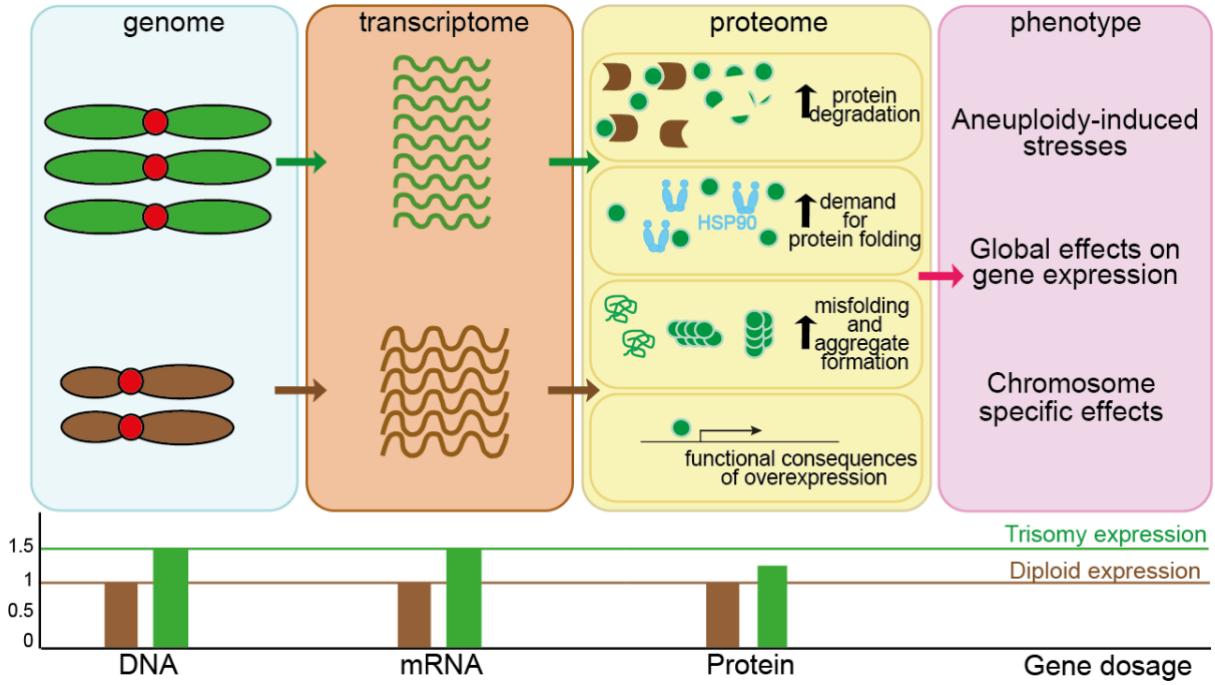

Figure 6. Impact of aneuploidy on the chromosome specific and global gene expression. Schematics show a summary of the impact of aneuploidy on genome, transcriptome, proteome and phenotypes. Gain of chromosome results in increased mRNA and proteins. Increased protein expression burdens protein folding machinery, leading to an increased protein misfolding, aggregation and protein degradation pathways. Further, increased mRNA expression of transcriptional factors encoded on aneuploid chromosome could increase the expression of genes across the entire genome. Combined protein homeostasis defects along with altered gene expression are responsible for inducing diverse phenotypes of aneuploidy. Histogram shows the gene dosage of DNA, mRNA and protein for diploids and aneuploids. Adapted from (Chunduri & Storchova, 2019).

1.4.2.2.2 Impact of aneuploidy on the global gene expression (trans- effects)

Besides the changes in expression of genes encoded on the supernumerary chromosomes, aneuploidy leads to changes in gene expression across entire genome. This may be simply explained by the increased or reduced expression of transcription factors or negative regulators encoded on the aneuploid chromosome which influence the expression of genes on the other chromosomes (Figure 6). In this case, the expression changes should be highly dependent on the chromosomal identity. Although there are chromosomal specific changes, they are not dominant. In contrary, several studies in mammalian and yeast models showed that aneuploidy leads to specific conserved pathway alterations. Intriguingly, these changes are not dependent on the chromosome identify. Aneuploidy in yeast elicits a transcriptional response that was similar to the so-called environmental stress response (ESR). ESR represents a common stress response triggered by environmental stresses such starvation, oxidative stress, heat shock and slow growth (Gasch et al., 2000; Sheltzer, Torres, Dunham, & Amon, 2012; Torres et al., 2007). Human and mouse aneuploid cells displayed consistent upregulation and downregulation of specific pathways. Gene ontology terms associated with DNA and RNA, such as DNA replication, repair, cytosolic ribosome subunits, cell cycle are downregulated in mammalian aneuploid cells (Sheltzer et al., 2012; Stingele et al., 2012) (Durrbaum et al., 2014). Upregulated pathways appear to be more specific to the species. Interestingly, inflammatory response, MHC complex, interferon signaling, lysosomes and autophagy are only observed in human aneuploid cell lines (Stingele et al., 2012) (Durrbaum et al., 2014) (Vigano et al., 2018).

How can aneuploidy of different chromosomes converge into similar stress responses? Studies in yeast suggest that aneuploidy increases cellular energy needs. This may be due to an increased transcription, translation and processing of excess mRNA and proteins. Increased energy demands alter the metabolic processes, leading to an increased concentration of reactive oxygen species which could elicit ESR (Torres et al., 2007) (Williams et al., 2008) (M. Li et al., 2010). Further, increased protein expression from supernumerary chromosome places a burden on protein homeostasis. Aneuploidy overwhelms protein folding and degradation pathways. This increases the chances of protein misfolding and aggregation of misfolded proteins (Oromendia, Dodgson, & Amon, 2012) (Donnelly, Passerini, Durrbaum, Stingele, & Storchova, 2014) (Brennan et al., 2019). Further, increased or reduced expression of dosage sensitive genes caused by aneuploidy reduces cellular fitness. Interestingly, all these individual stresses could alter cell cycle and reduce the cellular proliferation. Together, these findings suggest that altered mRNA and protein abundance caused by aneuploidy impairs various aspects of cellular physiology and elicits unique stress response.

Recently, analysis of yeast aneuploid populations harboring heterogeneous karyotypes suggested that aneuploidy induced a specific transcriptional response that the authors termed “Common Aneuploidy Gene Expression (CAGE)”. Comparison of CAGE with diverse transcriptional response revealed that CAGE positively correlated with transcriptional signatures of stresses such as hypo-osmotic stress, heat shock response, ER stress and metabolic stress. Interestingly, minor overlap of CAGE with ESR was observed with inverse expression changes. Further analysis of yeast and human aneuploid cells confirmed that they experience hypo-osmotic stress, which is responsible for inducing CAGE (Tsai et al., 2019). However, reanalysis of the transcriptome data suggested that CAGE may be a mere artifact of comparing stationary phase control cells with exponential growing aneuploid cells. Since aneuploid cells proliferate slower than the euploid control, control cells reach stationary phase much earlier than the aneuploid cells. Growth in stationary phase is a potent inducer of ESR. When gene expression profiles of exponentially growing control and aneuploid cells are compared, the CAGE signature was no longer evident. In fact, consistent with the previous findings, ESR signature was apparent in aneuploid cells (Terhorst et al., 2020). Since ESR is elicited by diverse stresses and slow proliferating cells, care should be taken while comparing cells with varying cell growth and proliferation to avoid potential artifacts.

In mammalian aneuploid models, although a common stress response was observed, the response differs from ESR. While the mammalian aneuploid cells proliferate slower than the diploid controls, the responses in human aneuploids are not proliferation dependent. Complex aneuploid cell lines that proliferate like diploids elicited similar responses as slowly proliferating aneuploid cells with single chromosome gains (Buccitelli et al., 2017; Durrbaum et al., 2014; Sheltzer et al., 2012). Further, transcriptome profiles of human aneuploid cells were similar to the cells treated with bafilomycin A1 (autophagy) and actinomycin D (DNA and rRNA transcription). No similarities were found with profiles of stresses caused by low or high glucose, hydroxyurea, hydrogen peroxide, hypoxia and nitric oxide (Durrbaum et al., 2014). This suggests that aneuploidy stress response is rather specific and not a common stress response such as ESR. Interestingly, the transcriptome and proteome changes in aneuploid cells were similar to cellular response of protein folding defects. Strong correlation of pathway changes was observed when expression data of aneuploid cells were compared with the expression of cells upon treatment with inhibitors of HSP90 and RNAi of HSF1 (Donnelly et al., 2014). Similarities between aneuploid cells and stresses due to defect in protein homeostasis (synthesis, folding and turnover) suggest that increased protein expression and the resulting burden on proteostasis network could be responsible for the observed transcriptional changes caused by aneuploidy.

Recent investigation of Down syndrome mice models and patient cell lines revealed that trisomy of 21 activates integrated stress response (ISR) and mediates behavioral and neurological abnormalities (P. J. Zhu et al., 2019). ISR is an elaborate signaling pathway activated by diverse stress conditions such as amino acid deprivation, viral infection, hypoxia, glucose deprivation and endoplasmic stress (reviewed in (Pakos-Zebrucka et al., 2016). Irrespective of stress condition, ISR induces phosphorylation of EIF2α and inhibits global protein translation, while allowing the translation of selected stress response genes such ATF4 to aid in cell survival and recovery (Lu , Harding , & Ron 2004). Although ISR was induced by trisomy 21, whether this a general response to aneuploidy or chromosome specific response remains undetermined. Taken together, aneuploidy elicits unique transcriptional signature independent of identity of the chromosome. While some pathways are conserved among different species, certain pathways are deregulated in only certain species. However, the genes responsible for inducing such response remains to be determined.

1.4.2.3 Impact of aneuploidy on protein homeostasis

Protein homeostasis or proteostasis is defined as the balance between the protein synthesis, processing (folding, post-translational processing, trafficking) and degradation (Hipp, Kasturi, & Hartl, 2019). Maintenance of protein homeostasis is essential for the normal functioning of a cell. It is enabled by a complex network of proteins such as chaperones (protein folding machines) and degradation pathways, such as autophagy and ubiquitin and proteasome system (UPS). Any disturbances in proteostasis result in accumulation of misfolded and cytotoxic aggregated proteins or increased degradation of essential proteins (Hipp, Park, & Hartl, 2014). Analysis of aneuploid cells with chromosome gains showed that the increased protein expression from extra chromosomes places additional burden on protein homeostasis network and causes proteotoxic stress (Donnelly et al., 2014; Oromendia et al., 2012) (Figure 6). Proteotoxic stress is manifested by impaired protein folding, increased cytoplasmic aggregation and activation of protein degradation pathways. Consistently, aneuploid yeast, murine and human cells showed increased sensitivity to protein folding inhibitors such 17AAG (HSP90 inhibitor) (Y.-C. Tang, B. R. Williams, J. J. Siegel, & A. Amon, 2011) (Donnelly et al., 2014; Oromendia et al., 2012). Accordingly, increased expression of HSF1, a crucial heat shock protein transcription factor, rescued the increased sensitivity to protein folding inhibitors (Donnelly et al., 2014). Increased dependence of aneuploid cells on chaperones suggest that the function of protein folding machinery is saturated, possibly due to the increased protein expression from extra chromosome. Impaired protein folding and the resulting misfolded proteins form cytoplasmic aggregates (Brennan et al., 2019). In particular, increased accumulation of ubiquitin-positive cytoplasmic foci that mark the proteins targeted for degradation was

observed in human aneuploid cells (Stingele et al., 2012). While any misfolded proteins could be responsible for forming the aggregates, a recent study showed that the proteins encoded on the aneuploid chromosomes that belong to multi-molecular protein complexes form aggregates in disomic yeast and trisomic human cell lines, albeit at a lower level in human cells (Brennan et al., 2019).

Accumulation of misfolded proteins and aggregates is toxic to cellular viability. Therefore, these proteins are often degraded by various mechanisms. Accordingly, aneuploid yeast and human cells are more sensitive to proteasome inhibitor MG132 suggesting they rely on protein degradation mechanisms (Torres et al., 2007) (Donnelly et al., 2014; Ohashi et al., 2015). A genetic screen to identify aneuploidy tolerating mutation discovered a loss-of-function mutation in Ubp6 increases tolerance to aneuploidy in yeast. Ubp6 is a deubiquitinating enzyme, which removes the ubiquitin from the substrates and allows them to escape degradation (Hanna et al., 2006). Therefore, loss of Ubp6 increases protein turnover, possibly helping aneuploid cells to degrade the excess proteins (Torres et al., 2010). Depletion of pleotropic deubiqutinase Ubp3, which is essential for efficient function of UPS pathway, reduced the fitness of aneuploid cells. Depletion of USP10, the human homolog of Ubp3, similarly reduced the fitness of human aneuploid cells (Dodgson, Santaguida, Kim, Sheltzer, & Amon, 2016). These findings together suggest that UPS pathway is essential for the fitness of the aneuploid cells.

Another pathway of protein degradation is autophagy. Human aneuploid transcriptome and proteome pathway analysis revealed increased gene expression of autophagy and lysosome related pathways (Stingele et al., 2012) (Durrbaum et al., 2014). In line with these findings, aneuploid cells are sensitive to inhibitors of autophagy, such as chloroquine (Y. C. Tang, B. R. Williams, J. J. Siegel, & A. Amon, 2011). LC3 foci, marking the autophagosomes and phagolysosomes are significantly increased in aneuploid cells (Stingele et al., 2012). Interestingly, autophagy is robustly induced immediately after chromosome missegregation. Although autophagosomes accumulate after chromosome missegregation, the capacity of lysosomes to degrade the cargo is not increased, leading to an activation of lysosomal stress pathway mediated by nuclear translocation of the lysosomal transcription factor TFEB (Santaguida, Vasile, White, & Amon, 2015). Whether the cells with chronic aneuploidy adapt and increase lysosomal activity to degrade the lysosomal cargo remains to be investigated. Of note, increased autophagy is evident only in mammalian aneuploid cells and is not observed in disomic yeast. This suggests that the trigger for the activation of autophagy could be species dependent. Identification of autophagy cargo in aneuploid cells should determine the underlying species specificity of autophagy activation.

1.4.2.4 Impact of aneuploidy on genomic stability

Aneuploidy is one of the hallmarks of cancer (Hanahan & Weinberg, 2011). Aneuploidy in cancers is associated with chromosomal instability (CIN), a process of ongoing chromosome losses and gains. Along with whole chromosome aneuploidy, cancers often possess structural aneuploidy that suggests ongoing defects in DNA replication and repair, collectively called genomic instability (GIN). Aneuploidy and genomic instability are observed during the early stages of tumorigenesis. It is believed that they help during the progression of tumors by generating and selecting beneficial mutations (Davoli et al., 2013) (Sansregret & Swanton, 2017). However, the origin of aneuploidy and GIN in cancer is still unclear and it is unknown whether the aneuploidy is causing GIN, or vice versa. Studies comparing the disomic yeast strains (*S. cerevisiae*) with isogenic controls revealed that presence of even one extra chromosome increases chromosome missegregation events and mutation rate. Disomic strains displayed increased accumulation of Rad52 foci, a marker of DNA damage and homologous recombination. Accordingly, aneuploid strains are sensitive to DNA damaging agents such as hydroxyurea and phleomycin. Similar findings were observed in aneuploid strains obtained in fission yeast *Schizosaccharomyces pombe,* as well as monosomic strains obtained from diploid budding yeast (Beach et al., 2017; Sheltzer et al., 2011).

Human aneuploid cells carrying one or two extra chromosomes displayed increased DNA damage and pre-mitotic errors, such as anaphase bridges and ultrafine bridges suggestive of defects in DNA replication and repair. Consistently, human aneuploid cells accumulated markers of replication stress including increased phosphorylation of RPA32 (Ohashi et al., 2015; Passerini et al., 2016; Santaguida et al., 2017). Aneuploid budding yeast accumulated Rad52 foci during the S phase suggesting problems in DNA replication. Interestingly, aneuploid cells often entered mitosis with persisting DNA damage (Blank, Sheltzer, Meehl, & Amon, 2015). Such damage provides a substrate for chromosomal rearrangements including chromosome deletions and translocations. Accordingly, 53BP1 containing nuclear bodies in cyclin-A negative G1 cells were elevated in human aneuploid cells (Passerini et al., 2016). 53BP1 foci mark the unrepaired replication-induced DNA damage that persists through mitosis (Lukas et al., 2011). Aneuploidy also results in replication stress at telomeres in human primary fibroblasts and murine hematopoietic stem cells (Meena et al., 2015). Interestingly, replication stress was shown to play an important role in generation of numerical and structural aneuploidy in cancer (Burrell et al., 2013). Therefore, current evidence implies the cooccurrence of replication stress, CIN and GIN in cancers.

What are the mechanisms underlying replication stress in aneuploidy? Current evidence from studies in aneuploidy yeast and human cells points to increased and unbalanced protein expression from supernumerary chromosome as a reason for replication stress. Yeast strains harboring yeast artificial

chromosome (YAC) with human DNA does not display increased DNA damage and sensitivity to genotoxic drugs, despite having comparable amount of extra DNA (Sheltzer et al., 2011; Torres et al., 2007). This suggest that the excess DNA *per se* is not responsible for observed defects. Interestingly, the expression of MCM2-7 helicase complex along with many other important proteins essential for replication are strongly downregulated in both acute and chronic aneuploidy (Ohashi et al., 2015; Passerini et al., 2016). Rescue of MCM levels attenuated the DNA damage, suggesting that the downregulation of these factors is responsible for DNA damage in human aneuploids (Passerini et al., 2016). Whether the downregulation of these proteins is a direct consequence of aneuploidy or a side effect of one of the other consequences of aneuploidy such as proteotoxic stress remains to be investigated.

1.4.2.5 Impact of aneuploidy on immune responses

Among the pathways altered in mammalian aneuploid model cell lines, GO terms related to type I interferon response and MHC complex were consistently upregulated. Increased expression of different factors involved in interferon signaling and response, such as IFIT1, OASL, OAS2, OAS3 and STAT1 was observed in aneuploid cells derived from HCT116, RPE1 and DLD1 cell lines (Durrbaum et al., 2014; Stingele et al., 2012; Vigano et al., 2018). Recent study observed an increased expression of pro-inflammatory cytokines and NK2D ligands in senescent complex aneuploid cell lines. These arrested aneuploid cells were further eliminated by natural killer (NK) cells (Santaguida et al., 2017). Pro-inflammatory cytokines along with many other genes are highly expressed in senescent cells, a signature commonly termed senescence associated secretory phenotype (SASP) (Coppe, Desprez, Krtolica, & Campisi, 2010). Interestingly, the gene expression in arrested aneuploid cells resembled SASP. Therefore, it is difficult to distinguish whether the increased expression in cytokines and NK cell mediated elimination is due to the senescence or due to aneuploidy itself. In a follow up study, the authors showed that pro-inflammatory cytokine signature and NK-cell mediated elimination was not specific to senescent aneuploid cells, but also for proliferating aneuploid cells. Further, they showed that NF-κB was responsible for eliciting the inflammatory response in aneuploid cells immediately after chromosome missegregation (R. W. Wang, Viganò, Ben-David, Amon, & Santaguida, 2020).

Interestingly, transcriptome analysis of cell lines derived from Down syndrome (DS) patients showed increased interferon responses (Sullivan et al., 2016). Consistently, proteomics approach identified increased levels of circulating pro-inflammatory cytokines, such as IL-6, IL-22, TNF-α and MCP-1, in blood samples from DS individuals (Sullivan et al., 2017). These molecular changes resemble chronic immune system deregulation and auto-inflammation. Several genes involved in immune control are encoded on chromosome 21, including 4 of the 6 interferon receptor subunits: IFNAR1, IFNAR2, IFNGR2 and IL10RB.

The frequent deregulation of immune response in DS patients has been previously attributed to upregulation of these genes in DS patients (Raz, Cheung, Ling, & Levy, 1995). Similarly, trisomy of chromosome arm 9p is associated with systemic lupus erythematosus and an increased expression INFa/b and IFN receptor signaling, possibly due to the increased expression INF cluster genes encoded on chromosome 9 (Zhuang et al., 2006). While the interferon response in these patients has also been attributed to the genes encoded on chromosome 9 and 21, recent work on aneuploid model systems suggest that activation of immune pathways is a general response to aneuploidy.

How aneuploidy per se can activate immune responses? Genomic instability and DNA damage caused by aneuploidy could explain the observed immune pathway activation in aneuploid cells. DNA is normally compartmentalized in the nucleus and mitochondria. Aberrant presence of foreign DNA in the cytoplasm, for example during infection, elicits robust immune responses. Initially discovered as a protein detecting cytoplasmic viral DNA, cyclic GMP-AMP synthase (cGAS) was recently identified to recognize double stranded DNA when present in cytoplasm (Sun, Wu, Du, Chen, & Chen, 2013). Once bound to dsDNA, cGAS converts ATP and GTP into a cyclic dinucleotide GMP-AMP (cGAMP). cGAMP then binds to stimulator of interferon genes (STING) and induces transcription of genes encoding type I IFNs and pro-inflammatory cytokines through IRF3 and NF-kB (H. Ishikawa & Barber, 2008; H. Ishikawa, Ma, & Barber, 2009; Motwani, Pesiridis, & Fitzgerald, 2019; Wu et al., 2013). Interestingly, genomic instability, DNA damage and replication stress were shown to increases cytoplasmic DNA in the form of cytoplasmic DNA speckles or micronuclei (Hartlova et al., 2015) (Shen et al., 2015) (Erdal, Haider, Rehwinkel, Harris, & McHugh, 2017) (Hatch et al., 2013) (Mackenzie et al., 2017) (Bartsch et al., 2017). Aneuploidy causes genomic instability, replication stress and increased cytoplasmic DNA levels (Sheltzer et al., 2011) (Passerini et al., 2016) (Vigano et al., 2018). Therefore, it is plausible to hypothesize that increased DNA damage and cytoplasmic DNA by aneuploidy activates immune response by cGAS-STING pathway. However, the direct link remains to be established.

These studies suggest that aneuploidy incites innate immune activation. However, cancers with a whole chromosome and arm level SCNAs are associated with escaping immune response (Davoli, Uno, Wooten, & Elledge, 2017). Therefore, aneuploid tumors must bypass and adapt to immune activation caused by aneuploidy. Given the important role of cGAS-STING in eliciting immune response, one could assume that loss-of-function mutations or inactivation of this pathway would be a way to adapt by the tumor cells. Analysis of large-scale cancer genome datasets revealed that the mutations in cGAS (0.6%) and STING (0.5%) are rare in cancer (S. F. Bakhoum & Cantley, 2018). SCNA of these genes are also rare, and on the contrary, they are often amplified. Interestingly, activation of cGAS-STING pathway is required for the

metastasis of CIN tumors (S. F. Bakhoum et al., 2018). Therefore, the impact of cGAS-STING pathway on immune activation to promoting tumors is highly dependent on the context. Potential factors determining the fate of cGAS-STING in promoting metastasis vs immune activation is an interesting aspect to investigate in future.

1.5. Monosomy and its occurrence

Monosomy is a state when cells lose one whole chromosome or an arm of a homologue pair. The occurrence of whole chromosomal loss in whole organisms is very rare, as the embryos die during the early stages of embryonic development. Turner syndrome, which occurs due to a loss of chromosome X in females, is the only exception. Since one copy of chromosome X is silenced in healthy females anyway, the loss of second copy does not lead to severe defects compared to loss of autosomes (Kesler, 2007). Partial fetal monosomy of autosomes, where only part of chromosome is lost, is observed during the clinical pregnancy (Watson, Marques-Bonet, Sharp, & Mefford, 2014). Interestingly, chromosome losses are better tolerated by uni-cellular organisms such as *Saccharomyces cerevisiae* or in pathogenic fungi *Candida albicans.* The impact of the loss on the viability and pathological consequences depends on the size and identity of the chromosome, and the genes encoded on the missing fragment.

The knowledge about the consequences of monosomy is very scarce due to the lack of defined model system for studying monosomy. Murine embryos with chromosome loss die significantly earlier than the trisomies (Magnuson et al., 1985). Although the monosomy and trisomy arise at similar frequency in human pre-implantation embryos, the generation of iPSC from these embryos showed a clear bias against the growth of autosomal monosomies. The viability for trisomic iPSC differed with chromosome, but none of the monosomic iPSC were viable except for chromosome X (Biancotti et al., 2012). Similarly, a study aimed to determine the extent of post-implantation development of human embryos for common aneuploidies identified that trisomy 21 embryos develop similar to diploid embryos, whereas monosomy 21 embryos exhibited higher rates of developmental arrest (Shahbazi et al., 2020). Although the underlying reasons for the lethality of monosomic condition is unknown, it is believed that the haploinsufficiency of genes essential for the viability might be contributing to the lethal effects of the monosomy. Moreover, chromosome loss is also associated with unmasking of recessive mutations (Egloff et al., 2018; Kuechler et al., 2010; Schwartz et al., 2018). Mutations are considered recessive when both alleles have to be mutated (homozygous) for the mutant phenotype to be observed. Heterozygous recessive mutation usually does not result in a phenotype, since a second functional allele can compensate for the mutated allele. However, in rare cases, heterozygous occurrence can display a specific phenotype. This can occur when deletion of normal chromosome leads to a loss of the wild type allele, thereby

exposing the recessive mutated allele. In these cases, the arising phenotype is a consequence of a loss of chromosomes and the genes encoded on the lost DNA, and/or due to the expression of recessive mutant allele.

Strikingly, loss of a whole chromosome or arm is frequently observed in cancers. For example, 1p deletion is often found in neuroblastoma (Gilbert, Balaban, Moorhead, Bianchi, & Schlesinger, 1982) (Kushner & Cheung, 1996) (Attiyeh et al., 2005), 3p deletion in lung tumors (Taylor et al., 2018), and the loss of 7 or 7q in myeloid leukemia (Hasle et al., 2007) (Honda, Nagamachi, & Inaba, 2015; Hosono et al., 2014; Will & Steidl, 2014) suggesting an important role of these chromosome abnormalities in tumorigenesis. However, the exact role of these chromosome abnormalities is not clear.

How are tumors able to survive monosomy, when the similar state is embryonically lethal? One possibility is that the loss of chromosome causes haploinsufficiency of tumors suppressor genes, thereby promoting tumor growth. For example, loss of 17p is frequently observed in a broad spectrum of tumors. This frequent occurrence was attributed to the loss of TP53, a crucial tumor suppressor gene. However, depletion of 17p in human cells identified several other tumor suppressor proteins that are contributing to TP53 loss in generating more aggressive tumors (Y. Liu, Chen, et al., 2016). Therefore, factors helping the tumors to survive with monosomic karyotype could act as potential therapeutic targets.

Previously, targeted elimination of chromosomes was performed using two methods. In one approach, targeted chromosome deletion was achieved by inserting oppositely oriented loxP sites. Cre mediated sister chromatid recombination in G2 and S phase generates dicentric or nullicentric chromosomes. These aberrant chromosomes are then eliminated during cell division (Ramirez-Solis, Liu, & Bradley, 1995) (Lewandoski & Martin, 1997). In the second approach, TKNEO fusion construct was inserted into one copy of chromosome (L. B. Li et al., 2012). TKNEO expression allows both positive and negative selection. Neomycin resistance can be used to select for the insertion of the gene and TK can be used for negative selection. In the presence of ganciclovir used for TK selection, cells that lost the thymidine kinase (TK) gene would survive. In this way, it is possible to obtain clones which survived in the presence of ganciclovir because they lost a chromosome where the TK gene was integrated. While these approaches can in principle eliminate a chromosome, they are quite laborious and the efficiency of obtaining clones with chromosome loss is very low. With the recent developments in CRISPR/Cas9, it became possible to delete the chromosome in a targeted manner. So far, CRISPR/Cas9 was used to eliminate additional chromosomes in cancer cell lines, aneuploid mouse embryonic stem cells with extra human chromosome, human induced pluripotent stem cells with trisomy 21 and sex chromosomes in cultured cells, embryos, as well as tissues *in vivo* (He et al., 2015; Taylor et al., 2018; Zuccaro et al., 2020; Zuo et al., 2017). Whether

it is possible to deplete one chromosome from a diploid cell needs to be validated. Attempts were made to understand the transcriptional consequences of chromosome loss using aneuploid blastocyst. Loss of chromosome resulted in reduced expression of genes encoded on the lost chromosomes but also deregulated the gene expression genome wide (Licciardi et al., 2018). However, the biggest limitation of this study is that the monosomic blastocyst are compared to genetically diverse diploid blastocyst. Therefore, studies comparing the genetically matched monosomy and diploid could provide a better understanding of cellular consequences to chromosome losses.

1.5.1 Monosomy and haploinsufficiency

The adverse effects of whole chromosomal monosomy and microdeletions were mainly attributed to the haploinsufficiency (HI) of genes encoded on the monosomic chromosome. The term haploinsufficiency describes the intolerance due to a loss of one allele in a diploid organism. The cells lose the function of one allele by various mechanisms. A) mRNA and protein expression at lower than diploid levels due to deletion of one allele (by chromosome loss) or due to the loss of function mutation; B) Reduced mRNA and protein stability, or C) Impaired translational control. Not every gene loss in the genome causes HI. In fact, high-throughput screens in budding yeast identified only about 3% (180 genes) of genes in entire genome to be haploinsufficient under normal growth conditions. This number increases up to 20% when the yeasts were grown in limited nutrient conditions (Deutschbauer et al., 2005). Similarly, high-dimensional single-cell morphological characterization of heterozygous yeast deletion strains revealed haploinsufficient phenotypes for more than half of 1,112 essential genes under normal growth conditions. Further, 40% of genes that did not show any phenotype under normal growth conditions exhibited HI under severe growth conditions (Ohnuki & Ohya, 2018). Together, these findings suggest that a gene loss that does not cause a phenotype under normal physiological conditions could display HI under stress conditions. In humans, approximately 300 genes were identified to be haploinsufficient and linked to many pathological conditions including cancer, developmental and neurological disorders and mental retardation (Dang, Kassahn, Marcos, & Ragan, 2008; Seidman & Seidman, 2002). Many of these genes belonged to various essential cellular processes such transcription, translation, cell cycle, development etc. Further, computational analysis predicts that the number of haploinsufficient genes could be much higher (Huang, Lee, Marcotte, & Hurles, 2010).

Why a dosage reduction of a few genes across entire genome causes HI? Two models have been proposed to explain the occurrence of HI. First is insufficient amount hypothesis (Figure 7A) which suggest that loss of one allele leads to reduced protein levels, thereby affecting the downstream functions of the protein (Veitia, 2002). A classic example for this hypothesis are transcription factors (TF). Reduced amount of TFs

could subsequently reduce the expression of its targets genes. For example, loss of function mutation in gene encoding homeobox transcriptional factor NKX2-5 impaired binding of NKX2-5 to DNA and resulted in haploinsufficiency, as documented by its association with different human congenital heart diseases (Schott et al., 1998). Similarly, haploinsufficiency of a zinc finger transcriptional factor GATA-4 caused by interstitial deletion of chromosome region 8p23.1 contributes to congenital heart diseases (Pehlivan et al., 1999). Haploinsufficiency of various other transcriptional factors and regulators has been associated with diseases (Seidman & Seidman, 2002). Haploinsufficiency of receptor and transduction molecules, such as RET and LIS-I, are associated with Hirschprung disease (Edery et al., 1994; Romeo et al., 1994) and Miller-Dieker syndrome, respectively (Reiner et al., 1993).

Second model is referred to as the dosage balance hypothesis (Figure 7B), where the haploinsufficiency is caused by disturbances in stoichiometry of multi-protein complexes (Papp, Pal, & Hurst, 2003). A classic example for dosage balance hypothesis is haploinsufficiency of ribosomal subunit genes (discussed in next chapter).

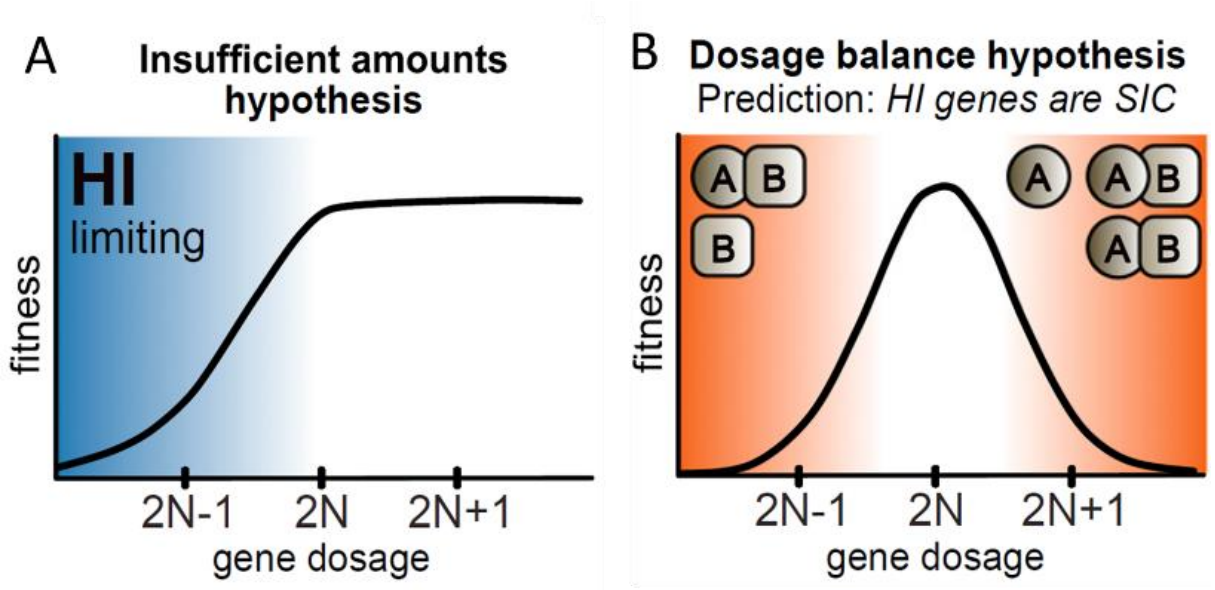

Figure 7. Models of haploinsufficiency. A. Insufficient amount hypothesis: Reduced expression of HI genes impairs cellular fitness in dose dependent manner. However, this model predicts that increased expression does not impact cellular fitness. **B.** Dosage balance hypothesis HI genes impairs cellular fitness when expressed at lower levels and at higher levels as well. HI-Haploinsufficiency, SIC- Sensitive to increased copy number. (Adapted and modified from (Morrill & Amon, 2019))

Loss of even one ribosomal gene significantly impairs the ribosome stoichiometry and impairs cellular fitness (Cheng et al., 2019). Interestingly, this model suggests that haploinsufficient genes also impair cellular fitness when gene copy is increased by just one allele. This model also explains why

haploinsufficient genes are neither evolutionarily eliminated, nor their expression is increased (Morrill & Amon, 2019).

Interestingly, haploinsufficiency is often associated with cancers. Tumor suppressor genes (TSG), as the name suggests, are involved in suppressing tumor growth. Loss of tumor suppressors is often associated with tumor development and progression. Haploinsufficiency of tumor suppressor genes involved in cell cycle regulators (p27kip1, p53, p21, RB and DMP1 (ARF1 regulator)), signaling molecules (PTEN, SMAD4 and LKB1) and genes involved in maintenance of genomic stability (MSH2, MAD2, BRCA1 and 2) have been associated with development of tumors (summarized in (Santarosa & Ashworth, 2004)). Apart from individual gene losses, chromosome arm deletions such 5q, 7q and 8q in cancers leads to loss of several TSG termed as compound haploinsufficiency (Boultwood, Pellagatti, McKenzie, & Wainscoat, 2010; Honda et al., 2015; Xue et al., 2012). While the impact of haploinsufficiency varies from gene to gene, it is clear that some gene losses impairs cellular fitness while others contribute to the development of tumors.

1.6 Ribosome haploinsufficiency and its consequences

Ribosomes are macromolecular machines involved mainly in protein synthesis through translation of mRNA. Eukaryotic ribosomes comprise of 40S subunit and 60S subunit, which assemble together to form functional 80S subunit. The generation of functional 80S subunit is achieved by coordinated synthesis of 4 ribosomal RNA (28S, 18S, 5.8S and 5S), nearly 80 ribosomal subunit genes (RPs), more than 150 associated proteins involved in synthesis, import, export and assembly of ribosomes and approximately 70 small nucleolar RNAs (snoRNAs). The 40S subunit is composed of about 33 distinct small ribosomal subunit genes (RPS) and one strand of 18S rRNA whereas 60S subunit is composed of 47 large subunit genes (RPL) and 28S, 5.8S and 5S rRNA (Figure 8). In eukaryotes, the synthesis and assembly of rRNA and ribosomal proteins takes place in nucleolus (pre 60S and 40S), which are then exported into cytoplasm to assemble and mature into functional ribosomes (Pelletier, Thomas, & Volarevic, 2018). The process of functional ribosome biogenesis (RiBi) is so intricate that even minor changes could influence the synthesis of ribosomes. Consistently, loss of function mutations or deletions in RPGs and associated factors are linked to several pathological conditions (Mills & Green, 2017).

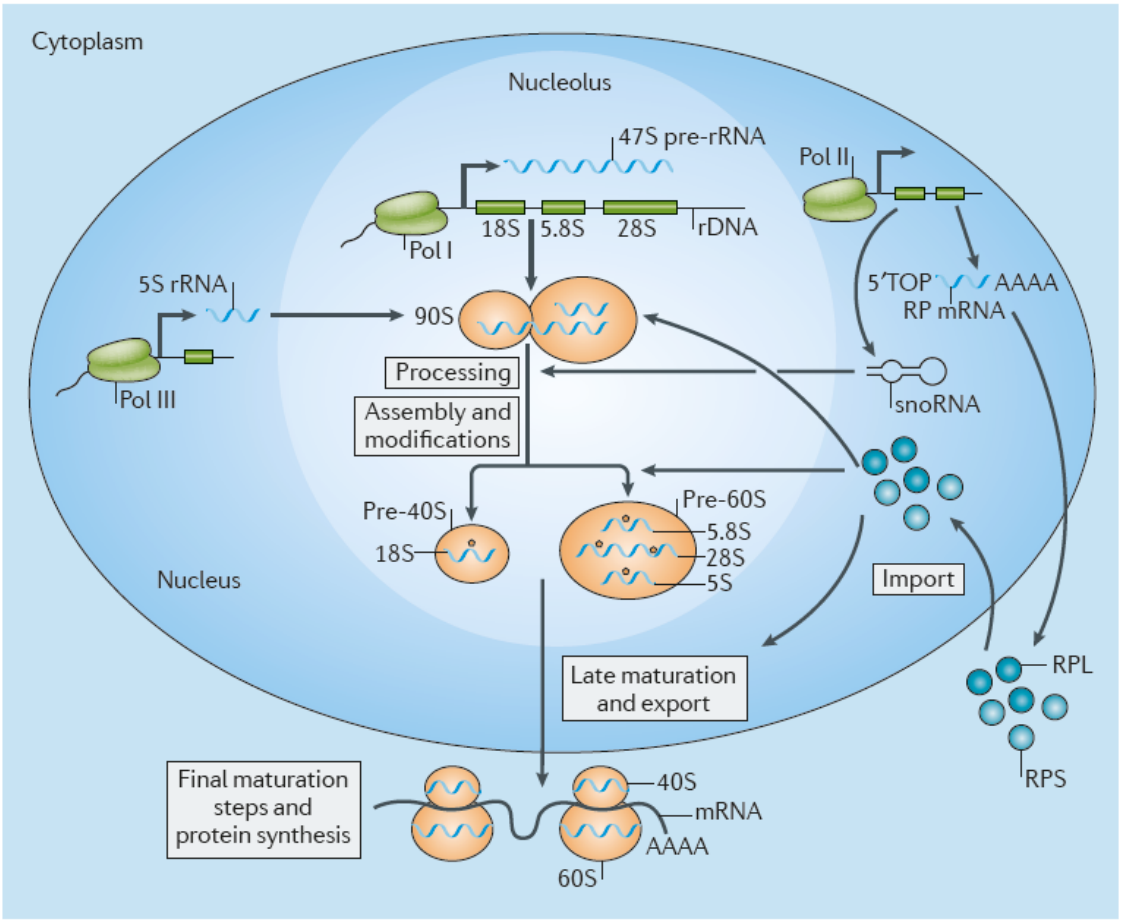

Figure 8. Multiple steps of ribosome biogenesis (RiBi). The functional 80S ribosomes are composed of 40S small subunit and 60S large subunit and different rRNAs. Majority of RiBi takes place in nucleolus, where rDNA is transcribed by RNA polymerase I (Pol I) to give rise to 47S pre-rRNA. 5S rRNA is transcribed by Pol III in nucleoplasm and RPs are transcribed by Pol II in cytoplasm and are exported into nucleolus. RPs along with 47s pre-rRNA and 5S rRNA form 90S processome. During the maturation of 90S processome into Pre-40S and Pre-60S ribosome subunits, the rRNA is processed and cleaved to give rise to 18S, 5.8 and 28S rRNA mediated by several snoRNA. Pre-40S and 60S subunits are further matured by addition of few more RPs and exported to cytoplasm where they assemble into functional ribosomes. RPL- ribosome protein large RPS- ribosome protein small. (Adapted from (Pelletier et al., 2018)).

Loss of RPGs are often associated with haploinsufficiency (Narla & Ebert, 2010). A very well-known and well-studied disease caused by ribosome haploinsufficiency is Diamond-Blackfan anemia (DBA) characterized by macrocytic anemia and cancer predisposition. DBA is mainly caused by inactivating mutations or deletion of RPS19 and few other ribosomal genes (Da Costa, Narla, & Mohandas, 2018). Further, haploinsufficiency of RPS14 was associated with 5q-syndrome, an independent subtype of myelodysplastic syndrome (MDS) (Ebert et al., 2008). Apart from the mutations directly affecting RPs,

mutations in genes involved in RiBi associated processes are also known to cause diseases. For example, Schwachman-Diamond syndrome (SDS) is caused by mutation in SBDS gene (Boocock et al., 2003). SDBS is involved in RiBi and shown to interact with rRNA. However, the exact role of this gene in RiBi is unknown. Further, the expression of several genes involved in rRNA processing, ribosomal subunit genes such as RPS9, RPS20, RPL6, RPL15, RPL22, RPL23 and RPL29 were reduced in SDS (Rujkijyanont, Adams, Beyene, & Dror, 2009). Interestingly, most of the ribosomal gene mutations seems to affect specifically the hematopoietic system. Although the ribosomal proteins are expressed abundantly in every tissue, the tissue-specific phenotypes of ribosomal gene mutations are unclear.

Several *in vitro* studies addressed the impact of ribosomal gene haploinsufficiency on cellular physiology. Partial loss of majority of ribosomal genes resulted in slower cellular growth and reduced bulk translation (Steffen et al., 2012). Analysis of ribosomal gene deletion mutants identified that loss of 60S subunit gene resulted in reduction of whole 60S and 40S subunit genes, whereas 40S deletion mutants resulted in reduction of only 40S subunit genes (Cheng et al., 2019). Besides being a part of ribosomes, ribosomal genes are involved in pre-rRNA processing. Yeast and human ribosomal protein reduction leads to impaired rRNA processing and alters the abundance of different rRNA (Ferreira-Cerca, Poll, Gleizes, Tschochner, & Milkereit, 2005; Nicolas et al., 2016; Poll et al., 2009; Robledo et al., 2008).

Intriguingly, ribosome haploinsufficiency and the resulting stoichiometric imbalances was shown to trigger p53 activation. Impaired stoichiometry leads to an increase in the abundance of free RPs. Some of the free RPs, such RPL5 and RPL18 could bind directly to E3 ubiquitin ligase MDM2. MDM2 is a negative regulator of p53. In the normal physiological states, p53 is bound to MDM2 and is marked for degradation. In the presence of stimuli, for example DNA damage, MDM2 interaction with p53 is inhibited, thereby prevents it from degradation. Once p53 is stabilized, it activates diverse genes that mediate cell cycle arrest or apoptosis. During ribosomal haploinsufficiency, free RPL5 and RPL18 bind to MDM2 and inhibit its interaction with p53, thereby stabilizing p53. Recently, more studies identified several other ribosomal proteins that could interact with MDM2, either directly or through 5S rRNA (reviewed in (Bursac, Brdovcak, Donati, & Volarevic, 2014)). The ability of ribosome genes to activate p53 makes one to think that their loss is not frequently observed in cancer. However, RPs mutations are observed in nearly 43% of 10,744 cancer specimens and cell lines. But these mutations are enriched in TP53 mutated tumors suggesting the negative selection RP mutations in TP53 positive cancers. Consistently, RP mutations are underrepresented in tumors with intact *TP53* (Ajore et al., 2017). Interestingly, several phenotypes of RP haploinsufficiency-associated diseases have been linked to p53 activation. Depletion of *TP53* rescued various phenotypes caused by RP mutations and RiBi mutations in general (Barlow et al., 2010; Jones et

al., 2008; Kamio et al., 2016; Stadanlick et al., 2011). Therefore, RP loss impairs cellular fitness not only through defective protein translation, but also by activation of tumor suppressor protein p53.

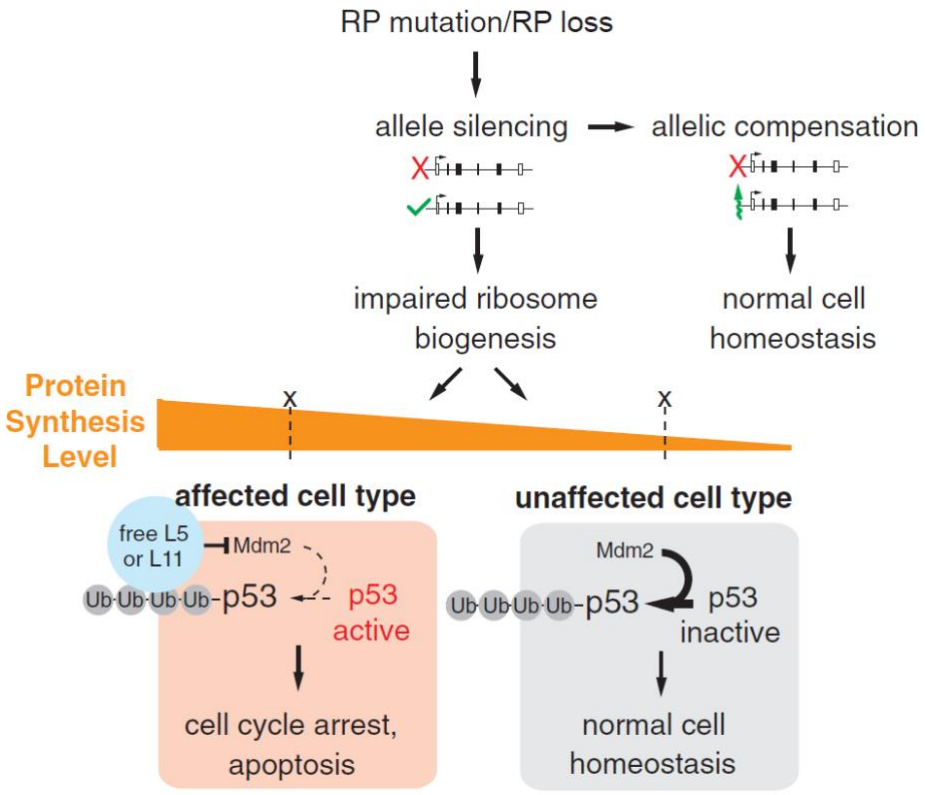

Figure 9. Impact of RP mutation on cellular physiology. RP mutations or RP loss caused by chromosome loss leads to either allele silencing or loss causing reduced RP expression. Increased RP expression from functional allele maintains normal cellular homeostasis. Absence of allelic compensation leads to reduced RPs and impaired RiBi. Impaired RiBi leads to reduced translation and protein synthesis. At the same time, reduced RPs leads to imbalances in ribosome assembly and accumulates free RPs. Increased free RPs competitively bind to MDM2 and relives the interaction of MDM2 and p53 thereby stabilizing p53. Increased p53 levels induces genes responsible for cell cycle arrest or apoptosis (Mills & Green, 2017).

1.7 TP53- a transcriptional factor and guardian of the genome

Originally, when it was discovered in 1979, p53 was believed to be an oncogene, since it was identified as an interacting partner of viral oncogene simian virus 40 (SV40) large T antigen, and due to its high expression in murine and human tumor cells (Dippold, Jay, DeLeo, Khoury, & Old, 1981; Kress, May, Cassingena, & May, 1979; Lane & Crawford, 1979; Linzer & Levine, 1979). A few years later, it was discovered that the highly expressed p53 in tumors is in fact a mutant derivative of p53 (Finlay, Hinds, & Levine, 1989). Subsequent studies showed that p53 is indeed a tumor suppressor protein that is frequently mutated in cancers and the underlying cause for Li Fraumeni syndrome (Baker et al., 1989; Nigro et al.,

1989; Srivastava, Zou, Pirollo, Blattner, & Chang, 1990; Takahashi et al., 1989). Since then, nearly after 40 years, p53 is still one of the most extensively studied protein for its role in tumor suppression as well as in various physiological states.

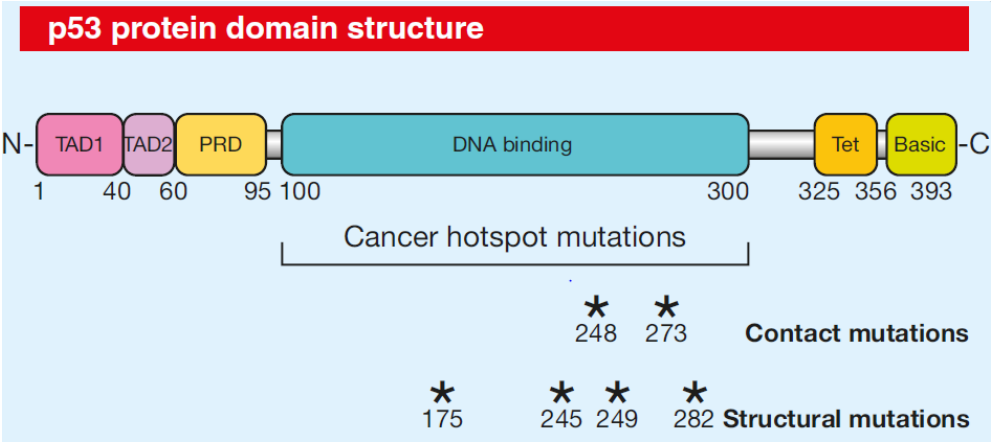

Figure 10. Structure of p53 protein. The figure depicts the various functional domains of p53 including N terminal transactivation domain (TAD1 and 2), Proline rich domain (PRD), DNA binding domain, Tetramerization domain (TET) and C terminal basic domain. Numbers represent the amino acids. * represent the most common mutations in the DNA binding domain of p53. Contact mutations prevents the interactions of p53 with target genes and Structural mutations leads to changes in p53 structure. (Adapted from (Brady & Attardi, 2010))

The p53 protein, as the name suggest, is a 53 kDa protein composed of various functional domains including two transactivation domains (TAD1 and 2), a proline-rich domain, a DNA binding domain, a tetramerization domain and a C-terminal basic regulatory domain (Joerger & Fersht, 2007a). While each of these domains are modified by post-translational modifications regulating its stability and activity, several mutations in the DNA binding domain have been identified as the hot spots in different cancers (Brosh & Rotter, 2009). Point mutation in DNA binding domain disrupts sequence specific binding of p53 to its target genes. Mutations in DNA binding domain impairs p53 function by altering the residues that are essential for direct contact with p53 response elements in target genes (contact mutations) or mutations that leads to impaired protein folding (structural mutations) (Joerger & Fersht, 2007b).

P53 is activated by diverse cellular and extra-cellular insults. Depending on the type of insult, p53 is activated either through protein stabilization or through post-translational modification. Once activated, p53 tetramers binds as dimers of dimers to the target genes containing p53 response element (RE) (Friedman, Chen, Bargonetti, & Prives, 1993; McLure & Lee, 1998). The p53 RE is composed of 5'-RRRCWWGYYY-3', where R is a purine, Y a pyrimidine, W is either adenine or thymine, G is guanine and C is cytosine. The p53 binding sites of target gene in various organisms is composed of RRRCWWGYYY sequence followed by a spacer of 0-21 bases and another RRRCWWGYYY sequence (Riley, Sontag, Chen,

& Levine, 2008). This pattern is commonly found in the promoters or in the first intron of the target genes. Once bound to the DNA, p53 activates diverse protein coding and non-coding genes and decides the fate of the cells.

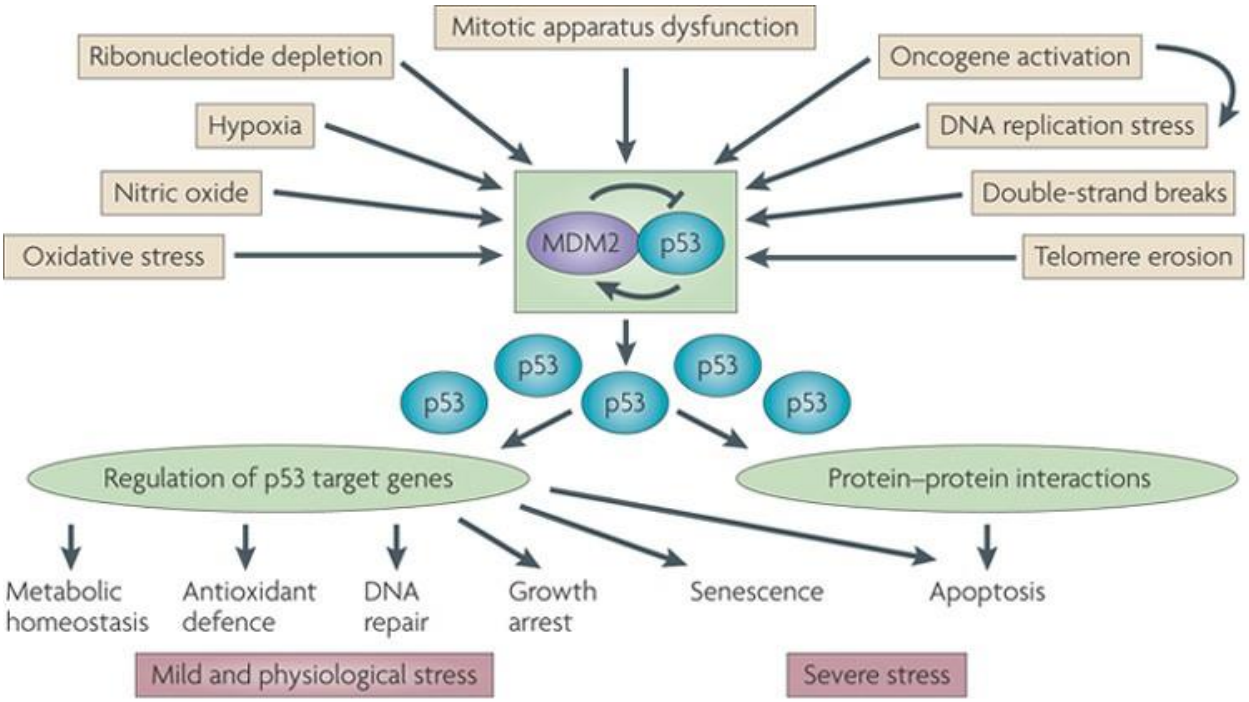

Figure 11. Diverse stress conditions activating p53. Under physiological conditions, p53abundance is maintained at the basal levels through interaction of p53 and MDM2. During stress, the interaction between p53 and MDM2 is relieved and p53 is stabilized. MDM2 is a transcriptional target of p53. Therefore, increased p53 negatively regulates MDM2 and reverts the p53 to basal levels. P53 is activated by diverse stress conditions, such as DNA damage, nucleotide depletion, telomere erosion, oxidative stress, nutrient deprivation, hypoxia, ribosomal dysfunction, mitotic dysfunction and oncogene expression. Some of the stresses leading to p53 activation are interconnected, such as DNA replication stress mediated by oncogene activation. Depending on the stress conditions, p53 induces diverse stress response genes to repair the defects or induces senescence/ apoptosis under severe stress conditions. (Adapted from (Levine & Oren, 2009)).

The p53 pathway is activated by diverse stresses that include DNA damage, hypoxia, mitotic spindle damage, impaired ribosome biogenesis, oxidative stress, nucleotide depletion, nutrient deprivation, telomere attrition, oncogene activation and others. Once activated, p53 induces transcriptional program to initiate either cell cycle arrest, senescence or apoptosis. The choice of the fate depends on the cell type, stress conditions and the severity of the stress. In response to severe and sustained stress signals, p53 induces either apoptosis or senescence (irreversible cell cycle arrest). P53 mediates these fates through transcriptional activation of apoptosis-causing genes such as BAX, FAS, NOXA, PUMA and few others, whereas senescence is mediated through p21, PAI1 and PML (Riley et al., 2008). However, when stress signal is not severe, for example during DNA damage, p53 activates genes that induces temporary cell

cycle arrest to allow for repair or directly activates DNA repair genes (Pellegata, Antoniono, Redpath, & Stanbridge, 1996). This protects the cells from propagating with unwanted mutations and keeps a check on genomic stability. Further, p53 is activated when the cells mis-segregate and becomes aneuploid (Ohashi et al., 2015; Santaguida et al., 2017; Soto et al., 2017; Thompson & Compton, 2010). Due to these functions of p53 in guarding the genome from unwanted mutations and chromosome aberrations, p53 is often referred to as "guardian of genome". Further, p53 protects the cells from oxidative stress by keeping a check on the redox status of the cells mediated through expression of anti-oxidant proteins such as Sestrins 1 and 2 (SESN 1 and SESN 2), GPX1 and TIGAR (B. Liu, Chen, & St Clair, 2008; Sablina et al., 2005). Cancer cells reprogram their metabolism to use glycolysis instead of more effective pathway for ATP generation, the oxidative phosphorylation. This reprogramming is referred to as "Warburg effect" (Vander Heiden, Cantley, & Thompson, 2009). P53 was shown to activate transcriptional program that inhibits glycolysis through activating TIGAR (Bensaad et al., 2006) and represses glucose transporters (GLUT1 and 4) (Schwartzenberg-Bar-Yoseph, Armoni, & Karnieli, 2004). Further, p53 promotes oxidative phosphorylation by activating SCO2 (Won et al., 2012) and glutaminase 2 (GLS2) (Hu et al., 2010). As described in the previous chapter, p53 is also activated during ribosomal biogenesis stress (Mills & Green, 2017). The list of stresses that activates p53 and effectors responding to p53 activation is expanding every day. It is important to note that p53 is activated by diverse stress conditions and eliminates the damaged cells or stops them cycling until damage is repaired.

To summarize, errors in chromosome segregation and the resulting chromosome copy number changes have significant impact on cellular physiology. Research in the past decade markedly improved our understanding of the cellular consequences of aneuploidy and shed light on the aneuploidy tolerance mechanisms. Large scale cancer genome studies underscore the frequent occurrence of aneuploidy in cancer and emerging evidence demonstrates that recurrent aneuploidies are commonly observed in certain tumor types. Moreover, aneuploidy positively correlate with poor patient prognosis and cancer treatment resistance. However, the exact role of the recurrent aneuploidies in cancer remains to be investigated and it is proposed that these karyotypes are selected for during tumor evolution. Therefore, understanding the diverse consequences of aneuploidy should aid in addressing the role of aneuploidy in cancer and potentially help to identify the vulnerabilities that could be targeted for the development of novel cancer therapeutics.

2. Aims of this study

Aneuploidy, a cellular state characterized by imbalanced chromosome number is embryonically lethal. In rare instances, embryos with aneuploidy survive postnatally, albeit with several pathological and developmental defects, such as Down's syndrome or Edwards' syndrome (trisomy of chromosome 21, or 18, respectively). Loss of a chromosome resulting in monosomy causes more severe phenotypes than the chromosome gains and mouse studies showed that monosomic embryos die significantly earlier than trisomies. In contrast, aneuploidy is frequently observed in cancers and high rates of aneuploidy are often associated with severe disease, poor prognosis and development of drug resistance. However, the exact role of aneuploidy in cancers remains unclear. In the past decade, a significant progress has been made towards the understanding of the consequences of aneuploidy and its role in tumorigenesis. While the impact of chromosome gains on cellular physiology is well understood, the impact of chromosome loss is unknown mainly due to the lack of model systems owing to its detrimental impact on viability. Yet, chromosome losses are frequently observed in cancers. Therefore, understanding the consequences of chromosome losses and factors determining the viability of cells with chromosomal losses could provide novel therapeutic opportunities for cancer treatments.

To uncover the cellular consequences of chromosome losses, we generated and characterized human cell lines with loss of one or two chromosomes in the human RPE1 cells line lacking p53. Previous analysis of chromosome gains showed that gain of even a single chromosome led to conserved common phenotypes such as slower proliferation, delayed cell cycle, proteotoxic stress, genomic instability, replication stress and innate immune pathway activation. Our first aim was to investigate whether the chromosome losses induce similar phenotypic responses as chromosome gains or whether the responses are different.

Next, we aimed to investigate if and how the mRNA and proteins abundance of the genes encoded on the monosomic chromosome scale with the DNA copy number. In other words, does reduced DNA amount always lead to reduced mRNA and protein? We performed global mRNA and protein quantification using RNA sequencing and mass spectrometry-based proteomics to investigate how the gene dosage of monosomy-encoded genes are regulated. Furthermore, we investigated the impact of chromosome loss on the global transcriptome and proteome and what genes or pathways are differentially regulated in response to chromosome loss. The findings suggested by the pathway analysis were then validated by functional studies.

Systemic analysis of monosomy in humans has never been performed before owing to its detrimental effect on cell viability and difficulties in obtaining isogenic monosomic model cell lines. For the first time, we obtained isogenic monosomic cell lines in the human RPE1 cell line lacking p53. We hypothesized that

the absence of p53 is probably a prerequisite for the viability of monosomies. To validate our hypothesis, we aim to reintroduce p53 and determine its impact on the monosomic cell viability and study the impact of p53 on the cellular responses to monosomy. Further, we made use of publicly available cancer genome data to investigate whether tumors with chromosome losses are preferentially enriched for p53 mutation in comparison to diploid cells and to chromosome gains.

Together, the findings from this study will reveal the cellular consequences of chromosome losses and the impact of p53 on the viability of monosomies. This study provides a rationale as to why monosomies are on one hand embryonically lethal, but, on other hand are frequently observed in cancers.

3. Results

3.1 Generation of monosomic cell lines

To understand the cellular consequences of monosomy, we, in collaboration with the laboratories of Jan Korbel (EMBL, Heidelberg) and Rene Medema (NKI, Netherlands) generated monosomic cell lines derived from RPE1, a human TERT-immortalized retina pigment epithelium cell line. The monosomic cells were derived by two approaches (Figure 12A). Both approaches involved depletion of p53 using CRISPR-Cas9 or TALENs (labeled as KO clones), or stable integration of shRNA against TP53 (KD clones). Single cell clones derived from p53 KO or KD generated several viable monosomic clones for different chromosomes (Figure 12A) (See methods for details). The genome changes of single cell derived clones were validated by whole genome sequencing (Figure 12B). The sequencing analysis of KD clones was published in (Soto et al., 2017). Chromosomal painting verified that at least 90% of the analyzed metaphases manifests the respective monosomic karyotype (Figure 12C, Table 1).

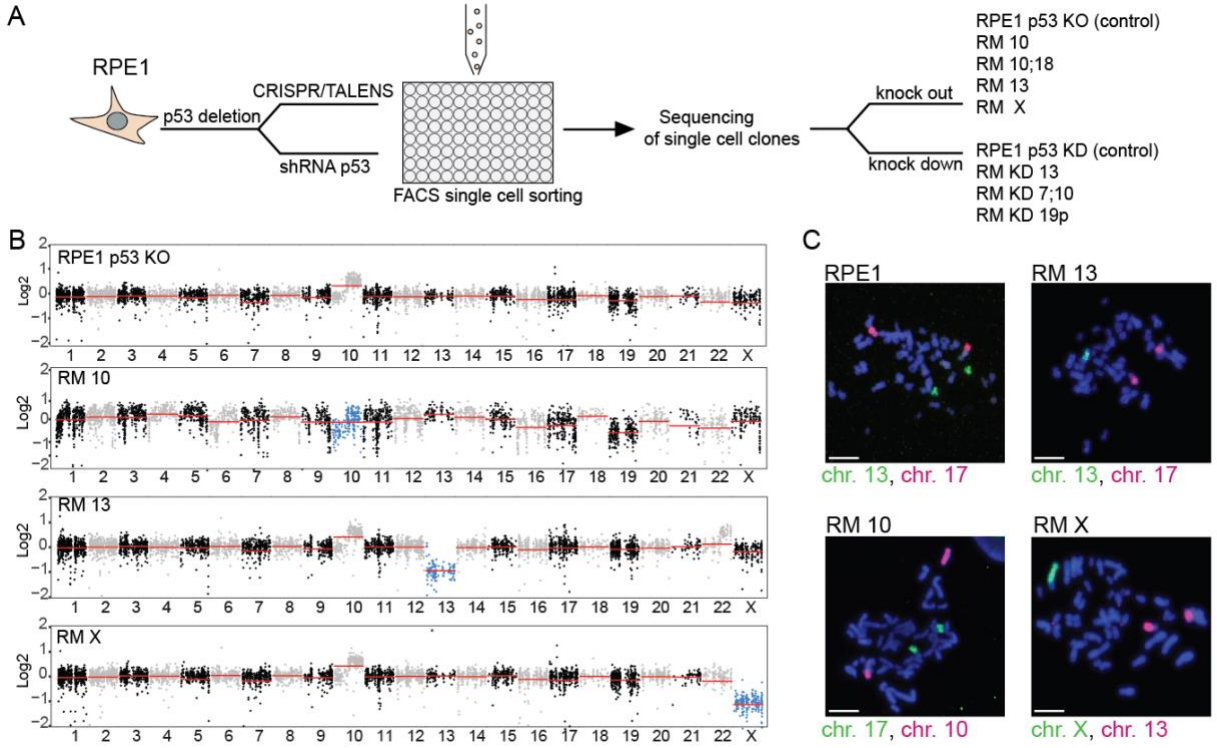

Figure 12. Generation of monosomic cell lines. A. Schematic depiction of the construction of monosomic cells. TP53 was mutated or depleted in RPE1-hTERT cell line via CRISPR/Cas9, TALENS, or shRNA expression, followed by single cell cloning and whole genome sequencing. **B.** Read depth plots of all chromosomes in control and RM samples. Chromosome losses are marked in blue. Red lines indicate the copy number of each individual chromosome. Note that the parental RPE1 cells contain an extra copy of 10q that is preserved in all monosomic derivatives. **C.**

Chromosomal paints of monosomic cell lines. The painted chromosomes are indicated with respective colors. Scale bar – 10 µm.

The monosomic cell lines were named **R**PE1-derived **M**onosomy (RM), followed by the number of the monosomic chromosome, i.e. RM 13 for monosomy 13; cell lines with the shRNA mediated knock-down of p53 are additionally labeled with KD, for example RM 13 KD (Figure 12A, Table 1). Of note, gain of chromosome 10q, a characteristic chromosomal aberration of the RPE1 cell line, is also observed in our analysis (Figure 12B). Some monosomic cell lines acquired variable partial or mosaic chromosome losses or gains (e.g. 22q gain RM 13). These changes can be likely attributed to the increased genomic instability of monosomic cells (discussed in later chapters) and to the relaxed checkpoint due to the p53 loss.

Table 1. List of monosomic cell lines and the karyotype

Fraction of monosomic cells - percentage of metaphase spreads having one copy of respective monosomic chromosome and 2 copies of diploid chromosome. N= number of metaphase spreads.

Name of the cell line	Parent	Altered chromosome	Fraction of monosomic cells	Remarks
RM10	RPE1-hTERT p53 -/-	10	Chr.10 100% (N=25)	This work
RM 10;18	RPE1-hTERT p53 -/-	10 and 18	Chr.10 100% (N=20)	This work
RM X	RPE1-hTERT p53 -/-	X	Chr. X 100% (N=15)	This work
RM 13	RPE1-hTERT p53 -/-	13	Chr. 13 91% (N=11)	This work
RM13 kd	RPE1-hTERT shRNA-p53; H2B-Dendra2	13	n/a	Soto et al, 2017
RM 7;10 kd	RPE1-hTERT shRNA-p53; H2B-Dendra2	7 and 10	n/a	Soto et al, 2017
RM 19p kd	RPE1-hTERT shRNA-p53; H2B-Dendra2	19p	n/a	Soto et al, 2017

3.2 Diverse phenotypic consequences of monosomy

3.2.1 Chromosome loss impairs proliferation and anchorage independent growth

Having isogenic monosomic cell lines at hand, we asked whether the loss of chromosome impairs proliferation similarly as observed in previous analysis of chromosomal gains. Strikingly, all of the analyzed monosomic cell lines proliferated slower than the respective diploid controls, albeit the strength of the defect varied among different monosomies (Figure 13A, B). Interestingly, the strength of proliferation defect correlated with the number of ORFs encoded of the monosomic chromosome for all but one monosomic cell line (Figure 13C). Notably, the loss of chromosome X from RPE1 impaired proliferation similarly as the loss of an autosome. RPE1 cell line is female-derived, with 2 copies of chromosome X. One

copy of chromosome X is transcriptionally inactivated by XIST-mediated silencing, but there are approximately 100 – 130 genes located on chromosome X known to escape the X-inactivation (Carrel & Willard, 2005). While proliferation defect in RM X could be attributed to DNA loss, previous analysis showed that DNA per se doesn't impact the proliferation of aneuploidy, but the gene expression from aneuploid chromosomes are responsible for such defects (Torres et al., 2007). Our observation therefore suggests that the loss of these few escapees is sufficient to impair cellular proliferation (Figure 13A, C).

Loss of chromosome(s) is frequently observed in a broad spectrum of tumors, suggesting its role in cancer pathogenesis (Kristin A. Knouse, Davoli, Elledge, & Amon, 2017). Therefore, we tested the tumorigenic potential of monosomic cells *in vitro*. One of the important properties of cancer cells is their ability to grow in an anchorage independent manner. We tested tumorigenic potential of monosomic cells by quantifying the anchorage independent growth on soft agar. While RPE1 cells with *TP53* does not form colonies on soft agar, depletion of *TP53* increased the cellular capacity of anchorage-independent growth of diploid RPE1 cells (Figure 13D). Strikingly, all of the monosomic cells formed significantly less colonies on soft agar compared to diploid control (Figure 13D). This suggests that loss of chromosome acts as tumor suppressor *in vitro.* Taken together, loss of chromosome impairs proliferation and the capacity of anchorage independent growth even in p53 deficient background.

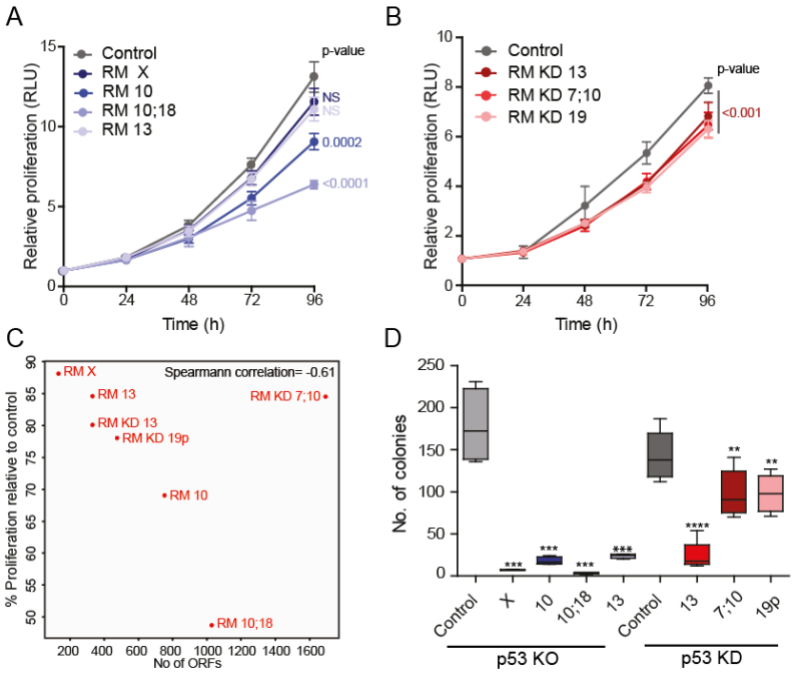

Figure 13. Proliferation and anchorage independent growth are impaired in monosomies.

A-B. Proliferation curves of monosomic cell lines in comparison to respective diploid controls. All the values are normalized to day 0. Each point represents the mean ± SEM from at least 3 independent experiments. RLU-relative luminescence unit. p-value was calculated using linear regression and shown in the plots.

C. Correlation between the proliferation and number of open reading frames (ORFs) on the monosomes. The number of ORFs was obtained from NCBI database; the estimated number of non-compensated ORFs was considered for chromosome X.

D. Quantification of a number of colonies growing on soft agar. Box and whiskers plots show the mean, highest and lowest value of at least 4 independent experiments. T-test; **<0.002; *** <0.0002, ****<0.0001

3.2.2 No consistent cell cycle changes in monosomic cells

Slower proliferation could be caused by a delay in different phases of the cell cycle. Therefore, we accessed the cell cycle profile of the monosomic and the corresponding control cells using FACS. For this purpose, we labelled the cells with EdU (nucleotide analogue, labels S phase cells) and DAPI (for DNA). FACS profiling based on the EdU and DAPI signals allow us to differentiate different cell cycle phases: G1 (Edu negative, 2N DNA content), S (Edu positive) and G2/M (EdU negative, 4N DNA content) (Figure 14A). Quantification of different cell cycle phases revealed no consistent differences between monosomies (Figure 14B). Immunoblotting of different proteins involved in regulating cell cycle also revealed no changes that were consistent with the defects in proliferation (Figure 14C). Based on our findings, we conclude that the cell cycle is not strikingly and uniformly impaired in response to monosomy.

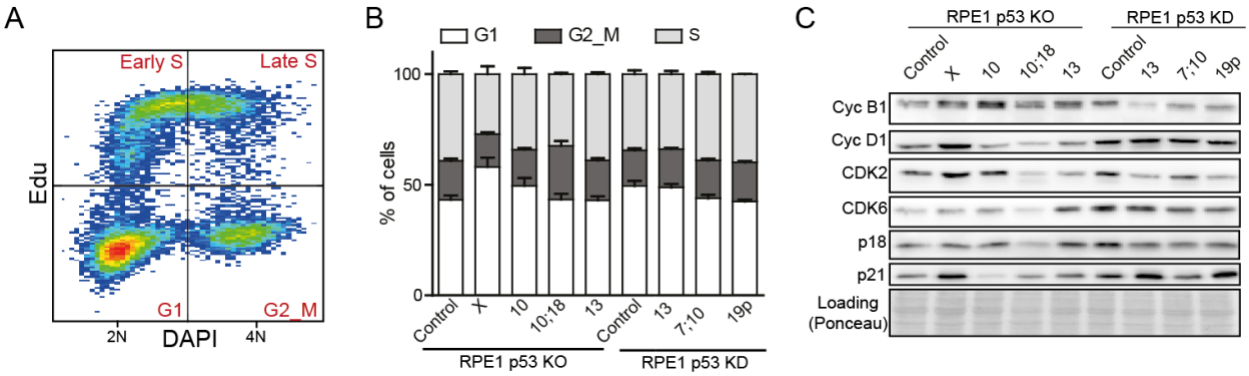

Figure 14. Cell cycle profile and the expression of proteins regulating cell cycle. A. Representative image of FACS profile of cell stained with Edu and DAPI. Different phases of cell cycle are depicted in the picture. **B.** Quantification of different cell cycle phases in control and monosomic cell lines (N=3). **C.** Representative Immunoblotting of different key cell cycle markers.

3.2.3 Chromosome loss impairs genomic stability

Previous studies in different organisms showed that genomic instability is one of the hallmarks of aneuploid state (Ohashi et al., 2015; Passerini et al., 2016; Santaguida et al., 2017; Sheltzer et al., 2011; Tumova, Uzlikova, Jurczyk, & Nohynkova, 2016). All of these studies used model systems with either a gain of chromosome or analyzed heterogeneous cell population immediately after chromosome missegregation. Whether the cells with chromosomes losses exhibit similar phenotypes has not been analyzed. Impaired genomic stability is characterized by increased micronuclei, anaphase bridges, DNA damage and increased accumulation of DNA damage checkpoint proteins. Therefore, we quantified the occurrence of micronuclei and anaphase bridges using fluorescence microscopy. Strikingly, majority of

monosomic cells showed increased incidence of micronuclei; this was significant in 5 out of the 7 monosomic cell lines (Figure 15A, B). Only a small proportion of micronuclei (20-30%) stained positive for Centromere Protein A or B that I used as a centromeric marker (CENP+), suggesting that the micronuclei enclose a chromosome fragment rather than a whole chromosome (Figure 15C, D). The fraction of CEN+ micronuclei was similar in diploid and monosomic cell lines (Figure 15D). Occurrence of anaphase bridges caused by under-replicated or incorrectly repaired DNA was significantly increased in 3 out of 7 monosomic cell lines (Figure 15E). Interestingly, the anaphase bridges accumulated only in p53 KO clones and no increase was observed in KD clones. The reasons underlying this difference remains unknown. Further, live cell imaging analysis revealed that monosomic cells on average spent 10 mins (28 min to 38 min) longer in mitosis that control cells (Figure 15F). This suggest that the mitosis of monosomies is more erroneous, thus leading to prolonged mitosis. At the same time this observation suggests that SAC is not impaired in monosomies.

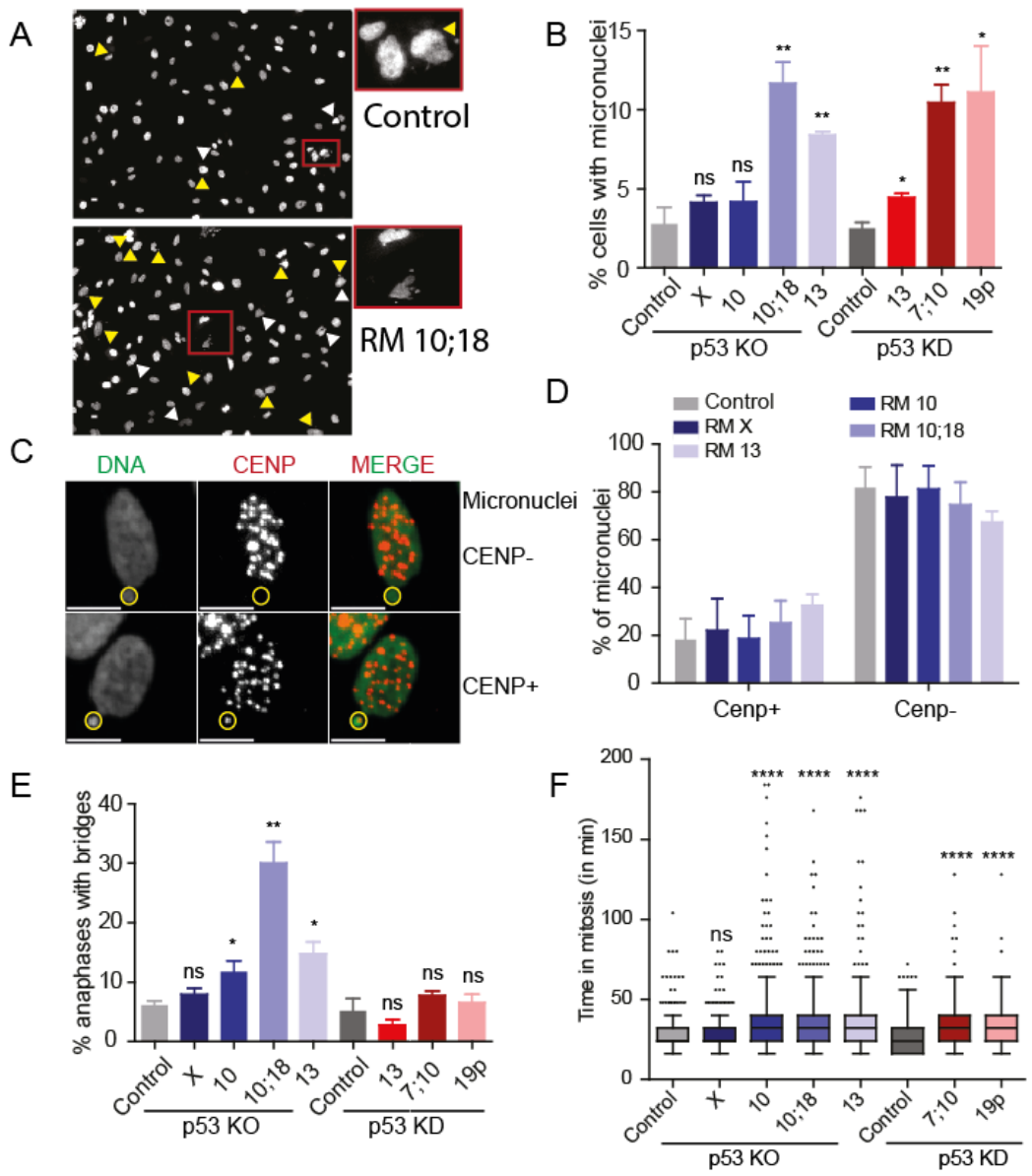

Figure 15. Genomic stability is impaired in monosomies. A. Representative images cells with micronuclei and nuclei structure abnormalities. Inset shows the enlarged field (white arrowhead – nuclear abnormalities, yellow arrowhead - micronuclei). Scale bar –10 µm. **B.** % of cells with micronuclei. **C.** Immunofluorescence images for micronuclei with CENP staining Scale bar – 10 µm. Yellow circle marks the micronuclei. **D.** Fraction of micronuclei positive/negative for CENP signal. **E.** % of anaphases with bridges. **F.** Quantification of time spent in mitosis. Time from nuclear envelope breakdown (NEBD) until the end of anaphase was measured. Box and whiskers plots show the mean and the outliers. Bar graphs display mean ± SEM of at least 3 independent experiments. 2 independent experiments for CENP staining. T-test; ns-not significant, *<0.05; ** 0.002. ****< 0.0001. At least 150 anaphases per cell line were counted.

Immunofluorescence staining for γH2AX, which marks DNA double strand breaks, was significantly increased in 3 out of 4 analyzed monosomic cell lines (Figure 16A, B). Together, our findings indicate that monosomies suffer from varying degree of DNA damage and genomic instability.

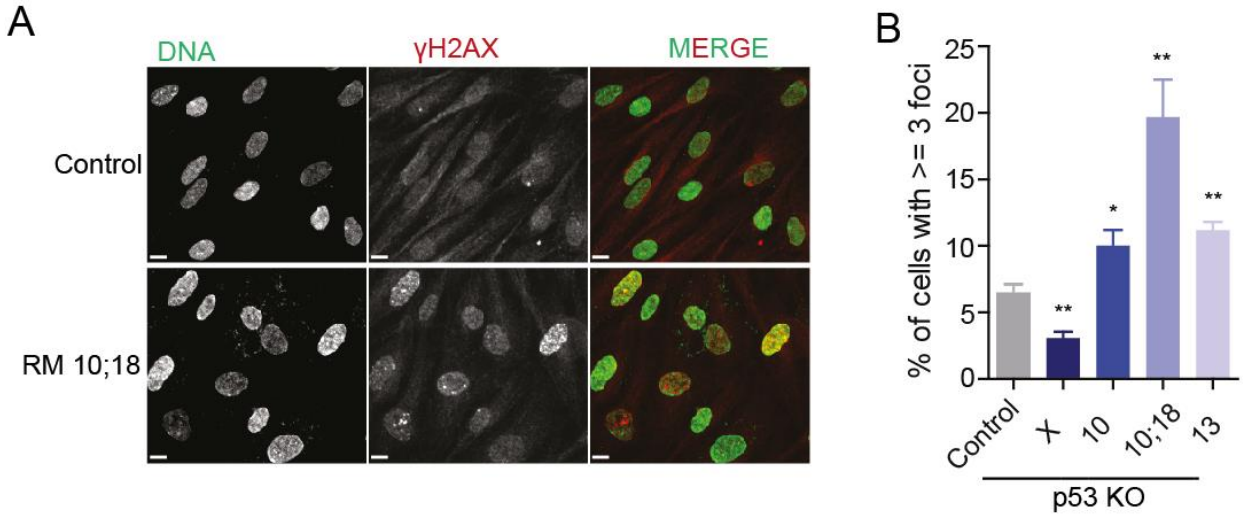

Figure 16. The occurrence of DNA double strand breaks is increased in monosomies. A. Representative images show immunofluorescence staining of the DNA damage marker γH2AX in control and RM10;18 cell lines. DNA is stained with Sytox green (green) and γH2AX (red). Scale bar - 10µm. **B.** Quantification of percentage of cells with >= 3 γH2AX foci per cell. Bar graphs display mean ± SEM of at least 3 independent experiments. T-test; *<=0.02 **<=0.003.

Genomic instability in aneuploid cells with a chromosome gain has been previously attributed to the replication stress caused by reduced expression of proteins regulating DNA replication and repair (Passerini et al., 2016). Proteome analysis (discussed in detail below) showed that, while the proteins involved in DNA replication and repair is markedly downregulated in trisomic cell lines, the expression of these proteins was largely unchanged in monosomies (Figure 17A). Immunoblotting for proteins of the MCM2-7 helicase complex confirmed that the expression of these proteins is unaltered in monosomic cells lines (Figure 17B, C).

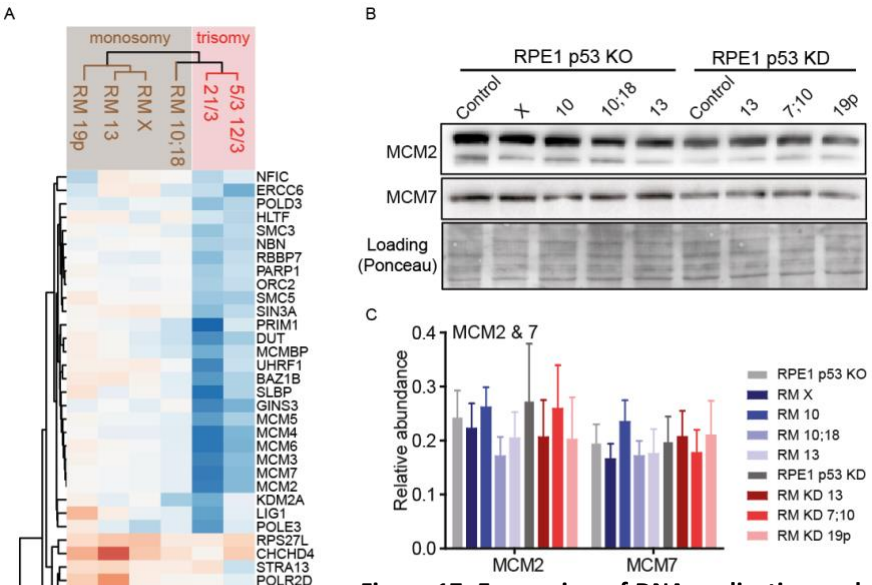

Figure 17. Expression of DNA replication and repair proteins in monosomies. A. Heat map and clustering analysis of top differentially expressed DNA replication and repair proteins. Log2FC outside -0.5 and 0.5 in at least 2 cell lines are shown. **B.** Immunoblotting for MCM2 and MCM7 helicases and **C.** Quantification. Ponceau staining was used as a loading control. Bars depict mean with SEM, at least three experiments were performed.

Further, immunoblotting of markers of replication stress (RPA32 and pRPA32 s4/8) and DNA damage checkpoint (CHK1 and pCHK1 s354) revealed no changes that would be consistent with replication stress in monosomies (Figure 18A, B). Of note, RM 10;18 being the monosomic cell line with the strongest genomic instability phenotypes, clustered more closely with trisomies and showed pattern of increased replication stress and damage markers (Figure 18A, B).

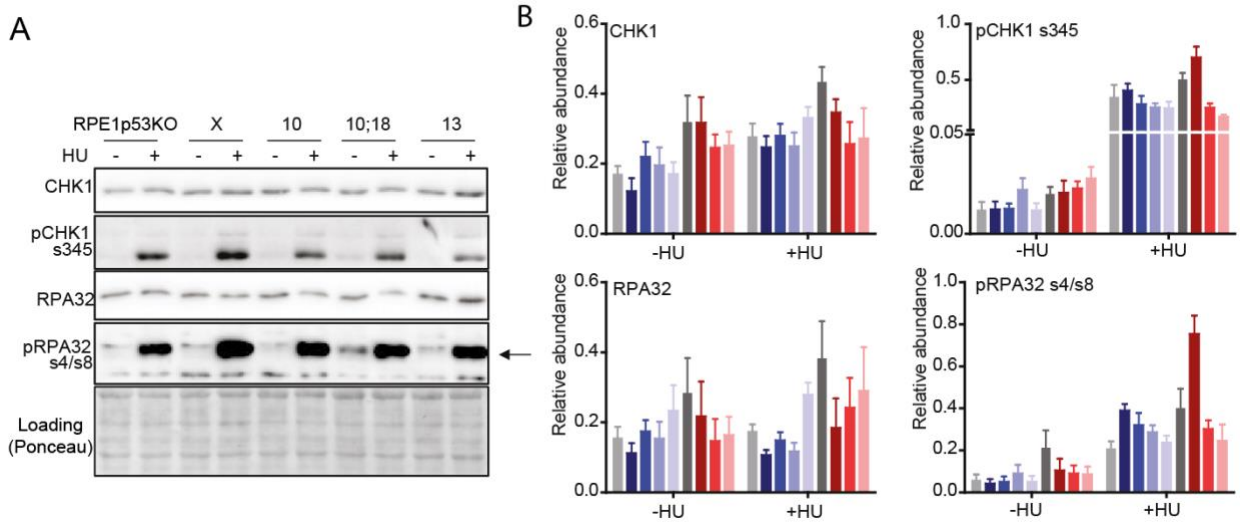

Figure 18. Expression of key replication stress and check point proteins. A. Representative Immunoblots of the key replication stress and checkpoint proteins and **B.** Quantification. Ponceau staining was used as a loading control. Bars depict mean with SEM, at least three experiments were performed.

Together, our findings suggest that DNA replication stress is not responsible for DNA damage and genomic instability in monosomies and the underlying reason for genomic instability is different to trisomic cells.

3.2.4 Proteotoxic stress is not a hallmark of monosomy.

Proteotoxic stress is a result of imbalance in the protein synthesis, folding and clearance mechanisms (Dai, Dai, & Cao, 2012). Previous studies showed that excessive protein production caused by aneuploidy (chromosome gains) disrupts protein homeostasis. This is manifested by impaired protein folding and increased sensitivity to inhibitors of protein folding and autophagy (17-AAG and chloroquine, respectively), as well as by increased autophagy and proteasomal activity (Dephoure et al., 2014; Donnelly et al., 2014; Ohashi et al., 2015; Oromendia et al., 2012; Santaguida et al., 2015; Stingele et al., 2012; Y.-C. Tang et al., 2011).

To evaluate whether the monosomies suffer from proteotoxic stress, we treated the cells with HSP90 inhibitor (17-AAG), which places an additional burden to cells suffering of proteotoxic stress. Thus, increased sensitivity to 17-AAG serves as a proxy of the proteotoxicity in monosomies. This analysis revealed that monosomies are not consistently sensitive to 17-AAG when compared to diploid control cell lines (Figure 19)

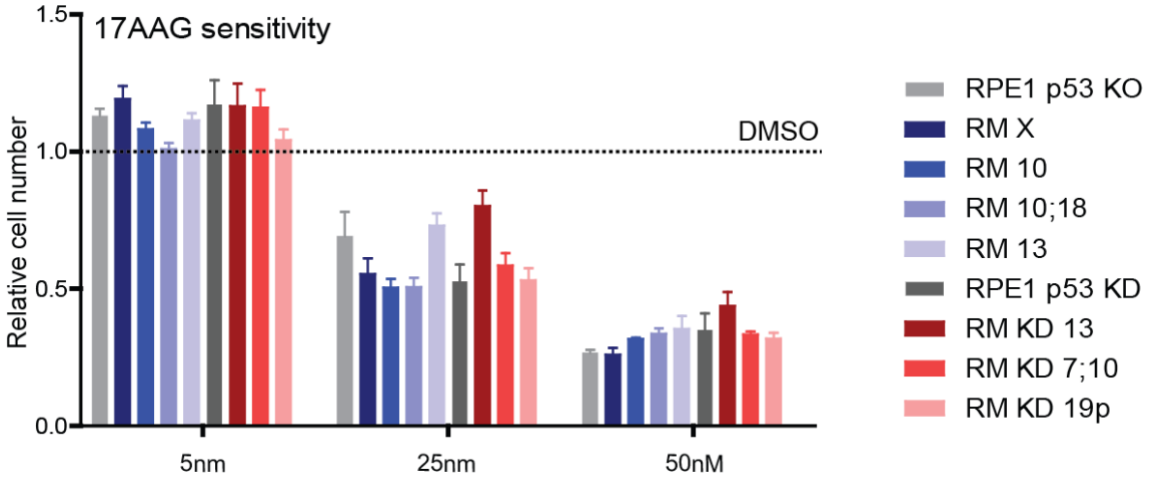

Figure 19. Monosomies are not sensitive to treatment with 17-AAG. Sensitivity to 17-AAG measured by Cell Titer Glo assay. All the values were normalized to DMSO control. DMSO was used as a solvent control. None of the values are statistically significant compared to control (bars in grey).

Further, expression of various heat shock proteins and markers of autophagy (LC3 I/II and SQSTM1) were not uniformly deregulated in monosomies (Figure 20).

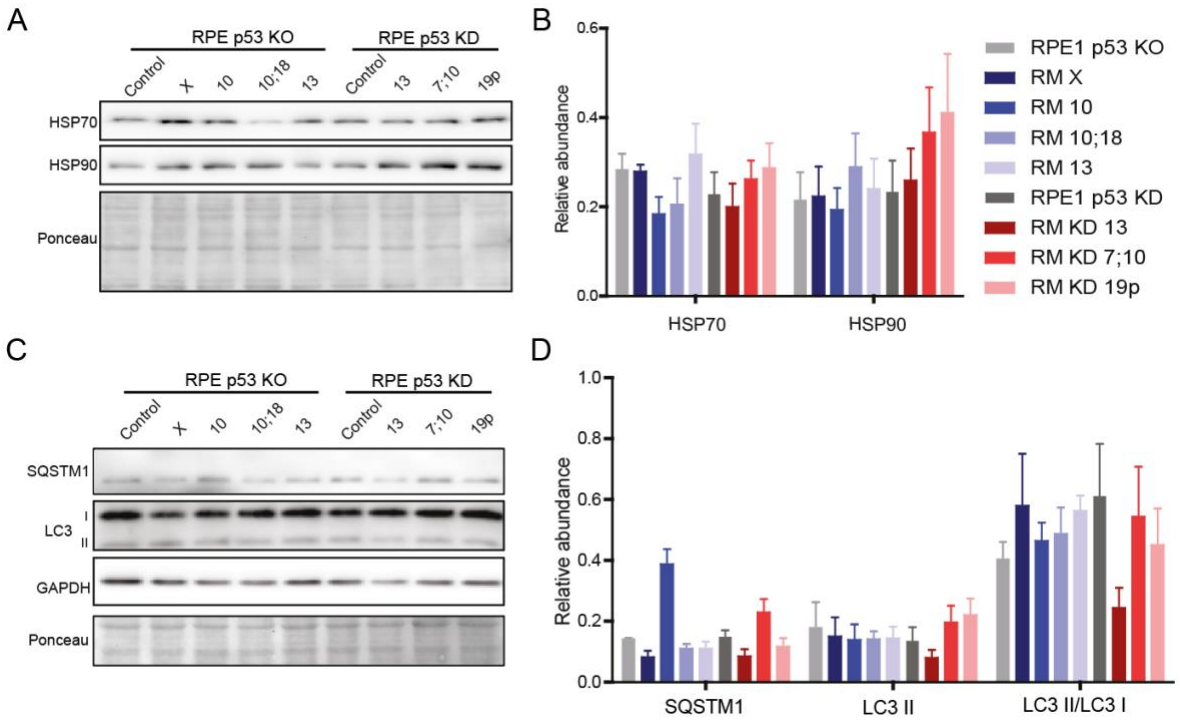

Figure 20. Expression of heat shock proteins and markers of autophagy are not altered in monosomies. A. Representative immunoblots for heat shock proteins and **B**. Quantification. **C.** Immunoblotting for markers of autophagy and **D.** Quantification. All the intensities were normalized to the Ponceau staining (Loading control). Quantification is from at least three independent experiments. Bars show mean and SEM.

Taken together, a loss of a single chromosome leads to proliferation defects and increased genomic instability, but does not trigger replication defects and proteotoxic stress, implying that the affected molecular processes in monosomies are different than those of chromosome gains.

3.3 Transcriptome and proteome analysis of monosomic cell lines

To understand the impact of chromosome loss on gene expression in *cis* (genes encoded on the monosomic chromosome) and *trans* (genes encoded on the other chromosomes), we analyzed the transcriptome and proteome of RM X, RM 10;18, RM 13, RM 19p and respective diploid controls. For transcriptomics, we performed RNA sequencing (see Methods for details), which provided quantification of approximately 14000 transcripts. For the proteomics, we employed multiplexed Tandem Mass Tag (TMT) labelling strategy (see Methods for details). In total, 7325 proteins were identified; 5887 proteins quantified with at least three valid values were used for further analysis. For combined analysis of

genome, transcriptome and proteome, we analyzed all genes for which both mRNA and protein expression values were quantified.

3.3.1 Expression of genes encoded on the monosomic chromosome are buffered towards diploid levels

To investigate, whether the mRNA and protein encoded on the monosomic chromosome is expressed at the levels according to the DNA copy number, we plotted the $\log_2$ **F**old **C**hanges (FC) (RM/control) of both mRNA and protein values along their chromosome positions. Such visualization revelaed that both mRNA and protein levels of genes encoded on monosomes were reduced (Figure 21A, B, S1A-F).

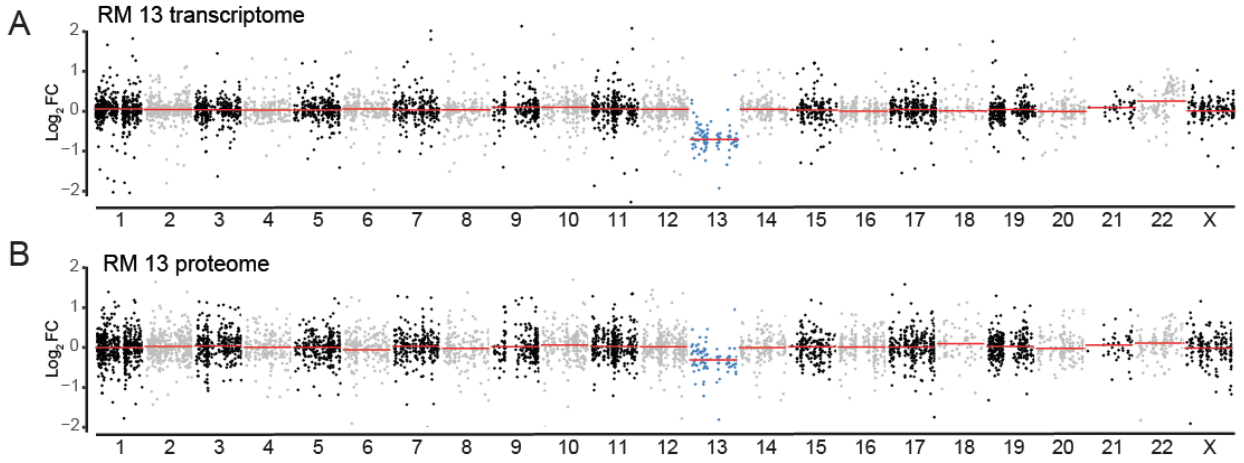

Figure 21. Expression of mRNA and protein encoded on the monosomic chromosome. A & B. The relative abundance of mRNAs and proteins of RM13 normalized to diploid isogenic parental control were plotted according to their chromosome location. The monosomic chromosome is marked in blue. Red line depicts the median for each chromosome. In cooperation with Paul Menges.

If all of the genes encoded on the monosomic chromosome were expressed according to the DNA copy number at 50%, then the median log2FC should be -1, while the median for the disomic chromosomes should be at 0. Analysis of transcriptome and proteome datasets revealed that the distribution of mRNA and protein abundances for genes encoded on the disomes was around 0 in all monosomic cells line (Figure 22, *lower panels in green*). However, the abundance of mRNAs encoded on the monosomic chromosomes (chromosomes 13, 10;18 and 19p, respectively) did not decrease to the expected levels; instead the median mRNA expression of monosomy encoded genes ranged from -0.5 to -0.75 (Figure 22, *upper panels in red*). The median of mRNA expression from X chromosome in RM X remains close to zero, as expected (Figure 22, *upper panels in red*). Analysis of proteome datasets revealed that the relative abundance of proteins encoded on monosomic chromosomes was further increased towards diploid levels (Figure 22, *upper panels in red*).

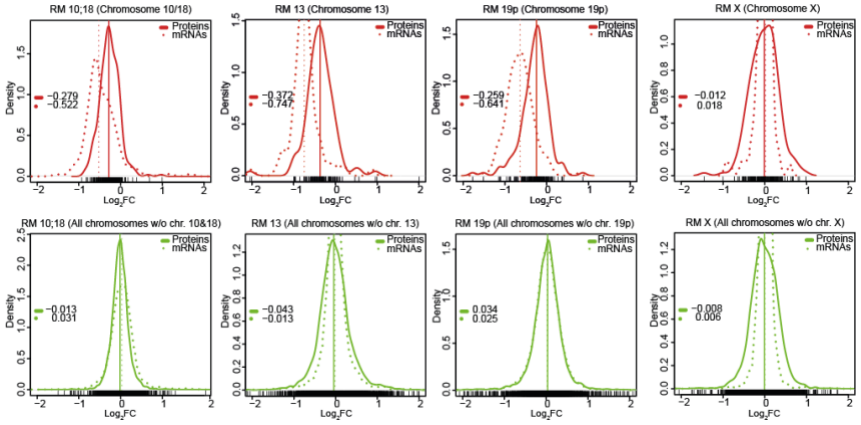

Figure 22. Dosage of mRNA and protein abundances of individual monosomic cell lines. Overlays of mRNA (dashed line) and protein (solid line) density histograms. Values of respective medians are plotted in the graph. Upper panels (in red) represent the monosomic chromosome; lower panel (green) display all other, disomic chromosomes. With Paul Menges.

When we combined the expression values of all genes encoded on the monosomic chromosomes of all cell lines, except of chr. X, the measured median of log_2FC of protein abundance was – 0.25, while the measured median of all corresponding transcripts was -0.59, both values being significantly higher than the expected -1 (Figure 23A). We then divided the monosomically encoded genes into four categories based on the cut off set at -0.5: down;down (both mRNA and protein log_2FC less than -0.5), up;down (mRNA>-0.5, protein< -0.5), down;up (RNA<-0.5, protein>-0.5) and up;up (both mRNA and protein more than -0.5) (Figure 23B). This analysis revealed that the expression of approximately 30 % of the genes encoded on the monosomes was adjusted to diploid levels transcriptionally (up; up) and 45 % were adjusted post-transcriptionally (down;up) (Figure 23C). Only about 20 % of monosome encoded genes were expressed at a relative abundance lower than -0.5 log_2FC of the parental control. Taken together, our data suggests that the expression of mRNA and proteins encoded on the monosomic chromosomes are compensated towards diploid levels by both transcriptional and posttranscriptional mechanisms.

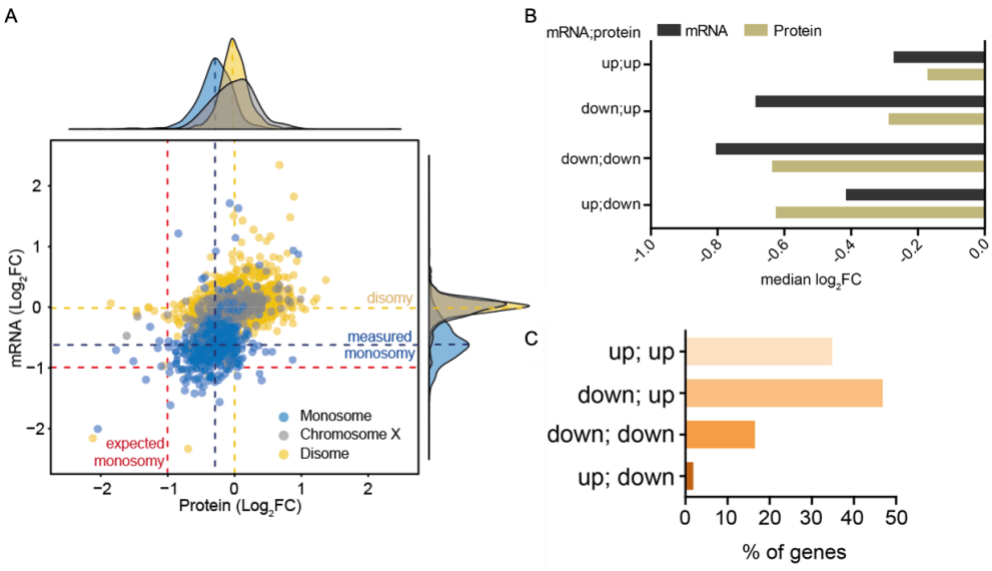

Figure 23. Combined mRNA and protein abundances of all genes encoded on all monosomic chromosomes. A. Scatter plot shows the log_2FC of mRNA and proteins encoded on monosomes (blue), disomes (yellow) and chromosome X (grey). The marginal density histograms show the distribution of respective mRNAs and proteins. The expected median fold change of monosomic genes is marked by red dashed lines. The measured median fold changes of monosomic and disomic genes is marked by blue and yellow dashed lines, respectively. **B.** Bar plots shows the median log2FC of mRNA and proteins assigned to different groups based on the log2FC cut off set at -0.5; up;up (both mRNA and protein more than -0.5), down;up (RNA<-0.5, protein>-0.5), down;down (both mRNA and protein log2 fold changes less than -0.5), up;down (mRNA>-0.5, protein< -0.5). **C.** Bar plot shows the percentage of genes assigned to different groups.

In the next step, we analyzed characteristics of genes belonging to respective dosage compensation groups. For this purpose, we performed pathway enrichment analysis using a web-based tool Enrichr (E. Y. Chen et al., 2013; Kuleshov et al., 2016). The top 10 pathways enriched for different groups are shown (Figure 24). Interestingly, the group down;up representing posttranscriptional compensation harbored genes enriched for ribosome biogenesis (rRNA metabolism and processing) and translation, while the group up;up representing transcriptional compensation enriched for pathways mRNA processing and mRNA splicing. The group down;down mainly enriched for mitochondrial related pathways. This was mainly due to the genes altered in RM 19p (discussed below). No such analysis could be performed for the group up;down due to the small sample size (no. of genes are 11).

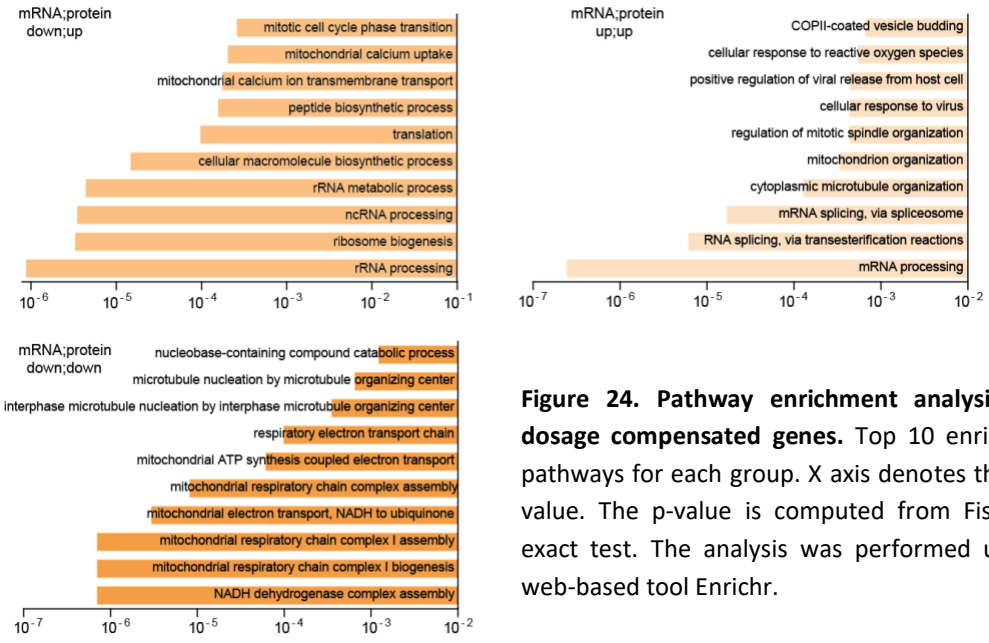

Figure 24. Pathway enrichment analysis of dosage compensated genes. Top 10 enriched pathways for each group. X axis denotes the p-value. The p-value is computed from Fischer exact test. The analysis was performed using web-based tool Enrichr.

Previous analysis of trisomic cell lines showed that the genes belonging to multi-molecular complexes defined by CORUM database are compensated towards diploid levels (Stingele et al., 2012). Similar analysis in monosomic cell lines revealed no consistent bias towards CORUM annotated protein in regards

to dosage compensation (Figure 25). Our results therefore suggest that the processes involved in dosage compensation is different for chromosome losses compared to chromosome gains.

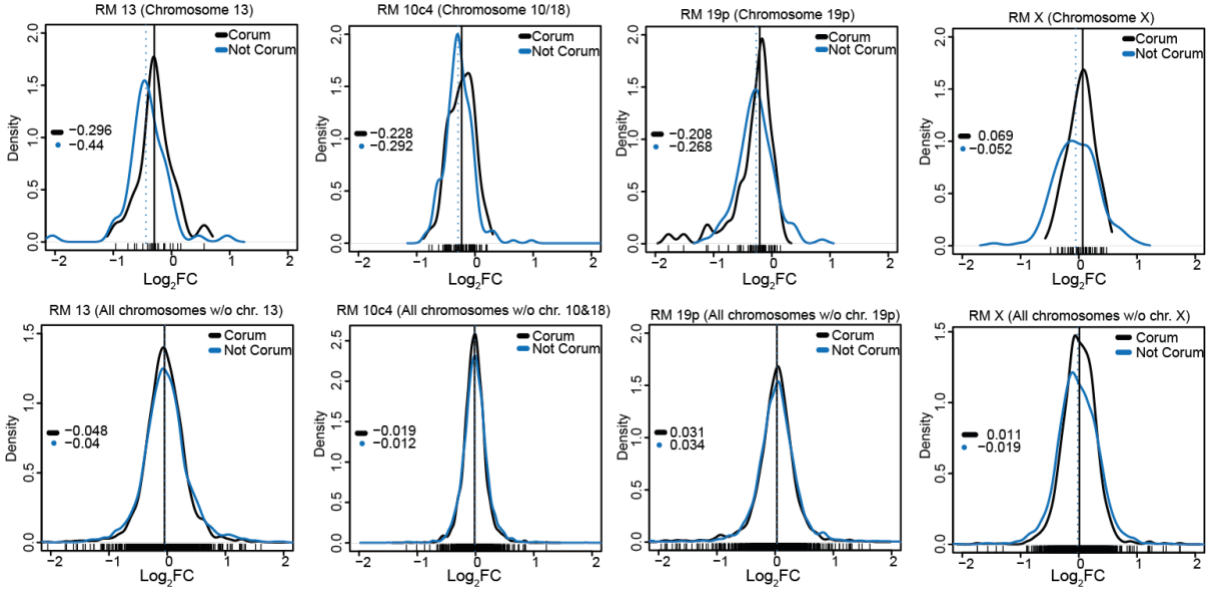

Figure 25. The dosage compensated proteins in individual monosomic chromosome are not enriched for CORUM. Overlays of Corum (black line) and Non-Corum (blue line) density histograms. Values of respective medians are plotted in the graph. Upper panels represent the monosomic chromosome; lower panel display all other, disomic chromosomes. With Paul Menges.

3.3.2 Global pathway alterations caused by chromosome loss

From the transcriptome and proteome analysis, we showed that the abundances of mRNA and protein of genes encoded on the monosomic chromosome were reduced, albeit not to the expected levels. Next, we were interested in revealing the impact of this reduction on the global deregulation of molecular pathways. In order to investigate this aspect, we used 2-dimensional (2D) pathway enrichment analysis as previously described (Cox & Mann, 2012). This analysis allows us to compare any two experimental samples or conditions and determine the correlated and anti-correlated changes between the two datasets. As shown in Figure 26, the correlation between the abundances of mRNA and protein was rather modest with Spearman correlation value ranging from 0.282 to 0.454- consistent with the previous studies showing the poor correlation between mRNA and protein (Schwanhausser et al., 2011).

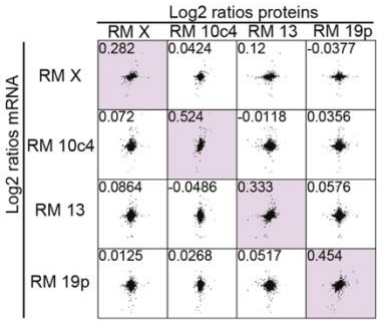

Figure 26. Correlation between the relative abundances of mRNA and protein. Scatter plots depicting the Spearman rank correlation coefficient between the relative abundances of mRNA and protein for all monosomies. The numbers in each plot represent the Spearman correlation coefficient.

However, comparison of pathway changes at transcriptional and proteome levels showed that the pathways changes are positively correlated in the respective monosomic cell line (Figure 27A, B S2 Blah).

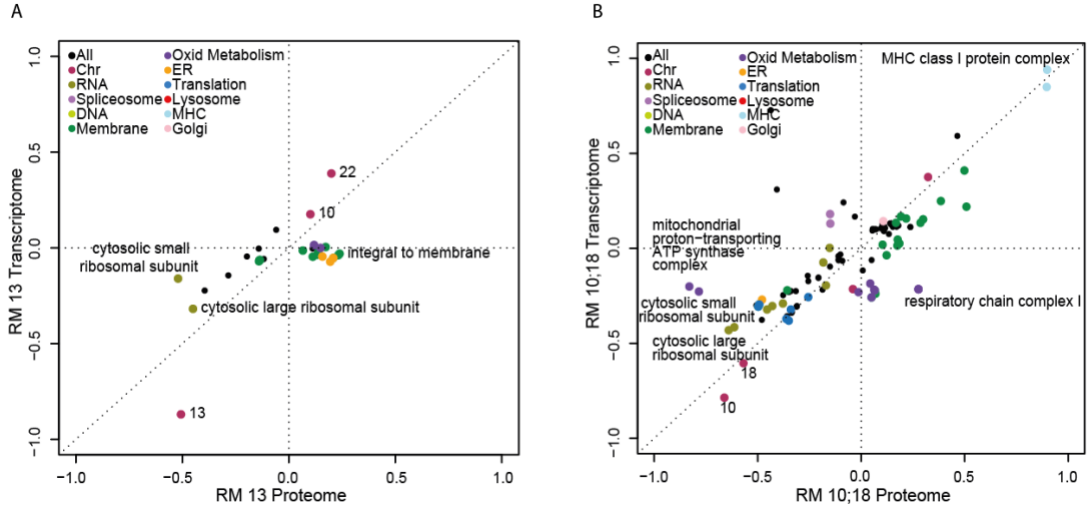

Figure 27. 2-dimensional pathway enrichment analysis of transcriptome and proteome of respective monosomic cell lines. 2D enrichment analysis based on the protein and mRNA changes in the monosomic cell line RM13 relative to the diploid parental cell line (**A**) and RM 10;18 (**B**). Each dot represents one category (GOBP, GOCC and chromosome location). Colors mark groups of related pathways as described in the inset. Axis-position represents scores of the pathways; negative values indicate downregulation; positive values indicate upregulation. Benjamini-Hochberg FDR Threshold < 0.02. With Paul Menges.

Next, we sought to compare previously obtained transcriptome and proteome of trisomic cell lines with monosomies to determine how gene expression is altered. Previous analysis of trisomic cell lines revealed that irrespective of the identity of the gained chromosome, majority of trisomic cell lines exhibited a uniform response, collectively called “aneuploidy stress responses (ASR)” (Durrbaum et al., 2014; Sheltzer et al., 2012). Comparison of the monosomy proteome datasets with two proteome datasets from RPE1 cell lines with extra chromosomes 5 and 12 (Rtr 5/12) and 21 (Rtr 21) revealed that the pathway deregulation in trisomies is different from that of monosomies (Figure 28A, Figure S).

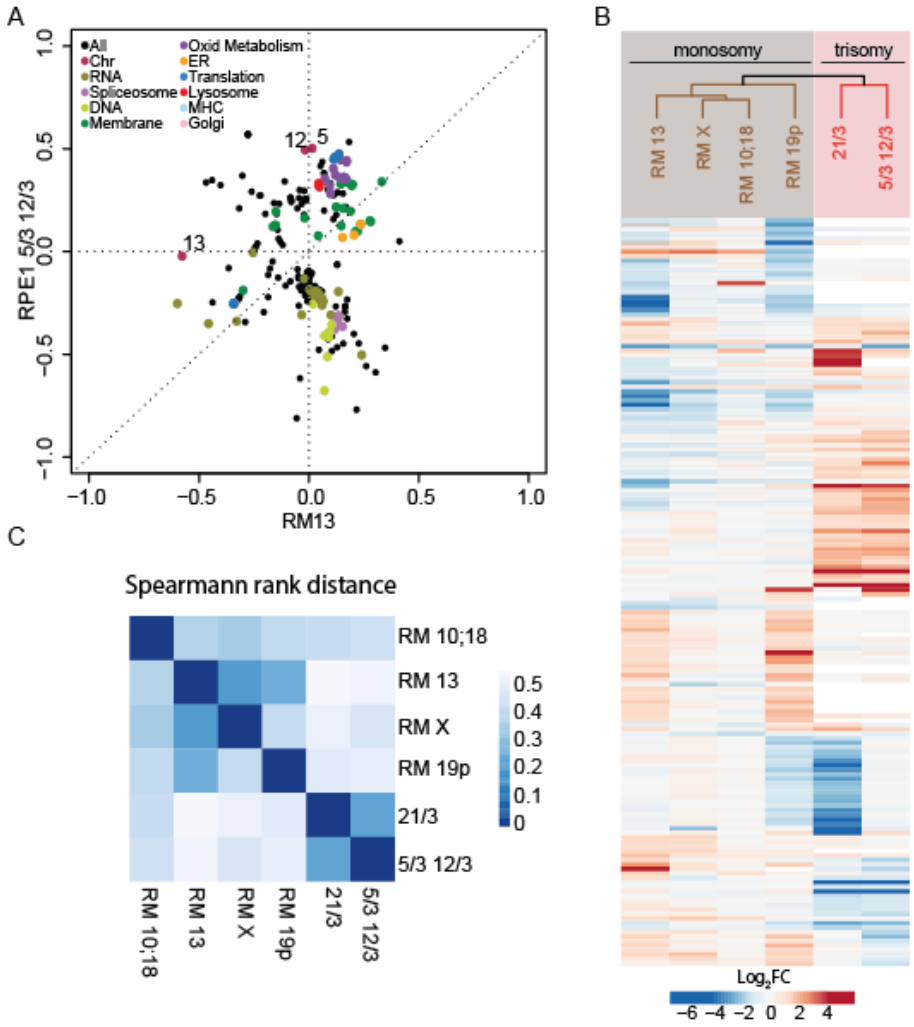

Figure 28. Responses to monosomies are different in comparison to trisomies. A. 2D pathway enrichment analysis comparing proteome of trisomy (RPE1 5/3 12/3) with monosomy (RM13), with Paul Menges. **B.** Heat map and clustering analysis of top differentially regulated proteins in monosomies and isogenic trisomies. Log_2FC of monosomy compared to diploid are depicted, Spearman correlation was used for the non-hierarchical clustering analysis. C. Distance matrix of the Spearman rank correlation of monosomic cell lines and trisomies. The Spearman distance metric is defined as the distance Spearman = (1- correlation Spearman)/2.

Unbiased clustering analysis of differentially expressed genes (genes outside log_2FC -1 and +1) showed that trisomies cluster together and away from monosomies (Figure 28B). Spearman rank correlation of all monosomies further confirmed the striking heterogeneity of genome-wide deregulation in monosomic and trisomic cell lines (Figure 28C). Based on our analysis, we conclude that ASR is specific to chromosomal gains and the responses to chromosome losses are heterogeneous.

Having determined that global responses to chromosome losses are different to chromosome gains, we were interested in identifying differentially expressed genes that emerged in response to the chromosome loss. For this purpose, we used proteome datasets and filtered for proteins with log_2FC greater than 1.5 or less than -1.5 folds and shared among at least two different monosomic cell lines. This analysis revealed only 5 upregulated and 13 down regulated proteins, suggesting that there is a little similarity in gene expression among different monosomic cell lines (Figure 29A, B).

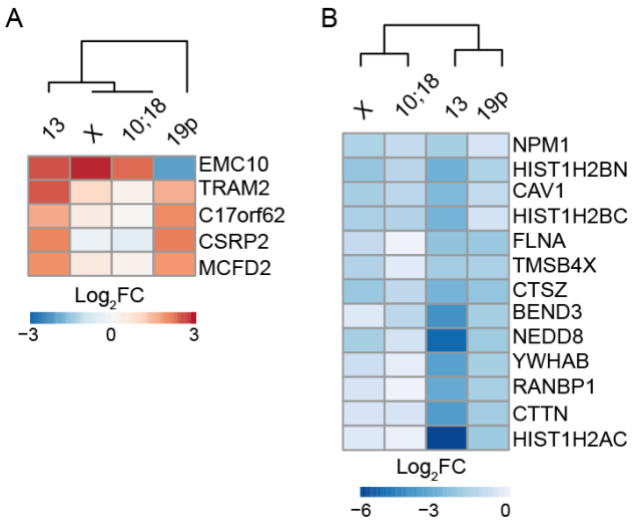

Figure 29. Differentially expressed genes and pathway deregulation in monosomies. A-B. Heat map of up and downregulated proteins, respectively, which were significantly altered in at least two monosomic cell lines. Log_2FC of monosomy compared to diploid are depicted. The proteins are filtered for Log_2FC outside -1.5 and +1.5.

All the analysis so far suggested that there is only limited shared common response to the monosomy in human cell. Consistently, pathway deregulation analysis and comparison of different monosomies showed that the deregulation of pathways is frequently specific for individual monosomic cell lines. For example, “MHC I and II protein complex” and immune related pathways (not shown on plot) were upregulated in RM 10;18 but downregulated in RM 13 (Figure 30A). Similarly, “O-glycan processing” was upregulated in RM X, while down regulated in RM 10;18 (Figure 30B). GO terms related to “Oxidative metabolism” was strongly downregulated in RM 10;18 and RM19p but upregulated in RM X (Figure 30B, C). Among the various pathways deregulated in monosomies, GO terms related to “Ribosomes” and “Translation” were the most consistently down regulated pathways among all the monosomies. Together,

these findings suggest that the cellular responses to chromosome losses differ from the responses to chromosome gains and that individual monosomic cell lines deregulate unique pathways.

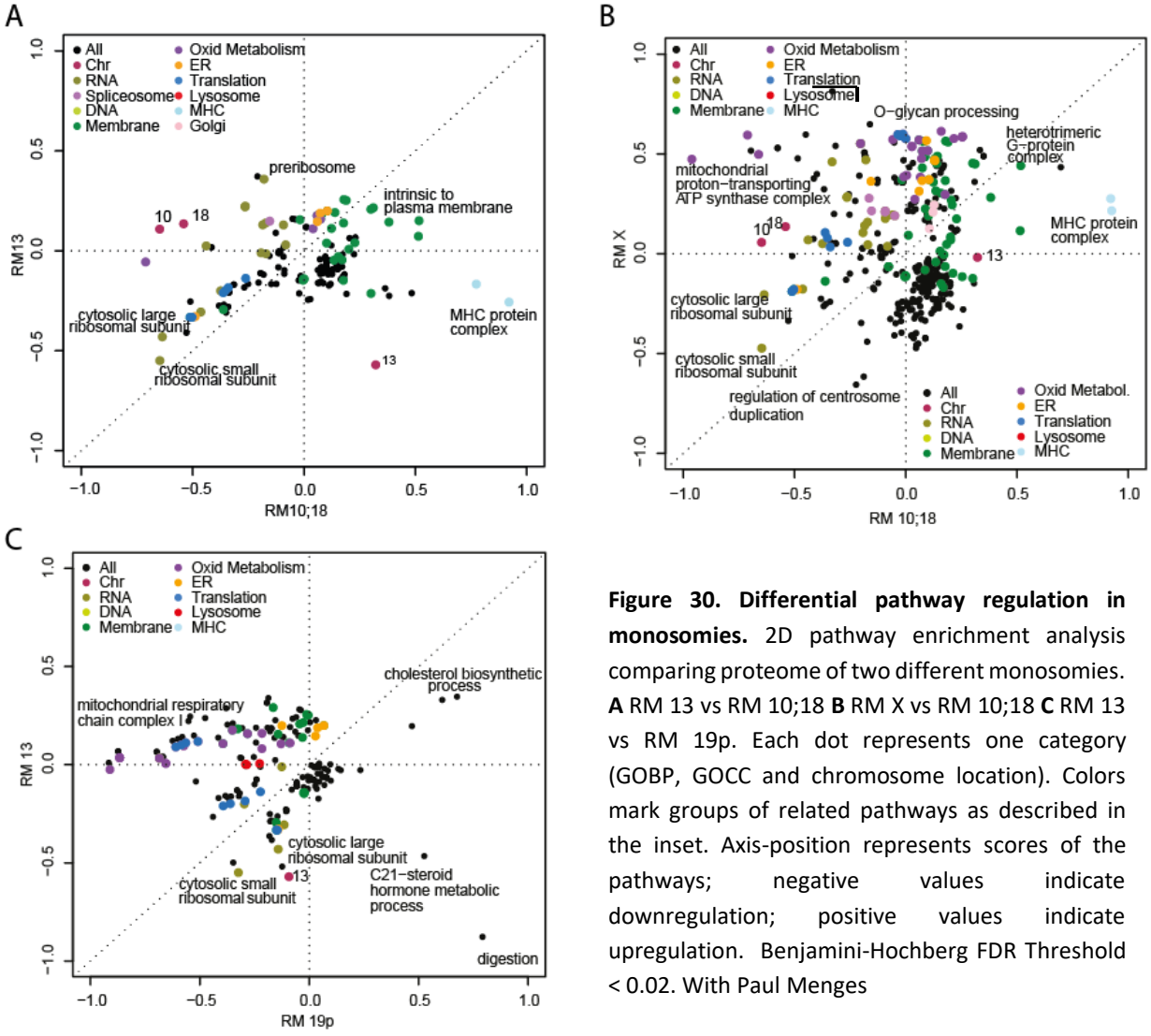

Figure 30. Differential pathway regulation in monosomies. 2D pathway enrichment analysis comparing proteome of two different monosomies. **A** RM 13 vs RM 10;18 **B** RM X vs RM 10;18 **C** RM 13 vs RM 19p. Each dot represents one category (GOBP, GOCC and chromosome location). Colors mark groups of related pathways as described in the inset. Axis-position represents scores of the pathways; negative values indicate downregulation; positive values indicate upregulation. Benjamini-Hochberg FDR Threshold < 0.02. With Paul Menges

3.3.3 Chromosome specific effects of monosomy

The transcriptome and proteome analysis showed that the cellular responses to chromosome losses is divergent compared to chromosome gains. Interestingly, the pathway alterations among different monosomic cell lines are inconsistent and an individual monosomic cell line up- or downregulated different pathways. To get a better insight and to validate these findings, we followed up on several pathways as discussed below.

3.3.3.1 Loss of chromosome 13 impairs transcriptional responses to interferon stimulation

One of the distinct differences we recognized in the 2D pathway enrichment analysis was the inverse correlation of pathways "interferon responses" and "MHC complex" in cell lines lacking chromosome 10 and chromosome 13. To validate these findings, we employed quantitative PCR to measure the abundance of different interferon stimulated genes (ISGs) upon treatment with various stimuli. ISGs are simply any genes that are stimulated by either type I IFNs or type II INFs or type III INFs. Once stimulated, such as during viral infection or treatment with recombinant interferons, several cascades of events lead to activation of ISGs (Schneider, Chevillotte, & Rice, 2014).

First, to validate our assay, we treated RPE1 WT cells with either Interferon β (1000 U) or polyinosinic:polycytidylic acid (Poly I:C) (1 µg) and measured the mRNA abundances of different ISGs. Interferon β is a recombinant interferon that stimulates ISGs when added to cell culture medium in dose dependent manner. Poly I:C is a immunostimulant, structurally identical to double-stranded RNA of some viruses (Matsumoto & Seya, 2008). As expected, the treatment resulted in a strong induction of ISGs, albeit to different levels. Poly I:C treatment resulted in maximal induction, while interferon treatment induced ISG expression to moderate levels (Figure 31).

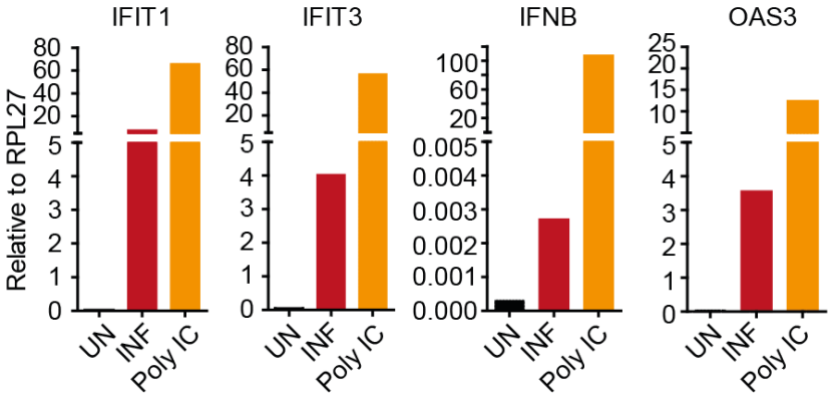

Figure 31. Expression of Interferon stimulated genes (ISGs) after treatment with Interferon β and Poly IC. mRNA expression of ISGs measured by quantitative PCR. All the values are normalized to the housekeeping gene RPL27. Bars show the expression from one experiment. UN- untreated, INF – treated with Interferon β.

Next, we treated monosomic cell lines and cell line 13_3 (Trisomy 13) with 1000 U of Interferon β and measured the abundance of ISGs. Although not statistically significant, the induction of ISGs was consistently diminished in RM 13, while they were unchanged or increased in RM 10 and RM 10;18 compared to control consistent with the proteome data (Figure 32). Interestingly, the induction of ISGs was increased in trisomic cell line 13_3 (Figure 32, *green bar*) suggesting that an yet to be identified gene or genes encoded on chromosome 13 is regulating the interferon responses.

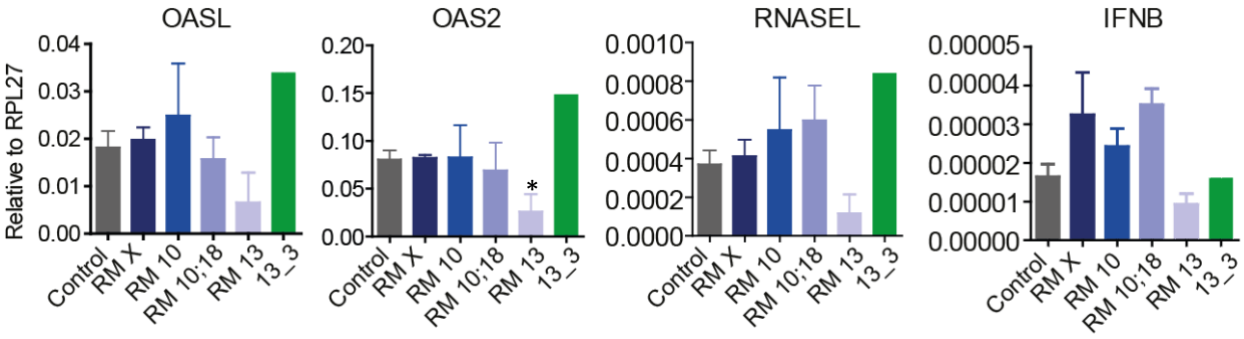

Figure 32. Expression of ISGs in monosomic and trisomic cell lines after treatment with Interferon β. mRNA expression of ISGs measured by quantitative PCR. All the values were normalized to the housekeeping gene RPL27. Bars show the mean and SEM of three independent experiments. For the trisomic cell line 13_3, only one replicate was performed. All the cell lines were treated with Interferon β (1000 U) for 8 h. *- p value < 0.05 derived using unpaired t-test. Rest of the values are statistically not significant.

3.3.3.2 Reduced expression of oxidative phosphorylation related genes in monosomy of 19p

Another interesting observation from our analysis of the proteomics data was the identification of alterations in mitochondrial pathways in various monosomic cell lines. 2D pathway analysis showed that GO terms related to mitochondria and oxidative phosphorylation were strongly downregulated in RM19p, while they were upregulated in RM X. To get a better insight, we filtered the datasets for mitochondria related genes with a log2FC outside -1 or 1 in at least one cell line, performed a clustering analysis and visualized as a heat map. We also included two trisomic cell lines for comparison. Clustering analysis revealed that while monosomies RM 10;18, RM 13 and RM X clustered together, RM 19p clustered together with the trisomic cell lines (Figure 33A). Further, a cluster of several genes was strongly downregulated in RM19p and 21_3 (Figure 33A, *black box*). This set of genes is probably responsible for the differences observed in the 2D pathway enrichment analysis.

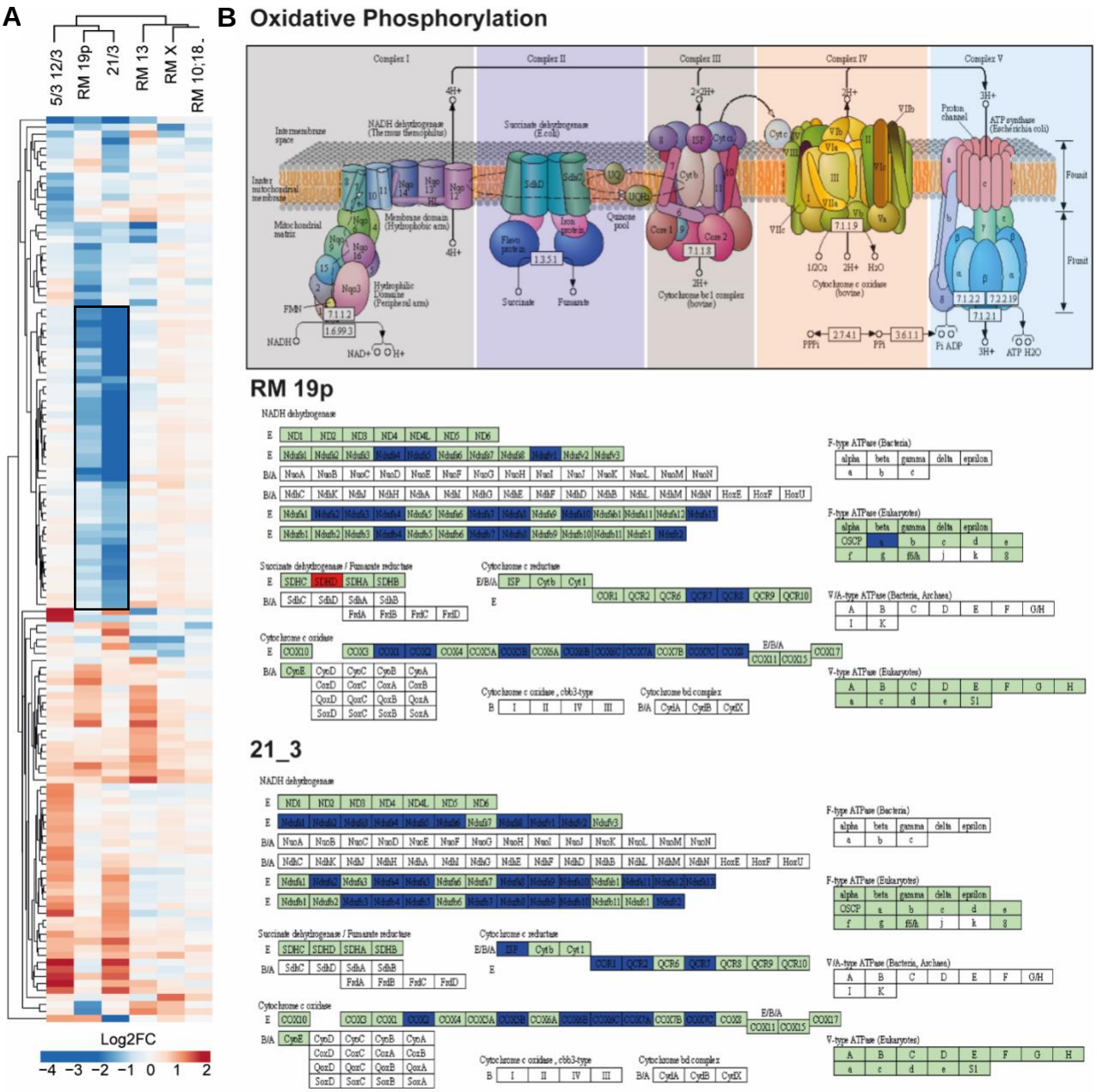

Figure 33. Mitochondria related pathway deregulation in monosomies. **A.** Heat map shows the genes of the GO terms associated with mitochondria. The genes were filtered for log2FC outside -1 and +1 in at least one cell line. **B.** *Top*: Individual complexes and steps of oxidative phosphorylation. *Bottom:* genes assigned to oxidative phosphorylation with fold changes outside -1 and +1 in RM 19p and 21_3 was mapped using KEGG mapper. Blue color denotes downregulation and red upregulation.

To investigate which of the mitochondrial genes were specifically differentially expressed, we performed statistical overrepresentation analysis using the web-based tool Panther. The analysis showed that a majority of genes belonged to oxidative phosphorylation pathway (Table 2). Further, KEGG mapping

revealed that large number of these genes belonged to NADPH dehydrogenase complex Cytochrome c oxidase complex (Figure 33B). However, these changes were specific only to cell lines RM 19p and 21_3. The underlying causes for these chromosome specific changes remain to be investigated.

Table 2. Statistical overrepresentation analysis of mitochondria related genes

The analysis was performed using Panther.db. Reference list (no. of genes belonging to process), Input (no. of monosomic genes belonging to process). P-value was calculated using Fischer exact test. FDR- False discovery rate (0.05).

GO biological process complete	Reference List	Input	fold Enrichment	raw P-value	FDR
oxidative phosphorylation	119	46	61.06	8.29E-65	1.32E-60
ATP synthesis coupled electron transport	89	43	76.32	7.90E-64	4.20E-60
mitochondrial ATP synthesis coupled electron transport	88	43	77.19	5.35E-64	4.27E-60
respiratory electron transport chain	108	44	64.35	1.04E-62	4.13E-59
electron transport chain	175	48	43.33	1.13E-61	3.62E-58
cellular respiration	158	46	45.99	5.21E-60	1.38E-56
generation of precursor metabolites and energy	411	56	21.52	1.88E-57	4.28E-54
ATP metabolic process	207	47	35.87	5.96E-57	1.19E-53
energy derivation by oxidation of organic compounds	228	46	31.87	1.36E-53	2.42E-50
oxidation-reduction process	962	64	10.51	2.92E-48	4.65E-45

3.3.3.3 Loss of chromosome 10 provides resistance to anti-cancer drug Paclitaxel

An experiment performed by our collaborator Jason Sheltzer (CSHL, USA) to investigate the mechanisms of Paclitaxel resistance revealed that the Paclitaxel resistant clones routinely lost chromosome 10. This suggests that loss of heterogeneity (LOH) of genes encoded on chr.10 could be responsible for the resistance. To validate this finding, we used monosomic cell lines for chr.10, treated them with an increasing concentration of paclitaxel for 72 h and measured the viability. We included RM 13 to test whether the resistance is a general response to monosomy, or a specific to the loss of chromosome 10.

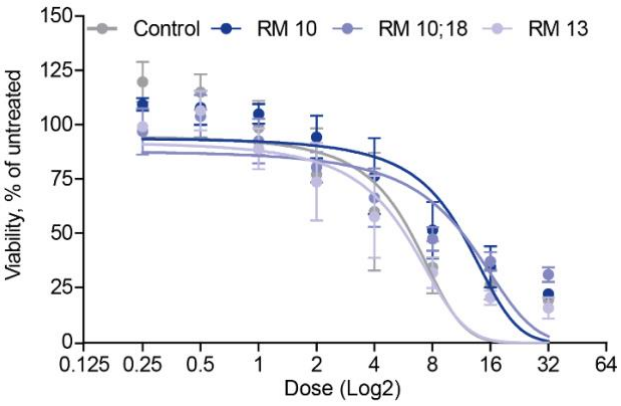

Consistent with our collaborator's findings, cell lines lacking chromosome 10 displayed an increased resistance to Paclitaxel treatment compared to the control and RM 13 cell line (Figure 34).

Figure 34. Loss of chromosome 10 increases resistance to Paclitaxel. Control and monosomic cells are treated with increasing doses of Paclitaxel. DMSO was used as a solvent control. All the values are normalized to DMSO control. Each point represents mean with SD of 5 independent experiments.

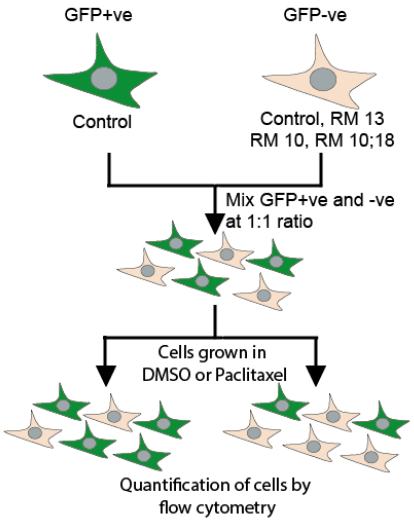

In order to directly validate if the loss of chromosome 10 provides growth advantage when treated with paclitaxel, we designed a cell competition assay. In this assay, the control cells expressing GFP was mixed in equal proportions with control and monosomic cells lacking GFP and grown in the presence of solvent control DMSO or paclitaxel at 8nM concentration. This concentration was chosen based on the paclitaxel dose response curves from figure 24. The proportion of cells in each competition was measured by flow cytometry (Figure 35).

Figure 35. Schematic outline of cell competition assay. Equal proportion of GFP positive and negative cells were mixed and grown in the presence of either DMSO or paclitaxel. The proportion of each cells were quantified by flow cytometry.

If the paclitaxel provides growth advantage to the cells compared to DMSO, then the proportion of cells increases over time in the presence of paclitaxel compared to DMSO. While the proportion of cells in DMSO and paclitaxel is not drastically changed in mixtures of control and RM 13, cell lines containing monosomy of 10, RM 10 and RM 10;18 outgrew the control cells treated with paclitaxel confirming that loss of chromosome 10 provides resistance to paclitaxel (Figure 36).

Taken together, these findings suggest that gene(s) encoded on the chromosome 10 are essential for the cell growth in the presence of paclitaxel. Future studies should aim to identify the genes responsible for this phenotype.

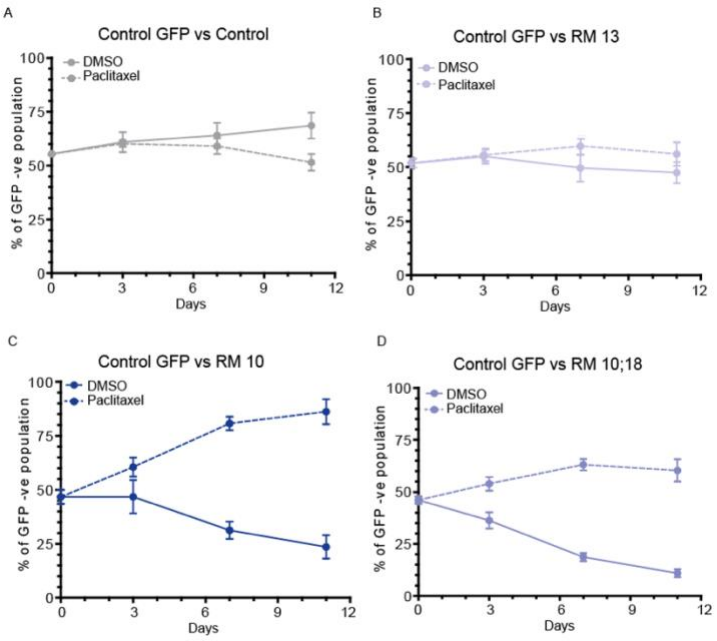

Figure 36. Loss of chromosome 10 confers resistance to paclitaxel. A-D Equal number of control GFP+ve cells were mixed with GFP-ve control and monosomic cells. The proportion of GFP+ve and -ve cells were quantified by flow cytometry. % of GFP-ve cells in cell mixtures treated with DMSO or paclitaxel are plotted. Each point represents the mean with SEM of 3 independent experiments.

3.4 Impaired ribosome biogenesis and translation are common defects in monosomies

3.4.1 Cytosolic ribosome subunit genes are consistently downregulated in monosomies

2D-enrichment analysis performed with different monosomies revealed consistent downregulation of pathways “translation” and “ribosomes”. However, this analysis did not show whether all of the genes in these pathways were downregulated, or only a few genes were affected. Therefore, we plotted the protein expression values of cytosolic ribosomal small and large subunits as a heat map. This visualization showed that majority of cytosolic small and large subunits genes were down regulated to different levels in monosomies, regardless of the identity of chromosome where they are located (Figure 37).

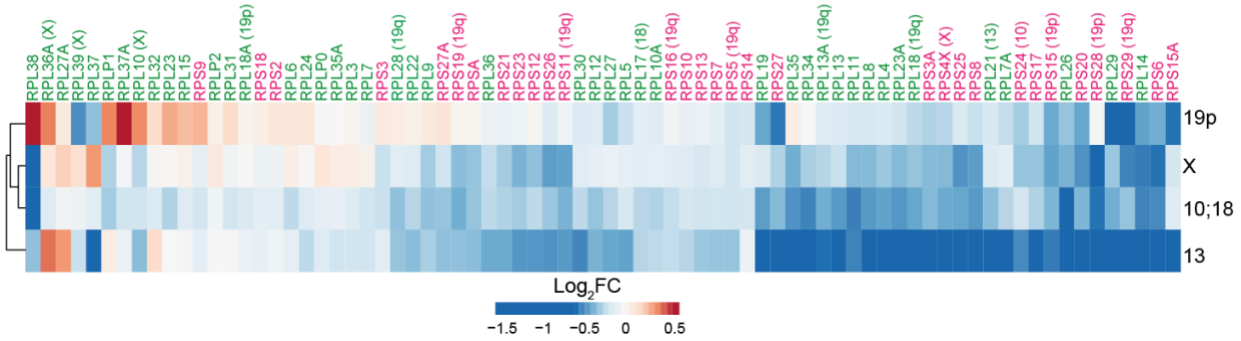

Figure 37. Cytosolic large and small subunit protein expression in monosomies. Heat map depicting the protein expression of ribosomal proteins in different monosomies. In brackets is the chromosome number for relevant ribosomal protein genes (RPGs). Ribosomal large subunit proteins (green) and small subunit proteins (pink) were included.

3.4.2 Protein synthesis is reduced consistently in all monosomies

Ribosome is an important organelle involved in translation of mRNA into protein. Therefore, we hypothesized that reduced ribosomal subunit gene (RPG) expression would impair translation. To determine translation activity, we used a puromycin-incorporation assay. In this assay, actively proliferating cells were treated with a short pulse of antibiotic puromycin (analog to aminoacyl-tRNA) (see Methods for details), which gets incorporated into the nascent polypeptide chain (Starck, Green, Alberola-Ila, & Roberts, 2004). Immunoblotting of cell lysates with an anti-puromycin antibody therefore approximates the translation rate in the cells. Indeed, translation was significantly decreased in all tested monosomic cell lines (Figure 38A, B). In yeast, growth rate correlates with the total translation levels (Cheng et al., 2019). In order to ascertain that the translation in monosomies is not reduced due to a slower proliferation, we measured the translation rate in trisomic cells, which proliferate similarly or slower than monosomic cells. Strikingly, we did not observe a uniform defect in puromycin incorporation in trisomic cells (Figure 38A, B).

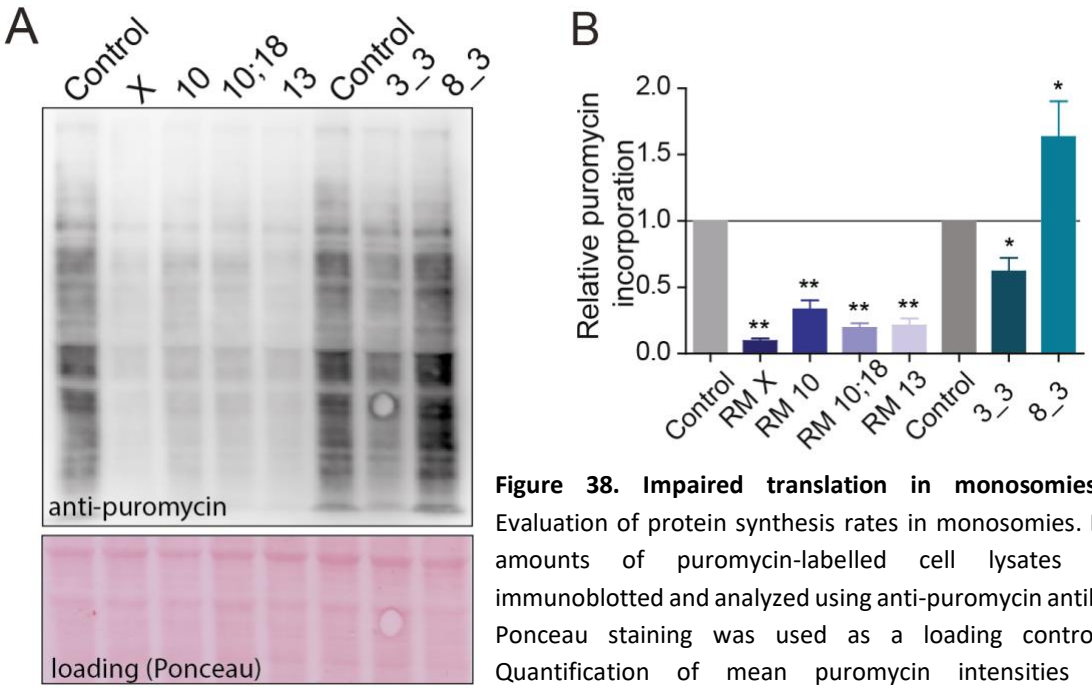

Figure 38. Impaired translation in monosomies. A. Evaluation of protein synthesis rates in monosomies. Equal amounts of puromycin-labelled cell lysates were immunoblotted and analyzed using anti-puromycin antibody. Ponceau staining was used as a loading control. **B.** Quantification of mean puromycin intensities from immunoblotting. The intensities were normalized to the Ponceau staining. Bars display mean ± SEM of at least three independent experiments. Non-parametric t-test; *<0.05, **< 0.005

3.4.2.1 Impaired translation in monosomies is not due to defects in mTOR pathway or activation of integrated stress response (ISR)

mTOR pathway is one of the important regulators of eukaryotic protein synthesis and ribosomal subunit gene expression (Iadevaia, Liu, & Proud, 2014). Since monosomies showed general reduction of ribosomal subunit genes and reduced translation in monosomies, we performed immunoblotting of the mTOR target p70S6K and its phosphorylation to evaluate the mTOR pathway activity. This demonstrated that there is no reduction of mTOR activity in monosomies (Figure 39A, B). Recent analysis of Down syndrome mice models and Down syndrome patients' derived cell lines identified translation defect similarly as in monosomies. However, the translation defect in Down syndrome was attributed to integrated stress response (ISR) (P. J. Zhu et al., 2019). Increased phosphorylation of eukaryotic initiation factor 2 alpha (eIF2α) is a marker of ISR (Pakos-Zebrucka et al., 2016). To test whether the reduced translation in monosomies is due to ISR activation, we performed immunoblotting of p-eIF2α, which showed no uniform increase of phosphorylation in monosomies. In fact, an increased phosphorylation level was identified

only in only RM 10;18 (Figure 39A, B). Together, our findings suggest that the decreased translational activity in monosomic cells is not caused by reduced mTOR activity or by activation of ISR.

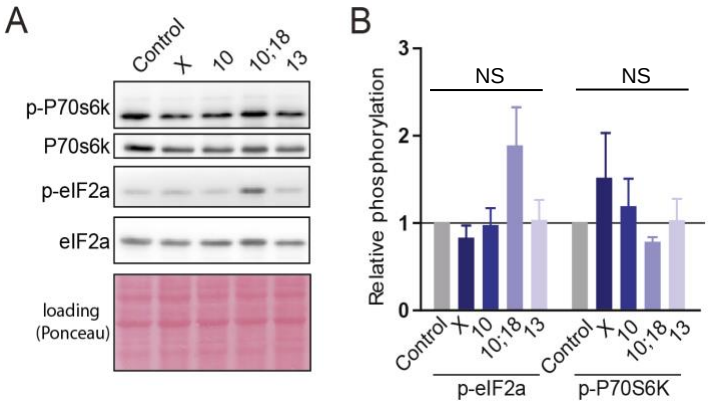

Figure 39. Impaired translation of monosomies is not due to reduced mTOR activity or integrated stress response (ISR). A. Immunoblotting of mTOR target p70S6k and phospho-p70S6K and the integrated stress response marker eIF2α and phospho-eIF2α. **B.** Quantification of relative phosphorylation levels of P70S6K and eIF2α normalized to total protein levels, respectively. Bar graphs display mean ± SEM of at least 3 independent experiments. NS-not significant.

3.4.3 Ribosome biogenesis is impaired in monosomies

To elucidate the nature of the translation defects in monosomic cell lines, we performed polysome profiling to determine the fraction of polysomes, 80S monosomes (composed of one ribosome residing on an mRNA), as well as unassembled small (40S eukaryotes, SSU) and large (60S in eukaryotes, LSU) ribosome subunits (Figure 40A). Polysome profiling revealed that the monosomic cell lines accumulated more individual ribosomal subunits than the parental diploid cell line and the ratio of unassembled large and small ribosomal subunits was altered (Figure 40A, B, C). Interestingly, the monosomic cell lines appear to contain more polysomes than the parental control (Figure 40A). The underlying reason for this finding remains to be investigated.

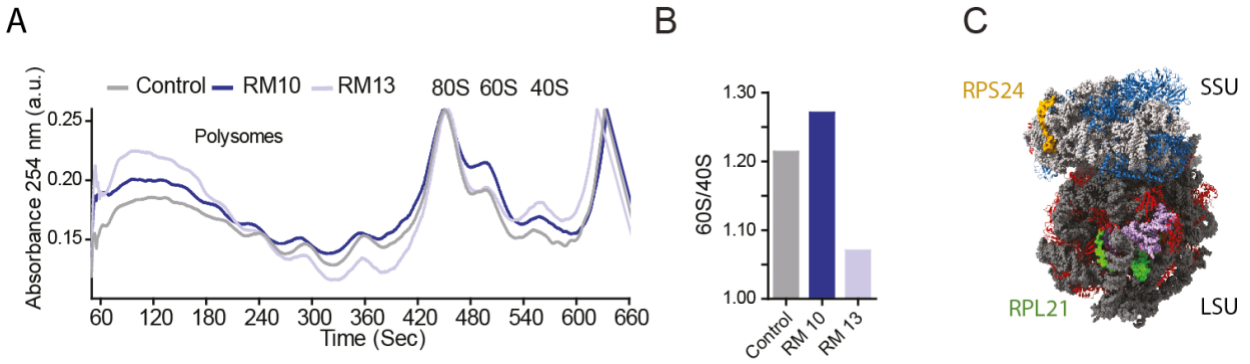

Figure 40. Polysome profiling of monosomies. A. Polysome profiles obtained from diploid and monosomic cell lines. Profiles are representative of at least two independent experiments. The profiles were adjusted to the 80S peak. **B.** Quantification of 60S/40S ratio of the representative polysome profiles. Peak absorbance for 60S and 40S were used for the calculations. **C.** Ribosome model shows the location of RPS24 (yellow) and RPL21 (green) proteins within the small and large ribosome subunit, respectively. C – courtesy of Vincent Gotsmann.

Ribosome biogenesis is an intricate multi-step process involving rRNA transcription and processing, ribosomal subunit synthesis, assembly and transport (Pelletier et al., 2018). Errors in any of the multi-step process would affect the ribosome synthesis and eventually translation. Our findings from polysome profiling and omics analysis indicate that indeed ribosome biogenesis is impaired in monosomies. In the next step, we investigated whether the rRNA transcription and processing is impaired in monosomies. To this end, we performed qPCR of different rRNAs, which revealed that the abundance of individual rRNAs is differentially expressed when compared to diploid control (Figure 41). However, the differences are not statistically significant and no consistent differences in the rRNA levels were observed among the monosomies. This suggests that the rRNA processing is not impaired in response to monosomy.

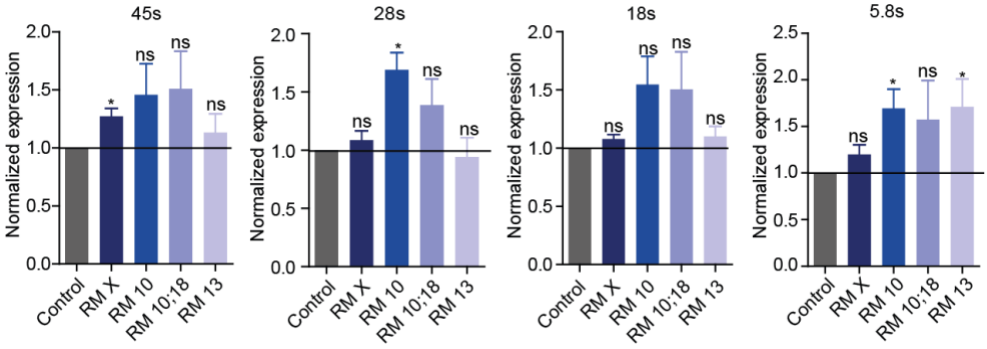

Figure 41. Expression of pre-rRNA and processed rRNA in monosomies. Quantitative PCR was performed from the cDNA synthesized using total RNA extracted from monosomies. Bars display the mean ± SEM of at least 4 independent experiments. *- p value <0.05. ns-not significant. P value was measured using Wilcoxon matched pair test.

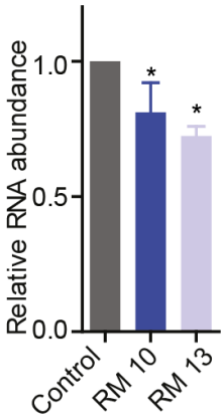

Finally, we determined the amount of total RNA in monosomic cells compared with the parental control. Since rRNA represents approximately 80% of all RNA in eukaryotic cells, the total RNA amount can serve as a proxy for rRNA abundance and ribosome content (Ebright et al., 2020). Strikingly, RM10 and RM13 comprised significantly less total RNA compared to the parental control (Figure 42). Based on our findings, we conclude that ribosome biogenesis is impaired in monosomies, most likely due to reduced expression of RPG.

Figure 42. Ribosome content in monosomies. Measurement of total RNA as a surrogate for rRNA levels and ribosome content. Bar graphs display the mean ± SEM of at least 3 independent experiments. Non-parametric T test. *0.03.

3.4.4 Haploinsufficiency of ribosome subunit gene (RPL21) caused by monosomy (RM 13) impairs translation

In humans, with the exception of chromosomes 7 and 21, every chromosome carries at least one RPG. Most of the RPGs are essential and are known for their haploinsufficiency (Danilova & Gazda, 2015). Therefore, we hypothesized that the impaired translation and ribosome biogenesis might be due to haploinsufficiency of RPGs caused by monosomy.

In order to validate our hypothesis, we used RNAi approach to deplete RPGs to the levels observed in monosomies. We depleted RPL21, the only RPG encoded on Chr.13, to the levels observed in RM 13 using siRNA and determined its impact on the translation using puromycin incorporation assay. Titrated knock down of Rpl21 resulted in a depletion of Rpl21 to approximately 50 % of the wild type abundance (Figure 43A, B).

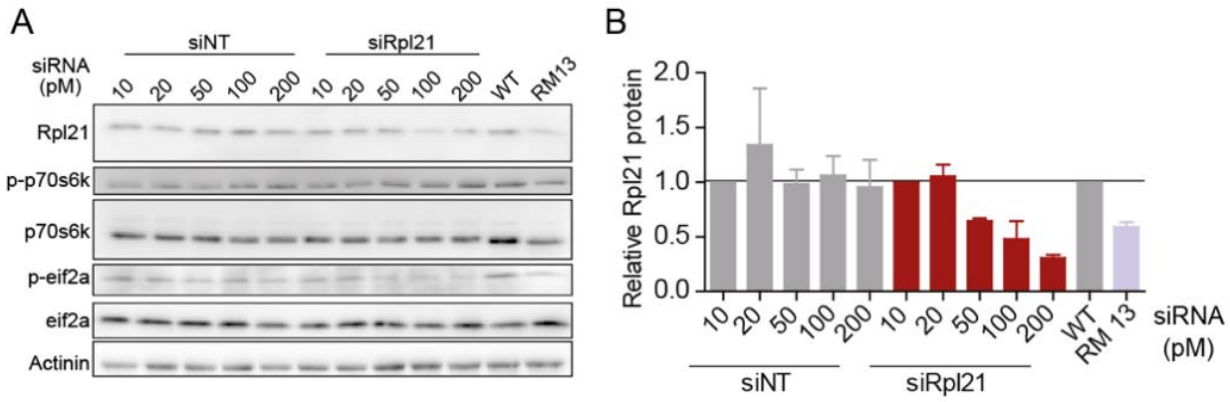

Figure 43. SiRNA mediated depletion of Rpl21. A. siRNA mediated titrated knockdown of RPL21 in RPE1 WT p53 KO cell line. siNT was used as a control; RPE1 p53 KO WT and RM 13 are shown as a non-transfected control. The western blots are representative of at least three independent experiments. **B.** Quantification of Rpl21 knock down efficiency. siNT and siRPL21 values were normalized to respective 10 pm samples. Bars display the mean ± SEM of at least 3 independent experiments.

Importantly, the knockdown of RPl21 resulted in a translation reduction similarly as in RM 13 cell line (Figure 44A, B).

Analysis of the activity of mTORC1 via phosphorylation of its target p70S6K (mTOR target) and analysis of p-eIF2α, a marker of integrated stress response, revealed no significant changes in phosphorylation of these proteins upon *RPL21* knock down (Figure 43A). Thus, in agreement with the observation in monosomic cells, the general translation machinery is not inhibited. Our findings therefore suggest that the haploinsufficiency of ribosomal subunit genes caused by monosomy is responsible for the impairment

of ribosomal biogenesis and reduced translation. Don't you want to add the data on RPS24? Even just briefly?

Data about rescue?

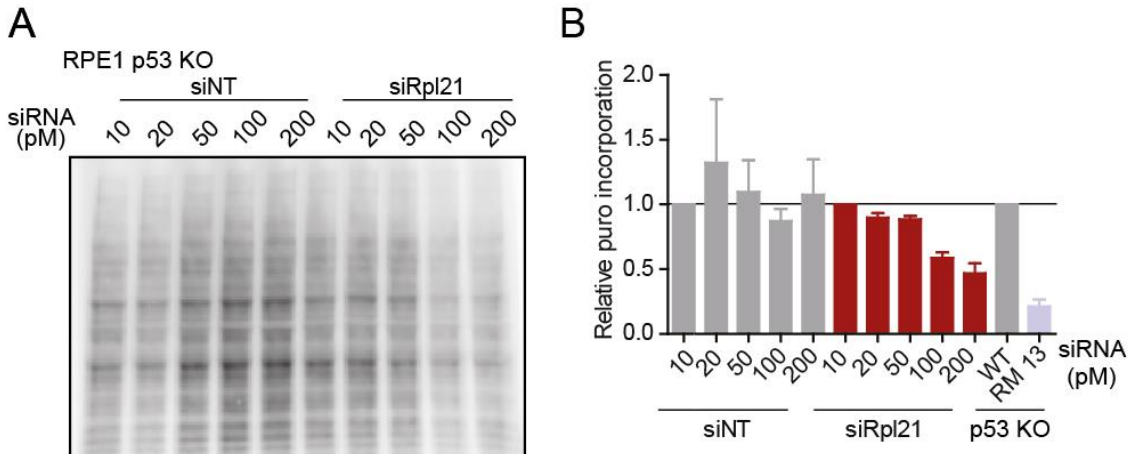

Figure 44. The impact of siRNA mediated knockdown of RPL21 on protein synthesis. A. Equal amounts of protein lysates from siNT and siRPL21 samples were immunoblotted against anti-puromycin antibody. Ponceau staining was used as a loading control. The western blots are representative of at least three independent experiments. **B.** Quantification of relative translation rate after RPL21 knockdown. siNT and siRPL21 values were normalized to respective 10 pm samples. Bars display the mean ± SEM of at least 3 independent experiments.

3.5 Impact of the p53 on the viability of monosomies

Since all the monosomic cell lines that we obtained so far are generated in a p53 negative background, we were interested to uncover the impact of p53 on the viability of monosomies. For this purpose, we transfected the RPE1 p53 KO and the respective monosomic cell lines with various different plasmids carrying WT *TP53* gene and its canonical cancer mutants (R273H and R175H), and an empty plasmid as a control. Immunoblotting of p53 96 h post transfection confirmed the expression of p53 in all cell lines, although at different levels, which was attributed to the differences in transfection efficiencies (Figure 45). However, immunoblotting after four weeks of antibiotic selection revealed that while control cell line retained the expression of p53 and its mutants, the p53 expression in all of the monosomic cell lines was lost, with the exception of mutant p53 expression in RM 13 (Figure 45). This suggests that monosomic cells do not tolerate p53 expression and thus cells expressing p53 or its mutants are eliminated during the antibiotic selection. We were surprised to see that the mutant p53 expression was also lost during selection, since these mutations render p53 transcriptionally inactive (Boettcher et al., 2019)(Figure 45).

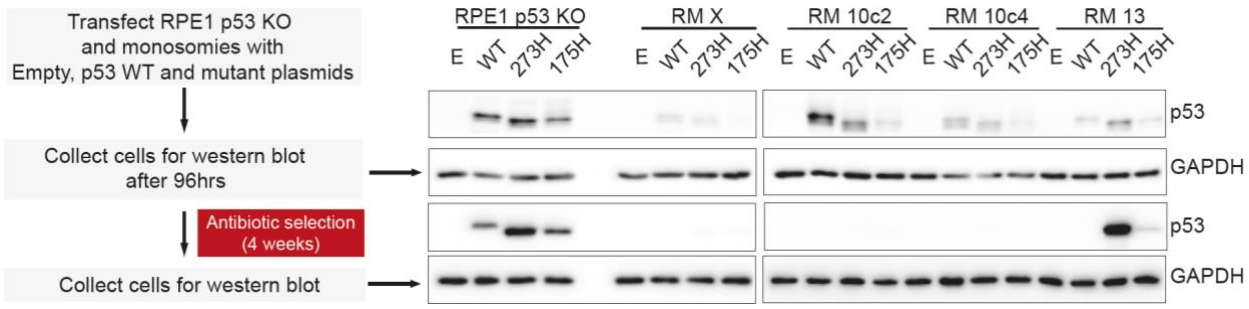

Figure 45. Monosomies are sensitive to p53 expression. On the left, schematic depiction of the experimental scheme to express p53 and mutant plasmids. On the right, immunoblotting of p53 and a housekeeping gene (GAPDH). GAPDH serves as a loading control.

3.5.1 Restoration of p53 expression in monosomic cell lines

To better understand the role of p53 in monosomic cell lines and due to the limited viability of monosomies with p53, we generated cell lines in which the p53 expression can be controlled in time and dose dependent manner. For this purpose, we employed a tetracycline-inducible gene expression system, where the gene of interest can be expressed reversibly by addition of tetracycline or its derivatives. After transfection and single cell cloning (see Methods for details), we screened for several clones to obtain clones with p53 expression and still maintaining the respective monosomic karyotype. This resulted in one clone each for monosomic cell lines RM 10;18 and RM 13, respectively, which we labelled as RM 10 ip53

and RM 13 ip53, respectively. The karyotype was confirmed by chromosomal painting (Figure 34). As an isogenic control, we obtained RPE1 p53 KO cell line with inducible p53 expression (RPE1 ip53).

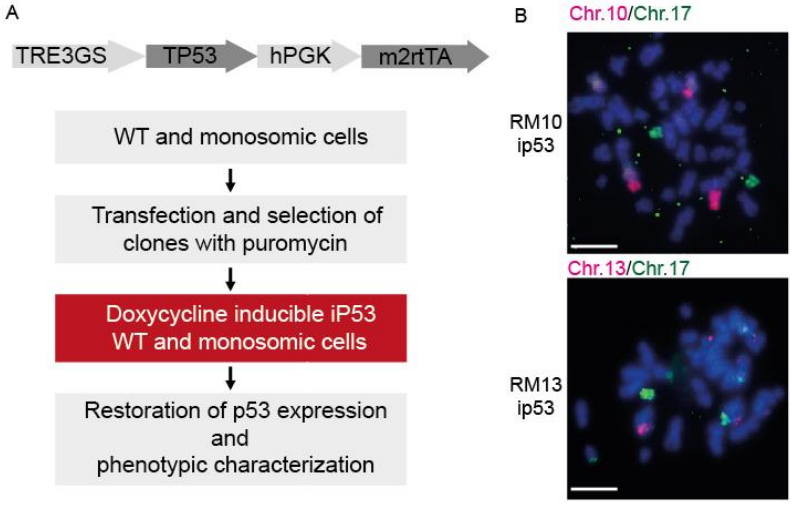

Figure 34. Generation of doxycycline inducible p53 monosomic cell lines. A. Schematic shows the steps involved in generation of ip53 monosomic cell lines. **B.** Chromosomal paints of monosomic cell lines. The painted chromosomes are indicated with respective colors. Scale bar – 10 µm.

3.5.2 Titration of the p53 expression levels

Next, we sought to determine the amount of doxycycline required to induce suitable p53 expression. Our aim was to restore p53 expression to the levels observed in RPE1 p53 +/+. For this purpose, we treated the cells with increasing dose of doxycycline and with doxorubicin (1 µM) to evaluate the expression levels of p53 and its functionality. As a control for the p53 expression, we used RPE1 p53+/+ cell line. Immunoblotting of p53, p-p53 (Ser 15) and p21 revealed that the doxycycline induced the p53 expression in a dose dependent manner (Figure 47). Further, doxorubicin treatment increased the phosphorylation of p53 and p21 expression, thus suggesting that the p53 is functional (Figure 47). For our further experiments, we used doxycycline dosage that resulted in expression levels similar to the RPE1 p53+/+ cell line.

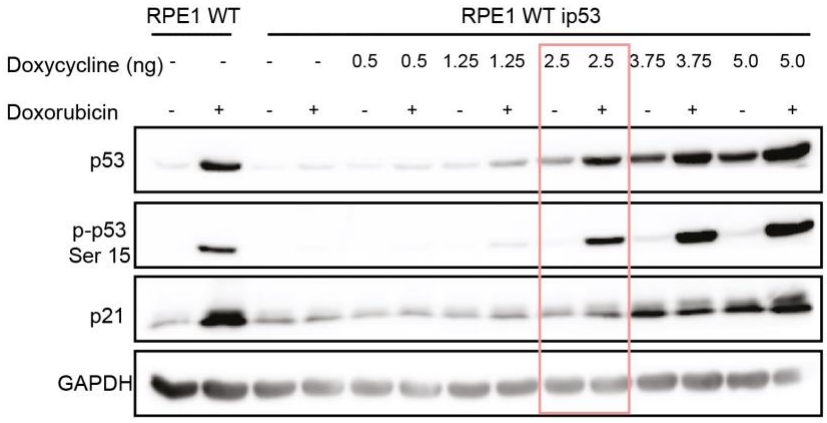

Figure 47. Functional evaluation of p53 inducible cell line with titrated doxycycline treatment. Immunoblotting of the protein lysates prepared from RPE1 WT (p53 positive and RPE1 WT ip53. Antibodies against p53, phospho-p53, p21 and GAPDH were used. GAPDH serves as loading control. Doxorubicin was used to induce DNA damage. The red box depicts the dose that induces p53 to the levels as in RPE1 WT cell line.

3.5.3 Expression of p53 is not tolerated by monosomies

To study the impact of p53 on the monosomies, we restored the expression of p53 by addition of doxycycline to the culture medium and incubated for 24 h and 120 h. Immunoblotting of cell lysates at these time points revealed that while at 24 h there was a strong expression of p53 in control and in monosomic cell lines, the expression gradually decreased by 120 h specifically in monosomies (Figure 48A, B). This finding suggests that the cells with p53 expression are either outgrown by cells without p53 expression, or that they are being eliminated by so far unknown mechanisms. This finding is in agreement with the transient transfection experiment (Figure 45) of monosomies, thus providing an independent evidence for the negative effect of p53 on monosomies.

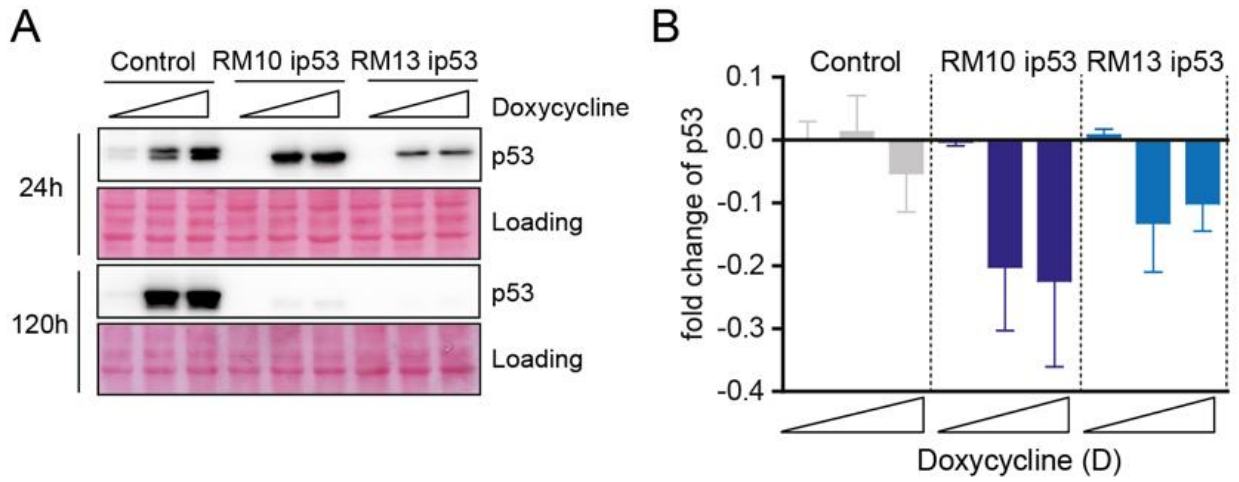

Figure 48. Expression of p53 is reduced in monosomies over time. A. Immunoblotting of p53 after an induction with doxycycline for 24 h and 120 h. Ponceau staining was used as a loading control. **B.** Quantification of the p53 intensities. The plots display the mean differential expression of p53 at 24 and 120 h of doxycycline treatment. All values were normalized to the respective loading control.

Single cell imaging analysis of p53 expression by immunofluorescence showed that the expression of p53 is heterogeneous among cell population. Quantification of cells expressing the p53 identified that the number of cells expressing p53 at 48 h is higher in diploid cell line compared to monosomies (Figure 49A, B). Further, the number of p53 expressing cells gradually reduced in monosomies by 96 h and 144 h while the control still retained the expression (Figure 49B). This demonstrates that the presence of p53 results in elimination of monosomic cells either by apoptosis or senescence. Alternatively, the p53 positive cells may be outgrown by the p53 negative cells.

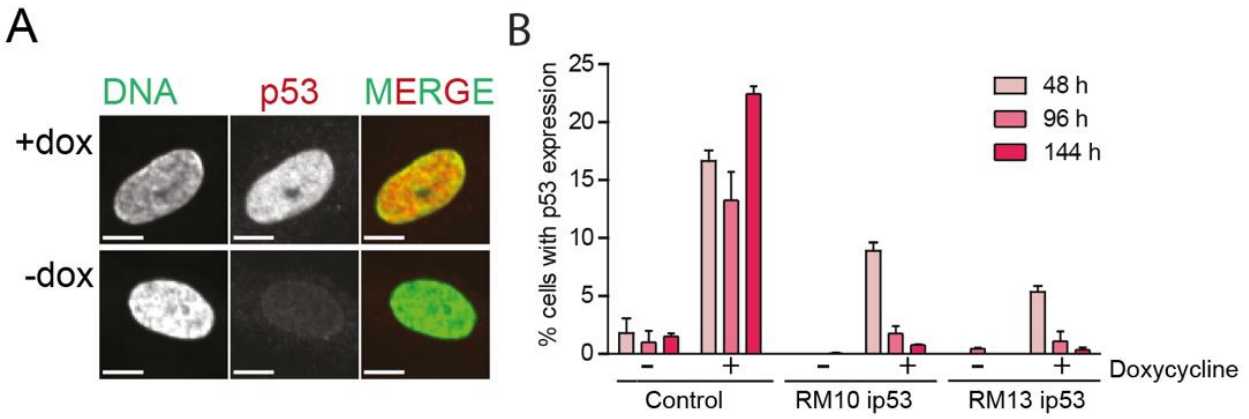

Figure 49. Single cell expression analysis of p53 by immunofluorescence staining. A. Representative images showing the cells with and without p53 expression. Dox- Doxycycline. DNA (Sytox green) and p53 (Red). Scale bar-10µm. **B.** Quantification of cells expressing p53 after 48 h, 96 h and 144 h of doxycycline treatment. Bars display the mean with SEM of two independent experiments.

3.5.4 Transcriptome analysis identifies the p53 pathway activation in monosomies

To obtain a global view on the impact of p53 on monosomies, we analyzed transcriptome changes in monosomic cells with restored p53 expression by RNA sequencing of RPE1 ip53, RM10ip53 and RM13ip53 after 48 h of doxycycline treatment**.** We choose 48 h, because the cells would have undergone at least one cell cycle in the presence of p53. Next, we addressed two important questions using the transcriptome data. 1) What is the impact of p53 on the cellular responses to monosomy? 2) How does monosomy affect the p53 pathway activity?

To address the first question, we normalized the transcriptome data of monosomies with and without p53 to the control cell lines with and without p53, respectively. This would allow us to identify the changes induced by p53 expression towards monosomic cellular responses. To do so, we filtered for genes with log_2FC outside -2 and +2 and visualized as a heat map. Interestingly, this analysis revealed that the gene expression remains largely unaltered in the presence of p53 (Figure 50A), suggesting that p53 has a minimal impact on the global gene expression caused by monosomy. To address the second question, we compared the transcriptome of doxycycline (p53+) treated and untreated (p53-) conditions in control and monosomic cell lines, respectively. We generated volcano plots to visualize the most significantly deregulated genes in the presence of p53 in control and in monosomies (Figure 50B, C). Interestingly, after p53 restoration, the p53 targets were significantly upregulated in monosomic cell lines, thereby suggesting that the p53 pathway is activated due to monosomy.

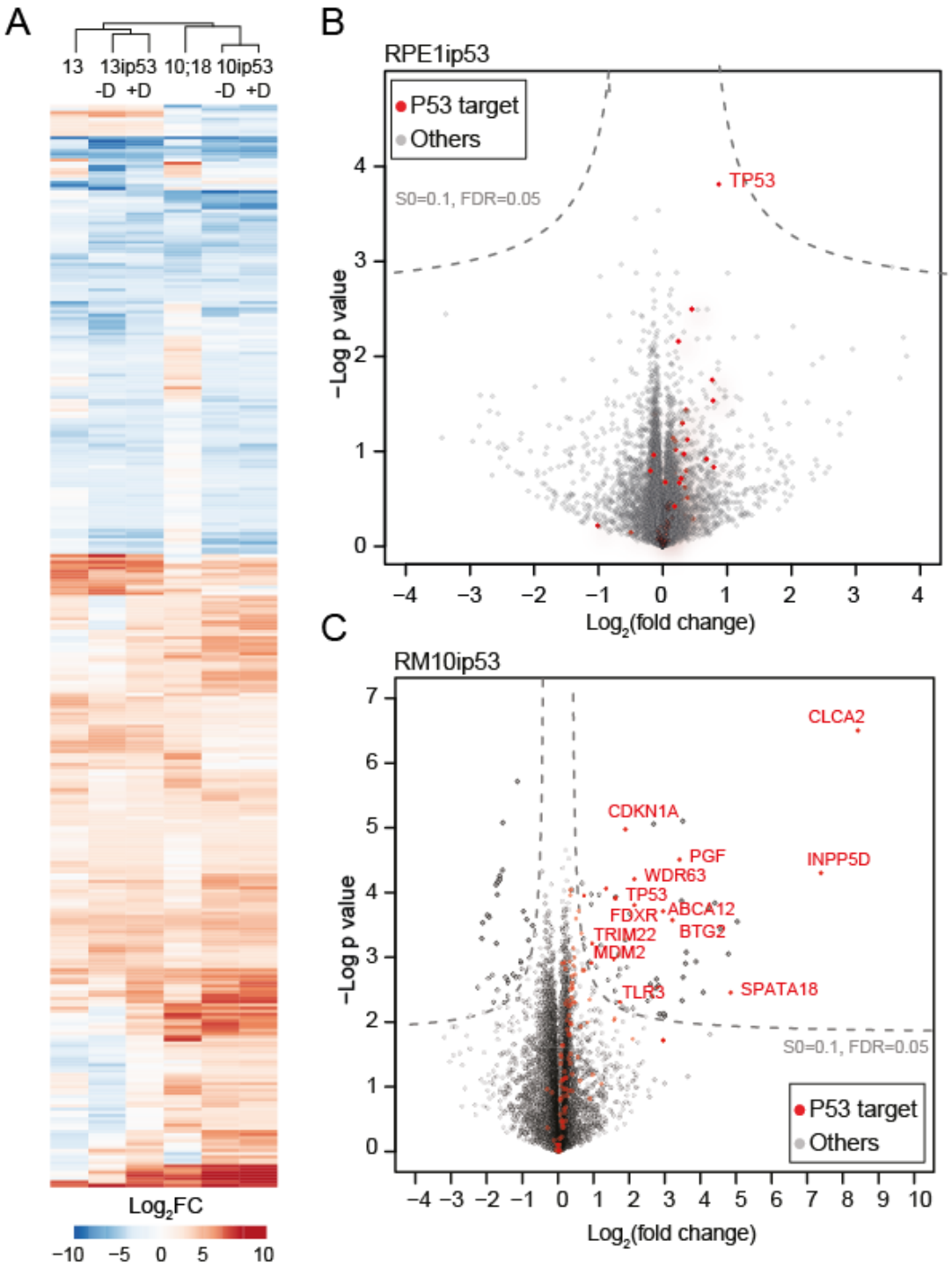

Figure 50. Impact of p53 on the cellular responses to monosomy. A. The heat map depicts the differentially regulated mRNA expression in monosomies compared to diploids. Hierarchical clustering of Euclidian distance. Gene expression fold changes greater than 2 or less than -2 are used for the heat map. D denotes doxycycline. **B-C.** Volcano plot showing the deregulated transcripts in RPE1 ip53 cell line upon doxycycline treatment compared to no doxycycline (log2FC). Red dots represent known p53 targets.

3.5.5 Ribosomal haploinsufficiency and p53 activity in monosomies

Defective ribosomal biogenesis and haploinsufficiency of ribosomes are known to activate the p53 pathway (Y. Liu, Deisenroth, & Zhang, 2016). Since the monosomies suffer from defects in ribosome biogenesis, we hypothesized that the ribosomal haploinsufficiency due to reduced RPG expression caused by monosomy leads to activation of p53 in monosomies. To validate this hypothesis, we depleted RPL21 in RPE1 p53 positive cell line using siRNA to the levels observed in RM 13. The depletion of RPL21 in RPE1 p53 positive cell line (Figure 51A, C) also reduced the translation efficiency (Figure 51B, D) similarly as in RPE1 p53 negative cell line, suggesting that p53 does not impact the translation efficiency. Importantly, we observed that already a minor reduction of Rpl21 protein abundance resulted in a robust accumulation of p53 and p21 (Figure 51A, B). Thus, a partial reduction of even single ribosomal subunit gene to the levels observed in monosomies activates p53 pathway. Based on our observations, we infer that the ribosomal haploinsufficiency caused by monosomy limits the viability through activation of p53.

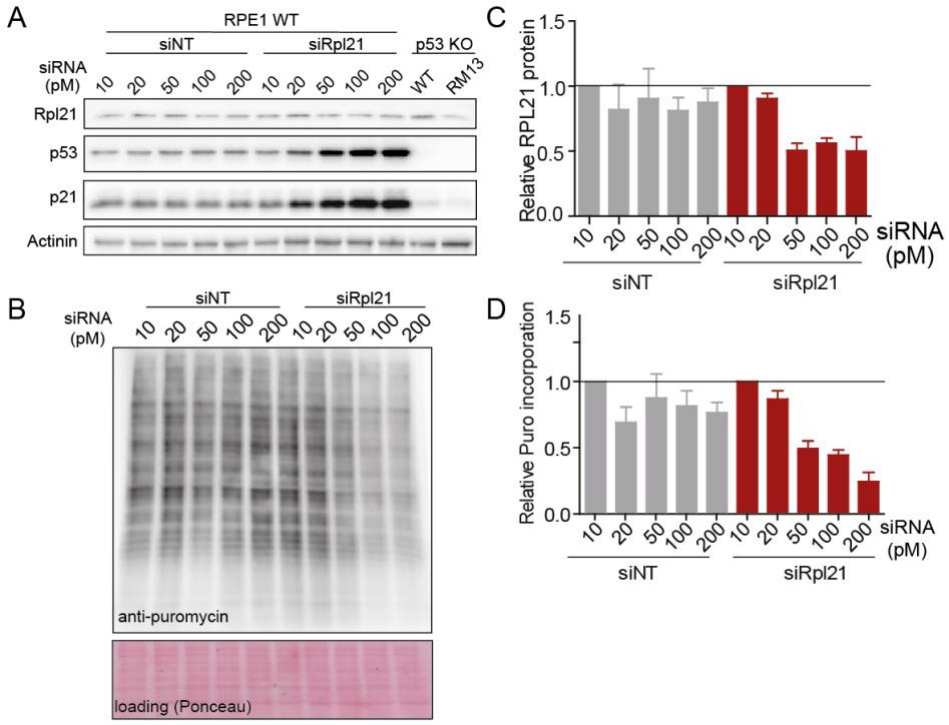

Figure 51. Knockdown of RPL21 leads to activation of the p53 pathway. A. siRNA mediated titrated knockdown of RPL21 in RPE1 WT p53+ cell line. siNT was used as a control; RPE1 p53 KO WT and RM 13 are shown as a non-transfected control. The western blots are representative of at least three independent experiments. **B.** Translation efficiency determined by immunoblotted against anti-puromycin antibody. Ponceau staining was used as a loading control. The western blots are representative of at least three independent experiments. **C.** Quantification of Rpl21 knock down efficiency and **D**. Puromycin incorporation. siNT and siRPL21 values were normalized to respective 10 pm samples. Bars display the mean ± SEM of at 3 independent experiments.

3.6. Computational analysis of CCLE and TCGA datasets reveal impaired ribosome biogenesis and loss of p53 in monosomic cancers

Our data collectively suggests that the loss of chromosome impairs ribosome biogenesis due to the haploinsufficiency of ribosomal subunit genes and shows the principle incompatibility of monosomy with p53. Therefore, we predicted that the cancers with monosomic karyotype should correlate with reduced ribosome gene expression, impaired ribosome biogenesis and are enriched for p53 pathway mutations. To validate our prediction, in collaboration with Maik Kschischo and XiaoXiao Zhang (HS Koblenz), we analyzed the transcriptome datasets available on the Cancer Cell Line Encyclopedia (CCLE) and The Cancer Genome Atlas (TCGA). Firstly, we categorized the cell lines into Monosomy and Disomy based on the ploidy values (see Methods for details). Then, using single sample gene set enrichment analysis (ssGSEA), we showed that GO terms related to ribosomes and rRNA are strikingly downregulated in Monosomy cancer cell lines compared to the Disomy ones (Figure 52).

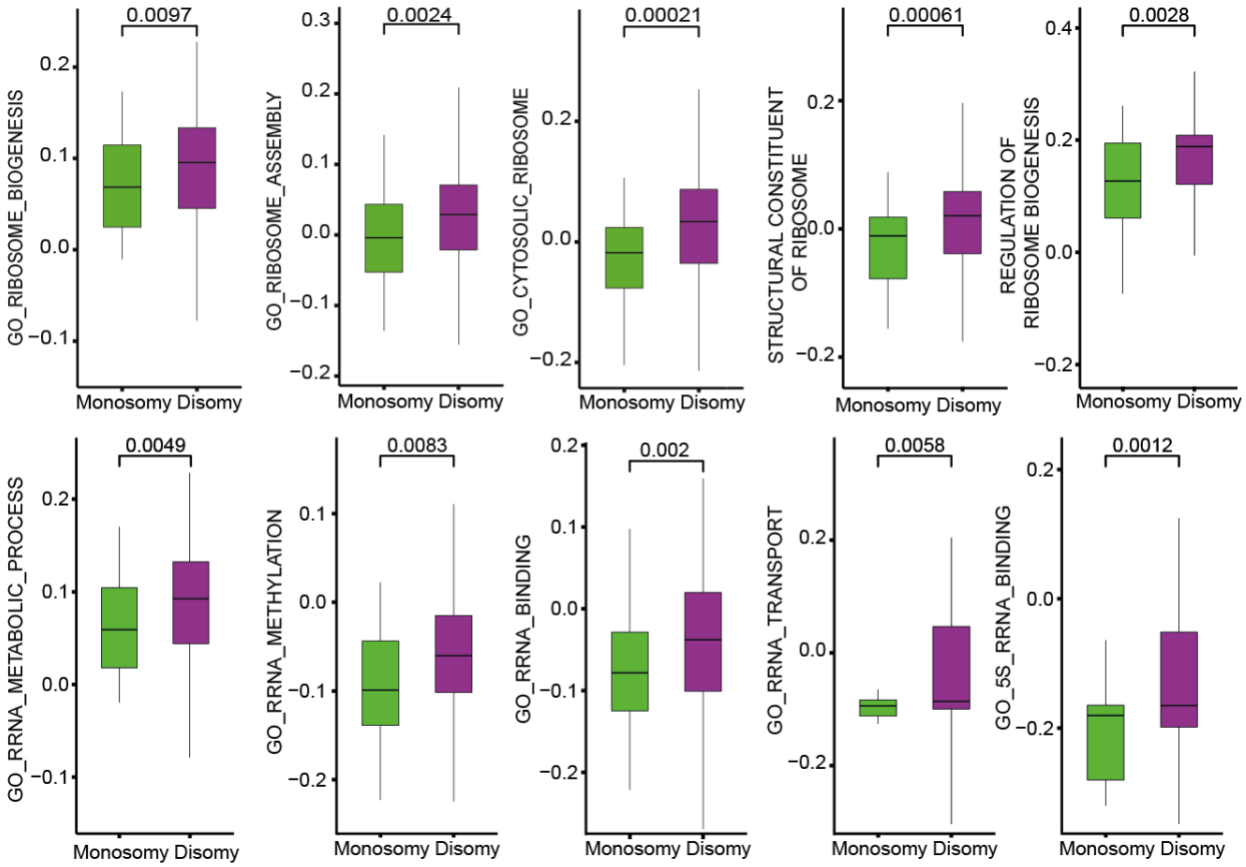

Figure 52. *In vitro* transcriptome analysis of CCLE datasets. Transcriptome analysis revealed the downregulation ribosome and rRNA related pathways in Monsomy compared to Disomy CCLE datasets. The y-axis shows the ssGSEA derived enrichment scores for gene ontology (GO) terms. All p-values are based on Wilcoxon rank sum tests. With Xiaoxiao Zhang.

Interestingly, similar analysis of The Cancer Genome Atlas (TCGA) datasets suggested that the GO terms related to ribosomes and rRNA are either increased or remains unchanged (Figure 53). These findings emphasize the differences in cellular responses *in vivo* and *in vitro* conditions. This observation indicates that the cancers with monosomic karyotype have to upregulate these pathways for their survival.

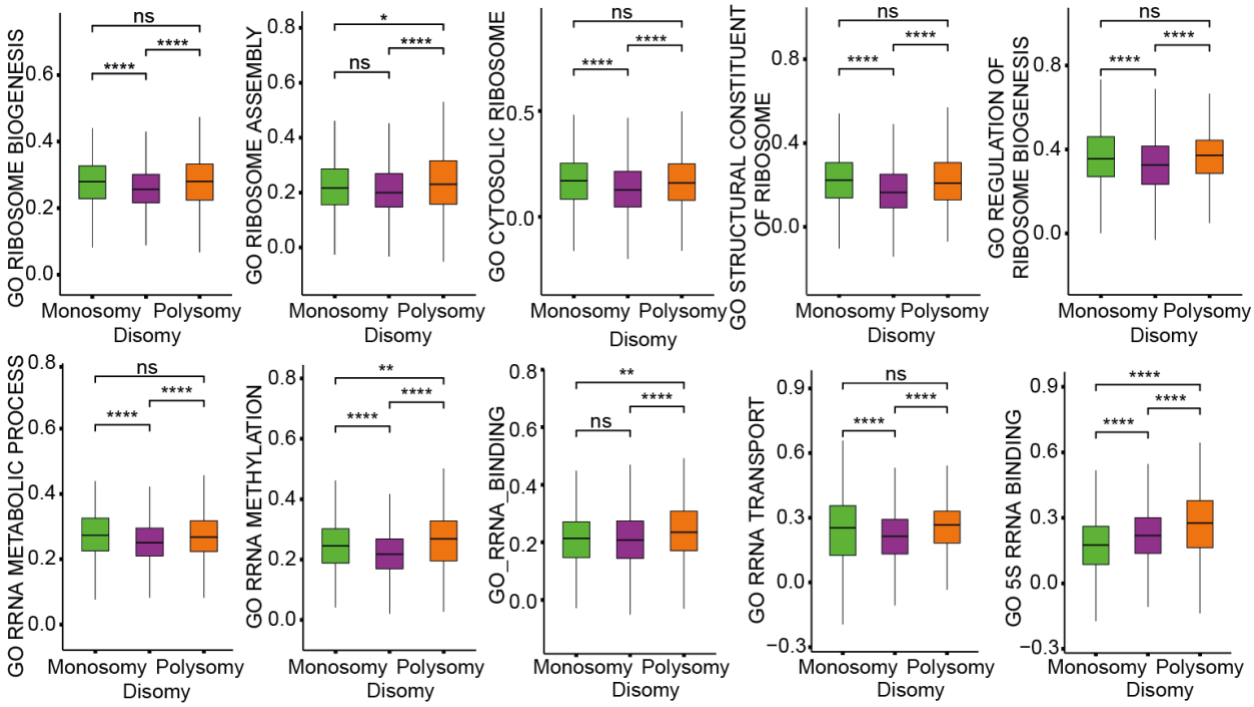

Figure 53. *In vivo* transcriptome analysis of TCGA datasets. Transcriptome analysis revealed the upregulation of ribosome and rRNA related pathways in categories Monsomy, Disomy and Polysomy. The y-axis shows the ssGSEA derived enrichment scores for gene ontology (GO) terms. ns- not significant. With Xiaoxiao Zhang.

To validate the prediction that the cancers with monosomic karyotype are positively correlated with increased p53 pathway mutations, we analyzed again the transcriptome datasets from the TCGA database. We calculated the "TP53 classifier score", which defines the extent of p53 pathway inactivation, including TP53 mutations, LOH, and also the mutations of TP53 targets (here should be citation of the paper). Therefore, the higher the TP53 classifier score, the lower the p53 activity. This analysis revealed that, across different cancer types, Monosomy cancers have higher TP53 classifier score compared to Disomy and Polysomy cancers (Figure 54).

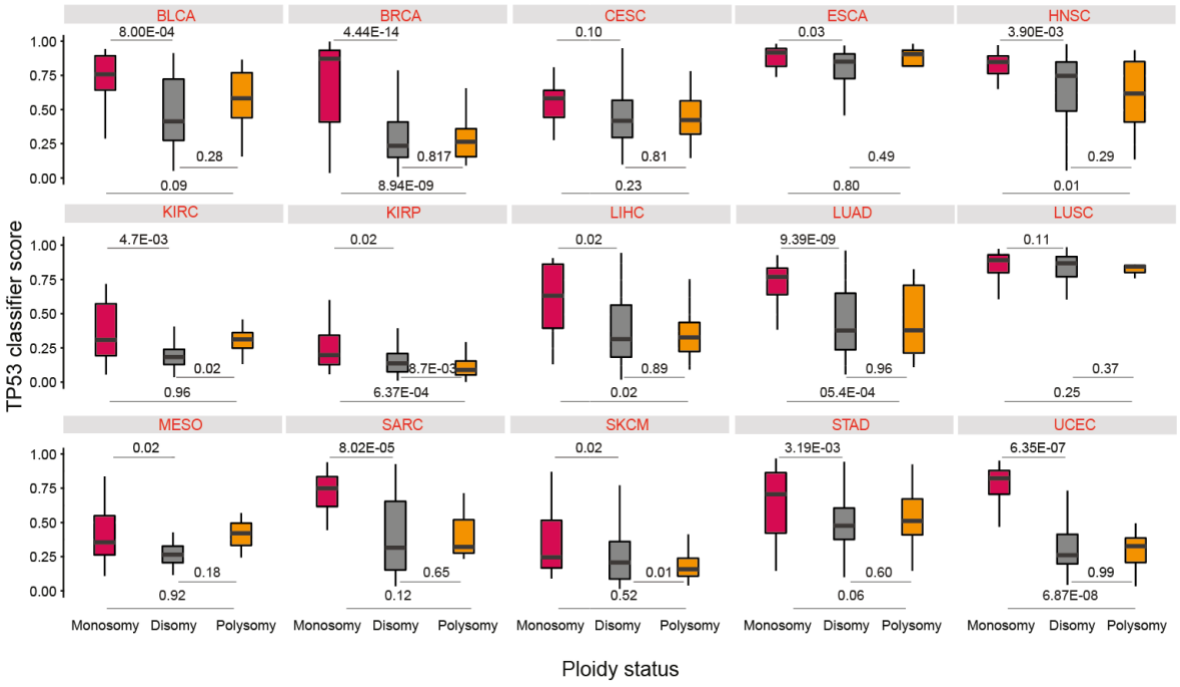

Figure 54. TP53 loss is a hallmark of monosomic cancers. TP53 classifier score estimating the extent of phenocopying TP53 loss in monosomy compared to diploid and polysomy tumors across pan cancer TCGA dataset. Cancer types are annotated as follows: BLCA - bladder urothelial carcinoma; BRCA - breast invasive carcinoma; CESC - cervical squamous cell carcinoma; ESCA - esophageal carcinoma; HNSC - head and neck squamous cell carcinoma; KIRC - kidney clear cell carcinoma; KIRP - kidney renal papillary cell carcinoma; LIHC - liver hepatocellular carcinoma; LUAD - lung adenocarcinoma; LUSC - lung squamous cell carcinoma; MESO – mesothelioma; SARC – sarcoma; SKCM - skin cutaneous melanoma; STAD - stomach adenocarcinoma; UCEC - uterine corpus endometrioid carcinoma. With Xiaoxiao Zhang.

Previous studies showed that tumors with high somatic copy number aberrations (SCNA) are enriched for TP53 mutations (Ciriello et al., 2013). To evaluate whether the increased TP53 classifier score in Monosomy might be a confounding effect of increased SCNA in this category, we measured the aneuploidy score of Monosomy and Polysomy tumors and compared to *TP53* mutations. While the aneuploidy score defining the SCNA levels is comparable in Monosomy and Polysomy, the *TP53* mutations are enriched in Monosomy (Figure 55).

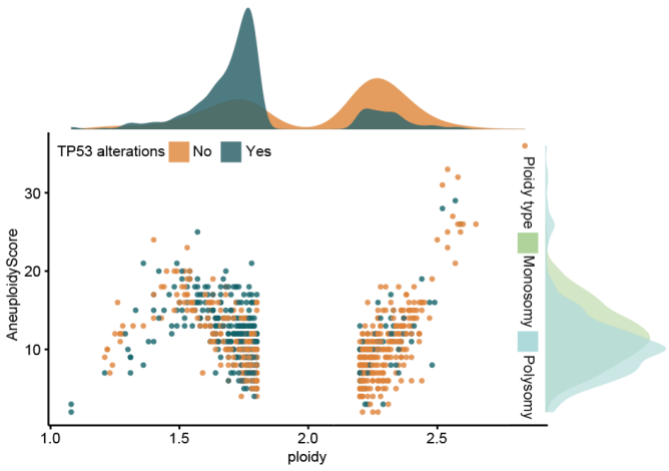

Figure 55. Impact of somatic copy number aberrations on TP53 alterations. Scatter plot showing the ploidy distribution. Samples with ploidy ranging from 1.80 to 2.19 are defined as disomic, 1.66 to 1.90 as Monosomy and

2.0 to 2.27 as polysomy. The top marginal density histogram shows that TP53 alterations. The right marginal density histogram depicts the aneuploidy score in monosomy and polysomy. With Xiaoxiao Zhang.

Based on our results, both experimental and computational, we propose that ribosome biogenesis defect is commonly associated with monosomy due to the haploinsufficiency of ribosomal genes and therefore, monosomy is incompatible with functional p53 pathway.

4. Discussion

Aneuploidy, a state of imbalanced chromosome number, often impairs cellular fitness and leads to severe pathological consequences. To understand why aneuploidy leads to such drastic consequences, several research laboratories investigated the impact of aneuploidy on cellular physiology using various aneuploidy model systems. This research showed that regardless the identity of the affected chromosome, aneuploidy leads to common phenotypes such as reduced proliferation mediated by slower progression from the G1 to S phase, altered protein homeostasis manifested by impaired protein folding, increased protein aggregation and activation of protein degradation pathways such as autophagy and UPS, increased genomic instability and replication stress, and activation of immune response pathways (reviewed in (Chunduri & Storchova, 2019; Santaguida & Amon, 2015; J. Zhu, Tsai, Gordon, & Li, 2018)). Multi-omics analysis revealed that the mRNA expression of the genes encoded on the aneuploid chromosomes scales according to the DNA copy number, although the abundance of some proteins compensates to diploid levels. This was apparent for proteins that were subunits of multi-molecular protein complexes (Dephoure et al., 2014; Oromendia et al., 2012; Pavelka et al., 2010; Stingele et al., 2012; Upender et al., 2004). Further, aneuploidy leads to specific pathway alterations termed “aneuploidy response pathways” in mammals (Durrbaum et al., 2014; Sheltzer et al., 2012). Aneuploidy is frequently observed in tumors. However, the exact role of aneuploidy in tumors is unclear. Intriguingly, aneuploidy was associated with tumor suppression *in-vitro* (Sheltzer et al., 2017). Therefore, aneuploid tumor cells must overcome aneuploidy associated stresses to survive and grow. Thus, identifying mechanisms that allow proliferation of aneuploid cancer cells could potentially offer novel therapeutic targets.

While a lot of progress had been made towards the understanding of aneuploidy and its consequences, majority of this knowledge was derived from model systems with a gain of chromosomes. Whether the cells with chromosome loss that leads to monosomy exert similar effects as chromosomal gain remains unknown. During my PhD, I focused on uncovering the impact of monosomy on the cellular viability and physiology. Using the monosomic cells derived from human immortalized RPE1-hTERT p53-/-, we showed that loss of a chromosome reduces cell proliferation and impairs genomic stability. Transcriptome and proteome analysis showed that the abundance of some of the mRNAs and proteins encoded on monosomic chromosome compensate towards diploid levels by both post-transcriptional and post-translational mechanisms. Further, pathway enrichment analysis identified chromosome specific pathway changes (for example, mitochondria & immune related) along with chromosome-independent pathway changes, among them most prominently are downregulation of ribosomes and translation. We validated these findings by a variety of biochemical assays. To study the impact of p53 on the viability of

monosomies, we reintroduced the p53 and identified that restoring the expression of p53 further reduced the proliferation. We propose that haploinsufficiency of ribosomal protein genes (RPG) caused by monosomy is responsible for p53-mediated cellular fitness impairment. Analyses of The Cancer Genome Atlas (TCGA) and Cancer Cell Lines Encyclopedia (CCLE) databases revealed a strong association of monosomy with p53 inactivation and ribosomal pathway impairment. *TP53* is the most frequent mutation in diverse cancer types. Our findings suggest that cancers with monosomy karyotype are enriched for p53 mutations. Based on these findings, we propose that the frequent occurrence of monosomy in cancer could be attributed to the loss of p53 which increases the tolerance to chromosome losses.

4.1 Model system for chromosome loss

Studies aimed to understand the consequences of chromosome loss are scarce owing to the lack of model systems. Few studies used embryonic material obtained from pre-implantation genetic screening samples (Biancotti et al., 2012; Licciardi et al., 2018; McCallie et al., 2016). However, there are several disadvantages of such models - they lack isogenic controls, the findings are limited to embryonic materials and these cells cannot be maintained in culture for extended periods. Few other studies attempted to eliminate entire chromosome using the Cre/loxP system (Lewandoski & Martin, 1997; Ramirez-Solis et al., 1995; Thomas, Marks, Chin, & Benezra, 2018), the TK-Neo transgene positive and negative selection (L. B. Li et al., 2012) and CRISPR/CAS9 mediated multiple chromosome cleavage (He et al., 2015; Taylor et al., 2018; Zuccaro et al., 2020; Zuo et al., 2017). However, in these studies they aimed to delete either the sex chromosomes, or the aneuploid chromosome from trisomic cells, or the cancer cells with chromosome gains. While these models allowed studying the impact of an extra chromosome deletion from trisomic cells, they did not provide the possibility to study the impact of chromosome loss that resulted in monosomy. During my PhD, we succeeded for the first time to obtain stable monosomic human cell lines. These cell lines were derived from single cell clones that spontaneously lost a chromosome following a *TP53* deletion (Figure 12, table 1). Loss of *TP53* alone does not cause aneuploidy (Bunz et al., 2002). However, it allows a propagation of cells with aneuploid karyotype (Lopez-Garcia et al., 2017; Ohashi et al., 2015; Soto et al., 2017; Thompson & Compton, 2010). Therefore, loss of *TP53* could have allowed the monosomic cells to survive despite losing a whole chromosome. This also suggest an important role of *TP53* in the viability of monosomies. While monosomy survival may not always depend on *TP53* deletion, future studies should consider genetic elimination or inactivation of p53 before attempting a whole or partial chromosome deletion.

4.2 Phenotypic consequences of chromosome loss

In this study, we investigated the impact of chromosome loss on diverse aspects of cellular physiology. While some phenotypes were similar in both chromosomal gains and losses, strikingly, several other phenotypes were observed only in chromosome gains.

Previous analysis of aneuploid model cells and organisms with chromosome gains revealed that gain of even one chromosome significantly slowed the proliferation (Beach et al., 2017; Ben-David et al., 2014; Stingele et al., 2012; Y. C. Tang et al., 2011; Torres et al., 2007; Williams et al., 2008). Similarly, we observed that the monosomic cells proliferate slower than the isogenic control cell lines (Figure 13A, B). In budding yeast, proliferation defect in monosomes is more severe in comparison to disomes and trisomes (Beach et al., 2017). Interestingly, the proliferation defect correlated with the relative ratio of aneuploid/euploid gene dosage. For example, gain of a chromosome in haploid yeast strain (disomes) led to doubling of the gene dosage, while gain of a chromosome in diploid yeast strain (trisomic) leads to only 1.5-fold increase in gene dosage relative to corresponding euploid strains (Beach et al., 2017). Similarly, human tetrasomic cells proliferate slower than trisomic cells (Stingele et al., 2012). However, direct comparison of proliferation of human monosomic cells to trisomic cells was not possible owing to the differences in p53 expression, as the monosomic cell lines were *TP53* deficient, while trisomic cells were *TP53* proficient. *TP53* is a well-known regulator of cell cycle and proliferation (Kastan, Canman, & Leonard, 1995; Milner, 1991). Therefore, lack of *TP53* could have a significant impact on the proliferation. Moreover, comparison of human cells with a loss or gain of the same chromosome would be a best match to study the impact of chromosome loss vs gains. Our attempts to generate *TP53* deficient trisomies were not successful due to an increased genomic instability and relaxed checkpoint caused by *TP53* loss in these cells. Future efforts should focus on obtaining cell lines with loss or gain of same chromosome and identical p53 status.

Interestingly, the strength of the proliferation defect in human monosomies correlated with the number of ORFs encoded on the lost chromosome (Figure 13C). This suggests that the combined loss of several genes could be responsible for the proliferation defect in monosomies. Of note, RM X cell line, monosomic for chromosome X, also proliferated slower than diploid. RPE1 is a female-derived cell line carrying two copies of chromosome X. However, a long non-coding RNA XIST silences one copy of X. Therefore, in a healthy female, the expression of majority of X-chromosome encoded genes are derived from one copy. Hence, loss of one chromosome should not influence the gene dosage. Nevertheless, XIST mediated silencing is not complete, as 100 to 130 genes escape from the XIST mediated silencing (Carrel & Willard, 2005). Based on our findings, we suggest that the loss of these few genes is sufficient to induce a significant proliferation defect upon chromosome X loss. Although the exact reason or the genes

underlying the proliferation defect is unknown, several genes across the genome are haploinsufficient. The lethality of monosomy is probably associated with haploinsufficiency or with unmasking of the recessive mutations. Previous analysis aimed to identify haploinsufficient genes across entire genome identified several genes involved in basic cellular processes such as transcription, translation, RNA processing, ribosomal proteins and cell cycle as haploinsufficient (Dang et al., 2008; Morrill & Amon, 2019). Defects in any of these processes negatively impact cell growth and proliferation. Additionally, recurrent chromosomal deletions in cancers had been associated with loss of so-called STOP genes. STOP genes comprise of several gene candidates known to restrain the cell cycle and proliferation (*CDK* inhibitors, *RB*, *TP53* etc.) (Solimini et al., 2012). Haploinsufficiency of these genes results in uncontrolled proliferation and tumorigenesis. Therefore, the impact of haploinsufficiency on the cell proliferation is context dependent. Further, proliferation defect in disomic yeast strain was associated with subtle increase in the expression of several genes that does not cause proliferation defect when deleted individually, and not due to increased expression of single dosage sensitive gene (Bonney et al., 2015). This means that the proliferation defect in disomic strain is determined by “mass action of genes” rather “few critical genes”. Whether the similar principle applies to chromosome losses have to be determined. Based on these observations, we propose that the proliferation defect in monosomy could be due to the combined loss of several genes or/and due to loss of one dosage sensitive/haploinsufficiency gene.

Chromosome losses are frequently found in cancers (Kristin A. Knouse et al., 2017), which may suggest their role in uncontrolled proliferation and tumorigenesis. Our analysis to investigate to monosomic cell growth in an anchorage independent conditions revealed that monosomic cells did not form any colonies on soft agar. Anchorage independency is one of the property of tumor cells and growth on soft agar is often used to determine transformation ability *in vitro.* Our findings suggest that the loss of chromosome act as tumor suppressor *in vitro* (Figure 13D). While similar observations were observed for chromosome gains, the precise reasons remain unknown (Sheltzer et al., 2017). The inhibitory potential is mediated by the same pathways or whether it varies between in trisomies and monosomies remains to be investigated. Another consequence of chromosome loss is an impaired genomic stability, manifested by an increased occurrence of micronuclei, anaphase bridges and γH2AX-marked DNA damage (Figure 15, 16). Centromere staining of micronuclei revealed that majority of the micronuclei did not stain positive for CENP A or B proteins, two different centromere markers (Figure 15C, D). This suggests that the micronuclei contain a fragment of a chromosome rather than a whole chromosome and the origin of micronuclei and anaphase bridges could be due to DNA replication and repair defects. Previous analysis of aneuploid cells immediately after chromosome missegregation, human trisomic and tetrasomic cells and yeast aneuploid

cells showed that a presence of even one extra chromosome increases genomic instability (Ohashi et al., 2015; Passerini et al., 2016; Santaguida et al., 2017; Sheltzer et al., 2011). However, the defect in human aneuploid cells was linked to replication stress and reduced expression of replication dependent proteins (Passerini et al., 2016) (Ohashi et al., 2015). No increase in expression of replication stress markers, such as phosphorylation of RPA32 and CHK1 proteins were observed in monosomies (Figure 18). Further, proteomic analysis showed that replication associated proteins such MCM2-7 helicases and others were down regulated only in trisomies, but not in monosomies (Figure 17A). These findings suggest that the replication stress presents as an inherent defect in trisomies leading to genomic instability, but the underlying causes of the genomic instability in monosomies is unknown. Wild type p53 is known to negatively regulate MCM2-7 helicases (Scian et al., 2008), and thus the reduced MCM2-7 helicases in trisomic cells could be mediated by p53. In line with this observation, trisomic cell lines lacking *TP53* did not down regulate MCM2-7 helicases (Vigano et al., 2018). Whether the lack of down-regulation of the replication proteins in monosomies is due to the absence of p53 remains to be investigated. However, p53 expression in monosomies could hamper such analysis, as monosomies cannot survive in the presence of p53 (discussed later). Another possibility is that the genomic instability occurs due to the haploinsufficiency of genes responsible for the maintenance of genomic stability. Genes such as PTEN (encoded on chromosome 10) (Hou, Ouyang, Brandmaier, Hao, & Shen, 2017), RB (van Harn et al., 2010), BRCA2 (Tutt et al., 1999) (both encoded on chromosome 13) are known to induce genomic instability, when expressed at lower levels. Experiments involving rescue of these proteins in monosomies should address whether the observed genomic instability in monosomies is due to reduced expression of such proteins.

Majority of the phenotypes observed in the models of chromosome gain were linked to the increased expression of genes encoded on the supernumerary chromosome (Bonney et al., 2015; Brennan et al., 2019; Y. Chen et al., 2019; Dephoure et al., 2014; Donnelly et al., 2014; Stingele et al., 2012; Torres et al., 2010; Torres et al., 2007). Increased protein expression places burden on the protein folding machinery, leading to an increased accumulation of misfolded and aggregated proteins (Brennan et al., 2019; Donnelly et al., 2014). Further, imbalanced increase in the abundance of some proteins disturbs the stoichiometry of the multimolecular complexes, contributes to the protein aggregation and disturbs the proteostasis network (Brennan et al., 2019; Ohashi et al., 2015; Oromendia et al., 2012; Stingele et al., 2012). Consistently, cells with chromosome gains rely on protein degradation pathways such as autophagy and ubiquitin - proteasomal system (Donnelly et al., 2014; Oromendia et al., 2012; Y.-C. Tang et al., 2011). However, in case of chromosome losses, the protein folding machinery may not be saturated, as there

are no excess proteins to be folded. Consistently, monosomies were not sensitive to 17AAG, an inhibitor of HSP90, suggesting that the protein folding machinery is not impaired or burdened in monosomies (Figure 19). Further, monosomy does not activate autophagy (Figure 20) as observed in trisomies (Stingele et al., 2012) (Santaguida et al., 2015). Together, these findings suggest that monosomic cells do not suffer from proteotoxic stress. Why loss of a chromosome does not lead to proteotoxic stress, but a gain of chromosome does? While the protein folding machinery is not burdened in monosomies, loss of chromosome should still impair protein stoichiometry, as one of the subunits would be expressed at lower levels. Several studies addressed the impact of increased protein expression on protein stoichiometry (Dephoure et al., 2014; K. Ishikawa, Ishihara, & Moriya, 2020; K. Ishikawa, Makanae, Iwasaki, Ingolia, & Moriya, 2017; McShane et al., 2016; Mueller et al., 2015; Stingele et al., 2012), but, not much is known about the impact of reduced protein levels. Is the protein synthesis of reduced proteins increased to balance the stoichiometry or the abundance of complexes adjusts according to the abundance of the subunits? Reduced expression of just one RPG was shown to reduce the whole ribosome complex in yeast ribosome mutant strains (Cheng et al., 2019). Similarly, our results suggest that haploinsufficiency of even a single ribosome protein caused by monosomy (discussed later) resulted in reduction of multiple other ribosomal proteins in the complex (Figure 37). This suggest that the complex levels are adjusted according to the availability of subunits. However, whether the reduction is mediated by reduced protein synthesis or by increased degradation remains unknown, as well as whether similar scaling applies to other protein complexes. In future, it would be interesting to investigate whether cells possess a feedback mechanism to adjust the levels of translation or degradation depending on the abundance of each proteins.

	Monosomies	Trisomies
Slower Proliferation	Yes	Yes
Decreased growth on soft agar	Yes	Yes
Genomic Instability	Yes	Yes
Replication stress	No	Yes
Defects in protein homeostasis	No	Yes

To summarize, loss of chromosome impairs proliferation, growth on soft agar and genomic stability similar to chromosome gains. Unlike gains, monosomies did not suffer from replication stress or proteotoxic stress, which suggests that the impact of aneuploidy varies depending on whether a chromosome was lost or gained.

4.3 Cis-effects of chromosome loss on the mRNA and protein expression

Cis-effects define the genetic changes caused by the loss of DNA on the corresponding mRNA and protein expression. Does DNA copy number loss lead to similar changes in mRNA and protein expression? Not much is known about the impact of monosomy on gene expression, mainly due to the lack of model systems. Recent transcriptome analysis of human monosomic blastocyst revealed that the abundance of several genes encoded on the monosomic chromosome as well as the other chromosomes were deregulated. However, this study was limited to embryonic material and number of transcripts analyzed were very low (about 3000 transcripts). Further, the analysis was complicated by the lack of isogenic diploid controls (Licciardi et al., 2018). Single cell RNA sequencing (scRNA-seq) of hematopoietic stem and progenitor cells of healthy donors and patients with monosomy 7 revealed that the expression of genes encoded on the chromosome 7 is reduced (Zhao et al., 2017). However, in both these studies, due to lack of isogenic controls, it was not possible to determine whether the mRNA expression scaled exactly according to the DNA copy number. To analyze whether the mRNA and protein express according to DNA copy number in monosomies, we performed RNAseq based transcriptome and TMT labelling based proteome quantification. This analysis revealed that only about 20% of the proteins are expressed according to the DNA copy number and majority of the genes are compensated towards diploid levels by both post-transcriptional as well as post-translational mechanisms (Figure 23). These findings were in contrast to what was observed in cells with chromosomal gains. While no compensation at the transcriptional level in aneuploid yeast, mice and human cells was observed, about 25 % of the proteins were compensated towards diploid levels in trisomic cells. Further analysis revealed that majority of these proteins belong to multi-subunit complexes (Stingele et al., 2012). We have tested whether similar bias explains the dosage compensation in monosomies. However, we did not find any bias for the multi-subunit complexes (Figure 25).

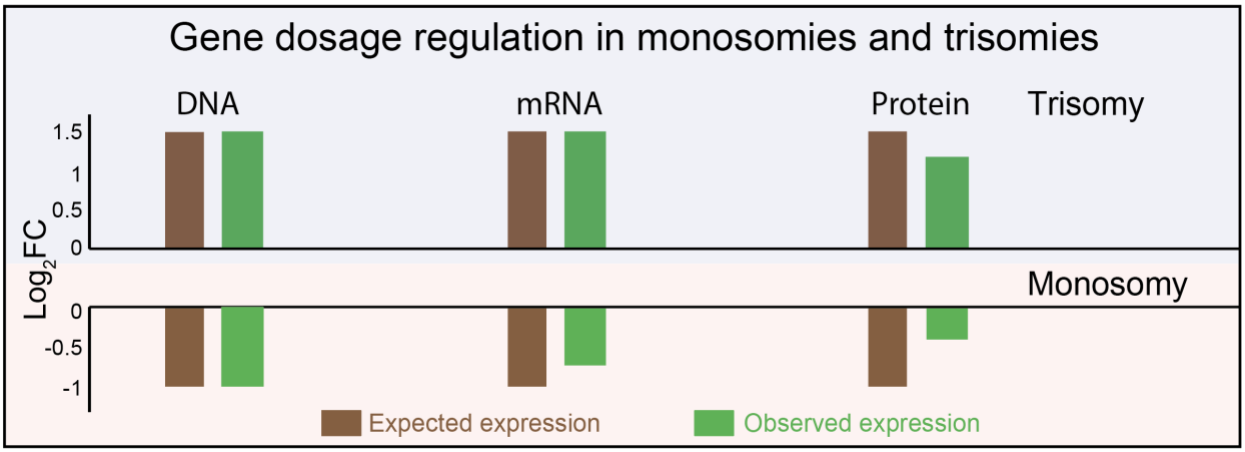

Interestingly, dosage compensation at the transcriptional level was observed in sex chromosomes and autosomal gains in *Drosophila melanogaster* and losses in *Candida albicans* (Stenberg et al., 2009; Y. Zhang et al., 2010). (Tucker et al., 2018). These findings suggest the existence of post-transcriptional mechanisms to compensate for chromosome copy number changes. Chromosome specific compensation was observed for chromosome 4 mediated by a protein painting of fourth (POF) (Johansson, Stenberg, Bernhardsson, & Larsson, 2007). However, existence of similar mechanisms to compensate for all autosomes is very unlikely. A model has been proposed by Birchler and colleagues defined as "inverse dosage effect" to explain the general transcriptional dosage compensation. It states that, in diploid cells, gene levels are regulated by the balance between a gene and its negative regulator (Veitia, Bottani, & Birchler, 2008). Interestingly, it was predicted that genes belonging to the similar complex or pathways tend to be clustered together in the genome (J. M. Lee & Sonnhammer, 2003) (Teichmann & Veitia, 2004). Therefore, in case of chromosome gain or loss, increased or reduced expression of negative regulators encoded on the same chromosome effects the gene expression inversely. However, it is unlikely that every gene has negative regulator encoded in close proximity, which also explains the non-pervasive dosage compensation.

The mechanisms of aneuploidy dosage compensation at protein levels are better understood, thanks to the increased sensitivity and improved protein quantification by mass spectrometry. However, majority of these studies are limited to only chromosome gains (Brennan et al., 2019; Dephoure et al., 2014; McShane et al., 2016). When the diploid cells lose one chromosome, the median log2 fold change of protein expression of the monosomic chromosome should be around -1 in comparison to euploid chromosome. However, the median protein expression of monosomes analyzed in this study is in range of -0.26 to -0.37 (Figure 22), suggesting a strong compensation towards diploid levels. Based on the median expression ranges of mRNA and protein abundances, it is apparent that the major adjustment occurs at protein levels. While the exact mechanism of such compensation is unknown, we envision two possible mechanisms of protein dosage compensation: 1) Increased protein translation of monosomy encoded genes, or 2) Increased protein stability by reduced degradation or post translational modifications.

Recent studies showed that the mRNA levels strongly determine the protein levels. For example, investigation of steady state mRNA and protein abundances in exponentially growing, non-synchronized mouse embryonic fibroblasts revealed that about 84% of protein abundance variation is determined by mRNA levels, while protein synthesis and degradation contributes to only 8% of protein variation (J. J. Li, Bickel, & Biggin, 2014; Schwanhausser et al., 2011). Similar findings were observed in unstimulated mouse

bone marrow-derived dendritic cells. However, when stimulated with lipopolysaccharide (LPS), the majority of the protein abundances were still determined by mRNA abundance dynamics, but the pre-existing proteome of proteins involved in basic cellular functions such translation, mitochondria were regulated at protein translation or degradation level (Jovanovic et al., 2015). Another study investigated the dynamics of transcript and protein abundance following induction of ER stress by dithiothreitol (DDT). Their results suggested that nearly equal contribution of both transcriptional and post transcriptional mechanisms in regulating the dynamic proteome profile following DTT (Cheng et al., 2016). Together, these findings suggest that the relative contribution of translation processes in regulating the protein abundances are determined by the cellular physiological states. Accordingly, we postulate that the chromosome loss and the resulting stresses determine the transcriptional and post transcriptional ways of regulating the protein expression.

Further, the derivation of monosomic cells involve several steps of single cell cloning and the clones that survive had managed to adapt to cellular stresses associated with monosomy. It might be that the cells survived because they managed to dosage compensate the genes to facilitate the viability. Yet, what determines the dosage compensation and the mechanisms underlying remains to be investigated.

Together, our findings suggest that cells possess mechanisms to alleviate or increase the mRNA and protein dosage on a global scale and the consequences of chromosomes losses are probably alleviated by the dosage compensation.

4.4 Trans-effects of chromosome loss and pathway deregulations

When the cells loose or gain a chromosome, it not only affects the gene expression of the aneuploid chromosome, but also across the entire genome. We compared the transcriptome and proteome of monosomic cells to previously obtained data from trisomic cells to understand the impact of monosomy on cellular pathways and how chromosome losses compare to chromosome gains. This analysis identified limited overlap among the deregulated pathways between monosomies and trisomies (Figure 28). Of note, the trisomic cells are p53 proficient, while the monosomies are p53 deficient. Therefore, the comparison is not a perfect one, as p53 can have an influence on the pathway changes. As will be discussed later, restored p53 expression leads to an upregulation of several p53 targets, but on a global scale, it has minimal impact. This suggests that p53 does not influence the monosomy associated gene expression. Although monosomies cluster away from trisomies (Figure 28B), the similarities among various monosomies is very low, as is evident from the small number of differentially regulated genes (Figure 29). Further, pathway analysis revealed that GO terms, such as ribosomes, cytosolic large and small ribosomal subunits and translation were among the few pathways consistently down regulated in all

monosomies. Pathways specific to aneuploidy response pattern (ARP), such as down regulation of DNA and RNA metabolism, DNA replication and repair and up regulation of lysosomes were not observed in monosomies. Together, these findings suggest that the aneuploidy stress response is specific to chromosome gains and monosomies instigate different responses.

Interestingly, we observed various chromosome-specific effects in monosomy. Particularly, GO terms related to mitochondria respiratory complex and oxidative phosphorylation were downregulated in RM 19p and RM 10;18, while they were upregulated in RM X (Figure 30A, B, C and 33A). Immune pathways such as type I interferon response were often upregulated as a common response to chromosomal gains. In monosomies it remained unchanged except for RM 13, where it was downregulated (Figure 30A and 32). Similarly, several other pathways were specifically deregulated in individual monosomic cell lines. These de-regulations could be attributed to the specific genes encoded on the individual chromosomes. However, the identity of the genes responsible for these effects remains unknown. In case of RM 19p, down regulation of mitochondrial respiratory chain and oxidative phosphorylation could be attributed to the several NADH dehydrogenases genes (*NDUFA11, NDUFA13, NDUFA3, NDUFA/, NDUFB7* and *NDUFS7*) encoded on 19p. *NDUF* genes are a part of respiratory chain complex I. We hypothesize that the loss of 19p and subsequent reduction of different subunits encoded on the 19p would impair the stoichiometry and results in down regulation of whole complex. While different pathways were identified to be deregulated by omics, the functional consequences of these deregulations remain to be explored. Further, small scale RNAi or CRISPR screen for genes encoded on the aneuploid chromosome would allow the identification of genes responsible for such deregulations, provided the existence of a reporter for the dysregulation.

4.5 Loss of chromosomes leads to ribosomal haploinsufficiency

One of the consistently down-regulated pathways among different monosomies were pathways related to ribosomes and translation. Ribosomes are composed of nearly 80 small and large ribosomal subunit proteins, along with rRNA. These subunit genes are distributed across entire genome on various chromosomes (Uechi, Tanaka, & Kenmochi, 2001). Except for chromosomes 7 and 21, each and every chromosome has at least one ribosomal subunit gene encoded on them. Further, rDNA arrays responsible for rRNA is encoded on five acrocentric chromosomes (13,14, 15, 21 and 22) in the genome (Kenmochi et al., 1998). Therefore, we hypothesized that loss of a chromosome may lead to a reduction in abundance of ribosomal subunit gene. Even partial reduction of RPG leads to slower cellular growth and reduced bulk protein synthesis, probably due to impaired ribosome assembly or stability of assembled ribosomes (Cheng et al., 2019). Consistently, monosomy and subsequent RPG haploinsufficiency significantly

reduced global protein translation. RM X also displayed defects in protein translation (Figure 38). Interestingly, *RPS4X* encoded on chromosome X is one among the few genes that escape dosage compensation (Carrel & Willard, 2005). Therefore, we propose that haploinsufficiency of *RPS4X* is probably responsible for the translation defects in RM X. To test our hypothesis that reduced ribosome gene expression led to translation defects, we depleted RPS24 and RPL21, the only RPGs encoded on chromosomes 10 and 13, respectively, in wild type cells. Depletion of these RPS24 and RPL21 to the levels observed in monosomies resulted in similar translation defect (Figure 43, 44). However, our attempts to rescue the RPG expression in monosomies were not successful. Lentiviral mediated expression of *RPL21* lead to accumulation of ribosomal proteins in insoluble fraction and was degraded by proteasome. Recent study suggested that the haploinsufficient genes such as RPG reduces cellular fitness when expressed at lower levels as well as at higher levels (Morrill & Amon, 2019). This means that the expression window of RPG is very narrow. Our failure to rescue ribosomal protein levels could be explained by this tight regulation of expression of RPGs. Consistently, previous studies showed that ectopic expression of RPGs resulted in accumulation of ribosomal proteins in insoluble fraction (Sung et al., 2016). In conclusion, we propose that haploinsufficiency of RPGs leads to impaired translation in monosomies, although the ultimate test remains for the future.

Alternative hypotheses for ribosome downregulation are also possible. Since we observed a downregulation of many ribosomal subunit proteins, we investigated the upstream regulators of ribosome biogenesis. mTOR pathway is known to positively regulate several steps of ribosome biogenesis such as rRNA transcription, synthesis of ribosomal proteins and other components required for the ribosome assembly (Iadevaia et al., 2014). However, we did not observe any defects in the mTOR activity measured by the phosphorylation of p70S6 kinase, a downstream target of mTOR (Figure 39). Further, integrated stress response (ISR) in Down syndrome patients and mice models was shown to reduce protein translation (P. J. Zhu et al., 2019). However, no ISR was detected in monosomies (Figure 39). Recent analysis of yeast complex aneuploid revealed that activation of ESR by aneuploidy leads to a ribosome loss (Terhorst et al., 2020). However, in mammalian monosomic cells, no apparent ESR was observed. Together, these findings exclude defects of upstream factors involved in ribosome biogenesis and further supports that the observed phenotypes are indeed caused by RP haploinsufficiency.

Interestingly, polysome profiling of monosomic cells displayed an increased abundance of the polysomes (Figure 40). This is in a stark contrast to the reduced translation efficiency observed in monosomies. It should be noted that monosomies reduce the translation rate and not the total protein levels, as the proteome analysis revealed that the relative abundance of majority of proteins is similar as in diploids.

Therefore, the translation defect in monosomies is probably due to slower elongation rates caused by RPG haploinsufficiency and the increased polysome peak is rather due to accumulation of defective ribosomes and ribosome stalling. Reduced expression of RPG leads to impaired ribosome assembly and stoichiometry, which leads to a production of defective ribosomes. We propose that these defective ribosomes either slower or stall the translation elongation when engaged in translation. Since the preceding ribosome cannot bypass the slower ribosome ahead, it leads to accumulation of several ribosomes on mRNA, which is reflected as heavier polysomes. Moreover, increased polysome fraction could also be due to an increased translation of mRNAs essential for the viability. This could be addressed by performing ribosome profiling combined with RNAseq of polysomes to identify whether and which mRNAs are being translated more efficiently.

Ribosomal haploinsufficiency has long been associated with different pathological conditions commonly called ribosomopathies. Diamond-Blackfan anaemia is a well-studied ribosomopathy caused by mutations or deletions of RP genes including *RPS7, RPS10, RPS17, RPS19, RPS24, RPS26, RPS29, RPL5, RPL11, RPL26,* and *RPL35A* (Boria et al., 2010). Another common disease associated with RPG haploinsufficiency is the 5q syndrome, an independent subtype of myelodysplastic syndrome. The pathology of 5q syndrome is associated with haploinsufficiency of *RPS14* encoded on chromosome 5 (Ebert et al., 2008). While the ribosomopathies are primarily characterized by bone marrow failure, growth defects and developmental abnormalities, recent evidence suggest a link between RP haploinsufficiency and cancer (Dutt et al., 2011; Vlachos, 2017). DBA and 5q patients are prone to develop acute leukemia and are at higher risk of developing malignancies. Mutations in *RPL5, RPL10* and *RPL22* increases chance of developing T-cell acute lymphoblastic leukemia (Vlachos, 2017). This suggest that RP genes could act as tumor suppressors and RPG haploinsufficiency could promote tumors. However, the role of RPG haploinsufficiency in tumors is unclear. Our analysis of *in vitro* CCLE database predicted that cancer cell lines with Monosomy karyotype display down regulation of GO terms such as ribosomes, ribosome biogenesis (Figure 52). However, analysis of *in vivo* TCGA data suggest that tumors with Monosomy karyotype upregulate these pathways (Figure 53). This observation suggests that cancer cells, despite missing chromosomes evolved to upregulate the ribosomes and proliferate. Indeed, increased expression of oncogenic factor such as c-MYC showed to increase ribosome biogenesis by influencing rRNA transcription, processing and synthesis of ribosomal proteins (van Riggelen, Yetil, & Felsher, 2010). Therefore, targeted disruption of ribosome biogenesis might be effective in targeting tumors and future studies should address what role RP haploinsufficiency plays in cancer.

4.6 Loss of p53 is essential for the viability of monosomies

Chromosome loss is embryonically lethal (Magnuson et al., 1985). It is believed that the lethality is caused by haploinsufficiency of genes essential for growth and development of embryos. In this study, we propose that the p53 activity determines the viability of monosomies. Several lines of evidence support this hypothesis. Our attempts to deplete chromosome using CRISPR/Cas9 genome editing in p53 proficient cell lines did not generate any viable monosomies. Further, several studies aimed to deplete chromosome succeeded to remove either supernumerary chromosome from aneuploid cells or chromosome X, but not from the diploid state. Partial depletion of chromosome 3 was possible in lung cancer cell line immortalized with SV40 T antigen, which inactivates RB and p53 (Taylor et al., 2018). *TP53* is the most frequently mutated gene in cancers and aneuploidy tightly correlates with impaired p53 activity (Lopez-Garcia et al., 2017). Recent evidence suggests that *TP53* mutated MDS and leukemia patients are enriched for chromosome 5(q) deletion and monosomy 7 (Leung et al., 2019). Consistently, our analysis of pan cancer TCGA data revealed that tumors with Monosomy karyotype display higher *TP53* classifier score which defines the *TP53* pathway mutation status compared to Disomy and Polysomy tumors. This suggest that the tumors with monosomic karyotype require dysfunctional p53 pathway. Accordingly, the viable monosomic cell lines that we obtained were also p53 deficient.

Previous studies suggested that p53 limits the proliferation of cells following missegregation. In those studies, p53 activation was attributed to aneuploidy and DNA damage (M. Li et al., 2010) (Soto et al., 2017) (Ohashi et al., 2015; Thompson & Compton, 2010). Recent studies suggested that aneuploidy *per se* does not activate p53 (Santaguida et al., 2017; Soto et al., 2017). Comparison of single cell DNA sequencing performed immediately following chromosome segregation and after 96h in the presence or absence of p53 revealed that the occurrence of chromosomal gains and losses are comparable with and without p53 immediately after chromosome missegregation. However, the occurrence of chromosome loss was drastically reduced in *TP53* proficient cells in comparison to *TP53* deficient cells after 96h, suggesting that p53 mediated negatively selection eliminates cells with chromosomal loss (Soto et al., 2017). To study the impact of p53 on the monosomies, we restored the expression of p53 using transient transfection or doxycycline inducible *TP53* expression (Figure 45, 48). While the cell lines obtained after the transfection showed heterogeneous p53 expression, the p53 expressing cells were soon eliminated in monosomies (Figure 49), which further supports the idea that monosomies cannot survive with functional p53 pathway. Further, transcriptome analysis to identify the impact of p53 revealed that global cellular response to the monosomy was not influenced by the p53 expression. However, p53 restoration leads to activation of several p53 transcriptional targets such as *CDKN1A, BTG2, FDXR, SPATA18, CLCA2* and others (Fischer, 2017) (Figure 50C). Several of these genes are mediators of the G1 cell cycle arrest (*CDKN1A,*

BTG2)(Abbas & Dutta, 2009; Rouault et al., 1996; Tanikawa, Nakagawa, Furukawa, Nakamura, & Matsuda, 2012), cellular senescence (*CLCA2*) (Tanikawa et al., 2012) and few others are activated under diverse stress conditions, e.g. mitochondrial stress (*SPATA 18*) (Bornstein et al., 2011; Kitamura et al., 2011) or ferroptosis, iron homeostasis (*FDXR*) (Y. Zhang et al., 2017). This suggest that p53 is activated in monosomies by diverse stresses.

One of the most common triggers of p53 pathway is the ribosomal biogenesis stress (Narla & Ebert, 2010; Pelletier et al., 2018). Although the mechanism of p53 activation during ribosome stress is not fully elucidated, it appears to be the consequence of free ribosomal subunits (individual proteins not assembled in ribosomes). Evidence from several studies suggest that the abundance of free ribosomal subunits increases during ribosomal biogenesis defects. Increased free subunits such as RPL5, RPL11, RPL23, RPL26 and RPS7 competitively interact physically with MDM2. This interaction relieves MDM2 and p53 binding and stabilizes p53 (Y. Liu, Deisenroth, et al., 2016). Since the monosomies suffer from RP haploinsufficiency, we hypothesized that ribosomal defects in monosomies probably activates p53. Consistently, depletion of RPL21, a large subunit gene encoded on chromosome 13 activates p53 in a concentration dependent manner (Figure 51A). While this only suggest that p53 activation in monosomies could be due to RPG haploinsufficiency, it does not provide concluding evidence. Experiments to assess the viability of monosomies in the presence of p53 and with restored RP haploinsufficiency should confirm causative link between p53 activation by RPG haploinsufficiency. However, such experiments were not possible owing to tight regulation of ribosomal protein subunits. Interestingly, the erythropoietic dysfunction and tissue specific phenotypes caused by RPG haploinsufficiency can be rescued by depletion of *TP53* or mutations in *MDM2* (Barlow et al., 2010; Jaako et al., 2015; Kamio et al., 2016). We concluded that p53 mediates the cellular dysfunction caused by RP haploinsufficiency.

In addition to ribosomal stress, p53 is activated various by other stresses such as DNA damage, nucleotide depletion, oncogenic activation, hypoxia, mitotic defects and so on (Brady & Attardi, 2010; Levine & Oren, 2009). While RP haploinsufficiency is one of the possible activators of p53, it should be noted that other phenotypes caused by chromosome loss, such as genomic instability, could also activate p53. Therefore, future studies should investigate the diverse stresses caused by monosomy and their impact on p53 activation and viability.

4.7 Impact of chromosome loss in cancers

Aneuploidy is one of the hallmarks of cancer (Hanahan & Weinberg, 2011). Analysis of large scale cancer datasets revealed that the some chromosome abnormalities are recurrently observed in cancers (Ben-David & Amon, 2020; Kristin A. Knouse et al., 2017; Taylor et al., 2018). While the exact role of these

recurrent aberrations is unclear, it is believed that cancers select for these changes at some point during tumorigenesis. In other words, cancers depend on these changes for their growth. Accordingly, deletion of chromosome 3p, which is frequently observed in lung squamous cell carcinoma, resulted in slower proliferation. This suggest that lung squamous cell carcinoma depends on 3p loss for efficient proliferation (Taylor et al., 2018). Further, monosomy 7 and 16 is frequently observed in myeloid malignancies (Porta et al., 2007) (McGhee, Cohen, Wolf, Ledesma, & Cotter, 2000). Single cell RNA sequencing identified that cells with monosomy 7 downregulates genes involved in immune response and genomic stability (Zhao et al., 2017).

Impaired genomic stability and immune inactivation are frequent in cancers. Aneuploidy in cancers are often associated with multi-drug resistance, metastasis and poor prognosis (S. F. Bakhoum et al., 2018; Kuznetsova et al., 2015; A. J. Lee et al., 2011; Rutledge et al., 2016; Swanton et al., 2009; Turajlic & Swanton, 2016; Vasudevan et al., 2020). Recently, we have observed that the induction of chromosome instability accelerates the gain of drug resistance in human cells lines. Single cell DNA sequencing of resistant clones revealed recurrent chromosome abnormalities. For example, paclitaxel resistant clones always lost chromosome 10 and the resistance phenotype was further confirmed by using monosomic cell lines RM 10 and RM 10;18 (Lukow et al., 2020)(Figure 34,36). These findings further confirm that cancers depend on such recurrent chromosome changes. Identifying how tumors overcome the negative impact of aneuploidy and become hyper-proliferative could be exploited for developing personalized cancer therapeutics.

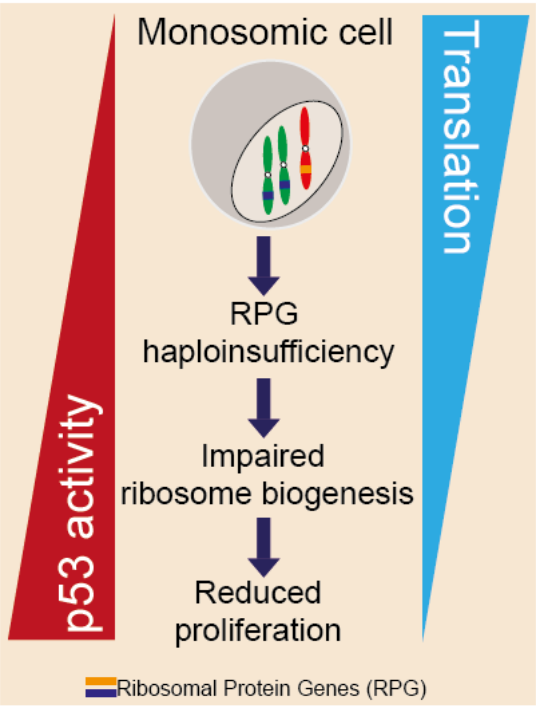

To summarize, this study for the first time evaluates the consequences of chromosome losses in human cells. The results suggest that the cellular consequences of chromosome losses are different then the consequences of chromosome gains. Further, the expression of genes encoded on the lost chromosome are compensated by transcriptional and post transcriptional mechanisms, thereby alleviating the drastic effects of reduced gene expression and enabling the monosomic cells to survive. Chromosome loss and the subsequent haploinsufficiency of ribosomal protein genes leads to impaired ribosome biogenesis and reduced translation.

Figure 56. Model depicting the cellular consequences of chromosome loss.

In addition, we show that survival of monosomic cells is incompatible with p53 expression and propose that the RPG haploinsufficiency is responsible for the activation of p53. We propose that the ribosomal haploinsufficiency associated with chromosome loss presents a major negative phenotype that is incompatible with a functional p53.

In the future, it would be important to understand how and what determines the dosage compensation. What genes are compensated and what determines transcriptional vs post transcriptional selection of compensation? This aspect would be of broad interest as this could uncover novel gene regulatory mechanisms.

5. Materials

List of buffers used in this study

Buffer/Solution	**Composition**
1x PBS	137 mM NaCl; 2.7 mM KCl; 10 mM Na2HPO4; 1.8 mM KH2PO4 in H2O
PBS-T	0.05% Tween 20 in 1x PBS
Fixation solution	37% formaldehyde solution diluted 1:10 in 1x PBS
Permeabilization solution	0.1% Triton X-100 in 1x PBS
Immunofluroscence Blocking solution	2% bovine serum albumin in PBS-T
RNase treatment	1:1000 RNase in PBS-T
Lower separating gels (for 2 x 12.5% gels)	6.15 ml 30 % (w/v) acrylamide; 3.75 ml lower SDS-buffer pH 8.8; 5.1 ml H2O; 150 µl 10 % APS; 15 µl TEMED pH 8.8
Upper stacking gels (for 2 x 5%)	0.8 ml 30 % (w/v) acrylamide; 1.2 ml upper SDS-buffer pH 6.8; 3 ml H2O; 50 µl 10 % APS; 5 µl TEMED pH 6.8
RIPA buffer (pH 7.5)	10 % NP-40; 10 % sodium deoxycholate; 5 M NaCl; 0.5 M EDTA; 1 M Tris, protease inhibitor (cOmplete Mini, EDTA-free) and phosphatase inhibitor (phosSTOP) according to the manufacturer's instructions
Lämmli buffer (1x)	50 mMTris-HCl pH 6.8; 2 % SDS; 10 % glycerol; 12.5 mM EDTA; 0.02 % bromphenol blue; 1 % β-mercaptoethanol
Lower SDS-buffer (pH 8.8)	1.5 M Tris-HCl, 0.4% (w/v) SDS
Upper SDS-buffer (pH 6.8)	0.5 M Tris-HCl, 0.4% (w/v) SDS
SDS-PAGE running buffer	25 mM Tris-HCl, 200 mM glycine, 0.1% (w/v) SDS
Bjerrum Schafer-Nielsen Buffer	48 mM Tris, 29mM glycine, 20% (w/v) methanol
TBS-T (pH 7.5)	50 mM Tris-HCl; 150 mM NaCl; 0.1 % Tween-20
Immuno blotting Blocking buffer	5% (w/v) skim milk in TBS-T
Ponceau solution	0.2 % Ponceau, 1 % acetic acid
EdUClickIt cocktail	0.5 mM CuSO4, 100 mMTris pH 8.8, azide fluorophore 1 uM, 100 mM ascorbic acid

RT-qPCR primers

Target gene	Primer sequence (5’ to 3’)
hIFIT1 F	TACCTGGACAAGGTGGAGAA
hIFIT1 R	GTGAGGACATGTTGGCTAGA
hIFIT3 F	CTTACGGCAAGCTGAAGAGT
hIFIT3 R	AATTGCCAGTCCAGAGGAGA
hIFNb F	TGCCTCAAGGACAGGATGAA
hIFNb R	TCCAGCCAGTGCTAGATGAA
hIL6 F	CTTCGGTCCAGTTGCCTTCT
hIL6 R	AGCTCTGGCTTGTTCCTCAC
hOAS3 F	CCCTGGTCTGAGACTCACGTTT
hOAS3 R	GACTTGTGGCTTGGGTTTGAC
hRPL27 F	ATCGCCAAGAGATCAAAGATAA
hRPL27 R	TCTGAAGACATCCTTATTGACG

List of primary antibodies

Name of the protein	Antibody dilution	Company	Identification number
P53 (DO-1)	1:500	Santa Cruz	Sc-126
Anti puromycin 12D10	1:1000	Merck Millipore	MABE343
p21 Waf1/Kip1	1:1000	Cell signaling	2947
p-eIF2 alpha (Ser51)	1:1000	Cell signaling	9721S
eIF2 alpha	1:1000	Cell signaling	9722S
LC 3a/b	1:1000	Cell signaling	4108
p70 S6 Kinase	1:1000	Cell signaling	2708
p-p70 S6 Kinase	1:1000	Cell signaling	9205
Ribosomal Protein L21 (D7)	1:500	Santa Cruz	Sc-393663
alpha-actinin	1:1000	Santa Cruz	sc-17829
HSP90	1:1000	Cell signalling	4874
HSP70/HSP72	1:1000	Enzo	ADI-SPA-902

Chk1	1:1000	Abcam	Ab32531-100
p-Chk1	1:1000	Cell signalling	2348
CDK2	1:1000	Cell signalling	2546
CDK6	1:1000	Cell signalling	3136
Cyclin D1	1:1000	Cell signalling	2978
Cyclin B1	1:1000	Cell signalling	4135
P16	1:1000	Cell singalling	2896
MCM2	1:2000	Abcam	Ab4461
MCM7	1:1000	Santa Cruz	Sc9966
pRPA32(s33)	1:1000	Bethyl	A300-246A
pRPA32(s4/s8)	1:1000	Bethyl	IHC-00422
RPA32	1:1000	Abcam	Ab2175
P62 lck ligand	1:1000	BD Transduction	610832
Cenp B	1:1000	Santacruz	Sc376392
γH2AX	1:1000	Abcam	Ab2893

siRNA		
siRPL21	Dharmacon	M-012910-01-0005 (Smartpool) Sequences: GUACCUGGGUUCAACUAAA GAGAAUUAAUGUGCGUAUU GAGGAGAGGCACCCGAUAU CCACAUAUAUGCGAAUCUA
siGENOME Non-Targeting Control siRNA Pool #1	Dharmacon	D-001210-01-05(Smartpool) Sequences: UAGCGACUAAACACAUCAA UAAGGCUAUGAAGAGAUAC AUGUAUUGGCCUGUAUUAG AUGAACGUGAAUUGCUCAA

6. Methods

6.1 Cell culture techniques

Cell lines generation and cultivation

Human retinal pigment epithelium cell line RPE1 immortalized with hTERT overexpression was used to derive monosomic cell lines utilized in this study. RPE-1 cells were cultured in DMEM + GlutaMAX™-I medium supplemented with 10% Fetal Bovine Serum and Pencillin-streptomycin (Gibco). RM 13 KO cell line was generated using pre-designed zinc finger nucleases (Sigma) as described previously. RM X, RM 10, RM 10;18 and RPE1 p53 KO cell lines were generated by CRISPR/Cas9 mediated deletion of *TP53* gene. For this purpose, the gRNA against *TP53* gene was cloned in pX330 vector (Addgene: 42230) according to a modified protocol from Shalem et al and transfected the RPE WT cells. Clones derived from single cells were isolated and tested for the loss of p53 expression by immunoblotting for p53 and p21. To assess the copy number status, single cell derived clones were subjected to low-pass whole genome sequencing. Chromosome loss was further validated by chromosome painting. The monosomic clones (KD) obtained from RPE1 cell line expressing TP53 shRNA was a kind gift from Dr. Rene Medema and are described in (Soto et al., 2017) (Netherlands Cancer Institute, The Netherlands).

For p53 restoration experiments, RM 10;18 and RM 13 cell lines were transduced with viral particles generated from an all-in-one tetracycline inducible plasmid with p53 (pMOV T11 p53) expressed under tet promoter (Heinz et al., 2010), selected in the presence of 2 µg/mL puromycin for 72 h and subsequently maintained in the presence of 0.5 µg/mL puromycin. RPE1 WT cells were transduced with *TP53* cloned into doxycycline inducible system (Tet on system, Clonetech) and selected with blasticidine (1 µg/mL) and puromycin (2 µg/mL). Several single cell clones were isolated and treated with doxycycline to induce the expression of p53. The expression of p53 was verified using immunoblotting for antibody against p53. The clones with minimal leakage without doxycycline and maximal induction in the presence of doxycycline were selected for further evaluation.

All lines were grown at 37°C in a humidified 5% CO_2 incubator. All cell lines were tested for mycoplasma contamination. To minimize the occurrence of secondary genomic changes, original stocks were thawed for every experiment and maintained for maximum of 4 to 5 passages.

Sub-culturing and passaging

Cell lines were grown in either 10 or 15cm dishes at 37°C in a 5% CO_2 until they reach an optimal confluency of 70-80%. Cells were washed once with PBS and trypsin-EDTA was added on the cells and placed in incubator at 37°C for 5 min. Cells were resuspended in DMEM supplemented with FBS and pen-strep and

passaged 1/10 of cells into a new 10 or 15 cm cell culture dish. The dishes are filled with appropriate amount of medium (10cm for 10cm dish and 20 ml for 15 cm dish) and cultivated at the optimal culture conditions.

Cryopreservation and thawing of cells

Cells were grown to the optimal density and trypsinized as described above. The cells were collected and centrifuged at 1500 rpm for 3 min to pellet the cells. The supernatant was aspirated and the pellet was resuspended in FBS containing 10% DMSO. The cells suspension was aliquoted in cryovials (0.5 to 1 ml/vial) and transferred to the freezing containing isopropanol and placed at -80°C overnight. On the following day, the vials were moved into liquid nitrogen containers for the long-term storage. For thawing of cells from frozen stocks, the frozen vials were thawed at 37°C and the cell suspension was mixed with 10ml of fresh medium. The suspension was centrifuged at 1500 rpm for 3 min to pellet the cells. The supernatant was aspirated and the pellet was resuspended in fresh medium and plated on appropriate cell culture dishes.

Lentivirus transfection and transduction

The pMOV T11 (kind gift of Dr. Bernhard Schiedlmeier, Medizinische Hochschule Hannover, Germany) and pRetroX-TRE3G and pRetroX-Tet3G vectors containing the *TP53* coding sequence were transfected along with pMDLg/pRRE (gift from Didier Trono, Addgene plasmid #12251) and pMD2.G (gift from Didier Trono, Addgene plasmid #12259) into 80% confluent HEK293T cells using Lipofectamine 2000 (Thermo Fischer Scientific) as per the manufacturer's instructions. On the next day, the transfection medium was replaced with fresh medium. Forty-eight hours post medium change, the viral supernatant was collected, filter sterilized and immediately used for transduction or stored at -80°C.

RPE1 p53 KO and RM 10;18 and RM13 were transduced with viral supernatant supplemented with 5 µg/mL polybrene and incubated 12-16 h at 37°C in a humidified 5% CO2 incubator. After 48 h, the medium was replaced with selection medium containing the respective antibiotics.

siRNA transfection

For the siRNA mediated knockdown of RPL21 and RPS24, $5x10^5$ were seeded on 6 cm dish on the day before transfection. Different concentrations (10 pm, 20 pm, 50 pm, 100 pm and 200 pm) of siNT (control) and siRPl21/siRPS24 were used. The transfection of siRNA was performed with Lipofectamine 2000 according to the manufacturer's instructions. 72 h post transfection, cells were collected for immunoblotting to verify the knockdown efficiency.

6.2 Karyotype validation

Chromosome spreads

For preparing the metaphase spreads, exponentially growing cells (70–80% confluence) were treated with 400 ng/mL colchicine for 5-6 h. The metaphase arrested cells were collected by trypsinization, and centrifuged at 1500 rpm for 10 min. Cell pellets were resuspended in 75 mM KCl and incubated for 10–15 min at 37°C in a water bath. Cells were pelleted by centrifugation at 1000 rpm for 10 min and suspended in 3:1 methanol/acetic acid to fix the cells. Fixed cells were washed several times in 3:1 methanol/acetic acid. To obtain the chromosome spreads, the fixed cells were dropped on a glass slide and dried at room temperature for 15 min

Chromosomal painting

The chromosome spreads were carried out as described above. Each sample was labeled with chromosome FISH probes (Chrombios) specific for a monosomic chromosome and a control chromosome as per manufacturer's instructions. Briefly, chromosome spreads were incubated with probe mixture (1 µL of each probe, adjusted to 10 µL with HybMix buffer). After denaturation at 72°C for 6 min, slides were kept at 37°C in a humid chamber overnight. Slides were washed for 5 min in 2x saline sodium citrate (SSC) solution and then for 1 min in prewarmed 70°C 0.4X SSC, 0.1% Tween solution, and, finally, in 4x SSC, 0.1% Tween solution for 5 min at room temperature. Then the slides were incubated for 30 min at 37°C with 100 µL fluorescein isothiocyanate (FITC) mouse anti-digoxin (Jackson Immuno Research) solution (1:300 in 4X SSC/0.1% Tween) and washed twice in 45°C pre-warmed 4x SSC/0.1% Tween solution for 5–10 min. Finally, cells were stained with DAPI and microscopic analysis was carried out using 3i software and spinning disc confocal microscopy (see below). For each sample, at least 25 metaphases were captured and analyzed.

6.3 Cell growth and cell cycle analysis

Cell proliferation

For proliferation assay, cells were seeded in triplicates into the wells of a 96 well plate ($1.5x10^3$ cells/well). In total 5 plates, one for each day, were prepared. To measure the proliferation, Cell Titer-Glo (Promega) was used according to the manufacturer's instructions. All the measurements were normalized to Day 0. The experiments were performed in multiple replicates.

Soft agar colony forming assay

For soft agar assay, 1% low melting agarose combined with an equal volume of DMEM was added to 12 well dish as a bottom layer. Subsequently, 0.7% low melting agarose was mixed with an equal volume of cell suspension containing 1000 cells and immediately layered on solidified agar base in duplicates per cell line. The wells were then filled with medium containing 10% FBS and 5% Pen-Strep. Medium was replaced

every 3 days and the colonies were counted after 3 weeks. Each well was divided into eleven fields and colonies in each field were counted using an inverted microscope (Motic AE2000).

17AAG sensitivity

To analyze the sensitivity to protein folding inhibitor 17-AAG (inhibitor of HSP90), $1.5x10^3$ were plated in triplicates on white 96-well glass bottomed plate. On the following day, the medium was replaced with fresh medium containing 17-AAG at desired concentrations or DMSO. Immediately, cells were placed in incubator with 5% CO_2 at 37°C. After 72 h, the cell viability was measured using Cell Titer-Glo according to manufacturer's instructions. All the values were normalized to DMSO control.

Cell cycle analysis using fluorescence activated cell sorting (FACS)

Cell cycle analysis was performed by labelling the replicating cells with EdU (5-ethynyl-2'-deoxyuridine) and DNA with DAPI (4',6-diamidino-2-phenylindole). Briefly, cells were cultured as described above and EdU was added 30 min before harvesting the cells. Subsequently, for EdU detection, the cells were fixed and permeabilized for 15 min with Fix perm (Thermo Fisher scientific), followed by incubation with EdU Click-iT cocktail (Invitrogen) as per the manufacturer's instructions. Cells were resuspended in PBS containing RNase (10 µg/mL) and DAPI and measured using Attune Nxt acoustic focusing cytometer (Life Technologies, Carlsbad, USA).

6.4 Cell and molecular biology techniques

RNA extraction and RT-PCR

mRNA was extracted using Qiagen RNeasy mini kit as per the manufacturer's instructions. 2 µg of genomic DNA-free mRNA was used for cDNA synthesis. cDNA was synthesized using iScript™ Advanced cDNA Synthesis Kit as per the manufacturer's instructions. As a control for cDNA synthesis efficiency, RNA spike (TATAA universal RNA spike I) was added in equal amounts into master mix of cDNA. cDNA was diluted 1:10 before using it for qPCR analysis. For qPCR, SYBR green based assay was used from Biorad (Sso advanced universal SYBR Green). The Ct values for the gene of interest is normalized either to RPL27 or Spike.

SDS-PAGE and immunoblotting

Whole-cell lysates were obtained using RIPA buffer supplemented with protease and phosphatase inhibitors (Roche). Protein concentration was measured using Bio-rad protein assay as per the manufacturer's instructions. Briefly, the Bio-rad assay reagent was diluted 1:5 and 1 µl of protein lysate was mixed with 799 µl of reagent and mixed well. As a blank, 1 µl of lysis buffer was added to 799 µl of reagent in a separate vial. 200 µl of mixed solutions were pipetted into 96 well plate in duplicates and the absorbance at 595 nm was measured using Promega Glomax explorer. Protein concentration was derived

by comparing the measured values to a standard curve previously generated using the same assay with known concentrations of BSA in the solution.

After determining the protein concentration, the protein lysates were mixed with 6x Lämmli-buffer to the concetration of 1 µg/ µl using water. An amount of 10 µg of protein was then resolved on self-made 10-12.5% polyacrylamide gels and ran using the Mini-PROTEAN II electrophoresis system at 200V for 45 min using SDS-running buffer.

After the SDS-PAGE, the proteins were transferred to a nitrocellulose membrane using the semi-dry technique. Ponceau staining was performed to evaluate the transfer efficiency by incubating the membrane for 5 min in Ponceau S solution (0.2 (w/v) in 1% (v/v) acetic acid). After blocking in low fat, 5% milk in Tris-Buffered Saline with Tween 20 for 1 h at room temperature, membranes were incubated overnight at 4°C with the primary antibodies. Antibodies used in this study are listed in Table S6. After incubation with horseradish peroxidase-conjugated secondary antibodies, horseradish peroxidase substrate was added and luminescent signals were quantified using an Azure c500. Protein bands were quantified using ImageJ software. For the normalization of western blotting results, we used housekeeping gene α-actinin or Ponceau staining as indicated in the figure legends. For Ponceau – based normalization, we used a large region between 35 to 60 kDa that contains several bands for normalization.

6.5 Microscopy

Immunofluorescence staining

RPE1 p53 KO and monosomic cells ($1x10^4$ cells) were plated in black 96-well flat glass-bottom plates and grown in DMEM to the desired confluence. Cells were fixed with freshly prepared 3.7% formaldehyde for 15 min at RT and permeabilized with 0.5% Triton X-100 in PBS for 5 min. For blocking, cells were incubated with 3% BSA for 30 min at RT and stained with anti-gamma H2AX (Abcam 2893), anti CENP B (Santa Cruz, sc376392), anti p53 (Santa Cruz, sc126) overnight at 4°C in humidified chamber. Next day, the primary antibody was washed off (3 times with PBS-T, 5 minutes each) and incubated with secondary antibody at room temperature in dark for 1 h. After secondary antibody was washed off, the nuclei were stained with Sytox green and DAPI. For micronuclei and anaphase bridge quantification, the cells were fixed as above and counter stained with DAPI and Sytox green.

Spinning disc confocal laser microscopy was performed using a fully automated Zeiss inverted microscope (AxioObserver Z1) equipped with a MS-2000 stage (Applied Scientific Instrumentation, Eugene, OR), the CSU-X1 spinning disk confocal head (Yokogawa) and LaserStack Launch with selectable laser lines (Intelligent Imaging Innovations, Denver, CO). Image acquisition was performed using a CoolSnap HQ camera (Roper Scientific) and a 20x-air (Plan Neofluar × 40/0.75, Plan Neofluar ×20/0.75) under the

control of the SlideBook 6 x64 program (SlideBook Software, Intelligent Imaging Innovations, Denver, CO, USA).

Live cell imaging

For the live cell imaging, cells expressing H2B-Dendra2 were seeded in a 96-well plate at $1x10^4$ cells per well in standard cell culture medium. Cells lacking the fluorescent tag to visualize DNA were labelled with Hoechst 33342 (1 µg/mL). The medium was replaced with FluoroBrite medium before live-cell imaging. Imaging was performed using an inverted Zeiss Observer Z1 microscope (Visitron Systems) equipped with a humidified chamber (EMBLEM) at 37°C, 40% humidity, and 5% CO_2 using CoolSNAP HQ2 camera (Photometrics) and X-Cite 120 Series lamp (EXFO) and Plan Neofluar 20x, or 10x magnification air objective NA 1.0 (Zeiss, Jena, Germany). Cells were imaged for 24 hours with 8 min time-lapse. Images were analyzed using Slidebook (Intelligent Imaging Innovations, Inc., Goettingen, Germany) and ImageJ (National Institutes of Health). To determine the time spent in mitosis, the period from nuclear envelope breakdown (NEBD) until end of anaphase was quantified.

6.6 Protein translation and polysome profiling

Puromycin labelling to determine translation rate

To determine the translation rate, $1.5x10^6$ cells were plated in 10 cm dish on the day before the puromycin labelling. Next day, cells should be actively growing with desired confluence of 70-80%. For labelling, 10 µM of puromycin was added directly to cell culture dish, mixed well and placed in incubator at 37°C for 15 min. Puromycin was washed off with PBS and the cells were collected for protein extraction and immunoblotting as described above. Equal amounts of protein lysates were loaded on 12.5 % acrylamide gel and the puromycin incorporated nascent peptides were identified using anti puromycin antibody. The intensity of puromycin was normalized to ponceau, which served as loading control.

Polysome profiling

Polysome profiling was performed as in (Pringle, McCormick, & Cheng, 2019). Cells were grown in 15 cm dishes (80% confluency at the time of experiment) and 10 dishes were used for each cell line. Cells were treated with 100 µg/ml cycloheximide (CHX) for 10 min and collected immediately by gently scraping with ice cold CHX/PBS. Cells were pelleted and flash frozen using liquid nitrogen and stored at -80°C until further use. Cells were lysed using ice cold low salt lysis buffer (50 mM KCL, 20 mM Tris HCL, pH 7.4, 10 mM MgCl2, 1% Triton X-100, 1 mM DTT, 0.5 % sodium deoxycholate, 100 µg/ml cycloheximide, RNAse inhibitiors, protease and phosphatase inhibitors) and incubated on ice for 10 min. The lysate was centrifuged at 2000 g for 5 min to pellet nuclei and large debris. The supernatant was transferred to a fresh tube and centrifuged at 13000 g for 5 min and the supernatant was transferred to a fresh tube. In

the meantime, a linear sucrose gradient (7-47%) was prepared using Biocomp Gradient Master 108. The RNA concentration of cleared lysate was measured using nanodrop and equal amounts of lysate was layered on the top of gradient and centrifuged at 39000 rpm on SW41 rotor for 90 min at 4°C. The UV absorbance of the gradients were measured starting at the bottom of the gradient using Bio Rad BioLogic FPLC system and BioLogic Optics Module OM-10.

The raw polysome profiles were smoothed using a Savitzky-Golay filter with a window size of 51 – 61 data points and a third order polynome in a Python script. For normalization by 80S maximum peak intensity, the data points of each monosomic cell line profile were multiplied by the ratio of its 80S maximum peak intensity to the wild types 80S maximum peak intensity. Based on the normalized profiles, the ratios of 80S, 60S and 40S maximum peak intensities between the wild type and monosomies were calculated. Ribosome structure modelling was performed using UCSF ChimeraX (Goddard et al., 2018).

6.7 Genome, transcriptome and proteome quantification

6.7.1 Genomic sequencing

DNA libraries

Genomic DNA was extracted from the cells using the DNA Blood Mini kit (Qiagen). Library preparation was performed with a Beckman Biomek FX automated liquid handling system, with 500ng starting material using SPRIworks HT chemistry (Beckman Coulter). Samples were prepared with custom 6 base pair barcodes to enable pooling. Library quantification and quality control was performed using a Fragment Analyzer (Advanced Analytics Technologies, Ames, USA).

Genomic sequencing and analysis

WGS was pursued on an Illumina HiSeq 2500 platform (Illumina, San Diego, USA), using 50 basepair single reads for low-pass sequencing. For all samples the GC-normalized data was aligned against the Genome Reference Consortium Human Build 38 patch release 13 (GRCh38.p13) using the intersect function of bedtools2 (version 2.29.1) to map the known genes to the measured coverages. The values were converted into log2 data and the median coverage per read was calculated for all known genes with at least one mapped coverage. To shift the values around zero, the median coverage of each cell line was subtracted for all values, resulting in a normalized population centered on 0.

6.7.2 Transcriptome quantification by RNA sequencing

RNA-seq library preparation and sequencing

NGS-Sequencing and library preparation was conducted at the NGS- Integrative Genomics Core Unit (NIG), Institute of Human Genetics, University Medical Center Göttingen (UMG).

RNA was extracted as described in the RNA extraction protocol above. Quality and integrity of RNA was assessed with the fragment analyzer from Advanced Analytical by using the standard sensitivity RNA analysis Kit (DNF-471). All samples selected for sequencing exhibited an RNA integrity number over 8. RNA-seq libraries were performed using 200 ng total RNA of a non-stranded RNA Seq, massively-parallel mRNA sequencing approach from Illumina (TruSeq stranded total RNA Library Preparation, Illumina). Libraries were prepared on the automation (Beckman Coulter's Biomek FXP workstation). For accurate quantitation of cDNA libraries a fluorometric based system, the QuantiFluor™dsDNA System from Promega were used. The size of final cDNA libraries was determined by using the dsDNA 905 Reagent Kit (Fragment Analyzer from Advanced Bioanalytical) exhibiting a sizing of 300 bp in average. Libraries were pooled and sequenced on the Illumina HiSeq 4000 (SE; 1 x 50 bp; 30-35 Mio reads/sample).Sequence images were transformed with Illumina software BaseCaller to BCL files, which was demultiplexed to fastq files with bcl2fastq v2.20.0.422. The quality check was done using FastQC.

Mapping & Normalization and analysis

Sequences were aligned to the genome reference hg38 sequence using the STAR aligner version 2.5.2a (Dobin et al., 2013). Subsequently, read counting was performed using featureCounts (Liao, Smyth, & Shi, 2014) (version 1.5.0-p1). Read counts were analyzed in the R/Bioconductor environment (version 3.6.1, www.bioconductor.org) using the DESeq2 package version 1.14.1(Love, Huber, & Anders, 2014). For further analysis, all counts were normalized by shifting the replicates to the same median, which was calculated without the monosomic genes to adjust the samples for the loss of a chromosome and the subsequent lower gene expression. For all monosomic cell lines, the log2 median intensity of three replicates was calculated and the log2 median intensity of three replicates of the wild type parental cell line was subtracted to calculate comparable fold changes.

6.7.3 Proteome quantification by TMT labelling

Preparation of Tandem Mass Tag (TMT) labeled peptides and high pH fractionation

Sample preparation and labelling

Cells were cultured as described above, $1x10^6$ cells were collected by scraping from plates and pellets were washed twice with PBS. Sample preparation and labelling peptides with TMT isobaric mass tags was performed as per the manufacturer's instructions. Briefly, cells were lysed in 100 µL lysis buffer (10% SDS in 100mM Triethyl ammonium bicarbonate (TEAB)) using strong ultrasonication. Lysates were cleared by centrifugation at 16,000 x g for 10 minutes at 4°C and protein concentration was determined using the BCA protein assay kit (Thermo Scientific). Fifty micrograms of protein was reduced with 5 mM Tris 2-carboxyethylphosphine (TCEP) for 1 h 55°C, and alkylated with 10 mM iodoacetamide for 30 min in the

dark at 25°C. Reduced and alkylated proteins were precipitated over night by adding six volumes of acetone at -20°C. Acetone precipitated proteins were resuspended in 100 mM TEAB, pH 8.5 and digested by incubation with sequencing-grade modified trypsin overnight at 37°C.

For TMT labelling, trypsinized peptide samples were subsequently labeled with isobaric tags (TMT 6-plex, Thermo Fisher Scientific). All samples were labelled with individual tags: RPE1 p53 KO- TMT126, RM X-TMT127, RM 10;18- TMT128, RM 13 -TMT129, RPE1 p53 KD- TMT130, RM 19p-TMT131.

High pH fractionation

After pooling the TMT labeled peptide samples, peptides were desalted on C18 reversed-phase columns and dried under vacuum. TMT-labeled peptides were fractionated by high-pH reversed-phase separation according to Wang et al., 2011 (Y. Wang et al., 2011) using a YMC Triart C18 column (3 µm, 120 Å, 2.1 mm × 100 mm; YMC Co., Ltd., Japan) on an Agilent 1100 HPLC system. Peptides were loaded onto the column in buffer A (ammonium formate [10 mM, pH 10] in water) and eluted using a 30 min gradient from 3-90% buffer B (90% acetonitrile/10% ammonium formate [20 mM, pH 10]) at a flow rate of 0.3 ml/min. Elution of peptides was monitored with a UV detector (280 nm). For each replicate, 48 fractions were collected and pooled into four fractions using a post concatenation strategy as previously described (Y. Wang et al., 2011), dried under vacuum and subjected to liquid chromatography (LC)-MS/MS analysis.

Liquid chromatography/Mass spectrometry

The concatenated and TMT-labelled peptide mixtures were analyzed using nanoflow liquid chromatography (LC-MS/MS) on an EASY nano-LC 1200™ system (Thermo Fisher scientific), connected to a Q Exactive HF (Thermo Fisher scientific) through a Nanospray Flex Ion Source (Thermo Fisher Scientific). 3 µL of each fraction was separated on a 40 cm heated reversed phase HPLC column (75 µm inner diameter with a PicoTip Emitter™, New Objective) in-house packed with 1.9 µm C18 beads (ReproSil-Pur 120 C18-AQ, Dr. Maisch). Peptides were loaded in 5% buffer A (0.5% aequeous formic acid) and eluted with a 3 hour gradient (5-95% buffer B (80% acetonitrile, 0.5% formic acid) at a constant flow rate of 0.25 µl/mL. Mass spectra were acquired in data dependent mode. Briefly, each full scan (mass range 375 to 1’400 m/z, resolution of 60,000 at m/z of 200, maximum injection time 80 ms, ion target of 3E6) was followed by high-energy collision dissociation based fragmentation (HCD) of the 15 most abundant isotope patterns with a charge state between 2 to 7 (normalized collision energy of 32, an isolation window of 0.7 m/z, resolution of 30,000 at m/z of 200, maximum injection time 100 ms, AGC target value of 1E5, fixed first mass of 100 m/z and dynamic exclusion set to 30 s).

Processing

MS data was processed with the MaxQuant software, version 1.6.3.3. All data was searched against the human reference proteome database (UniProt: UP000005640) with a peptide and protein FDR of less than 1%. All raw files as well as all MaxQuant output tables and parameters have been uploaded to PRIDE.

Analysis of proteome data

Identified protein groups were filtered to remove contaminants, reverse hits and proteins identified by site only. Next, Protein groups which were identified more than two times in at least one group of replicates (N=4) were kept for further processing resulting in a set of 5887 Protein groups in total. For LFQ, Protein groups which were identified more than three times in at least one group of replicates (N=4) were kept for further processing, resulting in a set of 5727 Protein groups in total Log2 TMT reporter intensities were cleaned for batch effects using the R package LIMMA (Ritchie et al., 2015) and further normalized using variance stabilization (Huber, von Heydebreck, Sultmann, Poustka, & Vingron, 2002). Next, protein intensities obtained from TMT of monosomic cell lines were normalized by shifting to diploid median and fold change calculation to the intensities of the wild type parental cell lines as described for the transcriptome analysis

Combined analysis of genomic, transcriptomic and proteomic datasets

For further analysis comparing genomic, transcriptomic and proteomic datasets, the DNA and mRNA datasets were matched to the corresponding protein entries and merged into a single table (Supplementary table S2).To compare monosomic and trisomic cell lines, proteome data of trisomic RPE cell lines (Stingele et al., 2012) was merged to the dataset. Chromosome/scaffold name, gene start (bp), gene stop (bp) and Ensembl gene stable ID (ENSG) were annotated through BioMart. Perseus was used to add additional annotation (GOBP, GOCC, CORUM) and to carry out 2D annotation enrichment analysis (Cox & Mann, 2012).

Density histograms were generated in R using the library k-density. The log2 ratios of the mRNA and proteome subsets were plotted as density histograms, including the median of both populations.

6.8 TCGA and CCLE data analysis

TCGA pan-cancer RNAseq data involving 11060 samples were downloaded from Pan-Cancer Atlas and filtered to remove tumors that underwent whole genome doubling (WGD). 5722 primary tumor samples were kept for further analysis. RNAseq profiles of 418 samples from the Broad-Novartis Cancer Cell Line Encyclopedia (CCLE) (Barretina et al., 2012), filtered to remove cell lines with WGD, were used for the analysis. Ploidy value annotated from (Knijnenburg et al., 2018) was used to define -somy status of pan-cancer dataset. Separation of ploidy values into Monosomy and Polysomy status relies was based on two

thresholds. As there are no clear minima in the distribution of ploidy values clearly separating monosomic, disomic and polysomic samples, we assessed how the thresholds affect the final results by varying them from 1.66 to 1.90 (monosomy-disomy) and from 2.0 to 2.27 (disomy-polysomy). All thresholds resulted in a significant enrichment of p53 alterations in monosomic samples. CCLE sample ploidy value was retrieved from CCLE database. Ploidy values of both Pan-cancer and CCLE cohorts were inferred using ABSOLUTE algorithm (Carter et al., 2012) using copy number data.

Ribosome related pathway GO terms and KEGG pathway gene sets created by MsigDB6 (Liberzon et al., 2011) were collected. ssGSEA (Hanzelmann, Castelo, & Guinney, 2013) was applied on CCLE RNA-seq data to calculate pathway activity scores. A lower pathway score indicates that the genes in a specific pathway for a sample are under-expressed compared to the overall population.

TP53 classifier scores of TCGA pan-cancer cohorts were annotated from (Knijnenburg et al., 2018). The p53 score is based on a logistic regression model where p53 functional inactivation status is the response and expression of genes are covariables. The logistic regression classifier is trained to estimate a set of parameters that can accurately predict the p53 alteration status. Given a new sample, this classifier uses a logistic sigmoid function to report a probability value representing to what degree p53 of a sample is likely to be altered, given the expression data of the sample.

7. References

Abbas, T., & Dutta, A. (2009). p21 in cancer: intricate networks and multiple activities. *Nat Rev Cancer, 9*(6), 400-414. doi:10.1038/nrc2657

Ajore, R., Raiser, D., McConkey, M., Joud, M., Boidol, B., Mar, B., . . . Nilsson, B. (2017). Deletion of ribosomal protein genes is a common vulnerability in human cancer, especially in concert with TP53 mutations. *EMBO Mol Med, 9*(4), 498-507. doi:10.15252/emmm.201606660

Attiyeh, E. F., London, W. B., Mosse, Y. P., Wang, Q., Winter, C., Khazi, D., . . . Children's Oncology, G. (2005). Chromosome 1p and 11q deletions and outcome in neuroblastoma. *N Engl J Med, 353*(21), 2243-2253. doi:10.1056/NEJMoa052399

Babu, J. R., Jeganathan, K. B., Baker, D. J., Wu, X., Kang-Decker, N., & van Deursen, J. M. (2003). Rae1 is an essential mitotic checkpoint regulator that cooperates with Bub3 to prevent chromosome missegregation. *J Cell Biol, 160*(3), 341-353. doi:10.1083/jcb.200211048

Baker, S. J., Fearon, E. R., Nigro, J. M., Hamilton, S. R., Preisinger, A. C., Jessup, J. M., . . . Vogelstein, B. (1989). Chromosome 17 deletions and p53 gene mutations in colorectal carcinomas. *Science, 244*(4901), 217-221. doi:10.1126/science.2649981

Bakhoum, S. F., & Cantley, L. C. (2018). The Multifaceted Role of Chromosomal Instability in Cancer and Its Microenvironment. *Cell, 174*(6), 1347-1360. doi:10.1016/j.cell.2018.08.027

Bakhoum, S. F., Ngo, B., Laughney, A. M., Cavallo, J. A., Murphy, C. J., Ly, P., . . . Cantley, L. C. (2018). Chromosomal instability drives metastasis through a cytosolic DNA response. *Nature, 553*(7689), 467-472. doi:10.1038/nature25432

Bakhoum, S. F., Thompson, S. L., Manning, A. L., & Compton, D. A. (2009). Genome stability is ensured by temporal control of kinetochore–microtubule dynamics. *Nature Cell Biology, 11*(1), 27-35. doi:10.1038/ncb1809

Barlow, J. L., Drynan, L. F., Hewett, D. R., Holmes, L. R., Lorenzo-Abalde, S., Lane, A. L., . . . McKenzie, A. N. (2010). A p53-dependent mechanism underlies macrocytic anemia in a mouse model of human 5q- syndrome. *Nat Med, 16*(1), 59-66. doi:10.1038/nm.2063

Barretina, J., Caponigro, G., Stransky, N., Venkatesan, K., Margolin, A. A., Kim, S., . . . Garraway, L. A. (2012). The Cancer Cell Line Encyclopedia enables predictive modelling of anticancer drug sensitivity. *Nature, 483*(7391), 603-607. doi:10.1038/nature11003

Bartsch, K., Knittler, K., Borowski, C., Rudnik, S., Damme, M., Aden, K., . . . Rabe, B. (2017). Absence of RNase H2 triggers generation of immunogenic micronuclei removed by autophagy. *Hum Mol Genet, 26*(20), 3960-3972. doi:10.1093/hmg/ddx283

Beach, R. R., Ricci-Tam, C., Brennan, C. M., Moomau, C. A., Hsu, P. H., Hua, B., . . . Amon, A. (2017). Aneuploidy Causes Non-genetic Individuality. *Cell, 169*(2), 229-242 e221. doi:10.1016/j.cell.2017.03.021

Ben-David, U., & Amon, A. (2020). Context is everything: aneuploidy in cancer. *Nat Rev Genet, 21*(1), 44-62. doi:10.1038/s41576-019-0171-x

Ben-David, U., Arad, G., Weissbein, U., Mandefro, B., Maimon, A., Golan-Lev, T., . . . Carlos Biancotti, J. (2014). Aneuploidy induces profound changes in gene expression, proliferation and tumorigenicity of human pluripotent stem cells. *Nat Commun, 5*, 4825. doi:10.1038/ncomms5825

Bensaad, K., Tsuruta, A., Selak, M. A., Vidal, M. N., Nakano, K., Bartrons, R., . . . Vousden, K. H. (2006). TIGAR, a p53-inducible regulator of glycolysis and apoptosis. *Cell, 126*(1), 107-120. doi:10.1016/j.cell.2006.05.036

Biancotti, J. C., Narwani, K., Mandefro, B., Golan-Lev, T., Buehler, N., Hill, D., . . . Benvenisty, N. (2012). The in vitro survival of human monosomies and trisomies as embryonic stem cells. *Stem Cell Res, 9*(3), 218-224. doi:10.1016/j.scr.2012.07.002

Blank, H. M., Sheltzer, J. M., Meehl, C. M., & Amon, A. (2015). Mitotic entry in the presence of DNA damage is a widespread property of aneuploidy in yeast. *Mol Biol Cell, 26*(8), 1440-1451. doi:10.1091/mbc.E14-10-1442

Boettcher, S., Miller, P. G., Sharma, R., McConkey, M., Leventhal, M., Krivtsov, A. V., . . . Ebert, B. L. (2019). A dominant-negative effect drives selection of TP53 missense mutations in myeloid malignancies. *Science, 365*(6453), 599-604. doi:10.1126/science.aax3649

Bonney, M. E., Moriya, H., & Amon, A. (2015). Aneuploid proliferation defects in yeast are not driven by copy number changes of a few dosage-sensitive genes. *Genes Dev, 29*(9), 898-903. doi:10.1101/gad.261743.115

Boocock, G. R., Morrison, J. A., Popovic, M., Richards, N., Ellis, L., Durie, P. R., & Rommens, J. M. (2003). Mutations in SBDS are associated with Shwachman-Diamond syndrome. *Nat Genet, 33*(1), 97-101. doi:10.1038/ng1062

Boria, I., Garelli, E., Gazda, H. T., Aspesi, A., Quarello, P., Pavesi, E., . . . Dianzani, I. (2010). The ribosomal basis of Diamond-Blackfan Anemia: mutation and database update. *Hum Mutat, 31*(12), 1269-1279. doi:10.1002/humu.21383

Bornstein, C., Brosh, R., Molchadsky, A., Madar, S., Kogan-Sakin, I., Goldstein, I., . . . Rotter, V. (2011). SPATA18, a spermatogenesis-associated gene, is a novel transcriptional target of p53 and p63. *Mol Cell Biol, 31*(8), 1679-1689. doi:10.1128/MCB.01072-10

Boultwood, J., Pellagatti, A., McKenzie, A. N., & Wainscoat, J. S. (2010). Advances in the 5q- syndrome. *Blood, 116*(26), 5803-5811. doi:10.1182/blood-2010-04-273771

Brady, C. A., & Attardi, L. D. (2010). p53 at a glance. *Journal of Cell Science, 123*(15), 2527. doi:10.1242/jcs.064501

Brennan, C. M., Vaites, L. P., Wells, J. N., Santaguida, S., Paulo, J. A., Storchova, Z., . . . Amon, A. (2019). Protein aggregation mediates stoichiometry of protein complexes in aneuploid cells. *Genes Dev, 33*(15-16), 1031-1047. doi:10.1101/gad.327494.119

Brosh, R., & Rotter, V. (2009). When mutants gain new powers: news from the mutant p53 field. *Nature Reviews Cancer, 9*(10), 701-713. doi:10.1038/nrc2693

Buccitelli, C., Salgueiro, L., Rowald, K., Sotillo, R., Mardin, B. R., & Korbel, J. O. (2017). Pan-cancer analysis distinguishes transcriptional changes of aneuploidy from proliferation. *Genome Res, 27*(4), 501-511. doi:10.1101/gr.212225.116

Bunz, F., Fauth, C., Speicher, M. R., Dutriaux, A., Sedivy, J. M., Kinzler, K. W., . . . Lengauer, C. (2002). Targeted inactivation of p53 in human cells does not result in aneuploidy. *Cancer Res, 62*(4), 1129-1133.

Burrell, R. A., McClelland, S. E., Endesfelder, D., Groth, P., Weller, M. C., Shaikh, N., . . . Swanton, C. (2013). Replication stress links structural and numerical cancer chromosomal instability. *Nature, 494*(7438), 492-496. doi:10.1038/nature11935

Bursac, S., Brdovcak, M. C., Donati, G., & Volarevic, S. (2014). Activation of the tumor suppressor p53 upon impairment of ribosome biogenesis. *Biochimica et Biophysica Acta (BBA) - Molecular Basis of Disease, 1842*(6), 817-830. doi:https://doi.org/10.1016/j.bbadis.2013.08.014

Carrel, L., & Willard, H. F. (2005). X-inactivation profile reveals extensive variability in X-linked gene expression in females. *Nature, 434*(7031), 400-404. doi:10.1038/nature03479

Carter, S. L., Cibulskis, K., Helman, E., McKenna, A., Shen, H., Zack, T., . . . Getz, G. (2012). Absolute quantification of somatic DNA alterations in human cancer. *Nat Biotechnol, 30*(5), 413-421. doi:10.1038/nbt.2203

Chen, E. Y., Tan, C. M., Kou, Y., Duan, Q., Wang, Z., Meirelles, G. V., . . . Ma'ayan, A. (2013). Enrichr: interactive and collaborative HTML5 gene list enrichment analysis tool. *BMC Bioinformatics, 14*, 128. doi:10.1186/1471-2105-14-128

Chen, Y., Chen, S., Li, K., Zhang, Y., Huang, X., Li, T., . . . Qian, W. (2019). Overdosage of Balanced Protein Complexes Reduces Proliferation Rate in Aneuploid Cells. *Cell Syst, 9*(2), 129-142 e125. doi:10.1016/j.cels.2019.06.007

Cheng, Z., Mugler, C. F., Keskin, A., Hodapp, S., Chan, L. Y., Weis, K., . . . Brar, G. A. (2019). Small and Large Ribosomal Subunit Deficiencies Lead to Distinct Gene Expression Signatures that Reflect Cellular Growth Rate. *Mol Cell, 73*(1), 36-47 e10. doi:10.1016/j.molcel.2018.10.032

Cheng, Z., Teo, G., Krueger, S., Rock, T. M., Koh, H. W., Choi, H., & Vogel, C. (2016). Differential dynamics of the mammalian mRNA and protein expression response to misfolding stress. *Mol Syst Biol, 12*(1), 855. doi:10.15252/msb.20156423

Chunduri, N. K., & Storchova, Z. (2019). The diverse consequences of aneuploidy. *Nat Cell Biol, 21*(1), 54-62. doi:10.1038/s41556-018-0243-8

Ciriello, G., Miller, M. L., Aksoy, B. A., Senbabaoglu, Y., Schultz, N., & Sander, C. (2013). Emerging landscape of oncogenic signatures across human cancers. *Nat Genet, 45*(10), 1127-1133. doi:10.1038/ng.2762

Conery, A. R., & Harlow, E. (2010). High-throughput screens in diploid cells identify factors that contribute to the acquisition of chromosomal instability. *Proc Natl Acad Sci U S A, 107*(35), 15455-15460. doi:10.1073/pnas.1010627107

Coppe, J. P., Desprez, P. Y., Krtolica, A., & Campisi, J. (2010). The senescence-associated secretory phenotype: the dark side of tumor suppression. *Annu Rev Pathol, 5*, 99-118. doi:10.1146/annurev-pathol-121808-102144

Cox, J., & Mann, M. (2012). 1D and 2D annotation enrichment: a statistical method integrating quantitative proteomics with complementary high-throughput data. *BMC Bioinformatics, 13 Suppl 16*, S12. doi:10.1186/1471-2105-13-S16-S12

Da Costa, L., Narla, A., & Mohandas, N. (2018). An update on the pathogenesis and diagnosis of Diamond-Blackfan anemia. *F1000Res, 7*. doi:10.12688/f1000research.15542.1

Dai, C., Dai, S., & Cao, J. (2012). Proteotoxic stress of cancer: implication of the heat-shock response in oncogenesis. *J Cell Physiol, 227*(8), 2982-2987. doi:10.1002/jcp.24017

Dang, V. T., Kassahn, K. S., Marcos, A. E., & Ragan, M. A. (2008). Identification of human haploinsufficient genes and their genomic proximity to segmental duplications. *Eur J Hum Genet, 16*(11), 1350-1357. doi:10.1038/ejhg.2008.111

Danilova, N., & Gazda, H. T. (2015). Ribosomopathies: how a common root can cause a tree of pathologies. *Disease models & mechanisms, 8*(9), 1013-1026. doi:10.1242/dmm.020529

Davoli, T., Uno, H., Wooten, E. C., & Elledge, S. J. (2017). Tumor aneuploidy correlates with markers of immune evasion and with reduced response to immunotherapy. *Science, 355*(6322). doi:10.1126/science.aaf8399

Davoli, T., Xu, A. W., Mengwasser, K. E., Sack, L. M., Yoon, J. C., Park, P. J., & Elledge, S. J. (2013). Cumulative haploinsufficiency and triplosensitivity drive aneuploidy patterns and shape the cancer genome. *Cell, 155*(4), 948-962. doi:10.1016/j.cell.2013.10.011

Dephoure, N., Hwang, S., O'Sullivan, C., Dodgson, S. E., Gygi, S. P., Amon, A., & Torres, E. M. (2014). Quantitative proteomic analysis reveals posttranslational responses to aneuploidy in yeast. *Elife, 3*, e03023. doi:10.7554/eLife.03023

Deutschbauer, A. M., Jaramillo, D. F., Proctor, M., Kumm, J., Hillenmeyer, M. E., Davis, R. W., . . . Giaever, G. (2005). Mechanisms of haploinsufficiency revealed by genome-wide profiling in yeast. *Genetics, 169*(4), 1915-1925. doi:10.1534/genetics.104.036871

Dippold, W. G., Jay, G., DeLeo, A. B., Khoury, G., & Old, L. J. (1981). p53 transformation-related protein: detection by monoclonal antibody in mouse and human cells. *Proc Natl Acad Sci U S A, 78*(3), 1695-1699. doi:10.1073/pnas.78.3.1695

Dobin, A., Davis, C. A., Schlesinger, F., Drenkow, J., Zaleski, C., Jha, S., . . . Gingeras, T. R. (2013). STAR: ultrafast universal RNA-seq aligner. *Bioinformatics, 29*(1), 15-21. doi:10.1093/bioinformatics/bts635

Dodgson, S. E., Santaguida, S., Kim, S., Sheltzer, J., & Amon, A. (2016). The pleiotropic deubiquitinase Ubp3 confers aneuploidy tolerance. *Genes Dev, 30*(20), 2259-2271. doi:10.1101/gad.287474.116

Donnelly, N., Passerini, V., Durrbaum, M., Stingele, S., & Storchova, Z. (2014). HSF1 deficiency and impaired HSP90-dependent protein folding are hallmarks of aneuploid human cells. *EMBO J, 33*(20), 2374-2387. doi:10.15252/embj.201488648

Duan, S. F., Han, P. J., Wang, Q. M., Liu, W. Q., Shi, J. Y., Li, K., . . . Bai, F. Y. (2018). The origin and adaptive evolution of domesticated populations of yeast from Far East Asia. *Nat Commun, 9*(1), 2690. doi:10.1038/s41467-018-05106-7

Duncan, A. W., Hanlon Newell, A. E., Smith, L., Wilson, E. M., Olson, S. B., Thayer, M. J., . . . Grompe, M. (2012). Frequent Aneuploidy Among Normal Human Hepatocytes. *Gastroenterology, 142*(1), 25-28. doi:https://doi.org/10.1053/j.gastro.2011.10.029

Durrbaum, M., Kuznetsova, A. Y., Passerini, V., Stingele, S., Stoehr, G., & Storchova, Z. (2014). Unique features of the transcriptional response to model aneuploidy in human cells. *BMC Genomics, 15*, 139. doi:10.1186/1471-2164-15-139

Dutt, S., Narla, A., Lin, K., Mullally, A., Abayasekara, N., Megerdichian, C., . . . Ebert, B. L. (2011). Haploinsufficiency for ribosomal protein genes causes selective activation of p53 in human erythroid progenitor cells. *Blood, 117*(9), 2567-2576. doi:10.1182/blood-2010-07-295238

Ebert, B. L., Pretz, J., Bosco, J., Chang, C. Y., Tamayo, P., Galili, N., . . . Golub, T. R. (2008). Identification of RPS14 as a 5q- syndrome gene by RNA interference screen. *Nature, 451*(7176), 335-339. doi:10.1038/nature06494

Ebright, R. Y., Lee, S., Wittner, B. S., Niederhoffer, K. L., Nicholson, B. T., Bardia, A., . . . Micalizzi, D. S. (2020). Deregulation of ribosomal protein expression and translation promotes breast cancer metastasis. *Science, 367*(6485), 1468-1473. doi:10.1126/science.aay0939

Edery, P., Lyonnet, S., Mulligan, L. M., Pelet, A., Dow, E., Abel, L., . . . Munnich, A. (1994). Mutations of the RET proto-oncogene in Hirschsprung's disease. *Nature, 367*(6461), 378-380. doi:10.1038/367378a0

Egloff, M., Nguyen, L. S., Siquier-Pernet, K., Cormier-Daire, V., Baujat, G., Attie-Bitach, T., . . . Malan, V. (2018). Whole-exome sequence analysis highlights the role of unmasked recessive mutations in copy number variants with incomplete penetrance. *Eur J Hum Genet, 26*(6), 912-918. doi:10.1038/s41431-018-0124-4

Ercan, S. (2015). Mechanisms of x chromosome dosage compensation. *J Genomics, 3*, 1-19. doi:10.7150/jgen.10404

Erdal, E., Haider, S., Rehwinkel, J., Harris, A. L., & McHugh, P. J. (2017). A prosurvival DNA damage-induced cytoplasmic interferon response is mediated by end resection factors and is limited by Trex1. *Genes Dev, 31*(4), 353-369. doi:10.1101/gad.289769.116

Faggioli, F., Wang, T., Vijg, J., & Montagna, C. (2012). Chromosome-specific accumulation of aneuploidy in the aging mouse brain. *Hum Mol Genet, 21*(24), 5246-5253. doi:10.1093/hmg/dds375

Ferreira-Cerca, S., Poll, G., Gleizes, P. E., Tschochner, H., & Milkereit, P. (2005). Roles of eukaryotic ribosomal proteins in maturation and transport of pre-18S rRNA and ribosome function. *Mol Cell, 20*(2), 263-275. doi:10.1016/j.molcel.2005.09.005

Finlay, C. A., Hinds, P. W., & Levine, A. J. (1989). The p53 proto-oncogene can act as a suppressor of transformation. *Cell, 57*(7), 1083-1093. doi:10.1016/0092-8674(89)90045-7

Fischer, M. (2017). Census and evaluation of p53 target genes. *Oncogene, 36*(28), 3943-3956. doi:10.1038/onc.2016.502

Foijer, F., Xie, S. Z., Simon, J. E., Bakker, P. L., Conte, N., Davis, S. H., . . . Sorger, P. K. (2014). Chromosome instability induced by Mps1 and p53 mutation generates aggressive lymphomas exhibiting aneuploidy-induced stress. *Proc Natl Acad Sci U S A, 111*(37), 13427-13432. doi:10.1073/pnas.1400892111

Fournier, R. E., & Ruddle, F. H. (1977). Microcell-mediated transfer of murine chromosomes into mouse, Chinese hamster, and human somatic cells. *Proc Natl Acad Sci U S A, 74*(1), 319-323. doi:10.1073/pnas.74.1.319

Friedman, P. N., Chen, X., Bargonetti, J., & Prives, C. (1993). The p53 protein is an unusually shaped tetramer that binds directly to DNA. *Proc Natl Acad Sci U S A, 90*(8), 3319-3323. doi:10.1073/pnas.90.8.3319

Garcia-Castillo, H., Vasquez-Velasquez, A. I., Rivera, H., & Barros-Nunez, P. (2008). Clinical and genetic heterogeneity in patients with mosaic variegated aneuploidy: delineation of clinical subtypes. *Am J Med Genet A, 146A*(13), 1687-1695. doi:10.1002/ajmg.a.32315

Gasch, A. P., Spellman, P. T., Kao, C. M., Carmel-Harel, O., Eisen, M. B., Storz, G., . . . Brown, P. O. (2000). Genomic expression programs in the response of yeast cells to environmental changes. *Mol Biol Cell, 11*(12), 4241-4257. doi:10.1091/mbc.11.12.4241

Gilbert, F., Balaban, G., Moorhead, P., Bianchi, D., & Schlesinger, H. (1982). Abnormalities of chromosome 1p in human neuroblastoma tumors and cell lines. *Cancer Genet Cytogenet, 7*(1), 33-42. doi:10.1016/0165-4608(82)90105-4

Goddard, T. D., Huang, C. C., Meng, E. C., Pettersen, E. F., Couch, G. S., Morris, J. H., & Ferrin, T. E. (2018). UCSF ChimeraX: Meeting modern challenges in visualization and analysis. *Protein Sci, 27*(1), 14-25. doi:10.1002/pro.3235

Gogendeau, D., Siudeja, K., Gambarotto, D., Pennetier, C., Bardin, A. J., & Basto, R. (2015). Aneuploidy causes premature differentiation of neural and intestinal stem cells. *Nat Commun, 6*, 8894. doi:10.1038/ncomms9894

Greco, E., Minasi, M. G., & Fiorentino, F. (2015). Healthy Babies after Intrauterine Transfer of Mosaic Aneuploid Blastocysts. *N Engl J Med, 373*(21), 2089-2090. doi:10.1056/NEJMc1500421

Gregan, J., Polakova, S., Zhang, L., Tolic-Norrelykke, I. M., & Cimini, D. (2011). Merotelic kinetochore attachment: causes and effects. *Trends Cell Biol, 21*(6), 374-381. doi:10.1016/j.tcb.2011.01.003

Gropp, A., Kolbus, U., & Giers, D. (1975). Systematic approach to the study of trisomy in the mouse. II. *Cytogenetic and Genome Research, 14*(1), 42-62. doi:10.1159/000130318

Guidotti, J. E., Bregerie, O., Robert, A., Debey, P., Brechot, C., & Desdouets, C. (2003). Liver cell polyploidization: a pivotal role for binuclear hepatocytes. *J Biol Chem, 278*(21), 19095-19101. doi:10.1074/jbc.M300982200

Hanahan, D., & Weinberg, R. A. (2011). Hallmarks of cancer: the next generation. *Cell, 144*(5), 646-674. doi:10.1016/j.cell.2011.02.013

Hanks, S., Coleman, K., Reid, S., Plaja, A., Firth, H., Fitzpatrick, D., . . . Rahman, N. (2004). Constitutional aneuploidy and cancer predisposition caused by biallelic mutations in BUB1B. *Nat Genet, 36*(11), 1159-1161. doi:10.1038/ng1449

Hanna, J., Hathaway, N. A., Tone, Y., Crosas, B., Elsasser, S., Kirkpatrick, D. S., . . . Finley, D. (2006). Deubiquitinating enzyme Ubp6 functions noncatalytically to delay proteasomal degradation. *Cell, 127*(1), 99-111. doi:10.1016/j.cell.2006.07.038

Hanzelmann, S., Castelo, R., & Guinney, J. (2013). GSVA: gene set variation analysis for microarray and RNA-seq data. *BMC Bioinformatics, 14*, 7. doi:10.1186/1471-2105-14-7

Hartlova, A., Erttmann, S. F., Raffi, F. A., Schmalz, A. M., Resch, U., Anugula, S., . . . Gekara, N. O. (2015). DNA damage primes the type I interferon system via the cytosolic DNA sensor STING to promote anti-microbial innate immunity. *Immunity, 42*(2), 332-343. doi:10.1016/j.immuni.2015.01.012

Hasle, H., Alonzo, T. A., Auvrignon, A., Behar, C., Chang, M., Creutzig, U., . . . Raimondi, S. C. (2007). Monosomy 7 and deletion 7q in children and adolescents with acute myeloid leukemia: an international retrospective study. *Blood, 109*(11), 4641-4647. doi:10.1182/blood-2006-10-051342

Hatch, E. M., Fischer, A. H., Deerinck, T. J., & Hetzer, M. W. (2013). Catastrophic nuclear envelope collapse in cancer cell micronuclei. *Cell, 154*(1), 47-60. doi:10.1016/j.cell.2013.06.007

He, Z., Proudfoot, C., Mileham, A. J., McLaren, D. G., Whitelaw, C. B., & Lillico, S. G. (2015). Highly efficient targeted chromosome deletions using CRISPR/Cas9. *Biotechnol Bioeng, 112*(5), 1060-1064. doi:10.1002/bit.25490

Heinz, N., Schambach, A., Galla, M., Maetzig, T., Baum, C., Loew, R., & Schiedlmeier, B. (2010). Retroviral and Transposon-Based Tet-Regulated All-In-One Vectors with Reduced Background Expression and Improved Dynamic Range. *Human Gene Therapy, 22*(2), 166-176. doi:10.1089/hum.2010.099

Hernando, E., Nahle, Z., Juan, G., Diaz-Rodriguez, E., Alaminos, M., Hemann, M., . . . Cordon-Cardo, C. (2004). Rb inactivation promotes genomic instability by uncoupling cell cycle progression from mitotic control. *Nature, 430*(7001), 797-802. doi:10.1038/nature02820

Hipp, M. S., Kasturi, P., & Hartl, F. U. (2019). The proteostasis network and its decline in ageing. *Nat Rev Mol Cell Biol, 20*(7), 421-435. doi:10.1038/s41580-019-0101-y

Hipp, M. S., Park, S. H., & Hartl, F. U. (2014). Proteostasis impairment in protein-misfolding and -aggregation diseases. *Trends Cell Biol, 24*(9), 506-514. doi:10.1016/j.tcb.2014.05.003

Honda, H., Nagamachi, A., & Inaba, T. (2015). -7/7q- syndrome in myeloid-lineage hematopoietic malignancies: attempts to understand this complex disease entity. *Oncogene, 34*(19), 2413-2425. doi:10.1038/onc.2014.196

Hose, J., Escalante, L. E., Clowers, K. J., Dutcher, H. A., Robinson, D., Bouriakov, V., . . . Gasch, A. P. (2020). The genetic basis of aneuploidy tolerance in wild yeast. *Elife, 9*. doi:10.7554/eLife.52063

Hose, J., Yong, C. M., Sardi, M., Wang, Z., Newton, M. A., & Gasch, A. P. (2015). Dosage compensation can buffer copy-number variation in wild yeast. *Elife, 4*. doi:10.7554/eLife.05462

Hosono, N., Makishima, H., Jerez, A., Yoshida, K., Przychodzen, B., McMahon, S., . . . Maciejewski, J. P. (2014). Recurrent genetic defects on chromosome 7q in myeloid neoplasms. *Leukemia, 28*(6), 1348-1351. doi:10.1038/leu.2014.25

Hou, S. Q., Ouyang, M., Brandmaier, A., Hao, H., & Shen, W. H. (2017). PTEN in the maintenance of genome integrity: From DNA replication to chromosome segregation. *Bioessays, 39*(10). doi:10.1002/bies.201700082

Hu, W., Zhang, C., Wu, R., Sun, Y., Levine, A., & Feng, Z. (2010). Glutaminase 2, a novel p53 target gene regulating energy metabolism and antioxidant function. *Proc Natl Acad Sci U S A, 107*(16), 7455-7460. doi:10.1073/pnas.1001006107

Huang, N., Lee, I., Marcotte, E. M., & Hurles, M. E. (2010). Characterising and predicting haploinsufficiency in the human genome. *PLoS Genet, 6*(10), e1001154. doi:10.1371/journal.pgen.1001154

Huber, W., von Heydebreck, A., Sultmann, H., Poustka, A., & Vingron, M. (2002). Variance stabilization applied to microarray data calibration and to the quantification of differential expression. *Bioinformatics, 18 Suppl 1*, S96-104. doi:10.1093/bioinformatics/18.suppl_1.s96

Iadevaia, V., Liu, R., & Proud, C. G. (2014). mTORC1 signaling controls multiple steps in ribosome biogenesis. *Semin Cell Dev Biol, 36*, 113-120. doi:10.1016/j.semcdb.2014.08.004

Ishikawa, H., & Barber, G. N. (2008). STING is an endoplasmic reticulum adaptor that facilitates innate immune signalling. *Nature, 455*(7213), 674-678. doi:10.1038/nature07317

Ishikawa, H., Ma, Z., & Barber, G. N. (2009). STING regulates intracellular DNA-mediated, type I interferon-dependent innate immunity. *Nature, 461*(7265), 788-792. doi:10.1038/nature08476

Ishikawa, K., Ishihara, A., & Moriya, H. (2020). Exploring the Complexity of Protein-Level Dosage Compensation that Fine-Tunes Stoichiometry of Multiprotein Complexes. *PLoS Genet, 16*(10), e1009091. doi:10.1371/journal.pgen.1009091

Ishikawa, K., Makanae, K., Iwasaki, S., Ingolia, N. T., & Moriya, H. (2017). Post-Translational Dosage Compensation Buffers Genetic Perturbations to Stoichiometry of Protein Complexes. *PLoS Genet, 13*(1), e1006554. doi:10.1371/journal.pgen.1006554

Iwanaga, Y., Chi, Y. H., Miyazato, A., Sheleg, S., Haller, K., Peloponese, J. M., Jr., . . . Jeang, K. T. (2007). Heterozygous deletion of mitotic arrest-deficient protein 1 (MAD1) increases the incidence of tumors in mice. *Cancer Res, 67*(1), 160-166. doi:10.1158/0008-5472.CAN-06-3326

Jaako, P., Debnath, S., Olsson, K., Zhang, Y., Flygare, J., Lindstrom, M. S., . . . Karlsson, S. (2015). Disruption of the 5S RNP-Mdm2 interaction significantly improves the erythroid defect in a mouse model for Diamond-Blackfan anemia. *Leukemia, 29*(11), 2221-2229. doi:10.1038/leu.2015.128

Jacob, H. S., Brain, M. C., Dacie, J. V., Carrell, R. W., & Lehmann, H. (1968). Abnormal haem binding and globin SH group blockade in unstable haemoglobins. *Nature, 218*(5148), 1214-1217. doi:10.1038/2181214a0

Janssen, A., van der Burg, M., Szuhai, K., Kops, G. J., & Medema, R. H. (2011). Chromosome segregation errors as a cause of DNA damage and structural chromosome aberrations. *Science, 333*(6051), 1895-1898. doi:10.1126/science.1210214

Jeganathan, K., Malureanu, L., Baker, D. J., Abraham, S. C., & van Deursen, J. M. (2007). Bub1 mediates cell death in response to chromosome missegregation and acts to suppress spontaneous tumorigenesis. *J Cell Biol, 179*(2), 255-267. doi:10.1083/jcb.200706015

Jiang, J., Jing, Y., Cost, G. J., Chiang, J. C., Kolpa, H. J., Cotton, A. M., . . . Lawrence, J. B. (2013). Translating dosage compensation to trisomy 21. *Nature, 500*(7462), 296-300. doi:10.1038/nature12394

Joerger, A. C., & Fersht, A. R. (2007a). Structural biology of the tumor suppressor p53 and cancer-associated mutants. *Adv Cancer Res, 97*, 1-23. doi:10.1016/S0065-230X(06)97001-8

Joerger, A. C., & Fersht, A. R. (2007b). Structure-function-rescue: the diverse nature of common p53 cancer mutants. *Oncogene, 26*(15), 2226-2242. doi:10.1038/sj.onc.1210291

Johansson, A. M., Stenberg, P., Bernhardsson, C., & Larsson, J. (2007). Painting of fourth and chromosome-wide regulation of the 4th chromosome in Drosophila melanogaster. *EMBO J, 26*(9), 2307-2316. doi:10.1038/sj.emboj.7601604

Jones, N. C., Lynn, M. L., Gaudenz, K., Sakai, D., Aoto, K., Rey, J. P., . . . Trainor, P. A. (2008). Prevention of the neurocristopathy Treacher Collins syndrome through inhibition of p53 function. *Nat Med, 14*(2), 125-133. doi:10.1038/nm1725

Jovanovic, M., Rooney, M. S., Mertins, P., Przybylski, D., Chevrier, N., Satija, R., . . . Regev, A. (2015). Immunogenetics. Dynamic profiling of the protein life cycle in response to pathogens. *Science, 347*(6226), 1259038. doi:10.1126/science.1259038

Kabeche, L., & Compton, D. A. (2012). Checkpoint-independent stabilization of kinetochore-microtubule attachments by Mad2 in human cells. *Curr Biol, 22*(7), 638-644. doi:10.1016/j.cub.2012.02.030

Kalitsis, P., Fowler, K. J., Griffiths, B., Earle, E., Chow, C. W., Jamsen, K., & Choo, K. H. (2005). Increased chromosome instability but not cancer predisposition in haploinsufficient Bub3 mice. *Genes Chromosomes Cancer, 44*(1), 29-36. doi:10.1002/gcc.20215

Kamio, T., Gu, B. W., Olson, T. S., Zhang, Y., Mason, P. J., & Bessler, M. (2016). Mice with a Mutation in the Mdm2 Gene That Interferes with MDM2/Ribosomal Protein Binding Develop a Defect in Erythropoiesis. *PLoS One, 11*(4), e0152263. doi:10.1371/journal.pone.0152263

Kastan, M. B., Canman, C. E., & Leonard, C. J. (1995). P53, cell cycle control and apoptosis: implications for cancer. *Cancer Metastasis Rev, 14*(1), 3-15. doi:10.1007/BF00690207

Kenmochi, N., Kawaguchi, T., Rozen, S., Davis, E., Goodman, N., Hudson, T. J., . . . Page, D. C. (1998). A map of 75 human ribosomal protein genes. *Genome Res, 8*(5), 509-523. doi:10.1101/gr.8.5.509

Kesler, S. R. (2007). Turner syndrome. *Child Adolesc Psychiatr Clin N Am, 16*(3), 709-722. doi:10.1016/j.chc.2007.02.004

Kitamura, N., Nakamura, Y., Miyamoto, Y., Miyamoto, T., Kabu, K., Yoshida, M., . . . Arakawa, H. (2011). Mieap, a p53-inducible protein, controls mitochondrial quality by repairing or eliminating unhealthy mitochondria. *PLoS One, 6*(1), e16060. doi:10.1371/journal.pone.0016060

Kneissig, M., Bernhard, S., & Storchova, Z. (2019). Modelling chromosome structural and copy number changes to understand cancer genomes. *Curr Opin Genet Dev, 54*, 25-32. doi:10.1016/j.gde.2019.02.005

Kneissig, M., Keuper, K., de Pagter, M. S., van Roosmalen, M. J., Martin, J., Otto, H., . . . Storchova, Z. (2019). Micronuclei-based model system reveals functional consequences of chromothripsis in human cells. *Elife, 8*. doi:10.7554/eLife.50292

Knijnenburg, T. A., Wang, L., Zimmermann, M. T., Chambwe, N., Gao, G. F., Cherniack, A. D., . . . Wang, C. (2018). Genomic and Molecular Landscape of DNA Damage Repair Deficiency across The Cancer Genome Atlas. *Cell Rep, 23*(1), 239-254 e236. doi:10.1016/j.celrep.2018.03.076

Knouse, K. A., Davoli, T., Elledge, S. J., & Amon, A. (2017). Aneuploidy in Cancer: Seq-ing Answers to Old Questions. *Annual Review of Cancer Biology, 1*(1), 335-354. doi:10.1146/annurev-cancerbio-042616-072231

Knouse, K. A., Wu, J., Whittaker, C. A., & Amon, A. (2014). Single cell sequencing reveals low levels of aneuploidy across mammalian tissues. *Proc Natl Acad Sci U S A, 111*(37), 13409-13414. doi:10.1073/pnas.1415287111

Kress, M., May, E., Cassingena, R., & May, P. (1979). Simian virus 40-transformed cells express new species of proteins precipitable by anti-simian virus 40 tumor serum. *J Virol, 31*(2), 472-483. doi:10.1128/JVI.31.2.472-483.1979

Kuechler, A., Hauffa, B. P., Koninger, A., Kleinau, G., Albrecht, B., Horsthemke, B., & Gromoll, J. (2010). An unbalanced translocation unmasks a recessive mutation in the follicle-stimulating hormone receptor (FSHR) gene and causes FSH resistance. *Eur J Hum Genet, 18*(6), 656-661. doi:10.1038/ejhg.2009.244

Kuleshov, M. V., Jones, M. R., Rouillard, A. D., Fernandez, N. F., Duan, Q., Wang, Z., . . . Ma'ayan, A. (2016). Enrichr: a comprehensive gene set enrichment analysis web server 2016 update. *Nucleic Acids Res, 44*(W1), W90-97. doi:10.1093/nar/gkw377

Kushner, B. H., & Cheung, N. K. (1996). Allelic loss of chromosome 1p in neuroblastoma. *N Engl J Med, 334*(24), 1608-1609. doi:10.1056/NEJM199606133342415

Kuznetsova, A. Y., Seget, K., Moeller, G. K., de Pagter, M. S., de Roos, J. A., Durrbaum, M., . . . Storchova, Z. (2015). Chromosomal instability, tolerance of mitotic errors and multidrug resistance are promoted by tetraploidization in human cells. *Cell Cycle, 14*(17), 2810-2820. doi:10.1080/15384101.2015.1068482

Kwon, M., Godinho, S. A., Chandhok, N. S., Ganem, N. J., Azioune, A., Thery, M., & Pellman, D. (2008). Mechanisms to suppress multipolar divisions in cancer cells with extra centrosomes. *Genes Dev, 22*(16), 2189-2203. doi:10.1101/gad.1700908

Lane, D. P., & Crawford, L. V. (1979). T antigen is bound to a host protein in SY40-transformed cells. *Nature, 278*(5701), 261-263. doi:10.1038/278261a0

Lee, A. J., Endesfelder, D., Rowan, A. J., Walther, A., Birkbak, N. J., Futreal, P. A., . . . Swanton, C. (2011). Chromosomal instability confers intrinsic multidrug resistance. *Cancer Res, 71*(5), 1858-1870. doi:10.1158/0008-5472.CAN-10-3604

Lee, J. M., & Sonnhammer, E. L. (2003). Genomic gene clustering analysis of pathways in eukaryotes. *Genome Res, 13*(5), 875-882. doi:10.1101/gr.737703

Leitao, A., Boudry, P., & Thiriot-Quievreux, C. (2001). Evidence of differential chromosome loss in aneuploid karyotypes of the Pacific oyster, Crassostrea gigas. *Genome, 44*(4), 735-737.

Leung, G. M. K., Zhang, C., Ng, N. K. L., Yang, N., Lam, S. S. Y., Au, C. H., . . . Leung, A. Y. H. (2019). Distinct mutation spectrum, clinical outcome and therapeutic responses of typical complex/monosomy karyotype acute myeloid leukemia carrying TP53 mutations. *Am J Hematol, 94*(6), 650-657. doi:10.1002/ajh.25469

Levine, A. J., & Oren, M. (2009). The first 30 years of p53: growing ever more complex. *Nat Rev Cancer, 9*(10), 749-758. doi:10.1038/nrc2723

Lewandoski, M., & Martin, G. R. (1997). Cre-mediated chromosome loss in mice. *Nat Genet, 17*(2), 223-225. doi:10.1038/ng1097-223

Li, J. J., Bickel, P. J., & Biggin, M. D. (2014). System wide analyses have underestimated protein abundances and the importance of transcription in mammals. *PeerJ, 2*, e270. doi:10.7717/peerj.270

Li, L. B., Chang, K. H., Wang, P. R., Hirata, R. K., Papayannopoulou, T., & Russell, D. W. (2012). Trisomy correction in Down syndrome induced pluripotent stem cells. *Cell Stem Cell, 11*(5), 615-619. doi:10.1016/j.stem.2012.08.004

Li, M., Fang, X., Baker, D. J., Guo, L., Gao, X., Wei, Z., . . . Zhang, P. (2010). The ATM-p53 pathway suppresses aneuploidy-induced tumorigenesis. *Proc Natl Acad Sci U S A, 107*(32), 14188-14193. doi:10.1073/pnas.1005960107

Liao, Y., Smyth, G. K., & Shi, W. (2014). featureCounts: an efficient general purpose program for assigning sequence reads to genomic features. *Bioinformatics, 30*(7), 923-930. doi:10.1093/bioinformatics/btt656

Liberzon, A., Subramanian, A., Pinchback, R., Thorvaldsdottir, H., Tamayo, P., & Mesirov, J. P. (2011). Molecular signatures database (MSigDB) 3.0. *Bioinformatics, 27*(12), 1739-1740. doi:10.1093/bioinformatics/btr260

Licciardi, F., Lhakhang, T., Kramer, Y. G., Zhang, Y., Heguy, A., & Tsirigos, A. (2018). Human blastocysts of normal and abnormal karyotypes display distinct transcriptome profiles. *Sci Rep, 8*(1), 14906. doi:10.1038/s41598-018-33279-0

Linzer, D. I., & Levine, A. J. (1979). Characterization of a 54K dalton cellular SV40 tumor antigen present in SV40-transformed cells and uninfected embryonal carcinoma cells. *Cell, 17*(1), 43-52. doi:10.1016/0092-8674(79)90293-9

Lippincott-Schwartz, J., Bonifacino, J. S., Yuan, L. C., & Klausner, R. D. (1988). Degradation from the endoplasmic reticulum: disposing of newly synthesized proteins. *Cell, 54*(2), 209-220. doi:10.1016/0092-8674(88)90553-3

Liu, B., Chen, Y., & St Clair, D. K. (2008). ROS and p53: a versatile partnership. *Free Radic Biol Med, 44*(8), 1529-1535. doi:10.1016/j.freeradbiomed.2008.01.011

Liu, S., Kwon, M., Mannino, M., Yang, N., Renda, F., Khodjakov, A., & Pellman, D. (2018). Nuclear envelope assembly defects link mitotic errors to chromothripsis. *Nature, 561*(7724), 551-555. doi:10.1038/s41586-018-0534-z

Liu, Y., Borel, C., Li, L., Muller, T., Williams, E. G., Germain, P. L., . . . Aebersold, R. (2017). Systematic proteome and proteostasis profiling in human Trisomy 21 fibroblast cells. *Nat Commun, 8*(1), 1212. doi:10.1038/s41467-017-01422-6

Liu, Y., Chen, C., Xu, Z., Scuoppo, C., Rillahan, C. D., Gao, J., . . . Lowe, S. W. (2016). Deletions linked to TP53 loss drive cancer through p53-independent mechanisms. *Nature, 531*(7595), 471-475. doi:10.1038/nature17157

Liu, Y., Deisenroth, C., & Zhang, Y. (2016). RP-MDM2-p53 Pathway: Linking Ribosomal Biogenesis and Tumor Surveillance. *Trends Cancer, 2*(4), 191-204. doi:10.1016/j.trecan.2016.03.002

Lopez-Garcia, C., Sansregret, L., Domingo, E., McGranahan, N., Hobor, S., Birkbak, N. J., . . . Swanton, C. (2017). BCL9L Dysfunction Impairs Caspase-2 Expression Permitting Aneuploidy Tolerance in Colorectal Cancer. *Cancer Cell, 31*(1), 79-93. doi:10.1016/j.ccell.2016.11.001

Love, M. I., Huber, W., & Anders, S. (2014). Moderated estimation of fold change and dispersion for RNA-seq data with DESeq2. *Genome Biol, 15*(12), 550. doi:10.1186/s13059-014-0550-8

Lu , P. D., Harding , H. P., & Ron , D. (2004). Translation reinitiation at alternative open reading frames regulates gene expression in an integrated stress response. *Journal of Cell Biology, 167*(1), 27-33. doi:10.1083/jcb.200408003

Lukas, C., Savic, V., Bekker-Jensen, S., Doil, C., Neumann, B., Pedersen, R. S., . . . Lukas, J. (2011). 53BP1 nuclear bodies form around DNA lesions generated by mitotic transmission of chromosomes under replication stress. *Nat Cell Biol, 13*(3), 243-253. doi:10.1038/ncb2201

Lukow, D. A., Sausville, E. L., Suri, P., Chunduri, N. K., Leu, J., Kendall, J., . . . Sheltzer, J. M. (2020). Chromosomal instability accelerates the evolution of resistance to anti-cancer therapies. *bioRxiv*, 2020.2009.2025.314229. doi:10.1101/2020.09.25.314229

Maass, K. K., Rosing, F., Ronchi, P., Willmund, K. V., Devens, F., Hergt, M., . . . Ernst, A. (2018). Altered nuclear envelope structure and proteasome function of micronuclei. *Exp Cell Res, 371*(2), 353-363. doi:10.1016/j.yexcr.2018.08.029

Mackenzie, K. J., Carroll, P., Martin, C. A., Murina, O., Fluteau, A., Simpson, D. J., . . . Jackson, A. P. (2017). cGAS surveillance of micronuclei links genome instability to innate immunity. *Nature, 548*(7668), 461-465. doi:10.1038/nature23449

Magnuson, T., Debrot, S., Dimpfl, J., Zweig, A., Zamora, T., & Epstein, C. J. (1985). The early lethality of autosomal monosomy in the mouse. *J Exp Zool, 236*(3), 353-360. doi:10.1002/jez.1402360313

Manning, A. L., Ganem, N. J., Bakhoum, S. F., Wagenbach, M., Wordeman, L., & Compton, D. A. (2007). The kinesin-13 proteins Kif2a, Kif2b, and Kif2c/MCAK have distinct roles during mitosis in human cells. *Mol Biol Cell, 18*(8), 2970-2979. doi:10.1091/mbc.e07-02-0110

Matsumoto, M., & Seya, T. (2008). TLR3: interferon induction by double-stranded RNA including poly(I:C). *Adv Drug Deliv Rev, 60*(7), 805-812. doi:10.1016/j.addr.2007.11.005

McCallie, B. R., Parks, J. C., Patton, A. L., Griffin, D. K., Schoolcraft, W. B., & Katz-Jaffe, M. G. (2016). Hypomethylation and Genetic Instability in Monosomy Blastocysts May Contribute to Decreased Implantation Potential. *PLoS One, 11*(7), e0159507. doi:10.1371/journal.pone.0159507

McCoy, R. C., Demko, Z. P., Ryan, A., Banjevic, M., Hill, M., Sigurjonsson, S., . . . Petrov, D. A. (2015). Evidence of Selection against Complex Mitotic-Origin Aneuploidy during Preimplantation Development. *PLoS Genet, 11*(10), e1005601. doi:10.1371/journal.pgen.1005601

McGhee, E. M., Cohen, N. R., Wolf, J. L., Ledesma, C. T., & Cotter, P. D. (2000). Monosomy 16 as the sole abnormality in myeloid malignancies. *Cancer Genet Cytogenet, 118*(2), 163-166. doi:10.1016/s0165-4608(99)00194-6

McLure, K. G., & Lee, P. W. (1998). How p53 binds DNA as a tetramer. *EMBO J, 17*(12), 3342-3350. doi:10.1093/emboj/17.12.3342

McShane, E., Sin, C., Zauber, H., Wells, J. N., Donnelly, N., Wang, X., . . . Selbach, M. (2016). Kinetic Analysis of Protein Stability Reveals Age-Dependent Degradation. *Cell, 167*(3), 803-815 e821. doi:10.1016/j.cell.2016.09.015

Meena, J. K., Cerutti, A., Beichler, C., Morita, Y., Bruhn, C., Kumar, M., . . . Rudolph, K. L. (2015). Telomerase abrogates aneuploidy-induced telomere replication stress, senescence and cell depletion. *EMBO J, 34*(10), 1371-1384. doi:10.15252/embj.201490070

Michel, L. S., Liberal, V., Chatterjee, A., Kirchwegger, R., Pasche, B., Gerald, W., . . . Benezra, R. (2001). MAD2 haplo-insufficiency causes premature anaphase and chromosome instability in mammalian cells. *Nature, 409*(6818), 355-359. doi:10.1038/35053094

Mills, E. W., & Green, R. (2017). Ribosomopathies: There's strength in numbers. *Science, 358*(6363). doi:10.1126/science.aan2755

Milner, J. (1991). The role of p53 in the normal control of cell proliferation. *Curr Opin Cell Biol, 3*(2), 282-286. doi:10.1016/0955-0674(91)90153-p

Mirkovic, M., Hutter, L. H., Novak, B., & Oliveira, R. A. (2015). Premature Sister Chromatid Separation Is Poorly Detected by the Spindle Assembly Checkpoint as a Result of System-Level Feedback. *Cell Rep, 13*(3), 469-478. doi:10.1016/j.celrep.2015.09.020

Morrill, S. A., & Amon, A. (2019). Why haploinsufficiency persists. *Proc Natl Acad Sci U S A, 116*(24), 11866-11871. doi:10.1073/pnas.1900437116

Motwani, M., Pesiridis, S., & Fitzgerald, K. A. (2019). DNA sensing by the cGAS-STING pathway in health and disease. *Nat Rev Genet, 20*(11), 657-674. doi:10.1038/s41576-019-0151-1

Mueller, S., Wahlander, A., Selevsek, N., Otto, C., Ngwa, E. M., Poljak, K., . . . Gauss, R. (2015). Protein degradation corrects for imbalanced subunit stoichiometry in OST complex assembly. *Mol Biol Cell, 26*(14), 2596-2608. doi:10.1091/mbc.E15-03-0168

Narla, A., & Ebert, B. L. (2010). Ribosomopathies: human disorders of ribosome dysfunction. *Blood, 115*(16), 3196-3205. doi:10.1182/blood-2009-10-178129

Nicklas, R. B. (1997). How Cells Get the Right Chromosomes. *Science, 275*(5300), 632. doi:10.1126/science.275.5300.632

Nicolas, E., Parisot, P., Pinto-Monteiro, C., de Walque, R., De Vleeschouwer, C., & Lafontaine, D. L. (2016). Involvement of human ribosomal proteins in nucleolar structure and p53-dependent nucleolar stress. *Nat Commun, 7*, 11390. doi:10.1038/ncomms11390

Nigro, J. M., Baker, S. J., Preisinger, A. C., Jessup, J. M., Hostetter, R., Cleary, K., . . . et al. (1989). Mutations in the p53 gene occur in diverse human tumour types. *Nature, 342*(6250), 705-708. doi:10.1038/342705a0

Ohashi, A., Ohori, M., Iwai, K., Nakayama, Y., Nambu, T., Morishita, D., . . . Iwata, K. (2015). Aneuploidy generates proteotoxic stress and DNA damage concurrently with p53-mediated post-mitotic apoptosis in SAC-impaired cells. *Nat Commun, 6*, 7668. doi:10.1038/ncomms8668

Ohnuki, S., & Ohya, Y. (2018). High-dimensional single-cell phenotyping reveals extensive haploinsufficiency. *PLoS Biol, 16*(5), e2005130. doi:10.1371/journal.pbio.2005130

Oromendia, A. B., Dodgson, S. E., & Amon, A. (2012). Aneuploidy causes proteotoxic stress in yeast. *Genes Dev, 26*(24), 2696-2708. doi:10.1101/gad.207407.112

Orr, B., & Compton, D. (2013). A Double-Edged Sword: How Oncogenes and Tumor Suppressor Genes Can Contribute to Chromosomal Instability. *Frontiers in Oncology, 3*(164). doi:10.3389/fonc.2013.00164

Orr, B., Godek, K. M., & Compton, D. (2015). Aneuploidy. *Curr Biol, 25*(13), R538-542. doi:10.1016/j.cub.2015.05.010

Orth, J. D., Loewer, A., Lahav, G., & Mitchison, T. J. (2012). Prolonged mitotic arrest triggers partial activation of apoptosis, resulting in DNA damage and p53 induction. *Mol Biol Cell, 23*(4), 567-576. doi:10.1091/mbc.E11-09-0781

Ottolini, C. S., Kitchen, J., Xanthopoulou, L., Gordon, T., Summers, M. C., & Handyside, A. H. (2017). Tripolar mitosis and partitioning of the genome arrests human preimplantation development in vitro. *Sci Rep, 7*(1), 9744. doi:10.1038/s41598-017-09693-1

Ottolini, C. S., Newnham, L., Capalbo, A., Natesan, S. A., Joshi, H. A., Cimadomo, D., . . . Hoffmann, E. R. (2015). Genome-wide maps of recombination and chromosome segregation in human oocytes and embryos show selection for maternal recombination rates. *Nat Genet, 47*(7), 727-735. doi:10.1038/ng.3306

Pakos-Zebrucka, K., Koryga, I., Mnich, K., Ljujic, M., Samali, A., & Gorman, A. M. (2016). The integrated stress response. *EMBO Rep, 17*(10), 1374-1395. doi:10.15252/embr.201642195

Papp, B., Pal, C., & Hurst, L. D. (2003). Dosage sensitivity and the evolution of gene families in yeast. *Nature, 424*(6945), 194-197. doi:10.1038/nature01771

Passerini, V., Ozeri-Galai, E., de Pagter, M. S., Donnelly, N., Schmalbrock, S., Kloosterman, W. P., . . . Storchova, Z. (2016). The presence of extra chromosomes leads to genomic instability. *Nat Commun, 7*, 10754. doi:10.1038/ncomms10754

Pavelka, N., Rancati, G., Zhu, J., Bradford, W. D., Saraf, A., Florens, L., . . . Li, R. (2010). Aneuploidy confers quantitative proteome changes and phenotypic variation in budding yeast. *Nature, 468*(7321), 321-325. doi:10.1038/nature09529

Pehlivan, T., Pober, B. R., Brueckner, M., Garrett, S., Slaugh, R., Van Rheeden, R., . . . Hing, A. V. (1999). GATA4 haploinsufficiency in patients with interstitial deletion of chromosome region 8p23.1 and congenital heart disease. *Am J Med Genet, 83*(3), 201-206.

Pellegata, N. S., Antoniono, R. J., Redpath, J. L., & Stanbridge, E. J. (1996). DNA damage and p53-mediated cell cycle arrest: a reevaluation. *Proc Natl Acad Sci U S A, 93*(26), 15209-15214. doi:10.1073/pnas.93.26.15209

Pelletier, J., Thomas, G., & Volarevic, S. (2018). Ribosome biogenesis in cancer: new players and therapeutic avenues. *Nat Rev Cancer, 18*(1), 51-63. doi:10.1038/nrc.2017.104

Peter, J., De Chiara, M., Friedrich, A., Yue, J. X., Pflieger, D., Bergstrom, A., . . . Schacherer, J. (2018). Genome evolution across 1,011 Saccharomyces cerevisiae isolates. *Nature, 556*(7701), 339-344. doi:10.1038/s41586-018-0030-5

Phillips, J. L., Hayward, S. W., Wang, Y., Vasselli, J., Pavlovich, C., Padilla-Nash, H., . . . Ried, T. (2001). The consequences of chromosomal aneuploidy on gene expression profiles in a cell line model for prostate carcinogenesis. *Cancer Res, 61*(22), 8143-8149.

Piló, D., Carvalho, S., Pereira, P., Gaspar, M. B., & Leitão, A. (2017). Is metal contamination responsible for increasing aneuploidy levels in the Manila clam Ruditapes philippinarum? *Science of The Total Environment, 577*, 340-348. doi:https://doi.org/10.1016/j.scitotenv.2016.10.193

Poll, G., Braun, T., Jakovljevic, J., Neueder, A., Jakob, S., Woolford, J. L., Jr., . . . Milkereit, P. (2009). rRNA maturation in yeast cells depleted of large ribosomal subunit proteins. *PLoS One, 4*(12), e8249. doi:10.1371/journal.pone.0008249

Pollack, J. R., Sorlie, T., Perou, C. M., Rees, C. A., Jeffrey, S. S., Lonning, P. E., . . . Brown, P. O. (2002). Microarray analysis reveals a major direct role of DNA copy number alteration in the transcriptional program of human breast tumors. *Proc Natl Acad Sci U S A, 99*(20), 12963-12968. doi:10.1073/pnas.162471999

Porta, G., Maserati, E., Mattarucchi, E., Minelli, A., Pressato, B., Valli, R., . . . Pasquali, F. (2007). Monosomy 7 in myeloid malignancies: parental origin and monitoring by real-time quantitative PCR. *Leukemia, 21*(8), 1833-1835. doi:10.1038/sj.leu.2404708

Pringle, E. S., McCormick, C., & Cheng, Z. (2019). Polysome Profiling Analysis of mRNA and Associated Proteins Engaged in Translation. *Curr Protoc Mol Biol, 125*(1), e79. doi:10.1002/cpmb.79

Ramirez-Solis, R., Liu, P., & Bradley, A. (1995). Chromosome engineering in mice. *Nature, 378*(6558), 720-724. doi:10.1038/378720a0

Raz, R., Cheung, K., Ling, L., & Levy, D. E. (1995). Three distinct loci on human chromosome 21 contribute to interferon-alpha/beta responsiveness. *Somat Cell Mol Genet, 21*(2), 139-145. doi:10.1007/BF02255789

Rehen, S. K., McConnell, M. J., Kaushal, D., Kingsbury, M. A., Yang, A. H., & Chun, J. (2001). Chromosomal variation in neurons of the developing and adult mammalian nervous system. *Proc Natl Acad Sci U S A, 98*(23), 13361-13366. doi:10.1073/pnas.231487398

Rehen, S. K., Yung, Y. C., McCreight, M. P., Kaushal, D., Yang, A. H., Almeida, B. S., . . . Chun, J. (2005). Constitutional aneuploidy in the normal human brain. *J Neurosci, 25*(9), 2176-2180. doi:10.1523/JNEUROSCI.4560-04.2005

Reiner, O., Carrozzo, R., Shen, Y., Wehnert, M., Faustinella, F., Dobyns, W. B., . . . Ledbetter, D. H. (1993). Isolation of a Miller-Dieker lissencephaly gene containing G protein beta-subunit-like repeats. *Nature, 364*(6439), 717-721. doi:10.1038/364717a0

Replogle, J. M., Zhou, W., Amaro, A. E., McFarland, J. M., Villalobos-Ortiz, M., Ryan, J., . . . Amon, A. (2020). Aneuploidy increases resistance to chemotherapeutics by antagonizing cell division. *Proc Natl Acad Sci U S A, 117*(48), 30566-30576. doi:10.1073/pnas.2009506117

Riley, T., Sontag, E., Chen, P., & Levine, A. (2008). Transcriptional control of human p53-regulated genes. *Nat Rev Mol Cell Biol, 9*(5), 402-412. doi:10.1038/nrm2395

Ritchie, M. E., Phipson, B., Wu, D., Hu, Y., Law, C. W., Shi, W., & Smyth, G. K. (2015). limma powers differential expression analyses for RNA-sequencing and microarray studies. *Nucleic Acids Res, 43*(7), e47. doi:10.1093/nar/gkv007

Robledo, S., Idol, R. A., Crimmins, D. L., Ladenson, J. H., Mason, P. J., & Bessler, M. (2008). The role of human ribosomal proteins in the maturation of rRNA and ribosome production. *RNA, 14*(9), 1918-1929. doi:10.1261/rna.1132008

Romeo, G., Ronchetto, P., Luo, Y., Barone, V., Seri, M., Ceccherini, I., . . . et al. (1994). Point mutations affecting the tyrosine kinase domain of the RET proto-oncogene in Hirschsprung's disease. *Nature, 367*(6461), 377-378. doi:10.1038/367377a0

Rouault, J. P., Falette, N., Guehenneux, F., Guillot, C., Rimokh, R., Wang, Q., . . . Puisieux, A. (1996). Identification of BTG2, an antiproliferative p53-dependent component of the DNA damage cellular response pathway. *Nat Genet, 14*(4), 482-486. doi:10.1038/ng1296-482

Rujkijyanont, P., Adams, S. L., Beyene, J., & Dror, Y. (2009). Bone marrow cells from patients with Shwachman-Diamond syndrome abnormally express genes involved in ribosome biogenesis and RNA processing. *Br J Haematol, 145*(6), 806-815. doi:10.1111/j.1365-2141.2009.07692.x

Rutledge, S. D., Douglas, T. A., Nicholson, J. M., Vila-Casadesus, M., Kantzler, C. L., Wangsa, D., . . . Cimini, D. (2016). Selective advantage of trisomic human cells cultured in non-standard conditions. *Sci Rep, 6*, 22828. doi:10.1038/srep22828

Sabat-Pospiech, D., Fabian-Kolpanowicz, K., Prior, I. A., Coulson, J. M., & Fielding, A. B. (2019). Targeting centrosome amplification, an Achilles' heel of cancer. *Biochem Soc Trans, 47*(5), 1209-1222. doi:10.1042/BST20190034

Sablina, A. A., Budanov, A. V., Ilyinskaya, G. V., Agapova, L. S., Kravchenko, J. E., & Chumakov, P. M. (2005). The antioxidant function of the p53 tumor suppressor. *Nat Med, 11*(12), 1306-1313. doi:10.1038/nm1320

Sansregret, L., & Swanton, C. (2017). The Role of Aneuploidy in Cancer Evolution. *Cold Spring Harb Perspect Med, 7*(1). doi:10.1101/cshperspect.a028373

Santaguida, S., & Amon, A. (2015). Short- and long-term effects of chromosome mis-segregation and aneuploidy. *Nat Rev Mol Cell Biol, 16*(8), 473-485. doi:10.1038/nrm4025

Santaguida, S., Richardson, A., Iyer, D. R., M'Saad, O., Zasadil, L., Knouse, K. A., . . . Amon, A. (2017). Chromosome Mis-segregation Generates Cell-Cycle-Arrested Cells with Complex Karyotypes that Are Eliminated by the Immune System. *Dev Cell, 41*(6), 638-651 e635. doi:10.1016/j.devcel.2017.05.022

Santaguida, S., Vasile, E., White, E., & Amon, A. (2015). Aneuploidy-induced cellular stresses limit autophagic degradation. *Genes Dev, 29*(19), 2010-2021. doi:10.1101/gad.269118.115

Santarosa, M., & Ashworth, A. (2004). Haploinsufficiency for tumour suppressor genes: when you don't need to go all the way. *Biochim Biophys Acta, 1654*(2), 105-122. doi:10.1016/j.bbcan.2004.01.001

Schliekelman, M., Cowley, D. O., O'Quinn, R., Oliver, T. G., Lu, L., Salmon, E. D., & Van Dyke, T. (2009). Impaired Bub1 function in vivo compromises tension-dependent checkpoint function leading to aneuploidy and tumorigenesis. *Cancer Res, 69*(1), 45-54. doi:10.1158/0008-5472.CAN-07-6330

Schneider, W. M., Chevillotte, M. D., & Rice, C. M. (2014). Interferon-stimulated genes: a complex web of host defenses. *Annu Rev Immunol, 32*, 513-545. doi:10.1146/annurev-immunol-032713-120231

Schott, J. J., Benson, D. W., Basson, C. T., Pease, W., Silberbach, G. M., Moak, J. P., . . . Seidman, J. G. (1998). Congenital heart disease caused by mutations in the transcription factor NKX2-5. *Science, 281*(5373), 108-111. doi:10.1126/science.281.5373.108

Schwanhausser, B., Busse, D., Li, N., Dittmar, G., Schuchhardt, J., Wolf, J., . . . Selbach, M. (2011). Global quantification of mammalian gene expression control. *Nature, 473*(7347), 337-342. doi:10.1038/nature10098

Schwartz, M., Sternberg, D., Whalen, S., Afenjar, A., Isapof, A., Chabrol, B., . . . Siffroi, J.-P. (2018). How chromosomal deletions can unmask recessive mutations? Deletions in 10q11.2 associated with CHAT or SLC18A3 mutations lead to congenital myasthenic syndrome. *American Journal of Medical Genetics Part A, 176*(1), 151-155. doi:10.1002/ajmg.a.38515

Schwartzenberg-Bar-Yoseph, F., Armoni, M., & Karnieli, E. (2004). The tumor suppressor p53 down-regulates glucose transporters GLUT1 and GLUT4 gene expression. *Cancer Res, 64*(7), 2627-2633. doi:10.1158/0008-5472.can-03-0846

Scian, M. J., Carchman, E. H., Mohanraj, L., Stagliano, K. E., Anderson, M. A., Deb, D., . . . Deb, S. (2008). Wild-type p53 and p73 negatively regulate expression of proliferation related genes. *Oncogene, 27*(18), 2583-2593. doi:10.1038/sj.onc.1210898

Segal, D. J., & McCoy, E. E. (1974). Studies on Down's syndrome in tissue culture. I. Growth rates and protein contents of fibroblast cultures. *J Cell Physiol, 83*(1), 85-90. doi:10.1002/jcp.1040830112

Seidman, J. G., & Seidman, C. (2002). Transcription factor haploinsufficiency: when half a loaf is not enough. *J Clin Invest, 109*(4), 451-455. doi:10.1172/JCI15043

Selmecki, A., Forche, A., & Berman, J. (2006). Aneuploidy and isochromosome formation in drug-resistant Candida albicans. *Science, 313*(5785), 367-370. doi:10.1126/science.1128242

Shahbazi, M. N., Wang, T., Tao, X., Weatherbee, B. A. T., Sun, L., Zhan, Y., . . . Zernicka-Goetz, M. (2020). Developmental potential of aneuploid human embryos cultured beyond implantation. *Nat Commun, 11*(1), 3987. doi:10.1038/s41467-020-17764-7

Sheltzer, J. M., Blank, H. M., Pfau, S. J., Tange, Y., George, B. M., Humpton, T. J., . . . Amon, A. (2011). Aneuploidy drives genomic instability in yeast. *Science, 333*(6045), 1026-1030. doi:10.1126/science.1206412

Sheltzer, J. M., Ko, J. H., Replogle, J. M., Habibe Burgos, N. C., Chung, E. S., Meehl, C. M., . . . Amon, A. (2017). Single-chromosome Gains Commonly Function as Tumor Suppressors. *Cancer Cell, 31*(2), 240-255. doi:10.1016/j.ccell.2016.12.004

Sheltzer, J. M., Torres, E. M., Dunham, M. J., & Amon, A. (2012). Transcriptional consequences of aneuploidy. *Proc Natl Acad Sci U S A, 109*(31), 12644-12649. doi:10.1073/pnas.1209227109

Shen, Y. J., Le Bert, N., Chitre, A. A., Koo, C. X., Nga, X. H., Ho, S. S., . . . Gasser, S. (2015). Genome-derived cytosolic DNA mediates type I interferon-dependent rejection of B cell lymphoma cells. *Cell Rep, 11*(3), 460-473. doi:10.1016/j.celrep.2015.03.041

Shintomi, K., & Hirano, T. (2009). Releasing cohesin from chromosome arms in early mitosis: opposing actions of Wapl-Pds5 and Sgo1. *Genes Dev, 23*(18), 2224-2236. doi:10.1101/gad.1844309

Simonetti, G., Bruno, S., Padella, A., Tenti, E., & Martinelli, G. (2019). Aneuploidy: Cancer strength or vulnerability? *International Journal of Cancer, 144*(1), 8-25. doi:https://doi.org/10.1002/ijc.31718

Simonetti, G., Bruno, S., Padella, A., Tenti, E., & Martinelli, G. (2019). Aneuploidy: Cancer strength or vulnerability? *Int J Cancer, 144*(1), 8-25. doi:10.1002/ijc.31718

Snape, K., Hanks, S., Ruark, E., Barros-Nunez, P., Elliott, A., Murray, A., . . . Rahman, N. (2011). Mutations in CEP57 cause mosaic variegated aneuploidy syndrome. *Nat Genet, 43*(6), 527-529. doi:10.1038/ng.822

Solimini, N. L., Xu, Q., Mermel, C. H., Liang, A. C., Schlabach, M. R., Luo, J., . . . Elledge, S. J. (2012). Recurrent hemizygous deletions in cancers may optimize proliferative potential. *Science, 337*(6090), 104-109. doi:10.1126/science.1219580

Soto, M., Raaijmakers, J. A., Bakker, B., Spierings, D. C. J., Lansdorp, P. M., Foijer, F., & Medema, R. H. (2017). p53 Prohibits Propagation of Chromosome Segregation Errors that Produce Structural Aneuploidies. *Cell Rep, 19*(12), 2423-2431. doi:10.1016/j.celrep.2017.05.055

Srivastava, S., Zou, Z. Q., Pirollo, K., Blattner, W., & Chang, E. H. (1990). Germ-line transmission of a mutated p53 gene in a cancer-prone family with Li-Fraumeni syndrome. *Nature, 348*(6303), 747-749. doi:10.1038/348747a0

Stadanlick, J. E., Zhang, Z., Lee, S. Y., Hemann, M., Biery, M., Carleton, M. O., . . . Wiest, D. L. (2011). Developmental arrest of T cells in Rpl22-deficient mice is dependent upon multiple p53 effectors. *J Immunol, 187*(2), 664-675. doi:10.4049/jimmunol.1100029

Starck, S. R., Green, H. M., Alberola-Ila, J., & Roberts, R. W. (2004). A general approach to detect protein expression in vivo using fluorescent puromycin conjugates. *Chem Biol, 11*(7), 999-1008. doi:10.1016/j.chembiol.2004.05.011

Steffen, K. K., McCormick, M. A., Pham, K. M., MacKay, V. L., Delaney, J. R., Murakami, C. J., . . . Kennedy, B. K. (2012). Ribosome deficiency protects against ER stress in Saccharomyces cerevisiae. *Genetics, 191*(1), 107-118. doi:10.1534/genetics.111.136549

Stenberg, P., Lundberg, L. E., Johansson, A. M., Ryden, P., Svensson, M. J., & Larsson, J. (2009). Buffering of segmental and chromosomal aneuploidies in Drosophila melanogaster. *PLoS Genet, 5*(5), e1000465. doi:10.1371/journal.pgen.1000465

Stingele, S., Stoehr, G., Peplowska, K., Cox, J., Mann, M., & Storchova, Z. (2012). Global analysis of genome, transcriptome and proteome reveals the response to aneuploidy in human cells. *Mol Syst Biol, 8*, 608. doi:10.1038/msb.2012.40

Storchova, Z., & Kuffer, C. (2008). The consequences of tetraploidy and aneuploidy. *J Cell Sci, 121*(Pt 23), 3859-3866. doi:10.1242/jcs.039537

Sullivan, K. D., Evans, D., Pandey, A., Hraha, T. H., Smith, K. P., Markham, N., . . . Blumenthal, T. (2017). Trisomy 21 causes changes in the circulating proteome indicative of chronic autoinflammation. *Sci Rep, 7*(1), 14818. doi:10.1038/s41598-017-13858-3

Sullivan, K. D., Lewis, H. C., Hill, A. A., Pandey, A., Jackson, L. P., Cabral, J. M., . . . Espinosa, J. M. (2016). Trisomy 21 consistently activates the interferon response. *Elife, 5*. doi:10.7554/eLife.16220

Sun, L., Wu, J., Du, F., Chen, X., & Chen, Z. J. (2013). Cyclic GMP-AMP Synthase Is a Cytosolic DNA Sensor That Activates the Type I Interferon Pathway. *Science, 339*(6121), 786. doi:10.1126/science.1232458

Sung, M. K., Reitsma, J. M., Sweredoski, M. J., Hess, S., & Deshaies, R. J. (2016). Ribosomal proteins produced in excess are degraded by the ubiquitin-proteasome system. *Mol Biol Cell, 27*(17), 2642-2652. doi:10.1091/mbc.E16-05-0290

Swanton, C., Nicke, B., Schuett, M., Eklund, A. C., Ng, C., Li, Q., . . . Downward, J. (2009). Chromosomal instability determines taxane response. *Proc Natl Acad Sci U S A, 106*(21), 8671-8676. doi:10.1073/pnas.0811835106

Takahashi, T., Nau, M. M., Chiba, I., Birrer, M. J., Rosenberg, R. K., Vinocour, M., . . . Minna, J. D. (1989). p53: a frequent target for genetic abnormalities in lung cancer. *Science, 246*(4929), 491-494. doi:10.1126/science.2554494

Tang, Y.-C., Williams, B. R., Siegel, J. J., & Amon, A. (2011). Identification of Aneuploidy-Selective Antiproliferation Compounds. *Cell, 144*(4), 499-512. doi:10.1016/j.cell.2011.01.017

Tang, Y. C., Williams, B. R., Siegel, J. J., & Amon, A. (2011). Identification of aneuploidy-selective antiproliferation compounds. *Cell, 144*(4), 499-512. doi:10.1016/j.cell.2011.01.017

Tanikawa, C., Nakagawa, H., Furukawa, Y., Nakamura, Y., & Matsuda, K. (2012). CLCA2 as a p53-inducible senescence mediator. *Neoplasia, 14*(2), 141-149. doi:10.1593/neo.111700

Taylor, A. M., Shih, J., Ha, G., Gao, G. F., Zhang, X., Berger, A. C., . . . Meyerson, M. (2018). Genomic and Functional Approaches to Understanding Cancer Aneuploidy. *Cancer Cell, 33*(4), 676-689 e673. doi:10.1016/j.ccell.2018.03.007

Teichmann, S. A., & Veitia, R. A. (2004). Genes encoding subunits of stable complexes are clustered on the yeast chromosomes: an interpretation from a dosage balance perspective. *Genetics, 167*(4), 2121-2125. doi:10.1534/genetics.103.024505

Terhorst, A., Sandikci, A., Keller, A., Whittaker, C. A., Dunham, M. J., & Amon, A. (2020). The environmental stress response causes ribosome loss in aneuploid yeast cells. *Proc Natl Acad Sci U S A, 117*(29), 17031-17040. doi:10.1073/pnas.2005648117

Thomas, R., Marks, D. H., Chin, Y., & Benezra, R. (2018). Whole chromosome loss and associated breakage-fusion-bridge cycles transform mouse tetraploid cells. *EMBO J, 37*(2), 201-218. doi:10.15252/embj.201797630

Thompson, S. L., & Compton, D. A. (2010). Proliferation of aneuploid human cells is limited by a p53-dependent mechanism. *J Cell Biol, 188*(3), 369-381. doi:10.1083/jcb.200905057

Torres, E. M., Dephoure, N., Panneerselvam, A., Tucker, C. M., Whittaker, C. A., Gygi, S. P., . . . Amon, A. (2010). Identification of aneuploidy-tolerating mutations. *Cell, 143*(1), 71-83. doi:10.1016/j.cell.2010.08.038

Torres, E. M., Sokolsky, T., Tucker, C. M., Chan, L. Y., Boselli, M., Dunham, M. J., & Amon, A. (2007). Effects of aneuploidy on cellular physiology and cell division in haploid yeast. *Science, 317*(5840), 916-924. doi:10.1126/science.1142210

Torres, E. M., Springer, M., & Amon, A. (2016). No current evidence for widespread dosage compensation in S. cerevisiae. *Elife, 5*, e10996. doi:10.7554/eLife.10996

Tsai, H. J., Nelliat, A. R., Choudhury, M. I., Kucharavy, A., Bradford, W. D., Cook, M. E., . . . Li, R. (2019). Hypo-osmotic-like stress underlies general cellular defects of aneuploidy. *Nature, 570*(7759), 117-121. doi:10.1038/s41586-019-1187-2

Tucker, C., Bhattacharya, S., Wakabayashi, H., Bellaousov, S., Kravets, A., Welle, S. L., . . . Rustchenko, E. (2018). Transcriptional Regulation on Aneuploid Chromosomes in Divers Candida albicans Mutants. *Sci Rep, 8*(1), 1630. doi:10.1038/s41598-018-20106-9

Tumova, P., Uzlikova, M., Jurczyk, T., & Nohynkova, E. (2016). Constitutive aneuploidy and genomic instability in the single-celled eukaryote Giardia intestinalis. *Microbiologyopen, 5*(4), 560-574. doi:10.1002/mbo3.351

Turajlic, S., & Swanton, C. (2016). Metastasis as an evolutionary process. *Science, 352*(6282), 169-175. doi:10.1126/science.aaf2784

Tutt, A., Gabriel, A., Bertwistle, D., Connor, F., Paterson, H., Peacock, J., . . . Ashworth, A. (1999). Absence of Brca2 causes genome instability by chromosome breakage and loss associated with centrosome amplification. *Curr Biol, 9*(19), 1107-1110. doi:10.1016/s0960-9822(99)80479-5

Uechi, T., Tanaka, T., & Kenmochi, N. (2001). A complete map of the human ribosomal protein genes: assignment of 80 genes to the cytogenetic map and implications for human disorders. *Genomics, 72*(3), 223-230. doi:10.1006/geno.2000.6470

Uetake, Y., & Sluder, G. (2010). Prolonged prometaphase blocks daughter cell proliferation despite normal completion of mitosis. *Curr Biol, 20*(18), 1666-1671. doi:10.1016/j.cub.2010.08.018

Uetake, Y., & Sluder, G. (2018). Activation of the apoptotic pathway during prolonged prometaphase blocks daughter cell proliferation. *Mol Biol Cell, 29*(22), 2632-2643. doi:10.1091/mbc.E18-01-0026

Upender, M. B., Habermann, J. K., McShane, L. M., Korn, E. L., Barrett, J. C., Difilippantonio, M. J., & Ried, T. (2004). Chromosome transfer induced aneuploidy results in complex dysregulation of the cellular transcriptome in immortalized and cancer cells. *Cancer Res, 64*(19), 6941-6949. doi:10.1158/0008-5472.CAN-04-0474

Valsecchi, C. I. K., Basilicata, M. F., Semplicio, G., Georgiev, P., Gutierrez, N. M., & Akhtar, A. (2018). Facultative dosage compensation of developmental genes on autosomes in Drosophila and mouse embryonic stem cells. *Nat Commun, 9*(1), 3626. doi:10.1038/s41467-018-05642-2

van Harn, T., Foijer, F., van Vugt, M., Banerjee, R., Yang, F., Oostra, A., . . . te Riele, H. (2010). Loss of Rb proteins causes genomic instability in the absence of mitogenic signaling. *Genes Dev, 24*(13), 1377-1388. doi:10.1101/gad.580710

van Riggelen, J., Yetil, A., & Felsher, D. W. (2010). MYC as a regulator of ribosome biogenesis and protein synthesis. *Nature Reviews Cancer, 10*(4), 301-309. doi:10.1038/nrc2819

Vander Heiden, M. G., Cantley, L. C., & Thompson, C. B. (2009). Understanding the Warburg effect: the metabolic requirements of cell proliferation. *Science, 324*(5930), 1029-1033. doi:10.1126/science.1160809

Vasudevan, A., Baruah, P. S., Smith, J. C., Wang, Z., Sayles, N. M., Andrews, P., . . . Sheltzer, J. M. (2020). Single-Chromosomal Gains Can Function as Metastasis Suppressors and Promoters in Colon Cancer. *Dev Cell, 52*(4), 413-428 e416. doi:10.1016/j.devcel.2020.01.034

Vazquez-Diez, C., & FitzHarris, G. (2018). Causes and consequences of chromosome segregation error in preimplantation embryos. *Reproduction, 155*(1), R63-R76. doi:10.1530/REP-17-0569

Veitia, R. A. (2002). Exploring the etiology of haploinsufficiency. *Bioessays, 24*(2), 175-184. doi:10.1002/bies.10023

Veitia, R. A., Bottani, S., & Birchler, J. A. (2008). Cellular reactions to gene dosage imbalance: genomic, transcriptomic and proteomic effects. *Trends Genet, 24*(8), 390-397. doi:10.1016/j.tig.2008.05.005

Vigano, C., von Schubert, C., Ahrne, E., Schmidt, A., Lorber, T., Bubendorf, L., . . . Nigg, E. A. (2018). Quantitative proteomic and phosphoproteomic comparison of human colon cancer DLD-1 cells differing in ploidy and chromosome stability. *Mol Biol Cell, 29*(9), 1031-1047. doi:10.1091/mbc.E17-10-0577

Virtaneva, K., Wright, F. A., Tanner, S. M., Yuan, B., Lemon, W. J., Caligiuri, M. A., . . . Krahe, R. (2001). Expression profiling reveals fundamental biological differences in acute myeloid leukemia with isolated trisomy 8 and normal cytogenetics. *Proc Natl Acad Sci U S A, 98*(3), 1124-1129. doi:10.1073/pnas.98.3.1124

Vlachos, A. (2017). Acquired ribosomopathies in leukemia and solid tumors. *Hematology Am Soc Hematol Educ Program, 2017*(1), 716-719. doi:10.1182/asheducation-2017.1.716

Wang, R. W., Viganò, S., Ben-David, U., Amon, A., & Santaguida, S. (2020). Aneuploid cells activate NF-κB to promote their immune clearance by NK cells. *bioRxiv*, 2020.2006.2025.172239. doi:10.1101/2020.06.25.172239

Wang, Y., Yang, F., Gritsenko, M. A., Wang, Y., Clauss, T., Liu, T., . . . Smith, R. D. (2011). Reversed-phase chromatography with multiple fraction concatenation strategy for proteome profiling of human MCF10A cells. *Proteomics, 11*(10), 2019-2026. doi:10.1002/pmic.201000722

Watson, C. T., Marques-Bonet, T., Sharp, A. J., & Mefford, H. C. (2014). The genetics of microdeletion and microduplication syndromes: an update. *Annu Rev Genomics Hum Genet, 15*, 215-244. doi:10.1146/annurev-genom-091212-153408

Weaver, B. A., Silk, A. D., Montagna, C., Verdier-Pinard, P., & Cleveland, D. W. (2007). Aneuploidy acts both oncogenically and as a tumor suppressor. *Cancer Cell, 11*(1), 25-36. doi:10.1016/j.ccr.2006.12.003

Weaver, B. A. A., & Cleveland, D. W. (2006). Does aneuploidy cause cancer? *Current Opinion in Cell Biology, 18*(6), 658-667. doi:https://doi.org/10.1016/j.ceb.2006.10.002

Will, B., & Steidl, U. (2014). Combinatorial haplo-deficient tumor suppression in 7q-deficient myelodysplastic syndrome and acute myeloid leukemia. *Cancer Cell, 25*(5), 555-557. doi:10.1016/j.ccr.2014.04.018

Williams, B. R., Prabhu, V. R., Hunter, K. E., Glazier, C. M., Whittaker, C. A., Housman, D. E., & Amon, A. (2008). Aneuploidy affects proliferation and spontaneous immortalization in mammalian cells. *Science, 322*(5902), 703-709. doi:10.1126/science.1160058

Won, K. Y., Lim, S. J., Kim, G. Y., Kim, Y. W., Han, S. A., Song, J. Y., & Lee, D. K. (2012). Regulatory role of p53 in cancer metabolism via SCO2 and TIGAR in human breast cancer. *Hum Pathol, 43*(2), 221-228. doi:10.1016/j.humpath.2011.04.021

Wong, C., & Stearns, T. (2003). Centrosome number is controlled by a centrosome-intrinsic block to reduplication. *Nature Cell Biology, 5*(6), 539-544. doi:10.1038/ncb993

Wu, J., Sun, L., Chen, X., Du, F., Shi, H., Chen, C., & Chen, Z. J. (2013). Cyclic GMP-AMP Is an Endogenous Second Messenger in Innate Immune Signaling by Cytosolic DNA. *Science, 339*(6121), 826. doi:10.1126/science.1229963

Xue, W., Kitzing, T., Roessler, S., Zuber, J., Krasnitz, A., Schultz, N., . . . Lowe, S. W. (2012). A cluster of cooperating tumor-suppressor gene candidates in chromosomal deletions. *Proc Natl Acad Sci U S A, 109*(21), 8212-8217. doi:10.1073/pnas.1206062109

Zhang, C. Z., Spektor, A., Cornils, H., Francis, J. M., Jackson, E. K., Liu, S., . . . Pellman, D. (2015). Chromothripsis from DNA damage in micronuclei. *Nature, 522*(7555), 179-184. doi:10.1038/nature14493

Zhang, Y., Malone, J. H., Powell, S. K., Periwal, V., Spana, E., Macalpine, D. M., & Oliver, B. (2010). Expression in aneuploid Drosophila S2 cells. *PLoS Biol, 8*(2), e1000320. doi:10.1371/journal.pbio.1000320

Zhang, Y., Qian, Y., Zhang, J., Yan, W., Jung, Y. S., Chen, M., . . . Chen, X. (2017). Ferredoxin reductase is critical for p53-dependent tumor suppression via iron regulatory protein 2. *Genes Dev, 31*(12), 1243-1256. doi:10.1101/gad.299388.117

Zhao, X., Gao, S., Wu, Z., Kajigaya, S., Feng, X., Liu, Q., . . . Young, N. S. (2017). Single-cell RNA-seq reveals a distinct transcriptome signature of aneuploid hematopoietic cells. *Blood, 130*(25), 2762-2773. doi:10.1182/blood-2017-08-803353

Zhu, J., Tsai, H.-J., Gordon, M. R., & Li, R. (2018). Cellular Stress Associated with Aneuploidy. *Developmental Cell, 44*(4), 420-431. doi:https://doi.org/10.1016/j.devcel.2018.02.002

Zhu, P. J., Khatiwada, S., Cui, Y., Reineke, L. C., Dooling, S. W., Kim, J. J., . . . Costa-Mattioli, M. (2019). Activation of the ISR mediates the behavioral and neurophysiological abnormalities in Down syndrome. *Science, 366*(6467), 843-849. doi:10.1126/science.aaw5185

Zhuang, H., Kosboth, M., Lee, P., Rice, A., Driscoll, D. J., Zori, R., . . . Reeves, W. H. (2006). Lupus-like disease and high interferon levels corresponding to trisomy of the type I interferon cluster on chromosome 9p. *Arthritis Rheum, 54*(5), 1573-1579. doi:10.1002/art.21800

Zuccaro, M. V., Xu, J., Mitchell, C., Marin, D., Zimmerman, R., Rana, B., . . . Egli, D. (2020). Allele-Specific Chromosome Removal after Cas9 Cleavage in Human Embryos. *Cell*. doi:10.1016/j.cell.2020.10.025

Zuo, E., Huo, X., Yao, X., Hu, X., Sun, Y., Yin, J., . . . Yang, H. (2017). CRISPR/Cas9-mediated targeted chromosome elimination. *Genome Biol, 18*(1), 224. doi:10.1186/s13059-017-1354-4

Barretina, J., Caponigro, G., Stransky, N., Venkatesan, K., Margolin, A. A., Kim, S., . . . Garraway, L. A. (2012). The Cancer Cell Line Encyclopedia enables predictive modelling of anticancer drug sensitivity. *Nature, 483*(7391), 603-607. doi:10.1038/nature11003

Carter, S. L., Cibulskis, K., Helman, E., McKenna, A., Shen, H., Zack, T., . . . Getz, G. (2012). Absolute quantification of somatic DNA alterations in human cancer. *Nat Biotechnol, 30*(5), 413-421. doi:10.1038/nbt.2203

Cox, J., & Mann, M. (2012). 1D and 2D annotation enrichment: a statistical method integrating quantitative proteomics with complementary high-throughput data. *BMC Bioinformatics, 13 Suppl 16*, S12. doi:10.1186/1471-2105-13-S16-S12

Dobin, A., Davis, C. A., Schlesinger, F., Drenkow, J., Zaleski, C., Jha, S., . . . Gingeras, T. R. (2013). STAR: ultrafast universal RNA-seq aligner. *Bioinformatics, 29*(1), 15-21. doi:10.1093/bioinformatics/bts635

Garcia-Castillo, H., Vasquez-Velasquez, A. I., Rivera, H., & Barros-Nunez, P. (2008). Clinical and genetic heterogeneity in patients with mosaic variegated aneuploidy: delineation of clinical subtypes. *Am J Med Genet A, 146A*(13), 1687-1695. doi:10.1002/ajmg.a.32315

Goddard, T. D., Huang, C. C., Meng, E. C., Pettersen, E. F., Couch, G. S., Morris, J. H., & Ferrin, T. E. (2018). UCSF ChimeraX: Meeting modern challenges in visualization and analysis. *Protein Sci, 27*(1), 14-25. doi:10.1002/pro.3235

Greco, E., Minasi, M. G., & Fiorentino, F. (2015). Healthy Babies after Intrauterine Transfer of Mosaic Aneuploid Blastocysts. *N Engl J Med, 373*(21), 2089-2090. doi:10.1056/NEJMc1500421

Hanks, S., Coleman, K., Reid, S., Plaja, A., Firth, H., Fitzpatrick, D., . . . Rahman, N. (2004). Constitutional aneuploidy and cancer predisposition caused by biallelic mutations in BUB1B. *Nat Genet, 36*(11), 1159-1161. doi:10.1038/ng1449

Hanzelmann, S., Castelo, R., & Guinney, J. (2013). GSVA: gene set variation analysis for microarray and RNA-seq data. *BMC Bioinformatics, 14*, 7. doi:10.1186/1471-2105-14-7

Heinz, N., Schambach, A., Galla, M., Maetzig, T., Baum, C., Loew, R., & Schiedlmeier, B. (2010). Retroviral and Transposon-Based Tet-Regulated All-In-One Vectors with Reduced Background Expression and Improved Dynamic Range. *Human Gene Therapy, 22*(2), 166-176. doi:10.1089/hum.2010.099

Huber, W., von Heydebreck, A., Sultmann, H., Poustka, A., & Vingron, M. (2002). Variance stabilization applied to microarray data calibration and to the quantification of differential expression. *Bioinformatics, 18 Suppl 1*, S96-104. doi:10.1093/bioinformatics/18.suppl_1.s96

Knijnenburg, T. A., Wang, L., Zimmermann, M. T., Chambwe, N., Gao, G. F., Cherniack, A. D., . . . Wang, C. (2018). Genomic and Molecular Landscape of DNA Damage Repair Deficiency across The Cancer Genome Atlas. *Cell Rep, 23*(1), 239-254 e236. doi:10.1016/j.celrep.2018.03.076

Liao, Y., Smyth, G. K., & Shi, W. (2014). featureCounts: an efficient general purpose program for assigning sequence reads to genomic features. *Bioinformatics, 30*(7), 923-930. doi:10.1093/bioinformatics/btt656

Liberzon, A., Subramanian, A., Pinchback, R., Thorvaldsdottir, H., Tamayo, P., & Mesirov, J. P. (2011). Molecular signatures database (MSigDB) 3.0. *Bioinformatics, 27*(12), 1739-1740. doi:10.1093/bioinformatics/btr260

Love, M. I., Huber, W., & Anders, S. (2014). Moderated estimation of fold change and dispersion for RNA-seq data with DESeq2. *Genome Biol, 15*(12), 550. doi:10.1186/s13059-014-0550-8

Magnuson, T., Debrot, S., Dimpfl, J., Zweig, A., Zamora, T., & Epstein, C. J. (1985). The early lethality of autosomal monosomy in the mouse. *J Exp Zool, 236*(3), 353-360. doi:10.1002/jez.1402360313

McCoy, R. C., Demko, Z. P., Ryan, A., Banjevic, M., Hill, M., Sigurjonsson, S., . . . Petrov, D. A. (2015). Evidence of Selection against Complex Mitotic-Origin Aneuploidy during Preimplantation Development. *PLoS Genet, 11*(10), e1005601. doi:10.1371/journal.pgen.1005601

Ottolini, C. S., Kitchen, J., Xanthopoulou, L., Gordon, T., Summers, M. C., & Handyside, A. H. (2017). Tripolar mitosis and partitioning of the genome arrests human preimplantation development in vitro. *Sci Rep, 7*(1), 9744. doi:10.1038/s41598-017-09693-1

Ottolini, C. S., Newnham, L., Capalbo, A., Natesan, S. A., Joshi, H. A., Cimadomo, D., . . . Hoffmann, E. R. (2015). Genome-wide maps of recombination and chromosome segregation in human oocytes and embryos show selection for maternal recombination rates. *Nat Genet, 47*(7), 727-735. doi:10.1038/ng.3306

Pringle, E. S., McCormick, C., & Cheng, Z. (2019). Polysome Profiling Analysis of mRNA and Associated Proteins Engaged in Translation. *Curr Protoc Mol Biol, 125*(1), e79. doi:10.1002/cpmb.79

Ritchie, M. E., Phipson, B., Wu, D., Hu, Y., Law, C. W., Shi, W., & Smyth, G. K. (2015). limma powers differential expression analyses for RNA-sequencing and microarray studies. *Nucleic Acids Res, 43*(7), e47. doi:10.1093/nar/gkv007

Snape, K., Hanks, S., Ruark, E., Barros-Nunez, P., Elliott, A., Murray, A., . . . Rahman, N. (2011). Mutations in CEP57 cause mosaic variegated aneuploidy syndrome. *Nat Genet, 43*(6), 527-529. doi:10.1038/ng.822

Soto, M., Raaijmakers, J. A., Bakker, B., Spierings, D. C. J., Lansdorp, P. M., Foijer, F., & Medema, R. H. (2017). p53 Prohibits Propagation of Chromosome Segregation Errors that Produce Structural Aneuploidies. *Cell Rep, 19*(12), 2423-2431. doi:10.1016/j.celrep.2017.05.055

Stingele, S., Stoehr, G., Peplowska, K., Cox, J., Mann, M., & Storchova, Z. (2012). Global analysis of genome, transcriptome and proteome reveals the response to aneuploidy in human cells. *Mol Syst Biol, 8*, 608. doi:10.1038/msb.2012.40

Taylor, A. M., Shih, J., Ha, G., Gao, G. F., Zhang, X., Berger, A. C., . . . Meyerson, M. (2018). Genomic and Functional Approaches to Understanding Cancer Aneuploidy. *Cancer Cell, 33*(4), 676-689 e673. doi:10.1016/j.ccell.2018.03.007

Vazquez-Diez, C., & FitzHarris, G. (2018). Causes and consequences of chromosome segregation error in preimplantation embryos. *Reproduction, 155*(1), R63-R76. doi:10.1530/REP-17-0569

Wang, Y., Yang, F., Gritsenko, M. A., Wang, Y., Clauss, T., Liu, T., . . . Smith, R. D. (2011). Reversed-phase chromatography with multiple fraction concatenation strategy for proteome profiling of human MCF10A cells. *Proteomics, 11*(10), 2019-2026. doi:10.1002/pmic.201000722

I. Acknowledgements

Foremost, I would like to express my sincere gratitude to my supervisor Prof. Dr. Zuzana Storchova, for giving me the opportunity to undertake my PhD in her group. I am really grateful for your constant enthusiastic support and patient guidance and for your many honest advices. The time I spent in your lab not only made me a better scientist but also a better person. I could not have imagined better advisor and supervisor for my PhD studies. I finally want to thank you for providing pleasant atmosphere and excellent working conditions in the lab.

Besides my advisor, I would like to Thank my PhD thesis committee members Prof. Dr. Johannes Hermann and Prof. Dr. Stefan Kins. Thank you for critical evaluation and insightful comments on my thesis.

I would like to thank several of our collaborators without whom this work would not be completed. Firstly, I want to thank Dr. Balca R Mardin, Dr. Christopher Buccitelli from lab of Prof. Dr. Jan O Korbel from EMBL, Heidelberg for providing us with several monosomic cell lines and support with data analysis. Next, I want to thank Dr. Mar Soto and Dr. Jonne Raaijmakers from lab of Prof. Dr. Rene Medema from NKI, Amsterdam for providing us with more monosomic cell lines. This project would not have started if not for your cell lines. I want to thank Dr. Anand Vasudevan and Devon Lekow from the lab of Dr. Jason Sheltzer from CSHL, USA for very interesting and productive collaboration. I am grateful to Vincent Leon Gottsmann from lab of Prof. Dr. Felix Willmund at University of Kaiserslautern for their help with polysome profiling and discussions on ribosomes. I would like to thank Xiaoxiao Zhang and Prof. Dr. Maik Kschischo for their help with computational analysis of TCGA and CCLE datasets. Last but not the least, I want to thank the members of sequencing facilities at EMBL, Heidelberg and NIG NGS sequencing center, University medical center Gottingen for their support with DNA and RNA sequencing and analysis.

I owe a special thanks to Dr. Markus Raeschle and Paul Menges for their help with transcriptomics and proteomic data analysis and for their helpful suggestions and ideas.

A special thanks to my girlfriend, partner in crime and also a dear colleague Sushweta Sen (Shonu) for her continuous support and encouragement during all the difficult times. Thank you for being part of my life and I hope to torture you many more years to come ☺

A special thanks to Angela Wieland, a dear friend and a wonderful colleague for helping me with revision experiments and for translating my thesis summary.

I am grateful to all the current members of Storchova lab: Sara (thanks for letting me steal your markers and buffers ☺ and for clicking bad pictures of me), Kristina (Yooo!!!), Galal (How are you doing my friend? Could not believe asking “How are you” will be so annoying ☺), Maja (Can’t forget your mix up of languages when you come back from Bogdan ☺), Kaisa and Mario (wonderful colleagues and roommates),

Maria Krivega, Clara, Lisa, Sahar, Steffi, Divya (thanks for designing my cover art), Aaron, Small Maria, Julia (Brasilian), Prince and many other students. I want to thank former lab members Chris, Neysan, Milena, Aline, Yehui, Verena for being wonderful colleagues and friends. Thanks for the fruitful discussions and for always being ready to listen and help. It was really a pleasure to work with you every day in the lab, I could not have asked for better labmates.

A special thanks goes to Carina, Phillip, Sven and many other students who helped with my experiments. I have learned from you all so much as you learned something from me (Hopefully ☺).

I am grateful to Isabell, Robin, Ingebourg and Arthur for your support and help with administration things, ordering, making buffers and everything that goes unnoticed. Isabell, a special thanks for bringing Nala into our life. Nala is the sweetest dog.

A great and warm thanks to my family in India, especially to my parents and my brother who always supported me in my life. I greatly appreciate how you care for me and at the same time leave me the freedom to make my own choices. A special thanks to my dear friend Jeshlee for bearing my torture for all these years. I am thankful to all my friends and well-wishers.

II. Abbreviations

17-AAG	17-N-allylamino-17-demethoxygeldanamycin
ASR	Aneuploidy Stress Response
BLCA	Bladder urothelial carcinoma
BRCA	Breast invasive carcinoma
CAGE	Common Aneuploidy Gene Expression
CCLE	Cancer Cell Line Encyclopedia
CENP	Centromere Protein
CESC	Cervical squamous cell carcinoma
CIN	Chromosome Instability
CRISPR	Clustered Regularly Interspaced Short Palindromic Repeats
DAPI	4’,6-diamidino-2-phenylindole
DBA	Diamond-Blackfan Anemia
DMSO	Dimethyl sulfoxide
DS	Down Syndrome
EdU	5-Ethynyl-2’-deoxyuridine
ESCA	Esophageal carcinoma
ESR	Environmental Stress Response
FACS	Flourscence Associated Cell Sorting
FISH	Flourescent In-Situ Hybridization
GFP	Green Flourescent Protein
GIN	Genomic Instability
GO	Gene Ontology
GOBP	Gene Ontology Biological Processes
GOCC	Gene Ontology cellular compartments
HI	Haploinsufficiency
HNSC	Head and neck squamous cell carcinoma
ISG	Interferon Stimulated Genes
ISR	Integrated Stress Response
KEGG	Kyoto Encylopedia of Genes and Genomes
KIRC	Kidney clear cell carcinoma
KIRP	Kidney renal papillary cell carcinoma
LIHC	Liver hepatocellular carcinoma
Lof2FC	Logarthmic Fold Changes
LOH	Loss Of Hetergozygosity
LSU	Large Subunit
LUAD	Lung adenocarcinoma
LUSC	Lung squamous cell carcinoma
MDS	Myelodysplastic Syndrome

MEF	Mouse Embryonic Fibrobalsts
MESO	Mesothelioma
MHC	Major Histocompatiability Complex
MTOC	Microtubule Organizing Center
MVA	Mosaic Variegated Aneuploidy
NK	Natural Killer cells
NT	Non Targetting
ORFs	Open Reading Frames
PCR	Polymerase Chain Reaction
Poly I:C	Polyinosinic:Polycytidylic acid
PRD	Proline Rich Domain
RiBi	Ribosome Biogenesis
ROS	Reactive Oxygen Species
RPE	Retinal Pigmental Epithelial
RPG	Ribosomal Protein Genes
RPL	Ribosome Protein Large
RPS	Ribosome Protein Small
SAC	Spindle Assembly Checkpoint
SARC	Sarcoma
SASP	Senescence Associated Secretory Phenotype
SCNV	Somatic Copy Number Abberations
scRNA seq	Singel Cell RNA sequencing
scSEQ	Single cell sequencing
SDS	Schwachman-Diamond syndrome
SEM	Standard Error of Mean
SKCM	Skin cutaneous melanoma
ssGSEA	Singel-Sample Gene Set Enrichment Analysis
SSU	Small Subunit
STAD	Stomach adenocarcinoma
TAD	Trans-activation Domain
TALENS	Transcription activator-like effector nuclease
TCGA	The Cancer Genome Atlas
TERT	Telomerase
TKNEO	Thymidine Kinase Neomycin
TMT	Tandem Mass Tag
UCEC	Uterine corpus endometrioid carcinoma
YAC	Yeast Artificial Chromosome

III. Curriculum Vitae

Name: Narendra Kumar Chunduri

Nationality: Indian

Education:

Since January 2021	**Postdoc** in the laboratory of Prof. Dr. Floris Foijer at European Research Institute for Biology of Ageing (ERIBA), Groningen
2015-2020	**PhD studies** in the Department of Molecular Genetics, Technical University of Kaiserslautern in the laboratory of Prof. Dr. Zuzana Storchova. Dissertation topic: "Multi-omics and functional analysis reveal novel consequences of monosomy"
2012-2015	**Masters in Molecular Life Sciences**, Friedrich Schiller University, Jena. Master thesis in Leibniz Institute on Aging - Fritz Lipmann Institute with Prof. Dr. Karl Lenhard Rudolph
2006-2010	**Bachelor of Sciences**, **Physician assistant**, Birla Institute of Technology and Sciences, Pilani, India

Professional experience:

2010-2011	Cardiovascular perfusionist, Cardio-thoracic surgery, Dr.Ramesh cardiac multispecialty hospitals, Vijayawada, India

Publications:

Published

1. Anand Vasudevan, Prasamit S Baruah, Joan C Smith, Zihua Wang, Nicole M Sayles, Peter Andrews, Jude Kendall, Justin Leu, Narendra Kumar Chunduri, Dan Levy, Michael Wigler, Zuzana Storchová, Jason M Sheltzer. **Single-Chromosomal Gains Can Function as Metastasis Suppressors and Promoters in Colon Cancer.** Developmental Cell 52 (4), 413-428. e6

2. Narendra Kumar Chunduri, Zuzana Storchova. **The diverse consequences of aneuploidy.** Nature Cell Biology. 21 (1), 54-62

3. Narendra Kumar Chunduri, Zuzana Storchova. **BCL9L and caspase-2—new guardians against aneuploidy.** Translational Cancer Research 6, S139-S142

In Revision

4. Narendra Kumar Chunduri, Paul Menges, Vincent Leon Gotsmann, Xiaoxiao Zhang, Balca R. Mardin, Christopher Buccitelli, Jan O. Korbel, Felix Willmund, Maik Kschischo, Markus Raeschle, Zuzana Storchova. **Haploinsufficiency of ribosomal genes limits the viability of monosomic human cells by activation of the p53 pathway.** (Accepted in Nature communications)

5. Maria Krivega, Clara Marie Stiefel, Sahar Karbassi, Narendra Kumar Chunduri, Neysan Donnelly, Andreas Pichlmair, Zuzana Storchova. **Genotoxic stress in constitutive trisomies induces autophagy and the innate immune response via the cGAS-STING pathway.** (Accepted in Communication Biology)

6. Devon A. Lukow, Erin L. Sausville, Pavit Suri, Narendra Kumar Chunduri, Zuzana Storchova, Jason M. Sheltzer. **Chromosomal instability accelerates the evolution of resistance to anti-cancer drugs.** (In revisions)

Workshops and Conferences:

2019	Poster presentation, EMBO Workshop - Chromosome segregation and aneuploidy, Cascais, Portugal
2016	International meeting of the German Society of Cell biology (DGZ) Participant